DIGITAL ACCESS TO SCHOLARSHIP AT HARVARD
DASH.HARVARD.EDU

HARVARD LIBRARY

The development of humoral breadth and protection against influenza

Citation

Boudreau, Carolyn M. 2021. The development of humoral breadth and protection against influenza. Doctoral dissertation, Harvard University Graduate School of Arts and Sciences.

Link

https://nrs.harvard.edu/URN-3:HUL.INSTREPOS:37371123

Terms of use

This article was downloaded from Harvard University's DASH repository, and is made available under the terms and conditions applicable to Other Posted Material (LAA), as set forth at
https://harvardwiki.atlassian.net/wiki/external/NGY5NDE4ZjgzNTc5NDQzMGIzZWZhMGFlOWI2M2EwYTg

Accessibility

https://accessibility.huit.harvard.edu/digital-accessibility-policy

Share Your Story

The Harvard community has made this article openly available.
Please share how this access benefits you. Submit a story

HARVARD UNIVERSITY
Graduate School of Arts and Sciences

DISSERTATION ACCEPTANCE CERTIFICATE

The undersigned, appointed by the

Division of Medical Sciences

Committee on Virology

have examined a dissertation entitled

The development of humoral breadth and protection against influenza

presented by Carolyn Boudreau

candidate for the degree of Doctor of Philosophy and hereby certify that it is worthy of acceptance.

Signature: Aaron G Schmidt (Sep 21, 2021 20:53 EDT)

Typed Name: Dr. Aaron Schmidt

Signature: Stephen Elledge

Typed Name: Dr. Stephen Elledge

Signature: Robert Anthony (Sep 21, 2021 17:52 EDT)

Typed Name: Dr. Robert Anthony

Signature: Adolfo Garcia-Sastre

Typed Name: Dr. Adolfo Garcia-Sastre

Date: September 21, 2021

The development of humoral breadth and protection against influenza

A dissertation presented

by

Carolyn Boudreau

to

The Division of Medical Sciences

in partial fulfillment of the requirements

for the degree of

Doctor of Philosophy

in the subject of

Virology

Harvard University

Cambridge, Massachusetts

September 2021

© Carolyn Boudreau

All rights reserved.

Dissertation Advisor: Dr. Galit Alter Carolyn Boudreau

The development of humoral breadth and protection against influenza

ABSTRACT

Influenza remains a serious global health concern, both as a seasonal pathogen and as a possible pandemic threat arising from novel strains against which the human population has no immunity. Current seasonal influenza vaccines provide a moderate level of protection, but complete protection is not achieved even where vaccination uptake is high. Furthermore, protection induced by both vaccines and infection is limited by lack of recognition of emerging zoonotic strains and seasonal strains that have undergone antigenic shift and/or drift. The current correlate of protection, hemagglutination inhibition, does not fully explain protection, particularly in high-risk groups. Emerging data suggests that antibody extra-neutralizing functions, which activate the innate immune system via interactions with Fc receptors (FcRs), can provide protection against seasonal and emerging pandemic strains. This work used an unbiased, polyclonal humoral profiling approach to explore the effects of an adjuvant, MF59, on the immune response to vaccination and define correlates of protection across multiple high-risk groups. In neonates, vaccine-induced maternal antibodies capable of binding to FcRs and transferring across the placenta provided increased protection. Similarly, in older adults, hemagglutinin- and neuraminidase-specific antibodies capable of activating NK cells provided increased protection. Linked to the importance of these mechanistic correlates of protection, the identification of strategies to broaden immunity is also key for the development of protective vaccines. Thus, to extend the correlates work, analysis of the role of antibody Fc-biology in the evolution of breadth of immunity across both influenza A and

B revealed that antibodies capable of binding to FcRs, and especially Fc γ receptor 2B, are both a correlate and a predictor of seroconversion to vaccine strains and seroconversion breadth. These antibodies, in addition to marking a matured humoral immune response, also act to promote this maturation upon repeated exposure, highlighting a target for increasing the potency of influenza vaccines. The data presented here implicate vaccine-induced Fc biology in tuning both the direct control and clearance of virus, but also, indirectly, the evolution of the Fab to recognize the breadth of influenza strain diversity, providing strategies for next generation vaccines, particularly in the context of universal influenza vaccine candidates.

TABLE OF CONTENTS

Abstract iii
Table of Contents v
Acknowledgements viii
List of Figures & Tables ix
Chapter 1: Introduction 1
Influenza virology and vaccinology 1
Influenza virology 1
Impact of influenza on human health 3
Current influenza vaccines 3
Antibody development against influenza 5
Original antigenic sin, or antigenic seniority 5
Antibody targets 6
Germinal Centers 7
FcR-mediated functions in influenza infection and vaccination 9
FCγR expression and functionality 10
Antibody-dependent cellular cytotoxicity by NK cells 12
Antibody-dependent macrophage phagocytosis and activation 15
Antibody-dependent neutrophil phagocytosis and activation 16
Antibody-dependent complement activation 17
Additional functions via non-classical FcR 19
Control of FcR-mediated functions by antibody properties 21
Subclass and isotype variation 21
Antibody Fc glycosylation 24
Optimizing antibody responses through vaccination 26
Adjuvants 26
Antigen Design And Glycosylation 28
Additional antigenic targets 31
Murine models in influenza and innate immune antibody functionality 32
Murine models in influenza 32
Antibody isotype and FCγR differences in mice and humans 33
Concluding remarks 33
Chapter 2: Selective induction of antibody effector functional responses using MF59-adjuvanted vaccination 35
Introduction 36

Methods 38
Results 43
MF59 induces a unique functional humoral response 43
MF59 enhances highly functional antibody subclass levels 46
MF59 selectively induces antibody-dependent innate immune functions 49
MF59 induces antibodies with differential low affinity Fcγ-receptor binding profiles 54
MF59 overcomes natural pre-existing HA specific antibodies 56
Discussion 58
Chapter 3: Impact of maternal influenza vaccination on antibody placental transfer and protection of infants in a placebo-controlled trial 64
Introduction 65
Methods 68
Resource availability 68
Experimental model and subject details 68
Method details 70
Results 75
Vaccination boosts antibody levels, FCGR binding, and functionality 75
FCγR-binding antibodies are selectively enhanced following vaccination in mothers and cord 80
FCγR-binding antibodies, rather than overall antibody concentrations, discriminate infants that later develop influenza infection 84
Cord blood from uninfected infants shows targeted humoral immune profile 87
Vaccination shapes the transfer of protective immunity to the cord 90
Discussion 92
Chapter 4: Vaccine-induced antibody mediated NK cell activation as a key correlate of immunity against influenza in older adults 96
Introduction 97
Methods 100
Results 107
Enhanced responses to egg-adapted HA correlate with responses to circulating HA 107
High dose vaccination induces a multipronged functional antibody response 110
Protected vaccinees induce more coordinated humoral immune responses 112
NK cell activation separates infected from uninfected vaccinees 114
Age decreases responsiveness to antibody-mediated protection against influenza in mice 117
NK cells in older adults are functionally different than NK cells in younger adults 119
Discussion 121
Chapter 5: Pre-existing Fc profiles shape the evolution of neutralizing antibody breadth to influenza 127
Introduction 128

Methods 130
Results 138
Response to seasonal influenza vaccination is highly heterogeneous 138
Defining correlates for the evolution of breadth of HAI 143
Validation of neutralizing breadth correlates in an orthogonal cohort of vaccinees 147
Pre-existing FCγR-binding antibody titers predict a broad neutralizing vaccine response 150
Pre-existing FCGR-binding antibodies increase humoral response to influenza vaccination in mice 153
Discussion 156
Chapter 6: Discussion 161
Use of systems serology in evaluating influenza vaccines 162
Innovations to the platform 162
Computational biology analyses 163
Humoral breadth: epitopes & functionality 164
Defining humoral breadth 164
Humoral breadth in response to vaccination 165
Epitopes and immunodominance 167
The development of the influenza-specific immune response across a lifetime 169
Placental sieving 170
Original antigenic sin 171
Repeated influenza exposure 172
Aging 173
Defining additional correlates of protection 174
Neutralization and antibody titers 174
NK cells as a key correlate of protection against influenza 175
FCγR-binding antibodies as a predictor of protection in neonates 177
Overall coordination of the humoral immune response alters susceptibility to influenza 178
Role of adjuvants in developing protective responses 179
Future Directions 180
Impact of repeated seasonal vaccination 180
Impacts of novel vaccine formulations 182
Antigenic targets beyond HA & NA 183
Conclusion 185
References 186

ACKNOWLEDGEMENTS

My thanks to my mentor, Galit Alter, for welcoming me into her lab, pushing me to do more, and providing countless opportunities to do interesting, impactful science with fantastic people. To all the members of the Alter lab (past and present) who answered my questions, shared snacks, and cracked jokes right when I needed a laugh. To Jackson, my right-hand man for three years of this PhD, who showed up every day ready to do whatever work needed to be done. To the Alter Lab grad student & tech crew who went on trips, launched our own beer hours, and had way more fun than we honestly had any right to.

My thanks to the Virology program, especially Maria Bollinger, and the members of my DAC (Daniel Lingwood, Michael Carroll, and Aaron Schmidt), who provided invaluable advice and support. To my cohort, who helped me remember how to take a class again, and to the Virology community for feedback and advice throughout.

My thanks to my comrades at the Harvard Graduate Student Union, who reminded me that we are stronger together. This dissertation was produced with union labor.

My thanks to the people who started out as coworkers and became best friends, Maddy and Stephanie. To all the friends who have been sources of joy throughout, especially Alecia, Sam, Emily, Licole, and Steph.

And finally, my thanks to my family: my in-laws, for their acceptance and love; my mother, who always offers guidance and support; my father, who always reminds me that I can do anything I put my mind to; my brother, who may not have moved to Boston just to be around me, but I know it was just so we could hang out. And finally, to Andrew, for unwavering and unrelenting support on every single day of this journey (all 1,857 of them).

LIST OF FIGURES & TABLES

Figure 1.1 Schematic structure of influenza virion. 3
Figure 1.2 Antibody structure highlighting functions of both the Fab and Fc regions. 9
Figure 1.3 Human FcRs associated with anti-influenza functionality and their affinities, expression, and functions. 11
Figure 1.4 Known FcR-dependent innate immune effector functions acting in influenza infection. 13
Figure 1.5 Structures of antibody isotypes and subclasses. 23
Figure 1.6 Structure of antibody glycan. 24
Figure 2.1 MF59 significantly alters the functional humoral profile following H5-vaccination. 45
Figure 2.2 Antibodies against H5 were compared for 90 vaccinees who received 15µg recombinant H5 unadjuvanted (none), with alum, or with MF59.. 45
Figure 2.3 MF59 selectively enhanced functional antibody subclass levels following H5 immunization. 47
Figure 2.4 MF59 alters specific antibody isotype levels following H5 immunization. 48
Figure 2.5 MF59 induces neutralization and specific antibody-dependent innate immune functions along with IgG1 titers. 50
Figure 2.6 MF59 induces higher titers, but not antibody-dependent monocyte or NK cell functions. 53
Figure 2.7 MF59 increases enhanced FcγRIIa, but not FcγRIIIa, H5-specific binding antibodies. 55
Figure 2.8 MF59 increases enhanced FcγRIIa, but not FcγRIIIa, H5-specific binding antibodies across FcγR polymorphisms. 55
Figure 2.9 MF59 induced antibody functionality is not influenced by pre-vaccination H1 specific immunity. 57
Figure 3.1 Schematic of samples included in this study. 67
Table 3.1 Table describing demographic data for study participants. 70
Figure 3.2 Vaccination boosts maternal and fetal antibodies, but not transfer efficiency. ...76
Figure 3.3 Vaccination has isotype- and subclass-specific effects. 78
Figure 3.4 FCGR binding levels separate vaccinee mother-child pairs from placebo recipients. 81
Figure 3.5 HAI is not a key feature separating vaccinees from placebo recipients. 82
Figure 3.6 FCGR binding levels separate infected infants from uninfected infants. 85
Figure 3.7 Correlations between LASSO-selected features and HAI. 87
Figure 3.8 Humoral intercorrelation in cord blood differentiates infected infants from uninfected infants. 88
Figure 3.9 Vaccination strongly affects the protective humoral features in cord blood. 91
Figure 3.10 Vaccine-induced features separate infected from uninfected infants. 91
Figure 4.1 Responses to circulating H3 and vaccine H3 are highly correlated but vaccine H3 responses have higher magnitude. 108
Figure 4.2 Regular and high dose vaccines induce different functional humoral responses. 111
Figure 4.3 Protected vaccinees induce more coordinated humoral immune response.. 113
Figure 4.4 Antibody-dependent NK cell activation is a predictor of protection from influenza infection. 115

Figure 4.5 Model significance for LASSO-Elastic Net in **Figure 4.4**.....116
Figure 4.6 Glycosylation and NK cell activation. 117
Figure 4.7 NK-activating Fc mutant increases protection in young mice while old mice remain susceptible.....119
Figure 4.8 NK cells from older adults are less responsive to FCGR3A-mediated stimulation than NK cells from younger adults. 120
Figure 4.9 Representative gating for NK cells in **Figure 4.8**.....121
Figure 4.10 Correlations across age and frailty to ADCC activation.. 121
Figure 5.1 Pairwise distances show subtype variation. 137
Table 5.1 Influenza strains tested in HAI assays and abbreviations used. 139
Table 5.2 Systems serologic measurements by sample cohort and influenza strain. 140
Figure 5.2 Seasonal influenza vaccine produces highly heterogeneous responses in healthy adults. 141
Figure 5.3 Accuracy and significance of non-converter vs converter model in **Figure 5.2**...142
Figure 5.4 HAI titers by group for vaccine antigens. 143
Figure 5.5 FCGR-binding titers are correlates of the development of neutralizing breadth. 144
Figure 5.6 Accuracy and significance of breadth model in **Figure 5.5**. 146
Figure 5.7 Additional univariate plots for LASSO-Elastic Net selected features (**Figure 5.5**). 146
Figure 5.8 Validation of breadth findings in an independent cohort. 148
Figure 5.9 Validation of the seroconversion model in **Figure 5.2** with an orthogonal cohort. 149
Figure 5.10 Breadth score distribution and comparison to percentage of strains neutralized for the larger cohort used for validation. 149
Figure 5.11 Additional univariate plots for LASSO-Elastic Net selected features (**Figure 5.8**). 150
Figure 5.12 FCGR2B-binding antibodies are a predictor of neutralizing breadth. 151
Figure 5.13 Accuracy and significance of breadth model in **Figure 5.12**. 152
Figure 5.14 Presence of FCGR-binding antibodies in immunization drives improved humoral immune response in mice. 154
Figure 5.15 Binding of CR9114 Fc variants to multiple H3N2 antigens. 156
Figure 6.1 Schematic depicting the systems serology analysis pipeline. 162
Figure 6.2 Effects of pre-existing antibodies at the time of vaccination.. 166
Figure 6.3 The development of the influenza-specific immune response over a lifetime. ...170
Figure 6.4 HAI breadth over multiple influenza vaccinations. 182

Chapter 1: INTRODUCTION

Sections of this introduction were published as:

> Boudreau, C. M. & Alter G. (2019). Extra-Neutralizing FcR-Mediated Antibody Functions for a Universal Influenza Vaccine. *Front Immunol, 10(440)*. doi: 10.3389/fimmu.2019/00440

While neutralizing antibody titers measured by hemagglutination inhibition have been proposed as a correlate of protection following influenza vaccination, neutralization alone is a modest predictor of protection against seasonal influenza. Instead, emerging data point to a critical role for additional extra-neutralizing functions of antibodies in protection from infection. Specifically, beyond binding and neutralization, antibodies mediate a variety of additional immune functions via their ability to recruit and deploy innate immune effector functions. Along these lines, antibody-dependent cellular cytotoxicity, antibody-mediated macrophage phagocytosis and activation, antibody-driven neutrophil activation, antibody-dependent complement deposition, and non-classical Fc-receptor antibody trafficking have all been implicated in protection from influenza infection. However, the precise mechanism(s) by which the immune system actively tunes antibody functionality to drive protective immunity against influenza has been poorly characterized.

INFLUENZA VIROLOGY AND VACCINOLOGY

INFLUENZA VIROLOGY

Influenza viruses are enveloped negative-strand RNA viruses with segmented genomes (**Figure 1.1**) that can infect a variety of mammals (*1*). Birds are the zoonotic reservoirs of many influenza viruses, but influenza can also infect pigs, horses, seals, and humans (*2*). Influenza viruses infect cells by binding to sialic acids on the cell surface via

the hemagglutinin (HA) protein, and the specificity of this receptor to sialic acid linkages determines host specificity (*3*). The neuraminidase (NA) protein, also expressed on the virion surface, mediates viral egress by cleaving sialic acids on the infected cell and allowing viral escape (*4*). The M1 matrix protein forms the capsid within the lipid envelope of the virus, and anchors the viral ribonucleoprotein (vRNP) complex (*5*). The M2 ion-channel protein, specific to influenza A viruses, is responsible for the release of vRNP complexes during an infection in response to pH changes in the endosome after the virion enters the cell (*6*). Influenza nucleoprotein (NP) encapsulates the viral RNA within the virion, interacting with RNA and the polymerase complex (PA,PB1,PB2) to form the vRNP complex (*7*). Additional nonstructural proteins, including the nuclear export protein (NEP), nonstructural protein (NS1), and the N40 truncated PB1 round out the protein coding regions of the genome.

Two families of influenza viruses, influenza A and influenza B, currently circulate in the human population. Influenza A strains are named by the hemagglutinin and neuraminidase molecules they express; there are 18 families of HA molecules and 11 families of NA molecules (*8*). Currently, H1N1 and H3N2 are the two influenza A strains causing seasonal outbreaks among the human population. H1N1 undergoes antigenic shifts, wherein major changes to the virus happen infrequently, often due to zoonotic emergence. H3N2, in contrast, primarily undergoes antigenic drift, wherein small changes occur consistently from season to season (*9*). While influenza A resides and reassorts in non-human hosts, influenza B has limited transmission outside of humans. Influenza B infections are typically more regionally contained than influenza A epidemics; however, influenza B contributes to seasonal epidemics, occasionally as the predominant subtype (*10*).

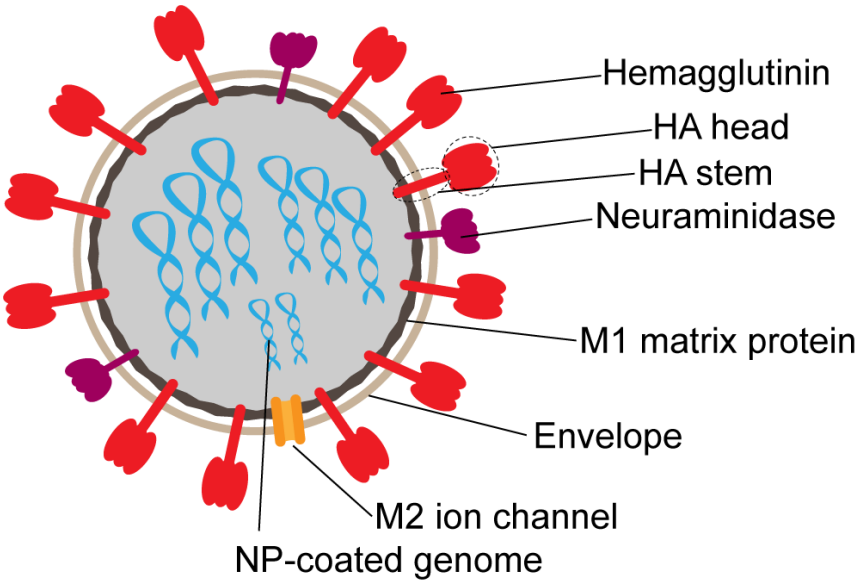

Figure 1.1 Schematic structure of influenza virion. Surface proteins hemagglutinin (HA) and neuraminidase (NA) are present on the surface at an approximate 3:1 ratio. The M2 ion channel also spans the envelope. M1 matrix protein forms the inner capsid, which surrounds the segmented RNA genome coated in nucleoprotein (NP).

IMPACT OF INFLUENZA ON HUMAN HEALTH

Seasonal influenza affects 10-20% of the world's population per year (*11*), which is estimated to cost $4.6 billion yearly for hospitalizations, doctor's visits, and medications in the United States alone (*12*). Additionally, influenza causes U.S. employees to miss approximately 17 million workdays, at an estimated cost of $7 billion a year in sick days and lost productivity (*12*). Increased infection and mortality occurred during four pandemics in the 20th and 21st centuries, in 1918, 1957, 1968, and 2009 (*13*), and could occur again if a new strain, such as avian influenzas H5N1 or H7N9, begins to circulate in the human population.

CURRENT INFLUENZA VACCINES

To address the looming threat of an influenza pandemic, the National Institute of Allergy and Infectious Diseases (NIAID) has named the development of a universal influenza vaccine, defined as one that provides protection against symptomatic disease from

≥75% of influenza A strains, as one of its research priorities (*14*). A key component of the strategic plan is the initial characterization of the correlates of immunity against influenza infection and disease (*15*). While antibody-mediated neutralization has been widely considered the major protective correlate of immunity, neutralization alone has been only modestly linked to protection from seasonal influenza infection (*16–19*). Moreover, currently licensed seasonal influenza vaccines provide only moderate (10-60%) protection against specific strains of seasonal influenza, and little to no protection from possible emerging pandemic influenza strains (*20*). Low vaccine efficacy is caused by subtype and strain variability of the two major viral antigens, HA and NA, as well as by antigenic drift (*4*). All the available seasonal influenza vaccines, including the inactivated influenza vaccine (IIV), adjuvanted IIV (FluAd), and live attenuated influenza vaccine (LIAV), are given yearly due to limited response durability and the need to induce *de novo* immunity to novel circulating strains. The development of yearly influenza vaccines relies on predictions published by the World Health Organization to determine the strain composition for a given year (*21*). Due to the long lead times in producing adequate quantities of the vaccine, the strains must be selected roughly 6 months in advance of vaccine administration (*21*), potentially leading to population vulnerability should a new strain enter circulation. During seasons when these predictions did not match well with seasonal circulating strains, vaccine effectiveness has been very low (*20*). For example, in the 2016-2017 flu season, the circulating H3N2 virus had an amino acid mismatch leading to the inclusion of a new glycosylation site that was not included in the egg-adapted viral strain used for vaccination. Thus, the virus readily evaded vaccine induced immunity, resulting in decreased vaccine effectiveness (*22*).

Beyond efforts to match sequences to ensure seasonal immunity, the current correlate of protection used to evaluate influenza vaccines is the hemagglutination inhibition (HAI) assay (*23*). HAI was identified as a predictor of protection from infection in the initial study of egg-grown inactivated vaccine efficacy conducted in 1943 by Salk, Menke, and Francis (*24*). HAI measures the ability of an antibody or serum sample to prevent HA binding to red blood cells, and is considered a proxy for neutralization by receptor blockade (*23*). HAI, however, does not fully explain or predict protection in humans (*16–18*). Indeed, individuals lacking detectable HAI titers were found to be resistant to influenza infection. Additionally, infection risk was clearly linked to age independent of HAI titer (*16*). While HAI is considered a classical correlate of protection from influenza infection, it alone is not sufficient to fully explain protection (*19*).

ANTIBODY DEVELOPMENT AGAINST INFLUENZA

ORIGINAL ANTIGENIC SIN, OR ANTIGENIC SENIORITY

Original antigenic sin was first defined over 50 years ago as the lifelong shaping of the anti-influenza immune response by the first exposure to influenza, typically occurring in infancy or early childhood (*25*). At a population level, this results in significant immunity towards the circulating strains that predominated at the time of first exposure (*26*). More recent explorations of this topic, which is now also called antigenic seniority, have provided significant detail into the effects of this phenomenon. Upon exposure, HAI titers of all previously encountered strains are boosted, resulting in the highest overall titers being those reactive to the earliest encountered strains (*27*). Early studies of repeated seasonal vaccination showed inconsistent results (*28–30*). However, more recent data indicated that, while vaccination causes the highest increase in total antibody titers upon the first dose,

current vaccination strategies provide increased protection even when administered repeatedly (*31*). Indeed, one recent study characterizing individual antibodies isolated from vaccinated adults indicated that vaccine-specific antibodies make up a large proportion of the antibody-secreting plasma cell population immediately following vaccination (*32*), suggesting that the impact of pre-existing antibodies may be more complex than originally described.

ANTIBODY TARGETS

Humoral immune responses to influenza are largely directed towards the hemagglutinin molecule. HA, the primary viral glycoprotein, exists as a trimer made of monomers composed of two subunits, HA1 and HA2 (*33*). The structure of HA is composed of a "head" and a "stem" domain (**Figure 1.1**). Heterosubtypic, or cross-reactive, antibodies to the HA head region are relatively rare due to heavy glycosylation and low sequence conservation in this region (*34*, *35*). Although highly variable, cross-reactive neutralizing antibodies have been discovered against the HA head. These antibodies bind primarily to specific conserved epitopes, including the receptor binding domain (*35*). While several protective antibodies have been identified against the HA stem, as it is more conserved, this region of the HA is poorly immunogenic (*34*).

As mentioned above, heterosubtypic protective antibodies against influenza primarily target either the receptor binding site on the HA head or the more conserved HA stem (*36*). However, the stem region is infrequently targeted compared to easily inducible strain-specific HA head responses (*37*). Antibodies that target the head region largely provide protection by preventing the virus from entering the target cell, and are thus referred to as neutralizing antibodies (*36*). Conversely, non-neutralizing yet protective influenza-specific antibodies have been documented against both the HA head and stem

(*38*, *39*); however, their mechanisms of action are more complex and varied (*40*). Although protective non-neutralizing antibodies have been documented across the HA molecule, these types of protective antibodies more dominantly target the stem region of HA and can exhibit wide reactivity, capturing most influenza A viruses (*37*).

Antibodies arising from influenza vaccination target different viral epitopes and develop along a distinct immune trajectory as compared to antibodies arising from natural infection. Infection-induced antibodies have more heavily mutated sequences than vaccine-induced antibodies; these infection-induced antibodies arise from repeated re-entry of antibody-producing B cells into the germinal center dark zone, while vaccination recalls more recent exposures than infection (*41*). Consistent with this mechanism, vaccine-induced antibodies are less likely to have cross-strain reactivity (*41*). Furthermore, vaccine-induced antibodies are targeted almost exclusively to HA, whereas antibodies arising from infection recognize a diverse array of viral proteins (*41*). During infection, additional viral antigens are also presented on virions and the surface of infected cells, including NA, NP, and M2 (*5*). Antibodies to all of these antigens are present in adults previously exposed to influenza, and as such, are possible candidates for novel vaccine designs (*42–47*). While the majority of the field is focused on HA as it is the immunodominant viral antigen in both vaccination and infection, immune responses directed towards highly conserved, non-neutralizing epitopes remain a promising area of investigation.

Germinal Centers

Antibodies develop in the germinal centers of lymph nodes following infection or vaccination, and the strength and character of the humoral immune response is largely determined by the conditions in the germinal centers as these B cells mature (*48*). Germinal

centers induced by protein model antigens last less than one month, while viral infection–induced germinal centers can persist for much longer as a result of differences in immune activation (*49*). Germinal center formation occurs upon the binding of antigen by resting B cells, leading to rapid B cell proliferation (*49*). Germinal centers select antibodies based on their affinity for the target antigen, and while this process typically results in some highly protective antibodies, germinal centers do not have a mechanism for assessing protective efficacy directly. There are two mechanistic models in the field currently for how germinal center selection works: (1) high affinity for antigens causes signaling through the B Cell Receptor (BCR) to germinal center light zone follicular dendritic cells (FDCs), which return to the dark zone of the germinal center to proliferate and (2) that germinal center B cells compete for limited T Follicular Helper (TFH) cell help by acquiring and presenting antigen in proportion to their affinity (*50*). Both of these models contribute to our understanding of germinal center steering, a phenomenon by which novel influenza exposures shift the humoral response towards conserved epitopes, whereas repeated exposures to the same strain bias the response towards the variable, immunodominant HA head (*50*).

Antibodies present in the serum and lymphoid organs shape the development of the immune response following vaccination and natural infection. Soluble antibodies present during the formation of the immune response mask antigen presentation by FDCs, competing with B cells and increasing the affinity threshold for B cell survival (*49*). Fc γ receptor IIB (FCGR2B), a transmembrane-receptor containing an immunoreceptor tyrosine-based inhibitory motif (ITIM) which binds to IgG in complex with antigen, is present on both B cells and FDCs and helps to shape the developing immune response (*51*). On B cells, it works in concert with soluble antibody to raise the B cell activation threshold and decrease antibody production by suppressing B cell-mediated antigen presentation to T

cells (*52*). On FDCs, FCGR2B traps the antigen-containing immune complexes and performs an activating role in driving the germinal center response (*51*). Overall, the impact of pre-existing antibodies on the immune response remains an open area of study, and will be explored in Chapter 5.

FcR-MEDIATED FUNCTIONS IN INFLUENZA INFECTION AND VACCINATION

While the mechanism of protection mediated by neutralizing antibodies is simple to comprehend, the mechanism of action of non-neutralizing antibodies is less well understood. Emerging evidence has suggested that mechanisms including the ability of antibodies to leverage the innate immune system may contribute to protection against influenza (*38–40*, *53–59*). Critically, antibodies possess two functional domains: the Fab, which recognizes the antigenic epitope, and the Fc, which interacts with Fc receptors (FcR) or complement to drive antibody-mediated effector functions (**Figure 1.2**). Passive transfer studies using both native IgG1 and FcR-binding ablated monoclonal antibodies (mAbs)

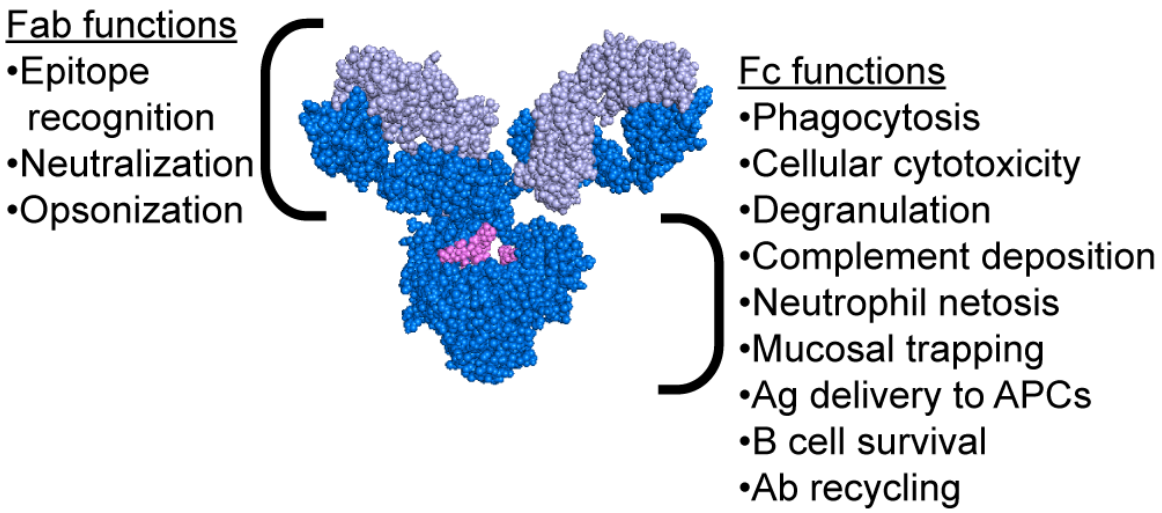

Figure 1.2 Antibody structure highlighting functions of both the Fab and Fc regions. Antibody image shows heavy chain in dark blue, light chain in light blue, and glycan in magenta. Antibody structure: PDB 1IGY.

clearly illustrated the importance of Fc-mediated functions in protection from infection in mice (*38*, *39*). Moreover, follow-up studies using FcR and complement knock out mice further clarified the critical nature of specific Fc-effector functions in protection (*38–40*, *53–59*). Antibody mediated macrophage phagocytosis (*56*, *60*), neutrophil production of reactive oxygen species (*56*), cellular cytotoxicity (*57*), and complement deposition (*54*, *55*, *60*, *61*) have all been implicated as protective functions leveraged by antibodies to drive protection from infection and/or viral clearance. Strikingly, even broadly neutralizing HA-stem targeting and pan-strain HA-head targeting mAbs require interaction with FcRs to confer protection (*39*).

FCγR EXPRESSION AND FUNCTIONALITY

Multiple human Fc γ receptors (FCγRs) and FcRn (**Figure 1.3**) have been implicated in protection from influenza, namely FCGR2A, FCGR2B, and FCGR3A (*62*). FCGR1A, 2A, and 3A are the activating Fc receptors, acting through immunoreceptor tyrosine-based activation motif (ITAM) domains to promote innate immune cell cytokine release, phagocytosis, and other immune functions. FCGR1A has high affinity for IgG1, IgG3, and IgG4 and is the sole FCγR capable of binding to monomeric IgG (*63*, *64*). FCGR2A has two allelic variants, H_{131} and R_{131}, both of which bind with low affinity to IgG1, IgG3, and IgG4, and only the H_{131} variant binds to IgG2 with appreciable affinity (*65*). FCGR2A is primarily associated with monocyte, macrophage, and neutrophil activation to trigger phagocytosis and cytokine release (*66*, *67*). FCGR3A also has two allelic variants, V_{158} and F_{158}, both of which bind with low affinity to IgG1 and IgG3; V_{158} binds with higher affinity than F_{158} to IgG1 and also binds to IgG4, with limited affinity for IgG2 (*65*). FCGR3A is primarily associated with natural killer (NK) cell activation to mediate antibody-dependent cellular cytotoxicity (ADCC) (*68*, *69*).

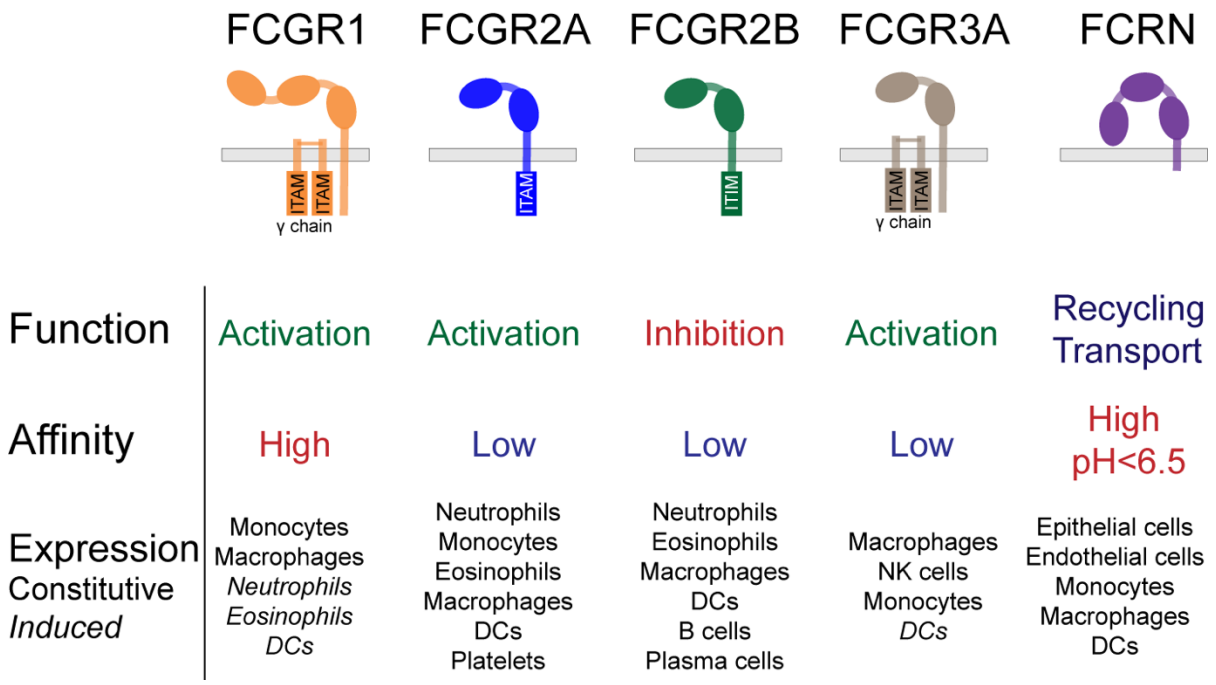

Figure 1.3 Human FcRs associated with anti-influenza functionality and their affinities, expression, and functions. Adapted from (*63, 64*). Additional information from (*70*).

FCGR2B is the classical inhibitory low affinity FCγR, which serves multiple roles depending on the cell type on which it is expressed. FCGR2B binds to IgG1, IgG3, and IgG4 isotypes (*63*). FCGR2B counteracts activating signals from other FCγRs via signaling through its ITIM domain and is expressed on macrophages, neutrophils, dendritic cells (DCs), and eosinophils (*51*). On B cells, FCGR2B raises the B cell activation threshold during a germinal center response (*51*). On FDCs, FCGR2B traps antigen-containing immune complexes and may serve to drive the germinal center response (*51*). The dual role of FCGR2B in both inhibiting certain anti-viral innate immune functions and enhancing the process of affinity maturation in germinal centers creates a unique opportunity to tune the developing immune response in the presence of pre-existing antibodies.

FcRn, also known as the neonatal Fc receptor, is not structurally similar to the other FcRs, but instead is similar to MHC class 1 molecules (*70*). FcRn is responsible for recycling

IgG from the serum and extending the half-life beyond other serum proteins (*71*). During pregnancy, FcRn is involved in the transport of IgG across the placental barrier (*72*). FcRn binds to IgG within acidified endosomes, protecting it from proteolytic cleavage, and transcytoses across to the basal cell surface or is recycled back to the apical surface of cells, where the return to physiological pH releases the IgG back into circulation (*70*). The sections below will explore in further detail the anti-influenza functions mediated by each FcR.

ANTIBODY-DEPENDENT CELLULAR CYTOTOXICITY BY NK CELLS

Antibody-dependent cellular cytotoxicity (ADCC) is largely mediated by the interaction of pathogen or cell-surface bound antibodies with FCGR3A on NK cells in humans (**Figure 1.4D**) and FCGR4 on monocytes, macrophages, and neutrophils in mice (*68*, *69*). FCGR3A is found on the surface of NK cells, monocytes, and macrophages (*67*). Engagement of FCGR3A by antibody causes the release of cytotoxic granules from NK cells, uptake by macrophages, apoptosis of infected targets, and secretion of antiviral cytokines and chemokines (*73–76*).

However, despite our emerging appreciation for the potential role of ADCC in protection from infection and disease, the seasonal influenza vaccine poorly induced broadly reactive ADCC-inducing antibodies in healthy children and adults (*77–80*). Conversely, the presence of cross-reactive HA-specific antibodies that can activate NK cells in older adults suggests that these functional antibodies accumulate over the course of many years of repeated natural infection with influenza (*79*, *81*). Moreover, some healthy American adults possessed ADCC activity against avian H7N9 and H5N1 viruses, viruses that do not circulate in North America but could cause pandemic outbreaks, indicating the natural evolution of cross-reactive functional antibodies to quite diverse HA antigens in the absence

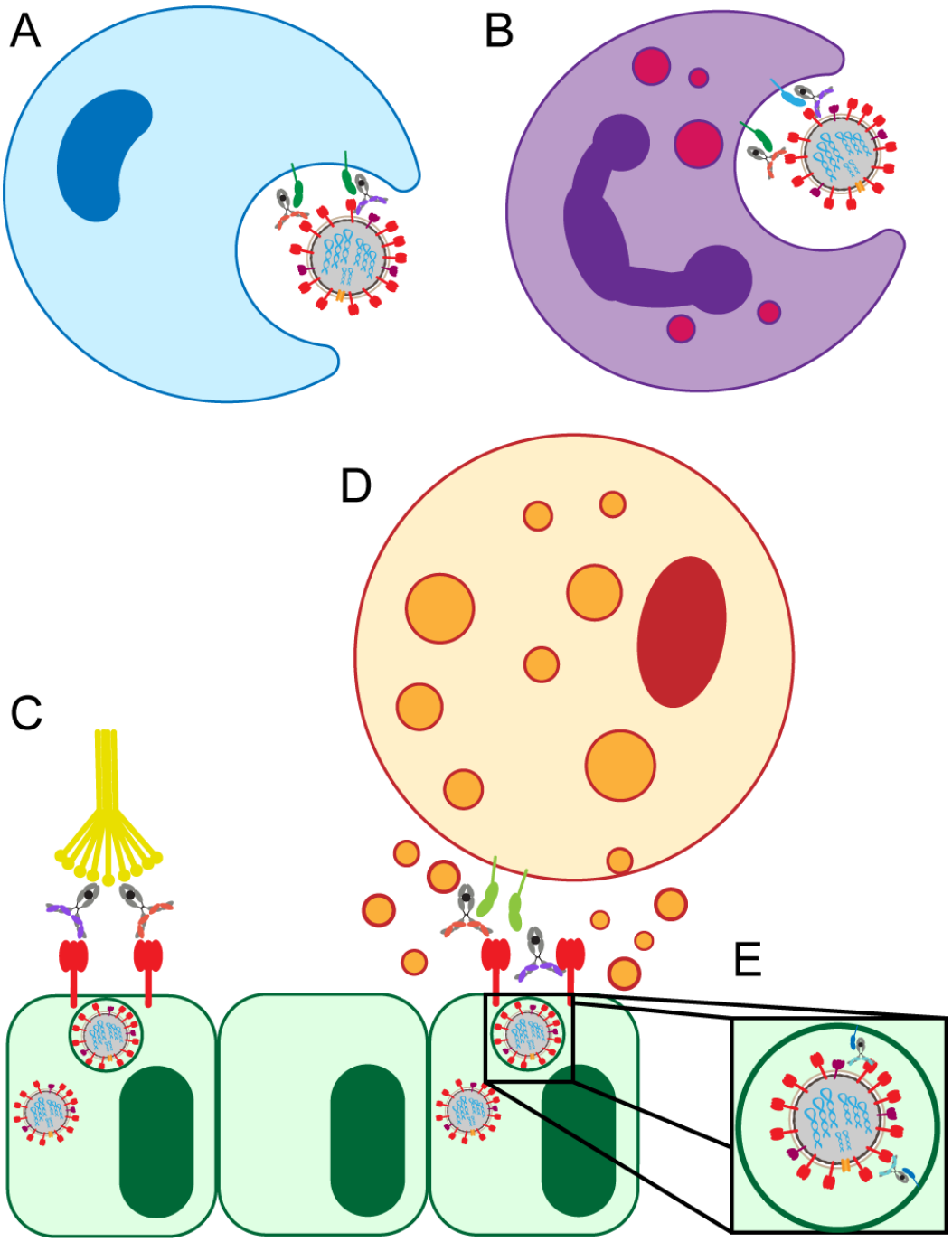

Figure 1.4 Known FcR-dependent innate immune effector functions acting in influenza infection. (A) Clearance of virions and infected cells by macrophage phagocytosis. (B) Clearance of virions and infected cells by neutrophil phagocytosis, and the release of cytokines and reactive oxygen species. (C) Clearance of infected lung epithelial cells and activation of the adaptive immune system by antibody interaction with C1Q. (D) Clearance of infected lung epithelial cells by ADCC. (E) Neutralization of virus by FcRn-bound HA-specific antibodies.

of exposure (*59*, *82*). Furthermore, broadly cross-reactive ADCC-inducing antibodies were reported in individuals who lack broadly neutralizing influenza-specific antibodies (*81–84*),

suggesting that these functions emerge separately and may evolve under distinct stimuli. Collectively, the data clearly demonstrate that broadly protective ADCC-inducing antibodies are associated with protection and evolve naturally over time.

HA head-specific mAbs induced less ADCC when compared to stalk-specific antibodies in an *in vitro* NK cell activation assay (*38*). This difference in function has been suggested to be related to the inability of the head-specific mAbs to efficiently multimerize when bound to antigen on the cell surface and interact with low-affinity FcRs to induce functional responses (*38*). A recent study suggested an alternative explanation in experiments using FLAG-tagged HA to direct FLAG-specific antibody to certain regions of the HA molecule. The data from this study suggested that two points of contact were required between infected and effector cells for efficient ADCC activity (*85*). These direct contacts are (1) between the mAb Fc and FcR and (2) between the cell surface sialic acid and viral HA (*85*). However, the co-ligation of FcR and viral protein has not been borne out by studies in other infection or disease contexts, or in polyclonal pools of antibodies directed against native HA.

An additional layer of complexity in dissecting non-neutralizing antibody mediated mechanisms of protection *in vivo* is the comparison of polyclonal versus monoclonal mediated antibody functions. Emerging data suggest that the level of *in vitro* ADCC is influenced by the ratio of ADCC-inducing to ADCC-inhibiting antibodies (*39*, *86*). ADCC-inhibiting antibodies, which can be neutralizing, were shown to compete for binding sites on HA on the surface of viral particles and infected cells (*39*, *86*). While the delivery of single protective ADCC-inducing mAbs demonstrated striking protection from infection *in vivo* (*38*, *39*), polyclonal pools of antibodies exhibited a much more complex balance of epitope targeted and functional competition that collectively may contribute to differential

protection from infection during seasonal exposure. While it is clear that functional antibodies play a vital role in protection against influenza infection, experimental approaches able to comprehensively dissect the nature of polyclonal antibody interactions are urgently needed to further define the nature of protective antibody activity to guide vaccine design.

ANTIBODY-DEPENDENT MACROPHAGE PHAGOCYTOSIS AND ACTIVATION

ADCC-inducing antibodies, as well as the direct cytopathic effects of the virus, drives infected cell apoptosis (*87*). These infected apoptosing cells are then cleared through phagocytosis to maintain tissue homeostasis (*88*). Post-infection, macrophages are rapidly recruited to the lung and are present in bronchoalveolar lavage (BAL), airway, and alveoli to support the rapid clearance of infected and dying cells (*89*). While the supernatant of influenza-infected cells can stimulate monocyte phagocytosis independently of antibody involvement (*89*), antibodies contribute to accelerated clearance of viral particles and infected cells through interactions with FCGR1A and FCGR2A on immune cells (*66*). Antibody mediated viral phagocytosis, resulting in viral degradation, was linked to decreased spread and severity of infection (*66*). While this mechanism was not directly associated with prevention of infection, it was linked to reduced severity of symptoms and viral shedding, and thus attenuating disease in humans.

Antibody-dependent cellular phagocytosis (ADCP) activity (**Figure 1.4A**) in healthy human serum, mediated by monocytes/macrophages, was shown to correlate with HAI titer both for circulating and non-circulating strains of influenza (*66*). Interestingly, ADCP activity was still detectable in diluted serum samples, even at dilutions where neutralization was no longer detectable (*66*), indicating that phagocytic antibodies may mediate antiviral clearance even at very low levels, and thus could still provide protection

or lessen the severity of disease. Along these lines, non-neutralizing protective mAbs in mice required alveolar macrophages to provide protection, which was partially dependent on the induction of a robust inflammatory response in the lung as shown by tissue histology and increased cytokine/chemokine production, and partially through direct phagocytosis (*58*). Additionally, broadly neutralizing HA-specific mAbs also exhibited enhanced protection in the presence of alveolar macrophages (*58*). This macrophage-mediated protection was dependent on interactions of the antibody with FcRs on the macrophage surface, as evidenced by experiments using FcR-binding null antibodies that failed to provide protection from infection (*58*). Together, these studies indicate that FcR-mediated macrophage activation reduces disease burden and protects mice from lethal influenza, and that healthy human serum has influenza-specific antibodies capable of inducing this function.

ANTIBODY-DEPENDENT NEUTROPHIL PHAGOCYTOSIS AND ACTIVATION

Neutrophils are among the first cell populations recruited to the site of infection and/or inflammation, and have been implicated in the protective response to influenza (*90*). Neutrophils are involved in the phagocytic clearance of both virions and infected cells, release immunostimulatory cytokines and chemokines to recruit additional immune cells, and form neutrophil extracellular traps (NETs) to capture and inactivate the virus (*91*). During influenza infection, neutrophils generate the chemokine CXCL12, required for efficient recruitment of cytotoxic $CD8^+$ T cells to the lung (*92*). However, beyond this indirect anti-viral role, human neutrophils express high levels of FCGR1A, FCGR2A, and FCGR3B after activation, enabling them to respond rapidly and efficiently to antibody coated targets (*67*). In addition, neutrophils constitutively express the FcαRI, an activating

receptor that binds IgA and activates cytotoxic and phagocytic responses via a shared FcR γ-chain (*93*).

Like macrophages, neutrophils are intimately involved in the phagocytic clearance of infected and apoptotic cells in the lung during influenza infection (**Figure 1.4B**) (*89*). Impaired neutrophil phagocytosis through depletion of neutrophils was linked to decreased survival in a mouse model of influenza infection (*89*, *94*). Following phagocytosis, neutrophils form phagolysosomes containing reactive oxygen species (ROS) to eliminate the virus (*91*). Both HA head- and stalk-specific mAbs induced the production of ROS by neutrophils *in vitro* in an FcR-dependent manner, as Fc-blockade resulted in reduced ROS production (*56*). Influenza-specific class-switched IgA antibodies were also implicated in neutrophil activation and ROS production (*56*). However, despite the ability of some antibodies to recruit neutrophil activity *in vitro*, the role of neutrophils in protection from infection remains controversial, as some animal studies using neutrophil depletions found no significant roles for neutrophils in protection mediated by passively transferred non-neutralizing mAbs (*58*), arguing that alveolar macrophages may play a more dominant role in protection. Conversely, in other studies, neutrophil recruitment and function was linked to protection from infection and reduction in disease (*94*, *95*). Thus, additional studies will be required to ultimately define the role of neutrophils in influenza infection.

ANTIBODY-DEPENDENT COMPLEMENT ACTIVATION

The complement system can recognize and eliminate viruses directly or can contribute to viral clearance via antibody mediated activation (**Figure 1.4C**) (*61*). The requirement for complement in protection from lethal influenza infection in mice was established in 1978 and has been more recently replicated with novel influenza strains (*54*, *96*). Recently, influenza virions were shown to be susceptible to both classical and

alternative complement–mediated lysis *in vitro* only when opsonized by antibodies (*55*). However, the level of susceptibility varied by strain. Synergy between the classical and alternative complement pathways was shown to provide protection against pandemic H1N1 strains in mice and the cooperativity of both pathways is associated with enhanced viral clearance, further supporting the involvement of antibody-mediated complement elimination in the influenza immune response (*55*). In these experiments, C3 knockout mice (deficient in all complement pathways because C3 is the central point of the cascade), C4 knockout mice (deficient in the classical and lectin pathways) and complement factor B (FB) knockout mice (deficient in the alternative pathway) were infected with influenza and disease progression was compared. While both C4- and FB-deficient mice showed increased mortality, neither pathway alone nor the additive mortality approached the level of mortality in C3 knockout mice, which have both pathways of complement ablated, indicating that the two complement pathways work synergistically to clear infection (*55*).

Beyond antibody driven virion elimination, the complement protein C3 has also been shown to promote higher titers of influenza-specific IgG antibodies, as well as improve CD4+ and CD8+ T cell responses, in mouse models of influenza infection (*61*). Following vaccination, C3 knockout mice showed dampened antibody titers and increased mortality when compared to wild type mice. The role of complement in driving immunity was proposed to be effectuated by the formation of pro-inflammatory complement degradation products C5a and C3a, which can serve a dual role of directly recruiting T cells and enhancing T cell priming by recruiting and subsequently stimulating antigen-presenting cells at the site of infection (*61*).

In humans, neutralization and complement-dependent lysis activities by influenza-specific mAbs have not always correlated, although stalk-specific neutralizing antibodies

can induce complement-dependent lysis (*97*). Both IgG1 and IgM antibodies have been implicated in the activation of the complement system in influenza infection (*55*). Complement-stimulating antibodies correlated with protection from infection in children in a serosurveillance study of seasonal influenza (*81*), which was potentially attributable to the complement-stimulating antibodies' generally higher cross-reactivity as compared to neutralizing antibodies (*59*). Importantly, if complement-inducing antibodies do in fact generally possess higher cross-reactivity as compared to neutralizing antibodies, complement lysis of virus is an attractive strategy for limiting initial infection with influenza by non-neutralizing antibodies thus broadening the epitopes that can be targeted by vaccination.

Additional functions via non-classical FcR

The neonatal Fc receptor, FcRn, is involved in transcytosing IgG across the placenta during fetal development, across the vascular endothelium to increase extravascular antibody levels, and across the mucosal epithelium to provide humoral defense within the mucosa (*98*). Additionally, FcRn has a non-canonical role in antiviral immunity against influenza. FcRn was implicated in facilitating antibody-mediated neutralization of influenza virions by HA head-specific antibodies that bind to the virus at acidic pH (**Figure 1.4E**) (*99*). These unusual head-specific antibodies were then shown to neutralize the virus by preventing trafficking of the viral ribonucleoproteins into the nucleus for replication (*99*).

Systems level analyses aimed at defining biomarkers of productive immunity of influenza vaccination pointed to pre-existing antibody titers as a negative predictor of response to vaccination (*100*), thought to act by capturing, destroying, and preventing response to vaccine antigens (original antigenic sin) (*25*). However, recent dissections of

vaccine-induced immunity suggested that pre-existing antibodies shape the immune response to influenza vaccination in ways that could be utilized to improve protection. It was observed that individuals with the most influenza-specific antibody affinity maturation had significant changes in antibody glycosylation, namely increased sialic acid (*101*). This led to a mechanism through which pre-existing cross-reactive influenza antibodies, which opsonize incoming vaccine antigen, drove the delivery of immune complexes to germinal centers of lymph nodes by subcapsular sinus macrophages or non-cognate B cells, preferentially when antibodies were sialylated (*102*, *103*). This delivery relied on interaction of immune complexes with the non-canonical IgG Fc-receptor, CD23, to capture antigen and move it to germinal center (*101*). This delivery of antigen to lymph nodes was speculated to increase and extend the contact between B cells and antigens of interest to drive affinity maturation, which can increase both the affinity and potential evolution of neutralization (*104*, *105*). Broadly cross-reactive neutralizing mAbs specific to influenza HA were shown to be highly affinity matured, indicating that this pathway may be essential for the development of broad humoral immunity (*106*).

Similar effects of glycosylation on shaping humoral immunity have also been observed in HIV infection, where broadly neutralizing antibodies (bNAbs), the most protective antibodies, undergo extensive somatic hypermutation and affinity maturation during their development (*107*). Conversely, while CD23 contributed negligibly to immune complex capture in this HIV model, complement-mediated capture of sialylated immune complexes appeared to be vital in driving antigen-deposition in germinal centers and in driving affinity maturation (*108*). Given the known role of complement in antigen-capture by FDCs, its role in prolonging the presentation of antigen on the surface of FDCs, as well as in increasing antigen recycling, it is likely that pre-existing sialylated antibodies can

selectively adjuvant immunity. In addition to trapping and delivery, these sialylated Fcs were also shown to increase B cell inhibitory FcR, FCGR2B, expression, resulting in elevated thresholds required to activate B cells during development in the germinal center (*109*). With elevated activation thresholds, B cells require higher affinity interactions or an ability to capture more antigen to become fully activated within the germinal center and may then experience more aggressive somatic hypermutation and subsequent affinity maturation. Because sialylated immune complexes bind to non-cognate B cells at high levels in the presence of both complement (*108*) and CD23 (*109*), it is possible that CD23- and complement-induced affinity maturation work synergistically to increase affinity maturation. This may offer a novel approach for the design of next generation vaccines able to leverage the potent immunomodulatory activity of the Fc-domain of antibodies.

Together, these recent data suggest that the quality of the antibody response may not only influence direct antiviral activity but may also be critical in influencing the response to a given vaccine, offering novel vaccination targets to improve universal immunity to influenza. Seasonal influenza infection in humans has been shown to induce moderate antibody cross-reactivity (*110*), and these pre-existing cross-reactive antibodies may be molding the affinity maturation of new antibodies following vaccination through mechanisms that increase somatic hypermutation, including increased antigen retention within germinal centers (*101*). Harnessing, increasing, and improving this pathway presents a novel method of improving the breadth and binding affinity of antibodies following influenza vaccination.

CONTROL OF FCR-MEDIATED FUNCTIONS BY ANTIBODY PROPERTIES

SUBCLASS AND ISOTYPE VARIATION

The functional potency of an antibody is significantly affected by the antibody's subclass, which determines the binding affinity of the antibody for FcRs (*111*). Antibody function is tuned at the time of B cell programming via class switch recombination (IgA, IgM, IgG, IgD or IgE; **Figure 1.5**). Because each isotype can interact with a distinct family of FcRs present on different innate immune cells within disparate compartments, each isotype has the capacity to drive unique antibody effector functions. Beyond the isotypes, there is additional capacity to select for subclasses of particular antibody isotypes. In humans, four IgG subclasses can be additionally selected during an immune response, each of which have further differential affinities for individual FcRs (*67*). IgG1 antibodies are the most prevalent at approximately 65% of total serum IgG, with the other three subclasses in decreasing fractions in numerical order (*112*). Because individual subclasses have different affinities for FcRs (*67*), subclasses drive different antibody effector functions. IgG1 and IgG3 are considered to be the most functional subclasses due to their enhanced ability to bind to FcRs, while IgG2 and IgG4 have lower affinities for FcRs (*65*, *113*). However, IgG3 has a shorter half-life, related to decreased binding affinity to FcRn and due to a proteolytically vulnerable hinge, although multiple allotypes of IgG3 with longer half-lives have been reported among non-Caucasian populations (*114*).

The relative magnitude and distribution of IgG subclass responses vary between acute influenza infection and vaccination. In adults and children previously exposed to natural infection, vaccination increased IgG3 production more than acute infection. However, this boost resulting from vaccination was not observed in those who were previously vaccinated (*115*). Interestingly, IgG3 levels following seasonal influenza vaccination correlated with cytokine production by peripheral blood mononuclear cells (PBMCs) stimulated *ex vivo* with infectious influenza virus, suggesting that enhanced IgG3

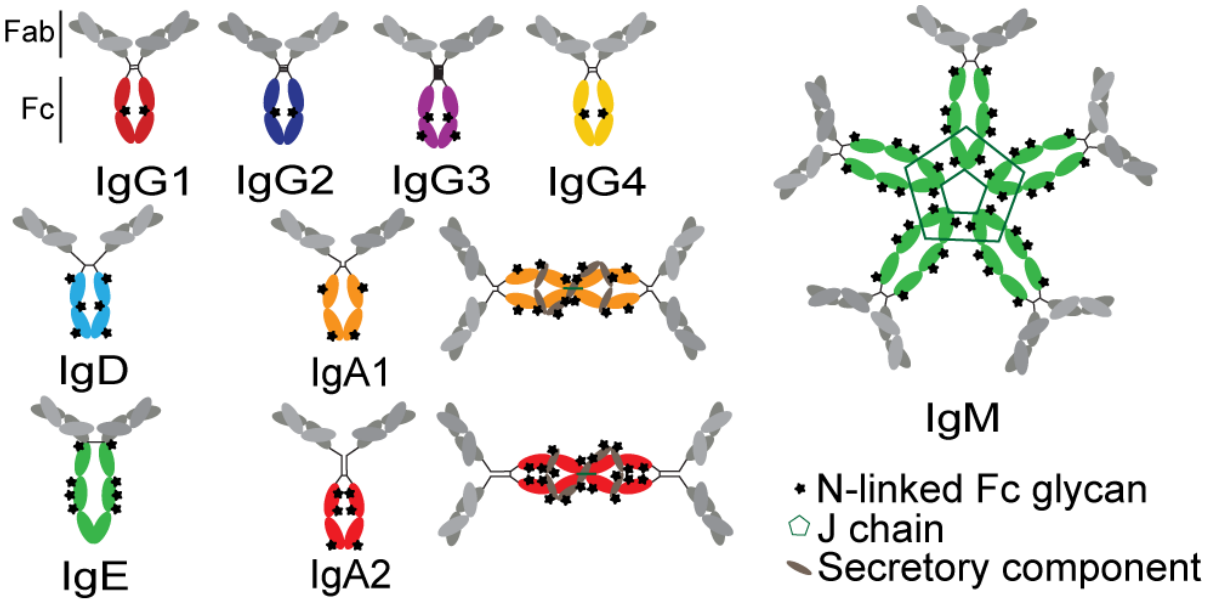

Figure 1.5 Structures of antibody isotypes and subclasses. Fc domains are in color while Fab domains are in grey. Stars indicate N-linked Fc glycans. IgA isotypes are shown as both monomers (predominant in serum) and dimers (predominant at mucosal surfaces).

responses were a marker of a more effective response to vaccination (*112*). While IgG3 is widely considered to be the most functional subclass due to its affinity for FcRs, the specific role of IgG3 in protection from influenza remains largely unclear.

While IgG is typically induced at higher levels in the blood, IgA antibodies are produced at considerable levels in mucosal tissues (*116*). Secreted IgA represents ~70% of the body's total antibody production and, in mucosa, is primarily dimeric, with only small fractions of monomer, trimer, and tetrameric IgA present; IgA in serum is primarily monomeric (*117*). Mucosal IgA can prevent influenza infection in the nasal and upper respiratory mucosa with higher heterologous neutralization than IgG with the same Fab (*116*, *118–120*). The protective activity of IgAs was linked to direct viral neutralization as well as viral capture and cross-linking to the mucosal surface, preventing cell entry in the absence of classical neutralization (*116*). However, beyond its direct antiviral effects, IgA may also recruit the indirect activity of the innate immune system, via the Fc-receptor for

IgA, FcαRI, which is constitutively expressed on neutrophils and increases in expression as neutrophils mature (*93*). Stimulation of this receptor by influenza-specific IgA was linked to increased ROS production (*56*), although the precise effect of this activation during influenza infection is unclear.

ANTIBODY FC GLYCOSYLATION

Beyond isotype and subclass selection, the humoral immune response additionally modifies antibodies via post-translational modifications in the form of Fc-glycosylation, further tuning antibody affinity for FcRs, and thus modulating antibody effector function (*121*). Each IgG molecule contains two N-glycosylation sites, at asparagine 297 (N297), one on each heavy chain (**Figure 1.6**). The core Fc glycan structure is biantennary, with a structure consisting of two-branched linked N-acetylglucosamine (GlcNAc), a mannose, followed by 2 branched mannoses, each followed by an additional GlcNAc on each mannose

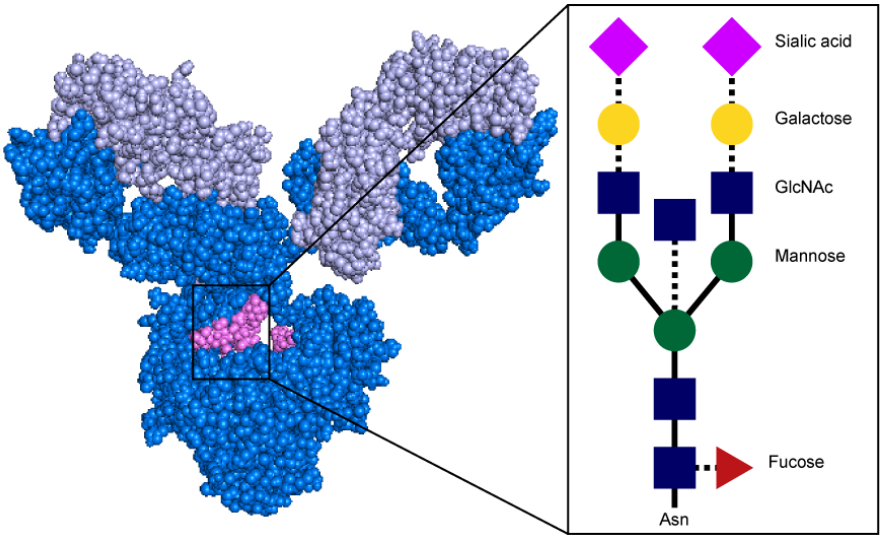

Figure 1.6 Structure of antibody glycan. Antibody image shows heavy chain in dark blue, light chain in light blue, and glycan in magenta. In glycan schematic, solid lines indicate core glycan consisting of two-branched linked N-acetylglucosamine (GlcNAc; blue rectangle), a mannose (green circle), followed by 2 branched mannoses, each followed by an additional GlcNAc on each mannose. Dotted lines indicate additional sugars that can be added at variable levels, including a core fucose on the first GlcNAc (red triangle), galactoses (yellow circle) to each terminal GlcNAc, sialic acids (pink diamond) to each galactose, and a bisecting GlcNAc to the core mannose. Antibody structure: PDB 1IGY.

(**Figure 1.6**). Three additional sugars can then be added at variable levels, including a core fucose on the first GlcNAc, galactoses that can be added to each terminal GlcNAc, sialic acids that can subsequently be added to the each galactose, and finally the addition of a bisecting GlcNAc to the core mannose (**Figure 1.6**) (*122*). Given the variable addition of each of the 4 additional sugars, a total of 36 distinct glycan structures can be added to any given IgG (*123*). Importantly, while the glycans themselves do not interact directly with FcRs, they influence the flexibility and structure of the antibody Fc, thereby changing interactions with FcRs (*124*). Complete removal of the Fc glycan nearly completely ablates low affinity FcR binding, with only high affinity FCGR1A retaining measurable binding ability, highlighting the importance of the glycan in shaping antibody function (*125*). Additionally, IgA and IgM antibodies are also Fc-glycosylated (**Figure 1.5**), although it is unclear how this glycosylation changes affinity for FcRs.

Across diseases, dramatic shifts have been identified in IgG glycosylation, such as a significant increase in agalactosylated antibodies in chronic inflammatory diseases such as autoimmune flares and HIV infection (*126*, *127*). In the monoclonal therapeutics field, the systematic removal of specific components of the Fc N-glycan have highlighted the critical role of individual sugars in shaping antibody effector function (*128*). Specifically, the presence of sialylation drives anti-inflammatory activity *in vivo* (*129*, *130*). The removal of fucose either directly or indirectly, through the upregulation of the bisecting GlcNAc, results in increased antibody affinity for FCGR3A and consequently enhanced ADCC (*121*, *131*). Conversely, agalactosylated antibodies decrease ADCC and drive pro-inflammatory responses (*121*).

Beyond our emerging appreciation for a role of sialylated antibodies in vaccine induced affinity maturation (*101*, *108*), influenza vaccination is known to alter Fc

glycosylation (*132*, *133*). Soon after immunization, influenza-specific antibodies rose rapidly, and had increased galactosylation, increased sialylation, and reduced bisection compared to pre-existing influenza-specific antibodies (*132*, *133*). However, these glycan shifts normalized after a month, suggesting that these transient changes in influenza-specific antibody glycan profiles may reflect differences in glycosylation by plasmablasts, not plasma cells. Even in the absence of vaccination, HA-specific antibodies exhibited unique glycan profiles compared to HIV-specific antibodies from the same individuals. Specifically, HA-specific antibodies were more highly galactosylated and sialylated and contained reduced b-GlcNAc (*132*), highlighting the unique glycan profiles that are naturally selected on influenza-specific antibodies. Whether individuals who control the virus more effectively tune antibody glycosylation in a specific or selective manner is unclear but represents a simple strategy to naturally modulate antibody function.

OPTIMIZING ANTIBODY RESPONSES THROUGH VACCINATION

ADJUVANTS

One of the greatest hurdles of influenza vaccination is overcoming response anergy caused by previous exposures to influenza in the aging immune system. An attractive strategy to overcome this anergy and generate protective humoral immunity, particularly for novel strains or universal vaccine formulations, is the use of adjuvants to enhance and tune the response to vaccination. There are currently four adjuvants licensed for use in influenza vaccines in the United States and/or in Europe: aluminum salts (alum), MF59, AS03, and virosomes (*134*). In addition to adsorbing antigens and creating multivalent lattices of antigens, alum activates the inflammasome promoting more effective responses upon antigen-presenting cell delivery (*135*). Alum induces primarily a Th2-driven response

(*134*). Conversely, Th1 responses are likely to be more critical in the clearance of intracellular pathogens, including influenza (*135*). Oil-in-water emulsions, such as MF59 and AS03, are predicted induce a more balanced Th1/Th2 response, enhancing both T cell and antibody responses via delivery to antigen presenting cells as well as through the recruitment of specific innate immune cells to the site of injection (*136*). Specifically, in an adjuvanted HIV vaccine trial in macaques, MF59 increased recruitment of neutrophils, monocytes, and MDCs to the site of injection and recruitment of neutrophils to the draining lymph node (*137*). In the context of influenza vaccination, MF59 increased a heterosubtypic, or broadly reactive, antibody response and increased neutralizing antibody responses to influenza (*138*, *139*). Unfortunately, MF59 also shifted the response even further towards the immunodominant HA head and away from the HA stem (*140*). Yet, MF59 increased the affinity of antibodies developed following both seasonal and novel pandemic influenza vaccines, suggesting that if skewed selectively to particular target antigenic sites, this adjuvant could drive enhanced affinity maturation to the correct sites of vulnerability (*140*). Virosomes, or phospholipid vesicles, have also been studied in the context of influenza HA and NA vaccines, showing similar profiles to MF59 (*134*). The effects of these adjuvants on FcR-mediated antibody functionality are only beginning to be studied (*137*).

Other adjuvants are currently under investigation to specifically and selectively enhance influenza specific immunity. For example, liposomes provide unique scaffolds for antigen delivery (*135*), and were shown to increase the humoral and Th1 response, boosting neutralization titers in mice following influenza vaccination (*134*). Additionally, virus-like particles, or nanoparticles, which deliver antigens in a multivalent manner, similar to their native conformation, increased heterosubtypic IgG2a neutralizing antibody titers in mice, the mouse analogue of IgG3, the most functional antibody subclass in humans (*63*).

Presentation of antigens in the form of a viral particle may play an essential role in driving functional antibody responses(*141–143*). Another type of adjuvant, ISCOMS (antigen, cholesterol, phospholipid and saponin-defined immunomodulatory complexes), created a balanced, protective immune response based on strong MHC class I presentation in trials with a pandemic influenza antigen (*134*). However, ISCOMS have been shown in other models to shift the response away from antibodies, and towards a cellular immune response comprising CD4+ and CD8+ T cells, with limited changes seen to antibody responses (*144*). Finally, Toll-like receptor (TLR) agonists, involved in early pathogen sensing, are known to tune the inflammatory response to tailor immunity in a pathogen specific manner (*134*). Several TLR agonists were shown to increase influenza-specific antibody titers following vaccination, however their effects on antibody-mediated functions beyond neutralization are unexplored (*134*, *145*). While previous studies with these adjuvants have primarily focused on neutralizing antibody responses, additional insights on the specific effects of adjuvants on shaping protective FcR activity will provide additional avenues to tune and direct protective immunity against influenza infection.

Antigen Design And Glycosylation

In addition to efforts to promote more effective immune stimulation through adjuvants, intense investigation is focused on the development and design of unique antigens able to selectively direct the immune response away from strain-specific immunodominant sites to those that are more conserved (*34*). These include the design of computationally enhanced globally relevant HA sequences, the design of mini-antigens, chimeric antigens, and glycan-enhanced antigens.

Computationally optimized broadly reactive antigens (COBRAs) are mosaic antigens designed based on computational modeling of influenza strains with the aim of focusing the

immune response on the evolution of heterosubtypic responses, and have had some success in eliciting broadly reactive HAI titers that target both seasonal and pandemic strains of influenza (*146–149*). In a recent study, COBRA H3s did not increase the breadth of HAI reactivity by vaccine-induced antibodies across a panel of strains. However, these COBRA H3s did increase the phylogenetic diversity of neutralized strains (*149*), meaning that the COBRA-induced responses altered which strains were recognized and neutralized without increasing the total number of strains recognized, providing evidence that this approach can successfully skew the immune response. COBRA antigens primarily increase receptor binding site targeting to create heterosubtypic neutralizing antibodies (*149*). These data suggest that COBRA antigens can increase heterosubtypic responses to conserved epitopes on the immunodominant head but are unable to create broadly reactive responses to the conserved HA stem.

Given the complexity of altering immunodominance using whole HA molecules, additional efforts have aimed to direct immunity against minimal antigenic regions associated with broadly protective responses including the stem (*150*, *151*) and the receptor binding site (*152*). Although broadly protective non-neutralizing responses can target the stem region of HA, these responses are typically subdominant (*153*). HA stem-only antigens or antigens with conserved stem domains but altered HA heads have been developed (*34*). For example, a "headless" HA vaccine tested in mice created a broadly protective non-neutralizing immune response (*154*). Furthermore, chimeric HA vaccines, which were used to immunize animals with "exotic" chimeric molecules that coupled unusual heads to a single stem region, have shown promise. Specifically, a vaccine strategy using heads that have not circulated in the population, coupled with conserved stem regions drove a robust

focused, stem-specific protective immune responses with higher cross-reactive HA-specific antibody titers, and are now being tested in clinical trials (*155*, *156*).

Seasonal influenza vaccines have been produced in eggs since the introduction of yearly vaccination, and the manufacturing techniques have remained largely unchanged for decades (*157*). Emerging data and technical advances are increasing the attractiveness of cell culture-based production strategies, rather than egg-based production. Beyond issues related to speed and cost of vaccine production across these platforms, qualitative differences in antigens from egg-based vaccines compared to circulating viruses may necessitate this shift. HA is highly N-glycosylated in a host-cell dependent manner (*158–160*). The glycosylation of egg-grown vaccine virus is different than that of naturally infecting virus (*161*). Emerging data points to the importance of glycosylation not only in shaping antigen-exposure on the surface of the HA molecule, such as the masking of specific epitopes (*160*, *162*), but also in contributing to the antigenicity of antibody binding epitopes (*22*, *163*, *164*). Differential HA glycosylation between egg- and cell culture-grown virus impacted innate immune interactions with the virus in the lung, including neutralization by surfactant protein D (SP-D) (*165*) and binding to mannose-specific lectins (*166*). Moreover, altered glycosylation was shown to change both cellular and humoral response kinetics *in vitro* and *in vivo* (*160*, *167*). These changes included significantly decreased CD4+ T cell activation and cytokine production, resulting in reduced HA-specific antibody titers and HAI titers in mice following vaccination with de-glycosylated HA (*160*, *167*). Studies of the antibody response using differentially glycosylated (not de-glycosylated) HAs showed that glycosylation alters the binding and neutralization of monoclonal antibodies, but lacked further detail about the effects of glycosylation on polyclonal antibody pools or on Fc-mediated function (*160*, *167*, *168*).

Epidemiological studies in recent years investigating poor vaccine protective efficacy have shown that antigen glycosylation has had a direct impact. In the 2016-2017 flu season, the circulating H3N2 virus had a new glycosylation site compared to previous seasons. However, the egg-adapted version of the viral strain used to produce the vaccine lacked this site through an amino acid mismatch in an antigenic site, resulting in decreased vaccine effectiveness (*22*). Given that glycosylation can strongly impact epitope antigenicity, a vital mismatch at a site of neutralization sensitivity resulted in the induction of non-protective immunity and rendered the circulating virus invisible to vaccine induced immune responses. Thus, shaping glycosylation to produce representative antigens is critical to achieving protective immune responses to vaccination.

ADDITIONAL ANTIGENIC TARGETS

While the majority of the humoral immune response is directed towards the immunodominant HA molecule, antibodies also emerge against other targets including NA, NP, and M2 (**Figure 1.1**). Antibodies targeting NA can be neutralizing (*4*), and have been associated with seasonal protection (*4*, *43*, *45*, *169*). Specifically, NA-specific antibodies can inhibit NA enzymatic activity, thereby neutralizing the virus. Additionally, NA-specific antibodies have also been shown to drive ADCC (*82*, *170*), suggesting that this less immunodominant target is still vulnerable to multiple modes of antibody mediated targeting.

The highly conserved internal viral proteins NP and M2 have been shown to induce an immune response that is also broadly reactive (*171*). NP-specific antibodies, which are always non-neutralizing (*172*), mediated viral clearance through interaction with FcRs and protection in mouse models of influenza infection (*43*, *173*). Similarly, non-neutralizing M2-specific antibodies mediated ADCC and ADCP to clear infected cells and promoted rapid

viral clearance (*45*, *169*). Thus, while current vaccination strategies largely focus on the development of broadly reactive immunity against HA, additional largely non-neutralizing conserved antigens exist within influenza that may represent next generation targets for protective universal immunity.

MURINE MODELS IN INFLUENZA AND INNATE IMMUNE ANTIBODY FUNCTIONALITY

MURINE MODELS IN INFLUENZA

Mice and ferrets are the two most commonly used model species in influenza research, although hamsters, guinea pigs, cotton rats, and rats have also been used. While ferrets are preferred for their similar symptomatic course to humans, mice are often the model of choice due to their availability, relatively low cost, well-characterized genetic backgrounds, and availability of relevant reagents (*174*). Human influenza viruses typically only cause disease in mice following adaptation to the species, and then cause symptoms including weight loss and mortality, but mice do not exhibit respiratory symptoms like humans (*175*). Mouse models are also difficult to use for transmission studies, with poor transmissibility of most influenza viruses between individuals (*175*). However, mice have been widely used in studies of the immune responses to both influenza infection and vaccination (*175*), with many preclinical vaccine candidates validated and immunological principles described in mice but await confirmation in humans (*176*). While mice provide a useful and convenient model system for understanding and testing mechanisms of protection, it is essential to keep in mind the differences between murine and human immune systems and influenza pathogenesis.

ANTIBODY ISOTYPE AND FCγR DIFFERENCES IN MICE AND HUMANS

In contrast to the IgG1, IgG2, IgG3, and IgG4 subclasses in humans, mice express the subclasses IgG1, IgG2a, IgG2b, and IgG3. Of the murine subclasses, mIgG2a is the most effective at binding FCγR (*63*). Mice have FCγRs 1, 2B, 3, and 4. mFCGR1 has a limited expression profile, on only monocyte-derived DCs (*177*). mFCGR2B plays a similar role to hFCGR2B but has a wider cellular expression profile (*63*). mFCGR3 is expressed as the only FCγR on NK cells, and has a dual activating/inhibitory role in modulating the threshold of activation depending on whether the binding of IgG is monomeric (inhibitory) or multimeric (activating) (*178*). mFCGR4 is responsible for the most potent ADCC in mice, which is primarily mediated by monocytes/macrophages (*179*). Mouse FCγRs and FcRn effectively bind human IgG subclasses (*179*), but the opposite is not true and human FCγRs and FcRn do not bind or poorly bind mouse IgG subclasses (*63*). Human IgG1 antibodies can potently induce ADCC on both mouse and human cells, binding to mFCGR1, mFCGR3, and mFCGR4 on monocytes, mFCGR3 on NK cells, and also mFCGR3 and mFCGR4 on neutrophils in a target-dependent manner (*179*). While mice are a useful and necessary tool in understanding the immunology of the humoral immune response, these nuances between mouse and human FCγR must be considered when designing and interpreting experiments.

CONCLUDING REMARKS

More than 4 decades of research has clearly illustrated the importance of both direct neutralization and non-neutralizing functional antibodies in protection against influenza infection and disease. Because neutralizing and non-neutralizing antibody activities are not induced in a mutually exclusive manner, vaccine strategies able to leverage both functions of antibodies are likely to confer the greatest level of protection. However, the precise innate immune effector functions to sites of viral vulnerability remain to be determined.

Thus, with emerging novel vaccine design strategies, coupled to emerging immune modulatory adjuvants, opportunities to drive universal protection are on the horizon.

Chapter 2: SELECTIVE INDUCTION OF ANTIBODY EFFECTOR FUNCTIONAL RESPONSES USING MF59-ADJUVANTED VACCINATION

Based on a published manuscript:

Boudreau, C.M., Yu, W.-H., Suscovich, T.J., Keipp Talbot, H., Edwards, K.M. & Alter G. (2019) Selective induction of antibody effector functional responses using MF59-adjuvanted vaccination. *JCI, 130(2).* doi: 10.1016/j.cell.2019.05.044

Author contributions: CMB, TS, and GA designed the research study. CMB conducted the experiments and acquired data. CMB and WHY analyzed data. HKT and KE provided study samples. CMB, TS, and GA wrote the manuscript. All authors contributed to the final version of the manuscript.

Seasonal and pandemic influenza infection remains a major public health concern worldwide. Driving robust humoral immunity in the face of pre-existing, often cross-reactive, immunity and particularly poorly immunogenic avian antigens has been a challenge. To overcome immune barriers, the adjuvant MF59 has been used in seasonal influenza vaccines to increase antibody titers and improve neutralizing activity, translating to a moderate increase in protection in vulnerable populations. However, its impact on stimulating antibody effector functions, including NK cell activation, monocyte phagocytosis, and complement activity, all of which have been implicated in protection against influenza, have yet to be defined. Using systems serology, changes in antibody functional profiles were assessed in individuals who received H5N1 avian influenza vaccine administered with MF59, with alum, or delivered unadjuvanted. MF59 elicited antibody responses that stimulated robust phagocytosis and complement activity. Conversely,

vaccination with MF59 recruited NK cells poorly and drove moderate monocyte phagocytic activity, both likely compromised due to the induction of antibodies that did not bind FCGR3A. Collectively, defining the humoral antibody functions induced by distinct adjuvants may provide a path to design next generation vaccines able to selectively leverage the humoral immune functions, beyond binding and neutralization, resulting in better protection from infection.

INTRODUCTION

Seasonal influenza infects 10-20% of the worldwide population each year, with a mortality rate of 0.1-0.2%, and increased mortality in the elderly (*180*, *181*). By contrast, avian influenza viruses that are endemic to global fowl populations, such as H5N1, infect significantly fewer humans per year but have a much higher mortality rate (approximately 60% for H5N1) (*182*). While these avian viruses cannot effectively spread from human to human, it has been suggested that we are on the precipice of highly lethal avian influenza viruses evolving to allow human-to-human transmission (*183*). This could result in the rapid global spread of the virus, causing the next influenza pandemic (*182*, *184*). To mitigate this concern, pandemic influenza vaccines are urgently needed. These vaccines will need to provide rapid and robust protection against the potential threat of an avian influenza pandemic. Current influenza vaccine design strategies, in the best-case scenario, require 5-6 months from determining the viral sequence to full-scale vaccine production, time that is not available during a pandemic. In addition, vaccine strategies that induce equivalent immunity using less antigen, termed antigen sparing, are needed to expand the quantity of vaccine available for the global population.

Adjuvants have the potential to not only decrease antigen quantity requirements but also to improve vaccine effectiveness by enhancing antigen delivery to antigen-presenting cells and by shaping the functional potency of the vaccine induced immune response(*185*). Currently, six adjuvants have been approved for use in licensed human vaccines, and of these, four have been assessed for use in influenza vaccines (*134*). Among these, MF59 is an oil-in-water emulsion licensed for use in seasonal influenza vaccines (*186*). In seasonal influenza vaccination, MF59 is known to induce monocyte and granulocyte chemoattractants (*187*), to alter the antibody-mediated immune response by inducing heterotypic antibody responses, increasing the breadth and affinity of the vaccine-induced antibodies, and to increase neutralizing antibody responses (*139*, *140*, *184*). Furthermore, MF59 also exhibits antigen sparing activity, driving robust neutralizing antibody responses at 3-fold lower doses of H5 antigen (*139*). However, despite its potent immunological effects, the addition of MF59 does not consistently afford equally potent enhanced protection from seasonal influenza infection to the level that would be predicted by the increased antibody responses (*188*, *189*). These data raise the possibility that while MF59 is able to drive enhanced vaccine-induced immunity, it may fail to raise a key humoral immune function required to achieve protection.

While the development of broadly neutralizing antibody responses against influenza remains a critical goal, emerging evidence suggests extra-neutralizing antibody functions also play an important role in protection from infection (*38–40*, *53–59*). Studies with passive transfer of neutralizing monoclonal antibodies in mice show that Fcγ receptors are required for protection from lethal infection, via mechanisms that do not block viral entry (*38*). In addition to binding pathogens and preventing infection of cells, antibodies mediate an array of functions, including complement activation and lysis; phagocytosis by

granulocytes, monocytes, and dendritic cells; NK cell activation; and dendritic cell maturation and antigen presentation (*190–192*). Influenza-specific antibodies have been shown to mediate macrophage phagocytosis (*56*, *60*), neutrophil production of reactive oxygen species (*56*), cellular cytotoxicity (*57*), and complement deposition (*54*, *55*, *60*, *61*). However, data using broadly neutralizing monoclonal antibodies suggest that NK cell driven antibody dependent cellular cytotoxicity (ADCC) may represent a key protective function against influenza (*38*, *39*, *79*).

While previous studies have demonstrated that MF59 can increase the breadth of the heterosubtypic immune responses and neutralizing titers, the goal of this study was to systematically probe the functional impact of MF59 induced immunity when administered in a potential pandemic avian influenza vaccine. Using an unbiased, high-throughput systems serology platform (*193*), we observed increased antigen-specific antibody functionality in serum of individuals who received MF59 adjuvanted vaccinations, with the notable exception of titer-dependent increases in NK cell activation or monocyte phagocytic activity, highlighting the robust induction of humoral immune responses programmed to induce selective antibody effector functions.

METHODS

Vaccine Schedule and Sample Collection

Samples were collected under NIAID-funded Vaccine and Treatment Evaluation Unit (VTEUs), ClinicalTrials.gov Identifier: NCT00280033. The results of this trial have been published previously (*139*). After informed consent, H5N1-naïve adult study participants (ages 18-64) were randomly assigned to receive 15µg of recombinant H5 A/Vietnam/1203/2004 antigen without adjuvant, with alum, or with MF59 in two doses administered 28 days apart. Samples from 90 individuals (30 without adjuvant, 29 with

alum, 31 with MF59) at four timepoints (0, 28, 56, and 208 days following the initial dose) were assayed.

Antibody-dependent cellular phagocytosis

THP-1 phagocytosis of HA-coated beads was performed as previously described(*194*). Briefly, H5 A/Vietnam/1203/2004 (Immune Technology Corp., New York, NY) or H1 A/New Caledonia/20/1999 (Immune Technology Corp.) was biotinylated with EZ-link NHS-LC-LC Biotin per manufacturer's instructions (Thermo Fisher Scientific, Waltham, MA). Biotinylated HA was adsorbed onto 1 μm fluorescent neutravidin beads at a ratio of 10μg of protein to 10μl of beads (Invitrogen, Carlsbad, CA). 10 μl of antigen-coated beads were then incubated with equal volume of serum samples diluted in PBS for 2 hours at 37°C in 96-well plates. Unbound antibody was washed away, and THP-1 cells (ATCC, Manassas, VA) added and incubated at 37°C for 16 hours, then fixed. Phagocytosis was measured by flow cytometry on a Becton Dickinson (BD, Franklin Lakes, NJ) LSRII cytometer with a high-throughput sampler. Phagocytic scores were calculated as the % of bead positive cells × geometric mean fluorescence intensity (GMFI)/1,000. Area under the curve was calculated using GraphPad Prism (San Diego, CA) based on three dilutions: 1:50, 1:500, and 1:5000. Each sample was assayed in two independent replicates performed on different days. Quality checks were performed to ensure that known positive samples were at least 2x higher than negative controls, and that replicate values correlated. Following quality checks, values from replicates were averaged.

Antibody-dependent neutrophil phagocytosis

HA-coated 1 μm fluorescent neutravidin beads were prepared and incubated with equal volume diluted serum samples as in the ADCP assay. For ADNP, optimal dilution

(1:50) was pre-determined by titration. Primary human leukocytes were isolated from healthy donors using Ammonium-Chloride Potassium (ACK) lysis, then added to the opsonized beads and incubated at 37°C for 1 hour. The cells were then stained with fluorescent anti-human CD66b (Biolegend Cat. No. 305112, San Diego, CA) and fixed prior to analysis on a BD LSRII cytometer with a high-throughput sampler. Phagocytic scores are calculated as the % of bead CD66+ positive cells × GMFI/1,000. Two healthy leukocyte donors were used to assay each sample in parallel. Quality checks were performed to ensure that known positive samples were at least 2x higher than negative controls, and that replicate values correlated. Following quality checks, values from replicates were averaged.

Antibody-dependent complement deposition

Serum samples were heat inactivated at 56°C for 30 minutes and centrifuged to remove aggregates. HA-coated 1 µm fluorescent neutravidin beads were prepared as in the ADCP assay and incubated with diluted, heat inactivated serum samples for 20 minutes at 37°C. Lyophilized guinea pig complement (Cedarlane, Burlington, Canada) was resuspended in ice cold water, then diluted 1:60 in veronal buffer with 0.1% gelatin added. 150µl diluted complement was added to the opsonized beads and incubated for 20 minutes at 37°C. Beads were then washed with 15 mM EDTA and stained with anti-guinea pig C3 (MP Biomedicals Cat. No. 855385, Santa Ana, CA). Samples were washed and analyzed on a BD LSRII cytometer with a high-throughput sampler. Complement scores are the % of C3-positive beads × GMFI/10,000. Area under the curve was calculated using GraphPad Prism based on three dilutions: 1:15, 1:30, and 1:60. Each sample was assayed in two independent replicates performed on different days. Quality checks were performed to ensure that known positive samples were at least 2x higher than negative controls, and

that replicate values correlated. Following quality checks, values from replicates were averaged.

Antibody-dependent NK Cell Activation

Antibody-dependent NK cell activation and degranulation were measured as previously described(*195*, *196*). ELISA plates (ThermoFisher NUNC MaxiSorp) were coated with H5 A/Vietnam/1203/2004, then blocked. Serum samples were then diluted 1:60 (dilution pre-determined by titration) and 100µl added to each well and incubated for 2 hours at 37°C. NK cells were isolated from buffy coats from healthy donors using the RosetteSep NK cell enrichment kit (STEMCELL Technologies, Vancouver, Canada) and rested in 1 ng/ml IL-15 at 37°C until needed. NK cells, with anti-CD107a PE-Cy5 (BD Cat. No. 555802), brefeldin A (Sigma-Aldrich, St. Louis, MO), and GolgiStop (BD), were added and incubated for 5 hours at 37°C. Cells were stained for surface markers using anti-CD56 PE-Cy7 (BD Cat. No. 557747), anti-CD16 APC-Cy7 (BD Cat. No. 557758), and anti-CD3 AF700 (BD Cat. No. 557943), then fixed and permeabilized using FIX & PERM® Cell Permeabilization Kit (ThermoFisher). Cells were stained for intracellular markers using anti-MIP1β PE (BD Cat. No. 550078) and anti-IFNγ APC (BD Cat. No 554702). Fixed cells were analyzed by flow cytometry on a BD LSRII equipped with a high-throughput sampler. NK cells were defined as CD3- and CD16/56+. Two healthy NK cell donors were used to assay each sample in parallel. Quality checks were performed to ensure that known positive samples were at least 2x higher than negative controls, and that replicate values correlated. Following quality checks, values from replicates were averaged.

Ig Subclassing/Isotyping and FcR binding

Antigen-specific antibody subclass/isotypes and FcR binding were determined using a high-throughput Luminex-based assay, which has been shown to correlate highly with more laborious SPR techniques (*197*). Antigens included were: H1 HA A/New Caledonia/20/99, H3 HA A/Brisbane/10/2007, H5 A/Vietnam/1203/2004, HA B/Florida/4/2006, EBV recombinant gH(D1-111)/gL/gp42 (Ectodomain) (Strain B95-8), all provided from Immune Technology Corp., and EBOV GPdTM from Mayflower Bioscience, St. Louis, MO. Antigens were coupled to carboxylate-modified microspheres (Luminex Corp., Austin, TX) by covalent NHS-ester linkages via EDC (ThermoFisher) and Sulfo-NHS (ThermoFisher) per manufacturer's instructions. These antigen-coated microspheres were added to non-binding 384-well plates (Grenier Bio-One, Kremsmunster, Austria) at 1000 beads per well (45µl). Serum samples were diluted 1:100 for IgG1, total IgG and all FcRs, and 1:10 for other antibody subclasses. 5µl of diluted serum samples were added and incubated with microspheres on a shaker for 2 hours at room temperature or overnight at 4°C. Sample dilutions were determined by assaying a dilution curve and selecting a dilution within the linear range of the assay. Microspheres were washed, and PE-conjugated anti-IgG1 (Cat. No. 9052-09), -IgG2 (Cat. No. 9060-09), -IgG3 (Cat. No. 9210-09), -IgG4 (Cat. No. 9200-09), -IgG (Cat. No. 9040-09), -IgM (Cat. No. 9020-09), -IgA1 (Cat. No. 9130-09), or -IgA2 (Cat. No. 9140-09) detection antibodies (all Southern Biotech, Birmingham, AL) or biotinylated FcRs (Duke University Protein Production Core) conjugated to streptavidin-PE (Prozyme, Hayward, CA) were added for 1 hour at room temperature. The microspheres were washed and read on a Bio-Plex 3D system (Luminex Corp.) or iQue Plus screener (Intellicyt, Albuquerque, NM). All samples were assayed in duplicate and values were averaged. Data were screened to ensure adequate bead counts (>20) per antigen per

sample, and values for sample/antigen pairs with inadequate counts were excluded from further analyses.

Statistics & Computational Analyses

For principal components analysis (PCA), data were normalized using Box-Cox transformation and z-scored. Missing values were imputed using k-nearest neighbor. PCA was performed to resolve differences between vaccination groups using all measured features as inputs using MATLAB (MathWorks, Natick, MA). To compare the difference between two groups (None v MF59 or Alum v MF59) of non-normally distributed PC1 values, Mann-Whitney U tests were calculated with GraphPad Prism.

For univariate analyses comparing multiple groups, ANOVA followed by Tukey's multiple comparison test was used with a p value of 0.05 considered significant. For correlations, Spearman's rank correlation coefficient was used with a p value of 0.05 considered significant.

Study Approval

Written informed consent was obtained before inclusion of subjects in the MF59 vaccine trial (*139*). The current work was approved by Massachusetts General Hospital Institutional Review Board approval #2015P000646.

RESULTS

MF59 INDUCES A UNIQUE FUNCTIONAL HUMORAL RESPONSE

Emerging data suggest that adjuvants may not only induce higher antibody titers and enhanced affinity maturation, but may also shape the Fc-profile of antibodies (*198*). To initially define whether adjuvants also shape influenza specific humoral immune responses, we applied a systems serology (*193*) approach to broadly and comprehensively profile the

functional and Fc-biophysical profiles of antibodies generated by vaccinees receiving pandemic influenza H5 immunization alone or adjuvanted with MF59 or alum. Using this suite of functional and biophysical assays, over 50 data points were collected per subject, encompassing the ability of antibodies to recruit NK cells, monocytes, neutrophils, and complement. In addition, differences in the subclass and isotype selection, and Fc γ receptor binding were analyzed across H5-specific immune responses. To determine whether induced profiles were any different at the peak response, 56 days following initial vaccination/28 days after 2nd dose, a principal components analysis was used to assess adjuvant effects (**Figure 2.1A**). While the alum-adjuvanted and unadjuvanted vaccine groups overlapped and were nearly indistinguishable, the majority of the MF59 group clearly separated, exhibiting a unique antibody Fc-profile. To further quantify the significance of the difference between MF59 and alum or unadjuvanted vaccines, scores along the first principal component (PC1) were analyzed (**Figure 2.1B**). As demonstrated in the PCA plot (**Figure 2.1A**), serum samples from individuals receiving MF59 exhibited a unique and separate response when compared to either the alum-adjuvanted or unadjuvanted groups. At baseline (day 0), the responses to H5 were indistinguishable from the other groups (**Figure 2.2**). These data suggest that, unlike alum, MF59 induces a significantly different functional humoral immune response compared to unadjuvanted vaccination (**Figure 2.1A**).

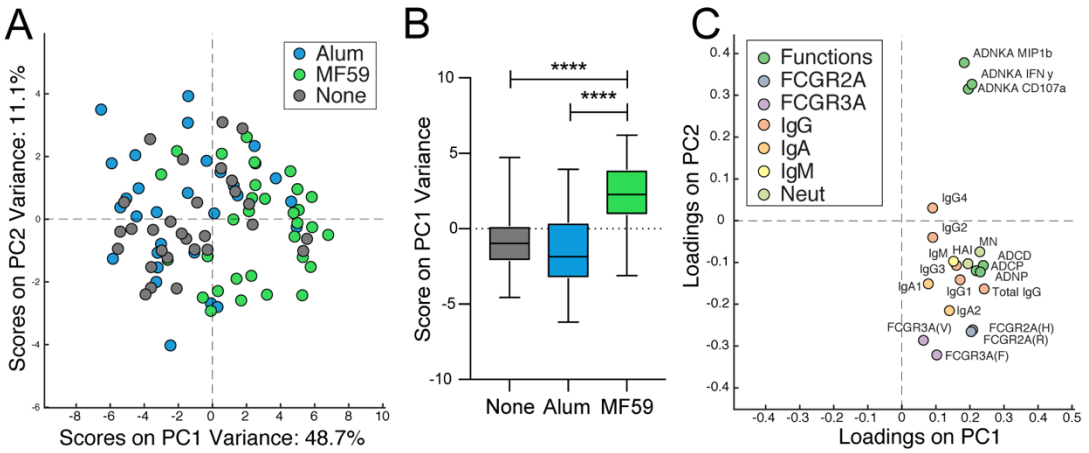

Figure 2.1 MF59 significantly alters the functional humoral profile following H5-vaccination. Antibodies against H5 were compared for 90 vaccinees who received 15µg recombinant H5 unadjuvanted (none), with alum, or with MF59. A principal components analysis (PCA) was used to identify differences in the functional responses of vaccinees by adjuvant. **A**. All H5-specific systems serology measurements (antibody isotypes, FCGR binding, and antibody-dependent functions) from post-vaccine day 56 samples were included in the PCA biplot, where dots represent individual samples (blue=alum, green=MF59, grey=none). **B**. Scores along the first principal component (PC1), which captures the greatest separation between samples, were plotted. Error bars show minimum to maximum. Differences were assessed using a Mann-Whitney U test. ****p<0.0001. **C.** Loadings in the PCA biplot are shown. Features are located in the loadings plot where they are enriched in samples in (A).

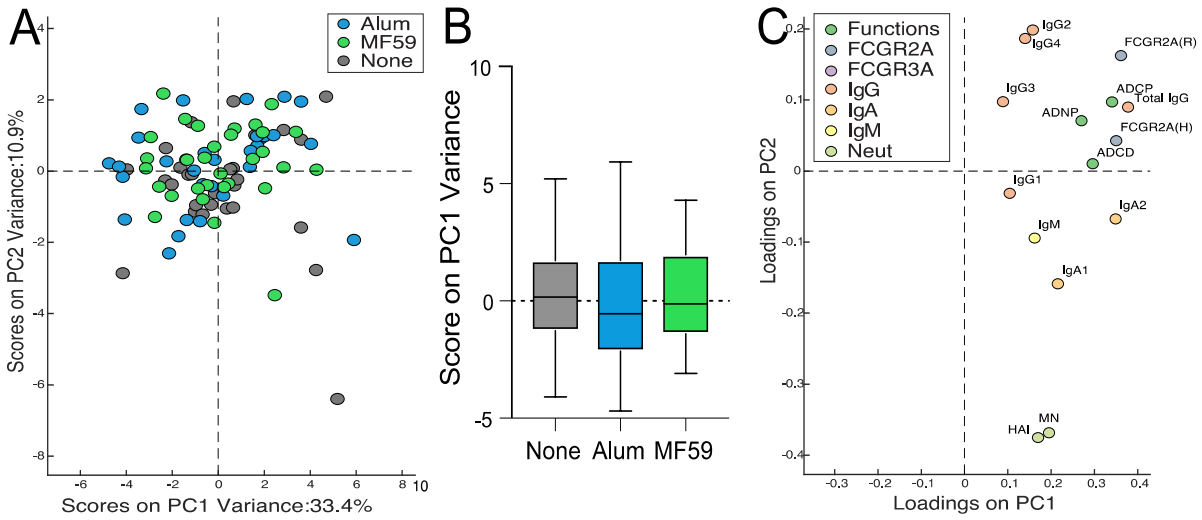

Figure 2.2 Antibodies against H5 were compared for 90 vaccinees who received 15µg recombinant H5 unadjuvanted (none), with alum, or with MF59. A principal components analysis (PCA) was used to identify differences in the functional responses of vaccinees by adjuvant. **A**. All H5-specific systems serology measurements (antibody isotypes, FCGR binding, and antibody-dependent functions) from baseline day 0 samples were included in the PCA biplot, where dots represent individual samples (blue=alum, green=MF59, grey=none). **B**. Scores along the first principal component (PC1), which captures the greatest separation between samples, were plotted. Error bars show minimum to maximum. Differences were assessed using a Mann-Whitney U test. ****p<0.0001. **C.** Loadings in the PCA biplot are shown. Features are located in the loadings plot where they are enriched in samples in (A).

To gain a deeper sense of the differences in the MF59 induced multivariate profile, a loadings plot was generated showing the specific features that were differentially enriched within each vaccine group profile (**Figure 2.1C**). Features cluster on the loadings plot in the same region as the samples in which they are enriched. Along these lines, nearly all features were enriched in the MF59-adjuvanted vaccine recipient profiles, except for the antibody-dependent NK cell activation (ADNKA) features, that clustered in a separate region of the graph. Consistent with previous studies (*138*, *139*), H5-specific IgG titers were enriched in the MF59 group. Antibody-mediated complement activity, the ability to drive monocyte phagocytosis, and neutrophil phagocytosis were also enriched in MF59 profiles when compared with the two other groups and contributed to the separation across the vaccine samples. Moreover, limited shifts were observed with IgG4, IgG2, and IgM responses that remained in the middle of the loadings plot (**Figure 2.1C**), whereas more pronounced shifts were observed in total IgG, surpassed by Fc-receptor binding antibodies, pointing to a combination of qualitative and quantitative, rather than strictly titer based, changes in H5-specific immunity. Thus, beyond strictly quantitative differences, MF59 induced a qualitatively different antibody profile compared to vaccine administered with alum or no adjuvant.

MF59 ENHANCES HIGHLY FUNCTIONAL ANTIBODY SUBCLASS LEVELS

While previous studies have demonstrated that MF59 can increase antibody titers, it is not clear whether alum and MF59 also drive differential isotype and subclass profiles. While alum induced both IgG1 (**Figure 2.3A**) and IgG3 antibodies (**Figure 2.3B**), levels were not different than those induced using the unadjuvanted vaccine. Conversely, MF59 drove significantly higher levels of total antigen-specific IgG1 at days 28 and 56 (**Figure 2.3A**), and higher IgG3 responses at day 56 (**Figure 2.3B**), consistent with previously reported

data (*138*, *139*). However, despite this significant increase in IgG1 and IgG3 antibodies, these responses were largely lost by day 208, when all the titers returned to near baseline levels irrespective of vaccine group.

Beyond IgG subclass level differences, all vaccine strategies slightly, but not significantly raised IgM levels by day 56 (**Figure 2.3C, Figure 2.4**). The unadjuvanted vaccine also tended to drive elevated levels of IgA1 and IgA2 H5-specific antibodies, although the difference was not always significant. While alum did not differ globally from the unadjuvanted vaccine profile, IgA1 was induced in the non-adjuvanted group at day 28 and 56 but not in the alum-adjuvanted group (**Figure 2.3C, Figure 2.4**). In contrast, MF59

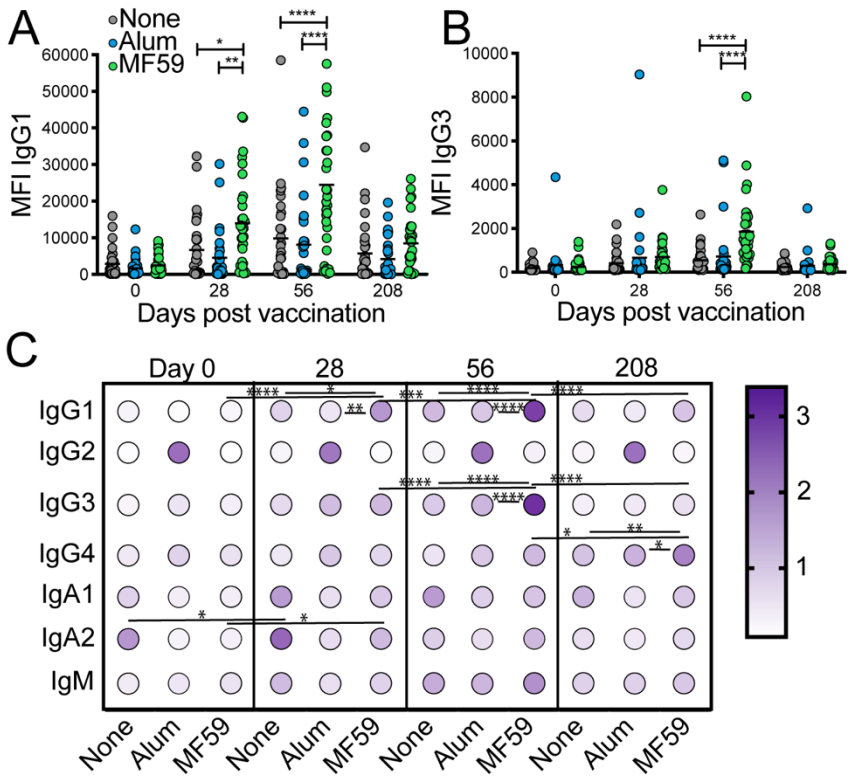

Figure 2.3 MF59 selectively enhanced functional antibody subclass levels following H5 immunization. **A.** The dot plot shows H5-specific IgG1 titers as measured by Luminex in all three vaccine groups over four timepoints. Each dot represents the average of two replicates for one serum sample. Bar represents group mean. **B.** The dot plot shows H5-specific IgG3 titers as measured by Luminex in all three vaccine groups over four timepoints. Each dot represents the average of two replicates for one serum sample. Bar represents group mean. **A-B.** Significance was determined by two-way ANOVA followed by Tukey's multiple comparisons test. Significance is noted only within timepoints. *p<0.05, **p<0.01, ****p<0.0001. **C.** Titers for other antibody isotypes and subclasses across all three vaccine groups are shown in the heatmap over four time-points, depicted as values normalized by dividing by row mean. Significance was determined on raw values by two-way ANOVA followed by Tukey's multiple comparisons test. *p<0.05, **p<0.01, *** p<0.001, ****p<0.0001.

drove significantly higher levels of functionally potent IgG1 and IgG3 responses (**Figure 2.3A-B**). MF59 did not drive significantly increased IgA in the serum when compared to unadjuvanted or alum-adjuvanted vaccination. These data suggest that all vaccine groups recruited IgM responses, however adjuvants shifted the unadjuvanted vaccine profile away from IgA dominated responses. Yet, unlike alum, MF59 drove an enhanced functional IgG1 and IgG3 dominated response, further suggesting that, in addition to quantitative changes, MF59 also induces a qualitative change in vaccine-induced immunity towards more functional IgG subclasses. Despite the more potent functional subclass induction, MF59 did not show evidence of enhanced durability of the vaccine response.

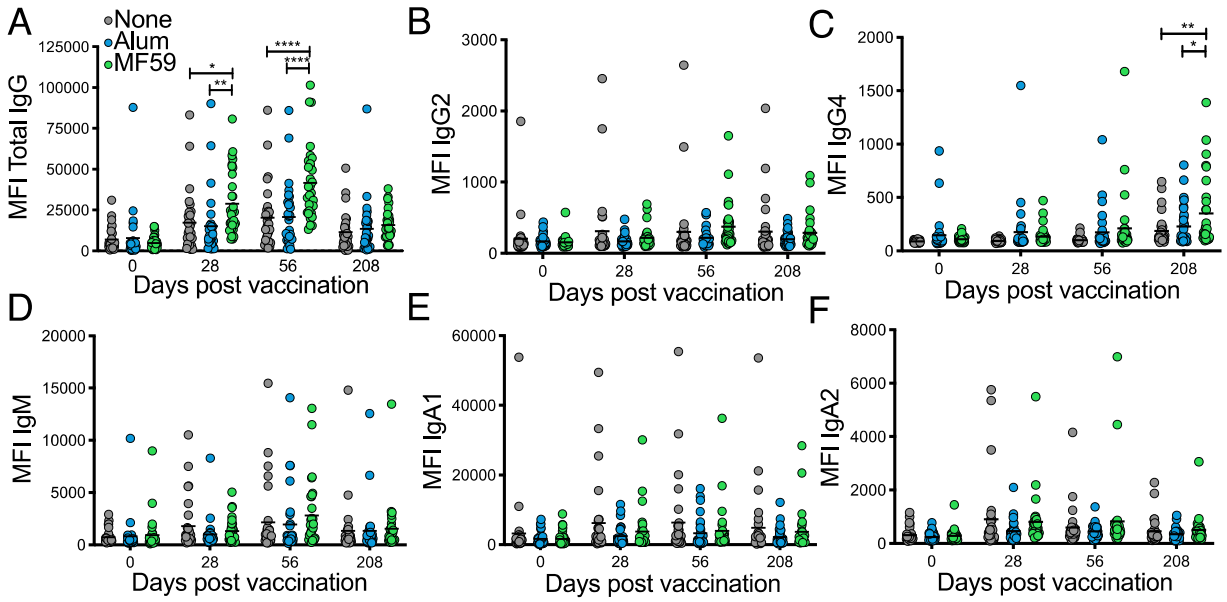

Figure 2.4 MF59 alters specific antibody isotype levels following H5 immunization. **A.** The dot plot shows H5-specific total IgG titers as measured by Luminex in all three vaccine groups over four timepoints. **B.** The dot plot shows H5-specific IgG2 titers as measured by Luminex in all three vaccine groups over four timepoints. **C.** The dot plot shows H5-specific IgG4 titers as measured by Luminex in all three vaccine groups over four timepoints. **D.** The dot plot shows H5-specific IgM titers as measured by Luminex in all three vaccine groups over four timepoints. **E.** The dot plot shows H5-specific IgA1 titers as measured by Luminex in all three vaccine groups over four timepoints. **F.** The dot plot shows H5-specific IgA2 titers as measured by Luminex in all three vaccine groups over four timepoints. **A-F.** Significance was determined by two-way ANOVA followed by Tukey's multiple comparisons test. *$p<0.05$, **$p<0.01$, ****$p<0.0001$. Significance is noted only within timepoints.

MF59 SELECTIVELY INDUCES ANTIBODY-DEPENDENT INNATE IMMUNE FUNCTIONS

Given the emerging appreciation for a critical role for antibody effector function in protection against influenza (*39*, *40*), we next probed whether the observed changes in antibody titer and isotype/subclass selection differences also tracked with changes in antibody effector functions. Previous studies demonstrated that the rapid increase in MF59 induced titers by day 28 was associated with a delayed increase in HAI and microneutralization at day 56 that declined to baseline levels by day 208 (**Figure 2.5A, C**). To gain a deeper appreciation for the relationship between HAI and vaccine-induced titers, HAI was normalized to titers at each time point (**Figure 2.5B**). Interestingly, HAI:titer ratios were consistent across all vaccine arms, with the exception of day 208, when HAI activity was disproportionately lower than H5-titers in the MF59 group. This selective reduction in HAI:titer ratio points to a selective loss of HAI-mediating antibodies among MF59 vaccinees at this late timepoint (**Figure 2.5B**). In contrast, no differences between groups were observed in the MN:titer ratios at all timepoints, highlighting the direct relationship between neutralization and titers across all vaccine arms (**Figure 2.5D**). These data point to a titer-based increase in HAI and MN across all vaccine arms, but the sharper decline in HAI, unlinked from titer, in the MF59 immunized group at day 208.

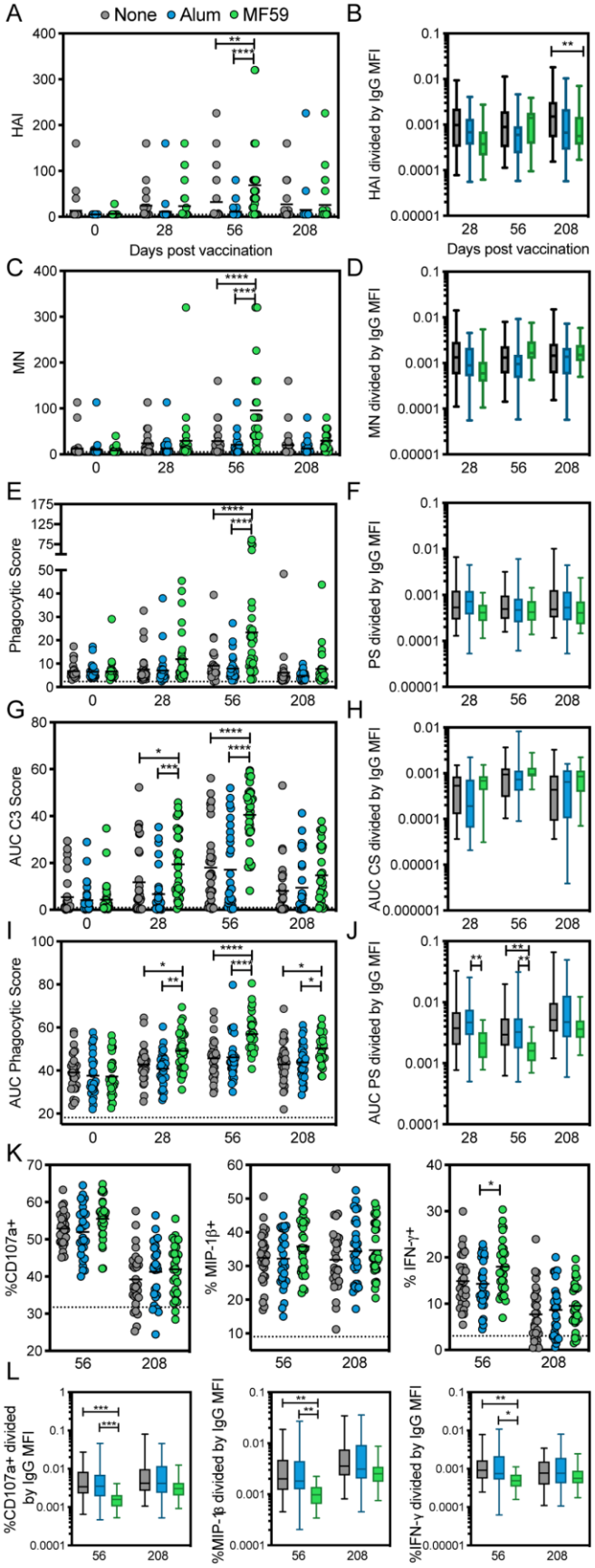

Figure 2.5 MF59 induces neutralization and specific antibody-dependent innate immune functions along with IgG1 titers. **A.** HAI activity for serum samples in all three vaccine groups over four timepoints (*139*). Each dot represents the average of two replicates for one serum sample. For all dot plots, bar shows group mean. The dotted line indicates the limit of detection. **B.** HAI activity divided by total IgG Luminex MFI as reported in Figure 2 for all three vaccine groups during the three post-vaccine timepoints. For all box plots, error bars show minimum to maximum. **C.** MN activity for serum samples (*139*). Each dot represents the average of two replicates for one serum sample. The dotted line indicates the limit of detection. **D.** MN activity divided by total IgG Luminex MFI for all three vaccine groups. **E.** Average ADNP activity for serum samples across two healthy WBC donors. Each dot represents the average of two replicates for one serum sample. The dotted line indicates flu negative serum background. **F.** ADNP activity divided by total IgG Luminex MFI for all three vaccine groups. **G.** ADCD by serum samples. Each dot represents the average of two replicates for one serum sample. The dotted line indicates the flu negative serum background. Values are indicated as the average area under the curve of three serum dilutions run in two independent replicates **H.** ADCD activity divided by total IgG Luminex MFI. **A-H.** Significance was tested by two-way ANOVA followed by Tukey's multiple comparisons test. Significance was only noted within timepoint. *p<0.05, **p<0.01, ***p<0.001, ****p<0.0001.

To probe if the same kinetics and titer-based relationships emerged for Fc-effector functions, the ability of vaccine-induced antibodies to drive antibody-dependent neutrophil phagocytosis (ADNP), antibody-dependent complement deposition (ADCD), antibody-dependent cellular phagocytosis (ADCP), and antibody-dependent natural killer (NK) activation (ADNKA) was assessed. A robust ADNP-inducing antibody response was observed following MF59-adjuvanted immunization (**Figure 2.5E**) following similar kinetics to those observed for both HAI and microneutralization in the MF59 arm (**Figure 2.5A, C**). Conversely, these antibodies were significantly lower in the alum or unadjuvanted arms (**Figure 2.5E**). ADNP peaked at week 56 in MF59 vaccinees and declined to baseline levels by day 208, similar to changes observed in antibody titers. Moreover, normalization of ADNP by titer demonstrated equivalent levels of ADNP per titer activity across all vaccine arms, highlighting that ADNP activity increased in an equally titer-dependent manner over time irrespective of adjuvant (**Figure 2.5F**).

Similarly to ADNP, MF59-adjuvanted vaccinees exhibited a significant increase in ADCD responses when compared to unadjuvanted and alum-adjuvanted vaccines. This increase occurred earlier than peak titers, with a significant increase in complement fixing activity by day 28, but a more significant increase of complement fixing antibodies by day 56 following vaccination (**Figure 2.5G**). ADCD-inducing antibodies declined by day 208 but remained slightly higher in the MF59 vaccinated group (**Figure 2.5G**). Normalization of ADCD to titer demonstrated the strong and equal association between titer and function across all vaccine groups, where ADCD:titer ratio did not change between groups over the vaccine study, suggesting that ADCD simply increased in a titer dependent manner across all vaccine strategies (**Figure 2.5H**), similarly to HAI and MN (**Figure 2.5B,D**).

ADCP increased in a similar manner to ADCD but remained significantly elevated in the MF59 group at day 208 (**Figure 2.6A**), despite the return to equal titers between vaccine arms (**Figure 2.3A**). However, normalization of ADCP to titer highlighted a disproportionate increase in titer compared to ADCP activity in the MF59 group, in such a way that lower levels of ADCP were induced per titer-level in the MF59 group compared to the unadjuvanted or alum adjuvanted groups at both days 28 and 56 (**Figure 2.6B**). These data suggest that while HAI, MN, ADNP and ADCD were induced in a titer dependent manner, MF59 induced antibodies possessed less ADCP per antibody generated when compared to responses in other vaccine arms, pointing to a functional divergence between the overall quantity and quality of adjuvanted vaccine-induced antibodies.

Finally, given the emerging appreciation for the importance of ADCC activity in protection against influenza (*172*), we profiled differences in NK cell activating ability of H5-specific antibodies following unadjuvanted, alum-adjuvanted or MF59-adjuvanted vaccination at days 56 and 208 (**Figure 2.6C-E**). While H5N1-vaccine induced antibodies were able to drive NK cell degranulation (upregulation of CD107a, a marker of NK cell cytotoxicity(*199*)) and NK cell chemokine secretion (macrophage inflammatory protein 1β - MIP1β), these responses were not different across the 3 vaccine groups (**Figure 2.6C,E**) despite observed titer differences (**Figure 2.3A**). MF59 was able to induce H5-specific antibodies able to stimulate more NK cell interferon-γ (IFNγ) secretion (**Figure 2.6D**). However, normalization of NK cell activating antibody levels to titer revealed disproportionately lower NK:titer ratios among MF59 vaccinees, across all NK cell functions (**Figure 2.6F-H**). These results suggest that despite the robust induction of antibody titers, HAI, MN, ADCD, and ADNP, MF59 induced antibodies possessed lower NK cell activating activity on a per antibody level compared to those induced by the vaccine

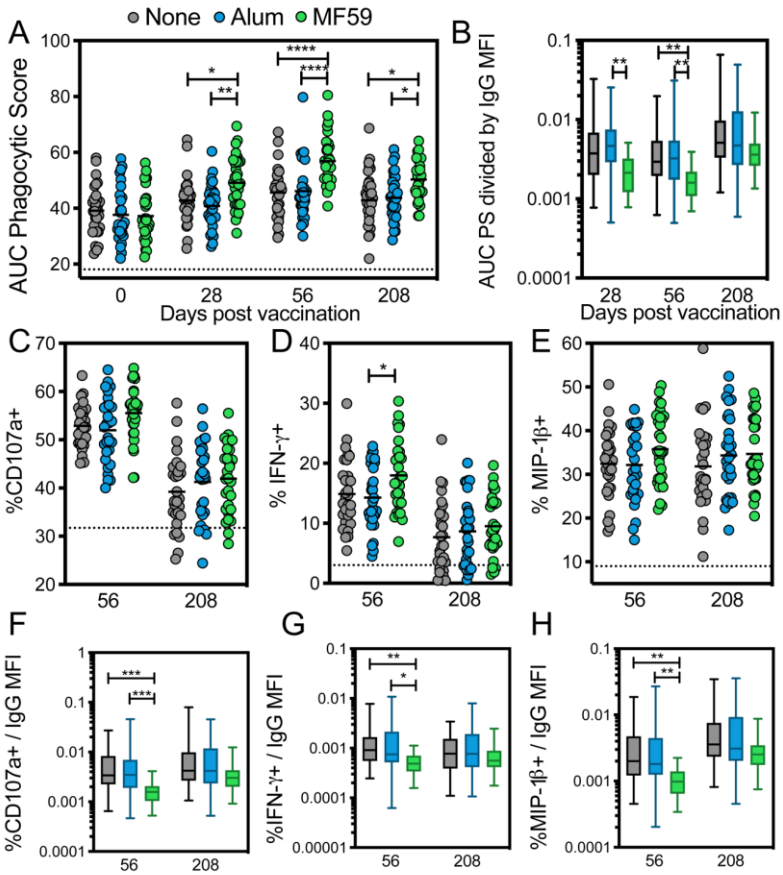

Figure 2.6 MF59 induces higher titers, but not antibody-dependent monocyte or NK cell functions. **A.** ADCP activity for serum samples in all three vaccine groups over four timepoints (*139*). Each dot represents the average of two replicates for one serum sample. For all dot plots, bar shows group mean. The dotted line indicates the flu negative serum background. Values are indicated as the area under the curve of three serum dilutions run in two independent replicates. **B.** ADCP activity divided by total IgG Luminex MFI. **C-E.** ADNKA activity by average percent of NK cells expressing each of three markers, CD107a (C), IFN-γ (D), and MIP-1β (E), for two healthy NK cell donors. The dotted line indicates flu negative serum background. **F-H.** ADNKA activity for three markers divided by total IgG Luminex MFI for all three vaccine groups. **A-H.** Significance was tested by two-way ANOVA followed by Tukey's multiple comparisons test. Significance was only noted within timepoint. *p<0.05, **p<0.01, ***p<0.001, ****p<0.0001.

alone or delivered with alum. Thus, MF59-adjuvanted vaccination may result in weaker induction of NK cell-activating humoral immune responses, on a per-antibody level. Taken together, these data point to a potent effect of MF59 in driving H5-specific functional antibodies, but with a reduced capacity to fully harness NK cell and monocyte functional responses.

MF59 INDUCES ANTIBODIES WITH DIFFERENTIAL LOW AFFINITY FCγ-RECEPTOR BINDING PROFILES

To gain further insights into the specific mechanics that could contribute to differential functional responses, we next aimed to explore changes in vaccine induced antibody interactions with Fc-receptors involved in directing innate immune effector function. Specifically, beyond changes in vaccine induced titers, the ability of H5-specific antibodies to interact with the two low affinity Fcγ-receptors involved in inducing phagocytosis (FCGR2A) and NK cell cytotoxicity (FCGR3A) were interrogated. In agreement with the functional data, all vaccine groups experienced an increase in FCGR2A binding (**Figure 2.7A**) at day 28 and day 56, however subjects receiving MF59 experienced a significantly higher increase in FCGR2A binding. Moreover, while all FCGR2A binding antibodies declined at day 208, the levels in MF59 vaccinees remained elevated, consistent with enhanced ADCP activity (**Figure 2.5E**) over time and unlinked from changes in overall H5-specific antibody titers (**Figure 2.3A**). Conversely, despite the increase in IgG1 and IgG3 titers, only a slight insignificant increase in FCGR3A binding antibodies at day 28 was observed in MF59-adjuvanted vaccine recipients compared to other groups. However, FCGR3A binding antibody levels declined rapidly across all groups over time (**Figure 2.7B**). Moreover, analysis of vaccine induced binding profiles across both high and low affinity variants of FCGR2A and FCGR3A showed consistent profiles, with a clear augmentation of FCGR2A binding across both allotypes, with a preferential significant increase among MF59 vaccinees (**Figure 2.7C, Figure 2.8**). Similarly, no evidence of increase in FCGR3A binding was observed across both FCGR3A variants (*65, 67*) highlighting the consistent lack of FCGR3A binding in all H5N1 vaccinees (**Figure 2.7C, Figure 2.8**). Given that both

NK cells and monocytes express FCGR3A (*67*), unlike neutrophils, these data are consistent with a lack of a NK cell activating and monocyte phagocytic activity.

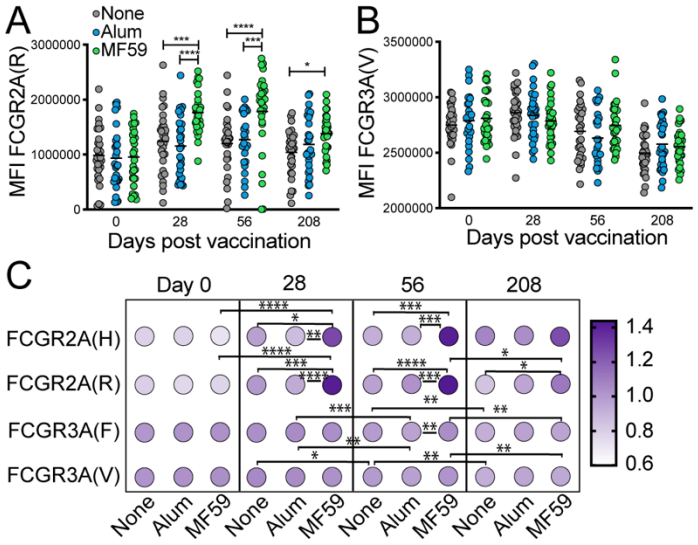

Figure 2.7 MF59 increases enhanced FcγRIIa, but not FcγRIIIa, H5-specific binding antibodies. **A.** The dot plot shows H5-specific antibody binding to FCGR2A(R) as measured by Luminex in all three vaccine groups over four timepoints. Each dot represents the average of two replicates for one serum sample. Bar shows group mean. **B.** The dot plot shows H5-specific antibody binding to FCGR3A(V) as measured by Luminex bead array in all three vaccine groups over four timepoints. Each dot represents the average of two replicates for one serum sample. Bar shows group mean. **A-B.** Significance was determined by two-way ANOVA followed by Tukey's multiple comparisons test. Significance is noted only within timepoints. *p<0.05, **p<0.01, ****p<0.0001. **C.** FCR binding for both allotypes of FCGR2A and FCGR3A for other antibody isotypes in all three vaccine groups over four timepoints are shown in a heatmap as values normalized by dividing by the row mean. Significance was determined on raw values by two-way ANOVA followed by Tukey's multiple comparisons test. *p<0.05, **p<0.01, *** p<0.001, ****p<0.0001.

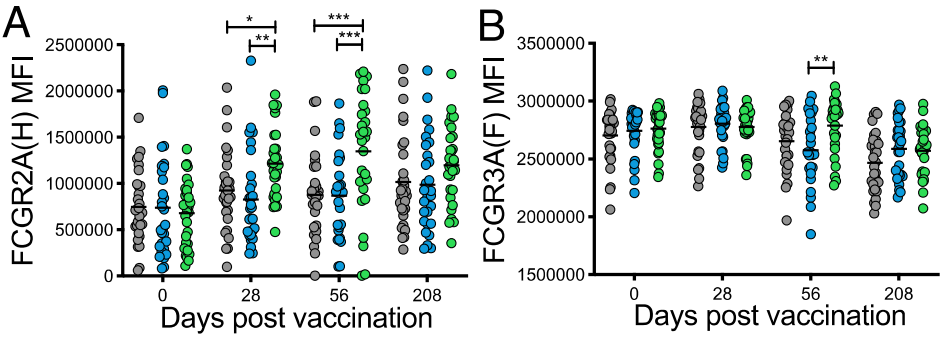

Figure 2.8 MF59 increases enhanced FcγRIIa, but not FcγRIIIa, H5-specific binding antibodies across FcγR polymorphisms. **A.** The dot plot shows H5-specific antibody binding to FCGR2A(H) as measured by Luminex in all three vaccine groups over four timepoints. **B.** The dot plot shows H5-specific antibody binding to FCGR3A(F) as measured by Luminex bead array in all three vaccine groups over four timepoints. **A-B.** Significance was determined by two-way ANOVA followed by Tukey's multiple comparisons test. *p<0.05, **p<0.01, ****p<0.0001. Significance is noted only within timepoints.

MF59 OVERCOMES NATURAL PRE-EXISTING HA SPECIFIC ANTIBODIES

Previous data suggest that pre-existing influenza immunity shapes the induction of the humoral immune response, even to distant HAs (*26*), so we finally sought to determine whether the functional profiles of vaccine induced antibodies were differentially influenced by natural pre-existing humoral immune responses. We hypothesized that individuals with generally higher levels of phagocytic antibodies in response to seasonal influenza may leverage these responses more effectively following H5N1 avian influenza vaccination. H1 responses were used a proxy for seasonal influenza responses. Vaccinees within each group were thus split into tertiles based on their pre-existing H1-specifc functional responses at baseline (**Figure 2.9A, D, G**). H5-specific responses were then compared across each group at peak immunogenicity (day 56). MF59 increased the H5-specific ADCP response at the peak time point in all three groups, suggesting that pre-existing H1 specific ADCP function did not influence the induction of H5-specific ADCP (**Figure 2.9B**). No significant differences were observed in H5-specific function between low, medium, and high baseline responders within the three different vaccine groups (**Figure 2.9B**). This points to a limited impact of previous influenza exposure in influencing antibody effector function to a novel influenza hemagglutinin. Importantly, this upregulation of phagocytic function, specifically in the MF59 group, was not associated with a concomitant increase in H1-specific functional activity (**Figure 2.9C**), further demonstrating the specific recruitment of H5-specific immune responses, rather than the co-recruitment of pre-existing H1-specific immune responses.

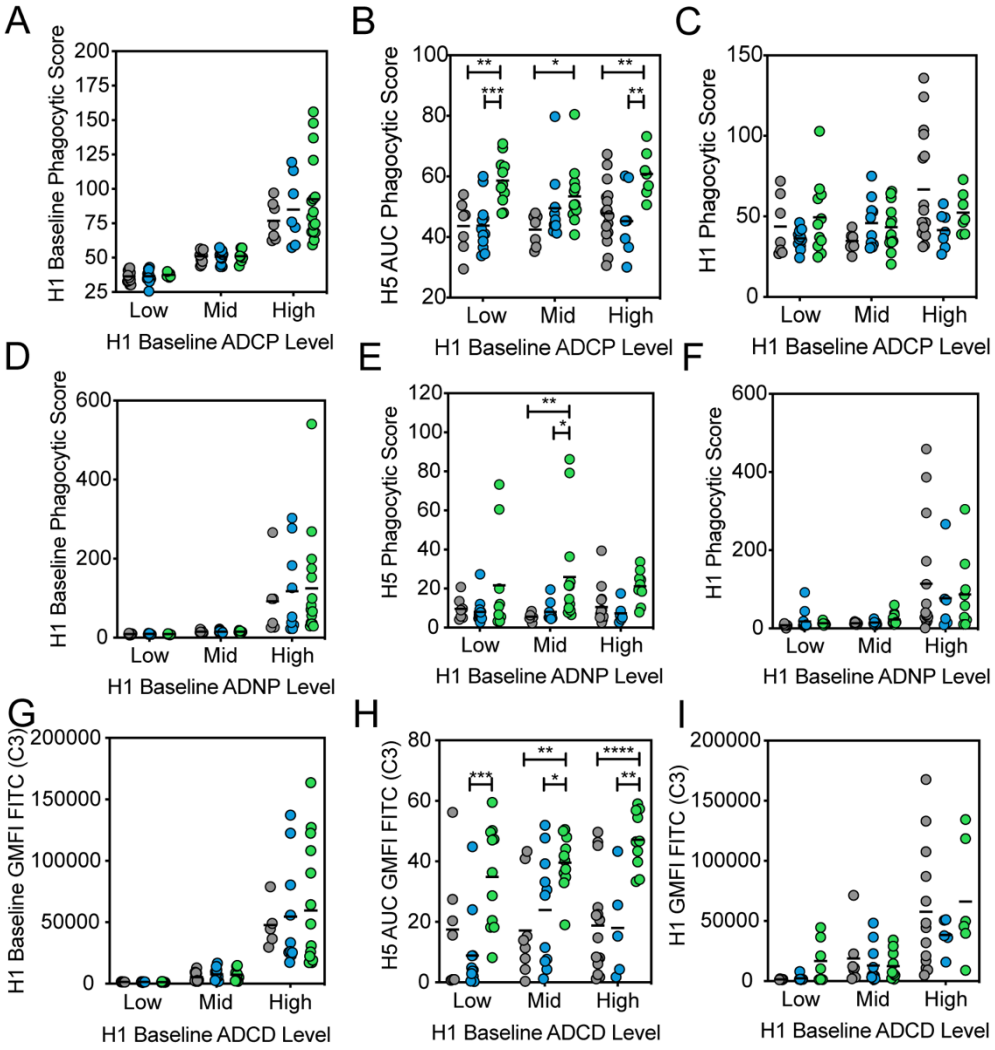

Figure 2.9 MF59 induced antibody functionality is not influenced by pre-vaccination H1 specific immunity. **A.** Samples were grouped into low, mid, or high based on their baseline (day 0) H1-specific ADCP. The dot plot indicates grouping strategy of baseline H1-specific ADCP among each vaccine group. **B.** H5-specific ADCP at peak immunogenicity (day 56) for H1 baseline ADCP groups. **C.** H1-specific ADCP at peak immunogenicity for each baseline reactivity group by vaccine adjuvant. **D.** Samples were grouped into low, mid, or high based on their baseline (day 0) H1-specific ADNP. The dot plot indicates the grouping strategy of baseline H1-specific ADNP among each vaccine group. **E.** H5-specific ADNP at peak immunogenicity (day 56) for H1 baseline ADNP groups. **F.** H1-specific ADNP at peak immunogenicity for each baseline reactivity group by vaccine adjuvant. **G.** Samples were grouped into low, mid, or high based on their baseline (day 0) H1-specific ADCD. Dot plot indicates grouping strategy of baseline H1-specific ADCD among each vaccine group. **H.** H5-specific ADCD at peak immunogenicity (day 56) for H1 baseline ADCD groups. **I.** H1-specific ADCD at peak immunogenicity for each baseline reactivity group by vaccine adjuvant. **A-I**. For all dot plots, each dot represents the average of two replicates for one serum sample, and bar shows group mean. significance was tested by two-way ANOVA followed by Tukey's multiple comparisons test and is noted only within timepoint. * $p<0.05$, ** $p<0.01$, *** $p<0.001$, **** $p<0.0001$.

Using a similar grouping strategy, no difference was observed in H5-specific neutrophil phagocytic activity (**Figure 2.9E**) or complement activity (**Figure 2.9H**) across

the H1 tertiles between the 3 vaccine groups, highlighting the lack of an impact of pre-existing potentially-cross reactive H1-specific immunity. In contrast, a trend towards higher ADNP and ADCD recruiting cross-reactive H1-specific responses were detected in subjects with the highest levels of pre-existing H1-specific immunity (**Figure 2.9F, I**). Taken together, these data suggest that pre-existing cross-reactive immunity does not influence the induction of functional antibodies to diverging HAs (H5N1) induced by MF59.

DISCUSSION

Over 100 years since the Spanish flu pandemic of 1918, strategies to prepare for an emerging pandemic influenza strain, such as the avian influenza H5N1, are still inadequate. Several strategies have been proposed including: 1) the acceleration of vaccine production pipelines (*200*), 2) the development of novel antigens able to drive immunity to sites of vulnerability like the HA stem (*201*), 3) the identification of immune correlates to induce targeted vaccine immune functions (*202*), 4) the generation of antigen-sparing vaccine approaches able to ensure sufficient material to cover the global population (*200*), as well as 5) the development of strategies to enhance the protective activity of vaccine-induced humoral immunity. Specifically, adjuvant technologies have been proposed to address the latter three efforts. Alum is both the most widely used adjuvant and the standard comparator for novel adjuvant formulations, but did not satisfy these goals for avian influenza vaccination, consistent with previous studies (*203*, *204*). MF59, in contrast, exhibits both antigen-sparing and immune boosting functions, and has shown promise in seasonal and avian influenza vaccines by significantly increasing antibody response titers following vaccination (*138*, *140*, *184*, *205*). However, despite these increases in titer, MF59-adjuvanted vaccination still provided only partial protection from seasonal infection in large studies (*188*, *189*). Specifically, while MF59 conferred much higher protection among

the youngest age group (6-23 months) compared to un-adjuvanted vaccination, this level of protection was not observed across the whole study population (*188*). Thus, the level of protection did not reach the level expected to be conferred by enhanced antibody titers, pointing to a critical disconnect between the quality and quantity of influenza-specific humoral immunity. This is reflected in the data presented here, wherein MF59 significantly augmented H5-specific antibody titer but did not equally enrich for all antibody-dependent innate immune cell functions in a titer-dependent manner, with notable gaps in monocyte phagocytic and NK cell functions.

Given our emerging appreciation for the importance of adjuvants in shaping antibody function (*206*), here we aimed to deeply profile and compare the functional quality of the antibody response driven by distinct adjuvants. We found that while alum slightly enhanced the Th1 character of the humoral immune response, marginally moving the isotype profile away from IgA1 and IgA2 (**Figure 2.3C, Figure 2.4E-F**), MF59 drove significant IgG1 and IgG3 responses able to drive highly neutrophil phagocytic- and complement-inducing responses. Both IgG and IgA antibodies are critical for the control of influenza infection, with mucosal and serum IgA complementing IgG in serum and the lung for both the prevention and clearance of infection (*118*). IgA alone has been shown to be sufficient to prevent influenza transmission (*120*), a proxy for decreasing infection severity. The dampening of the IgA response by alum, which could decrease the effectiveness of the vaccine at generating a protective humoral immune response, may explain its' substandard performance as an adjuvant in influenza vaccination in this and previous vaccine trials (*139*, *203*). Additionally, as MF59 did not enhance the IgA levels as compared to unadjuvanted vaccination (**Figure 2.3C, Figure 2.4E-F**), this may also be an area of concern

for future influenza vaccination regimens using MF59 to boost immunity, if this critical protective isotype is not induced at sufficient levels.

Beyond neutralization and HAI, many antibody functions have been implicated in protection from and clearance following influenza infection. Complement activation has been implicated in protection from influenza pathogenesis in mouse models (*54*, *96*), and was transiently boosted with MF59 (**Figure 2.5G**). Additionally, neutrophils also play a role in the phagocytic clearance of influenza-infected lung cells (*89*). Similarly, macrophage activity in the lung has been linked to protection from lethal influenza infection in mice (*58*), and human serum is known to have ADCP activity against circulating influenza strains that can clear both virus and infected cells (*66*). MF59-induced increases in ADCP did not occur in a titer-dependent manner, although significantly increased ADCP activity persisted to day 208 (**Figure 2.6A**). Importantly, while IgG-mediated neutrophil-mediated phagocytosis occurs in a largely FCGR2A-dependent manner (*67*), monocytes are able to phagocytose in both an FCGR2A- and FCGR3A-dependent manner (*67*). Thus, compromised monocyte, but not neutrophil phagocytic function, is likely related to the inability of MF59-induced antibodies to bind to FCGR3A (**Figure 2.7B**). These data point to enhanced clearance of ADNP antibodies, that may solely function through FCGR2A, but the potential slower clearance of antibodies potentially harboring distinct Fc-glycan profiles able to drive ADCP through non-canonical Fc-receptors, such as lectin-like receptors, known to drive monocyte mediated activity (*207*). Defining the unique antibody subpopulations as well as their functional durability may provide important insights for next generation long-lived vaccine design. However, despite the significantly increased titers and function of influenza-specific antibodies, MF59 showed poorly enhanced protection in clinical trials

(*188*, *189*), raising the possibility that these functions alone may not be sufficient for generalized protection from influenza.

Antibody-driven NK cell function has been implicated in protection against multiple infections, including HIV (*208*, *209*), malaria (*210*, *211*), and Ebola (*212*). Likewise, while the protective role of NK cells in influenza is not fully understood, emerging data point to a critical role for NK cells in the protection against severe disease and the clearance of influenza infection (*40*, *79*, *213*). The importance of NK cells has emerged in relationship to the disconnect between broadly protective antibodies that show limited HAI activity (*39*). Specifically, antibodies that bind to the stalk region of influenza HA and are protective in animal models require FCGR interactions to provide their protective effect, regardless of *in vitro* neutralization capability (*38*). Further, only stalk-specific and broadly-reactive head-specific monoclonal antibodies, not head-targeting strain-specific mAbs, were shown to mediate ADCC (*38*). Recent studies in this field suggest that stalk-specific, but not head-specific, antibodies can mediate ADCC by NK cells owing to a requirement for contact both between the antibody Fc and the receptor binding site of HA with sialic acids on the NK cell (*85*, *214*). Strain-specific head-targeting antibodies typically block the receptor binding site interactions with sialic acid needed to efficiently induce ADCC (*214*). Owing to this involvement of NK cells in HA stalk-specific antibody-mediated protection, it has been speculated that NK cell activation may represent a vital Fc-effector function in broadly reactive humoral immunity against influenza. However, MF59 was unable to efficiently promote the development of NK-cell activating, FCGR3A-binding antibodies (**Figure 2.6C-E**).

Monocytes and NK cells may mediate protection through multiple mechanisms. Following the recognition of antibody-opsonized cells or virus, monocytes and/or NK cells

may contribute to direct lysis and destruction, clearance of influenza-infected cells, or to the indirect arming of antiviral immunity via the release of IFN-γ required to potentiate T cell immunity and efficient antigen-uptake and activation of pulmonary dendritic cells (*215*). Recent data and opinion in the field has suggested a particular role for ADCC- or FCGR3A-binding antibodies (*172*), with studies in mice finding protection by ADCC-inducing antibodies and correlations in human studies between ADCC titers (*38*, *216*) and reductions in disease burden (*78*). FCGR3A is the primary Fc-receptor expressed on NK cells, responsible for NK cell activation (*68*, *69*), but is also expressed on mature macrophages (*67*) . Affinity for binding to this receptor is influenced by the selection of antibody subclass and Fc glycosylation (*67*). Surprisingly, while MF59 induced higher levels of IgG1 and IgG3, known to bind to FCGR3A, MF59 did not induce antibodies able to enhance binding to FCGR3A (**Figure 2.7B**) or drive enhanced NK cell activation (**Figure 2.6C-E**). The consistent deficit in FCGR3A and NK cell or incomplete monocyte responsiveness suggests that the induced IgG3, that typically exhibit enhanced affinity for FCGR3A, may be functionally distinct from typical IgG3 responses, thought classically to drive enhanced ADCC activity. However, like IgG1 antibodies, IgG3 also possess an Fc-glycan, that may also change following vaccination and infection, potentially resulting in differential affinity for Fc-receptors. Thus, future studies focused selectively on IgG3 glycosylation differences across adjuvant-platforms may point to opportunities to shape overall and subclass specific antibody functionality.

Pre-existing antibodies from previous influenza exposure or vaccination have been an issue in the development of influenza vaccination both seasonal and pandemic, while cross-reactive antibodies to conserved epitopes like the HA stem have been considered a possible benefit (*26*, *100*). While pre-existing antibodies have been shown to influence the

magnitude, epitope targeting, and neutralizing capacity of vaccine induced immunity, it was uncertain whether pre-existing immunity could also influence antibody effector function. Here, we observed limited evidence of an influence of pre-existing H1 responses on H5-induced antibody functionality (**Figure 2.9**), which was induced equivalently with MF59 across groups. While the influence of stem-specific pre-existing responses, that are likely to interact more readily with H5, were not investigated here, these responses could potentially be leveraged to drive enhanced immunity to this diverging strain. Thus, future studies focused on the interrogation of epitope-specific functional responses may uncover additional roles for pre-existing antibodies on shaping vaccine induced immunity.

The robust induction of antibody titers and neutralization using MF59 have resulted in only a modest increase in protection against seasonal and pandemic influenza in vulnerable populations(*188*, *189*), although the effectiveness of the adjuvant has yet to be studied against human avian infections. This disconnect may be related to the ability of MF59 to significantly augment neutralization and antibody function that appears to harbor a functional "hole" in NK cell and monocyte activation. Given our emerging appreciation for opportunities to combine adjuvants, due to their complementary immune stimulating capabilities (*206*, *217*, *218*), defining the landscape of qualitative modifications induced by individual and combined adjuvants, may offer a unique opportunity to fully control both the quantity and quality of the humoral immune response. Thus with our growing appreciation for the importance of particular Fc-effector functions across infections (*40*, *208–212*), next generation rational vaccine design efforts may benefit from a comprehensive understanding of the functional impact and opportunities to conditionally elicit vaccine-induced antibody effector function to maximize on both the potency of the antigen binding and constant domain-driven function of vaccine induced antibodies.

Chapter 3: IMPACT OF MATERNAL INFLUENZA VACCINATION ON ANTIBODY PLACENTAL TRANSFER AND PROTECTION OF INFANTS IN A PLACEBO-CONTROLLED TRIAL

Based on a manuscript in press:

Boudreau, C.M., Burke, J.S. IV, Shuey, K.D., Wolf, C., Katz, J., Tielsch, J., Khatry, S., LeClerq, S.C., Englund, J.A., Chu, H.Y., & Alter G. Dissecting Fc signatures of protection in neonates following maternal influenza vaccination in a placebo-controlled trial.

Author contributions: CMB, JAE, HYC, and GA designed the research study and wrote the manuscript. JK, JT, SK, and SCL designed and led the original clinical sample from which samples were drawn. KDS and CW provided study samples. CMB and JSB conducted experiments, acquired data, and analyzed data.

Influenza is an important cause of illness and morbidity for infants. Seasonal influenza vaccination during pregnancy protects both mothers and infants; however, the precise influence of maternal vaccination and how vaccine-elicited antibodies provide protection in some but not all infants is incompletely understood. We comprehensively profiled the transfer of functional antibodies and defined humoral factors contributing to immunity against influenza in a clinical trial of maternal influenza vaccination. Influenza-specific antibody subclass levels, Fc γ receptor (FCγR) binding levels, and antibody-dependent innate immune functions were all profiled in the mothers during pregnancy and at birth, and in cord blood. Vaccination increased influenza-specific antibody levels, antibody binding to FCγR, and specific antibody-dependent innate immune functions in both maternal and cord blood, with FCγR binding most enhanced via vaccination.

Influenza-specific FCγR binding levels were lower in cord blood of infants who subsequently developed influenza infection. Collectively these data suggest that in addition to increased antibody amounts, the selective transfer of FCγR-binding antibodies contributes to the protective immune response in infants against influenza.

INTRODUCTION

Influenza is a major cause of respiratory disease and hospitalization in children under 5 years of age globally (*219–221*). Moreover, infants and young children without underlying medical conditions are hospitalized for influenza-associated-illness at higher rates than adults with high-risk conditions, including the elderly (*222*, *223*). These data have revealed the critical need for global vaccine campaigns to protect high risk groups, including young children, elderly, and pregnant people, leading to the recommendation of year-round influenza vaccination during pregnancy to protect both the mother and child (*224*).

While pregnancy is not associated with an increased risk of influenza virus infection, pregnancy is associated with an increased risk of hospitalization and adverse outcomes following an influenza infection, particularly during the third trimester (*225*, *226*). Specifically, influenza infection during pregnancy is associated with an increased risk of low infant birthweight, preterm birth, neonatal and maternal ICU admission, and even infant death (*227*). Influenza vaccination during pregnancy decreases rates of respiratory illness in both the mother and the infant (*228–233*), with efficacy rates among mothers estimated at 31-70% and efficacy rates in infants estimated at 30-63% across multiple randomized, controlled trials (*234*), clearly highlighting the public health impact of influenza vaccination during pregnancy.

Influenza vaccination during pregnancy has been linked to elevated vaccine-specific antibody concentrations in the cord blood that persist in the neonate for at least 2 months post-partum (*230*, *235*, *236*). However, the mechanism(s) through which these transferred antibodies afford protection against influenza remains incompletely understood. The current standard for evaluating influenza vaccination immunogenicity is the hemagglutination inhibition (HAI) assay (*18*), which is a proxy measurement for viral neutralization. While neutralizing antibodies that opsonize the virus and prevent infection are undoubtedly important for protection, increasing evidence points to additional antibody-induced functions in protection from influenza infection (*62*). Extra-neutralizing antibody functions mediate protection against influenza in animal models (*38–40*, *53–59*) and have been observed following infection and vaccination in humans (*40*, *83*, *237*, *238*). Specifically, the ability of influenza-specific antibodies to drive Fc γ receptor (FCγR) dependent functions, namely antibody-dependent cellular phagocytosis (ADCP) (*56*, *60*), neutrophil production of reactive oxygen species (*56*), antibody-dependent cellular cytotoxicity (ADCC) (*57*), and antibody-dependent complement deposition (ADCD) (*54*, *55*, *60*, *61*), have been linked to protection from influenza infection and disease. Whether influenza vaccination during pregnancy can induce functional antibodies, and whether these antibodies are transferred to the fetus and provide protection in infants, remains unknown.

During pregnancy, antibodies are actively transported across the placenta to the fetus, where they enter fetal circulation and provide protection during the first months of life (*227*, *230*, *235*). The neonatal Fc receptor (FcRn) preferentially transfers IgG1 antibodies across the placenta (*239–243*). Recent studies have further indicated that the placenta may selectively transfer subsets of IgG1 antibodies with enhanced NK cell function to provide protection to infants in early life (*244*). Thus, we aimed to define the

influence of influenza vaccination on tuning influenza-specific immunity during pregnancy, to define how vaccination impacts antibody transfer to neonates, and ultimately to probe the specific patterns of antibodies that track with protection in early life. Using systems serology (*193*), we profiled the influenza-specific immune response among a cohort of pregnant women in rural Nepal (**Figure 3.1**), where women were enrolled in a randomized clinical trial of influenza vaccination, and were administered vaccine or placebo between 17 and 34 weeks of gestation (*225*, *245*). Influenza-specific antibody profiles were then comprehensively assessed in the maternal and cord blood among infants with and without influenza infection from birth to six months (*225*).

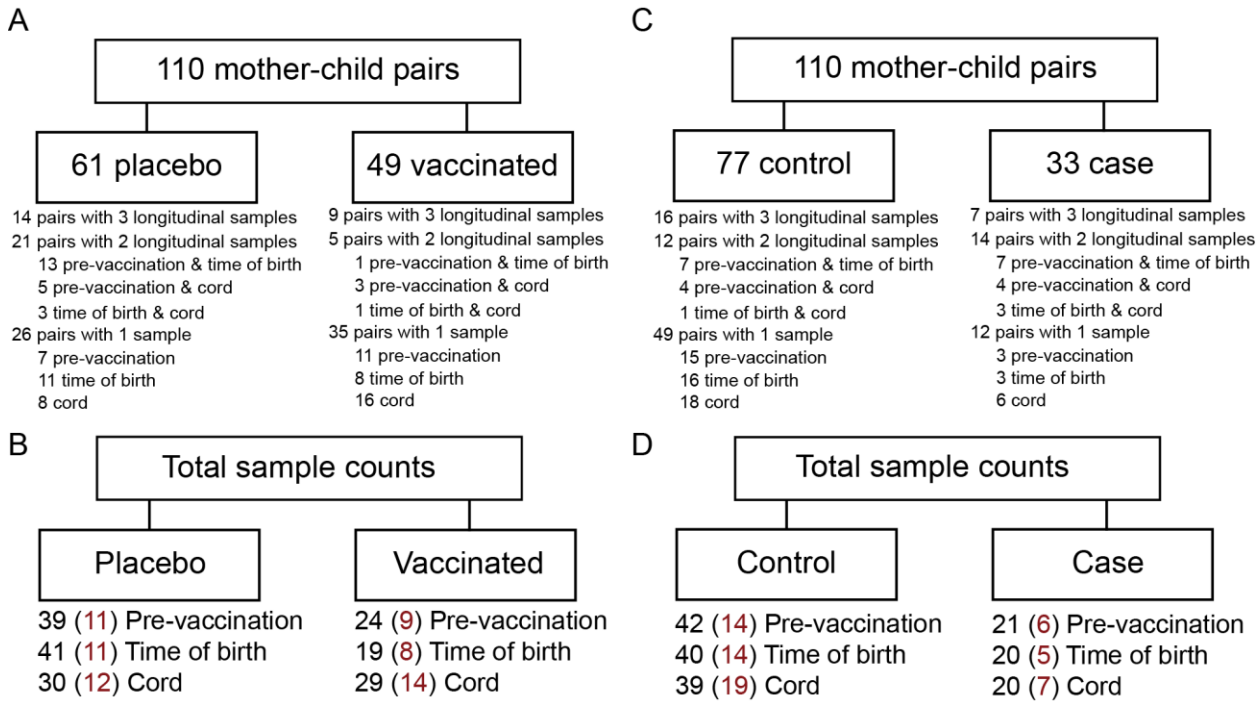

Figure 3.1 Schematic of samples included in this study. Schematic (**A**) shows dyads with number of longitudinal samples across placebo and vaccinated groups. Schematic (**B**) shows number of samples at each timepoint in each group. Numbers in red indicate samples for which HAI data is available. Schematic (**C**) shows dyads with number of longitudinal samples across control (uninfected infants) and case (infants who became infected). Schematic (**D**) shows number of samples at each timepoint in each group. Numbers in red indicate samples for which HAI data is available.

METHODS

RESOURCE AVAILABILITY

Lead contact

Further information and requests for resources and reagents should be directed to and will be fulfilled by the lead contact, Galit Alter (galter@mgh.harvard.edu).

Materials availability

This study did not generate new unique reagents.

Data and code availability

Data reported in this paper will be shared by the lead contact upon request.

Any additional information required to reanalyze the data reported in this paper is available from the lead contact upon request.

EXPERIMENTAL MODEL AND SUBJECT DETAILS

Human subjects

Serum samples from a community-based, placebo-controlled trial of influenza vaccination in the rural Sarlahi district of Nepal in 2011-2014 (*228*) drawn from pregnant study participants prior to vaccination, at the time of birth, and from the umbilical cord, were obtained for systems serology analysis. Informed consent was obtained from all subjects. Saline placebo was used for those assigned to the placebo group and vaccinees received the Vaxigrip vaccine (Sanofi Pasteur Ltd.) (*222*). More details about the demographic data of these subjects can be found in months post-partum for fever or . The primary outcomes of the original trial were maternal influenza-like-illness, laboratory-confirmed influenza in infants, and low birthweight (*222*, *225*, *228*). Multiple secondary outcomes, including preterm birth, maternal laboratory-confirmed influenza, and effect of timing of vaccination, have already been investigated (*222*, *225*, *228*). Subjects were actively

followed weekly for 6 months post-partum for fever or respiratory symptoms to track influenza infection. We selected a convenience subset of mother-infant pairs with and without evidence of infant influenza infection from the vaccine and the placebo arms of the trial and performed a 1:2 match of cases:controls for each time point by vaccine status, month, and year of birth, as well as infant sex and preterm birth. Cases were defined as mother-infant pairs with infant laboratory-confirmed influenza infection and controls were defined as mother-infant pairs without infant influenza infection. Serum sample sets from a total of 114 mother-child pairs were included in the analysis presented here (**Figure 3.1**). Within this study cohort, 23 infants were infected with H3N2, 2 infants were infected with H1N1, and 6 infants were infected with influenza B. In two dyad pairs with infant influenza infection and one pair without infant influenza infection, maternal influenza infection was also documented during the study period. A smaller subset of these samples had HAI data available from a previous study (*228*) (**Figure 3.1**). HAI assays were used to test for antibodies to influenza antigens contained in the vaccines by a CLIA certified laboratory at Cincinnati Children's Hospital. Laboratory staff were blinded to the vaccine assignments and timing of vaccine. The parent trial is registered at clinicaltrials.gov (NCT01034254). This study was approved by the Massachusetts General Hospital Institutional Review Board.

Table 3.1 Table describing demographic data for study participants.

	Placebo	Vaccine	Control	Case
Demographic Data Available	60	49	77	32
Missing Demographic Data	1	0	0	1
Male infants	16.7% (10)	26.5% (13)	23.4% (18)	15.6% (5)
Preterm infants	28.3% (17)	20.4% (10)	23.4% (18)	28.1% (9)
Vaccine Strains				
A/CA/07/2009, A/Perth/16/2009, B/Brisbane/60/2008	23.3% (14)	30.6% (15)	28.6% (22)	21.9% (7)
A/CA/07/2009, A/Victoria/361/2011, B/Wisconsin/1/2010	76.7% (46)	69.4% (34)	71.4% (55)	78.1% (25)
Vaccination Season				
Dec-Feb	55% (33)	30.6% (15)	41.6% (32)	50% (16)
Mar-May	21.7% (13)	34.7% (17)	27.3% (21)	28.1% (9)
Jun-Aug	1.7% (1)	4.1% (2)	4.9% (3)	0% (0)
Sep-Nov	21.7% (13)	30.6% (15)	27.3% (21)	21.9% (7)
Birth Season				
Dec-Feb	18.3% (11)	40.8% (20)	32.5% (25)	18.8% (6)
Mar-May	48.3% (29)	14.3% (7)	29.9% (23)	40.6% (13)
Jun-Aug	31.7% (19)	32.7% (16)	32.5% (25)	31.3% (10)
Sep-Nov	1.7% (1)	12.2% (6)	5.2% (4)	9.4% (3)
Approx. Gestational Age at Vaccination				
1st Trimester	3.3% (2)	6.1% (3)	5.2% (4)	3.1% (1)
2nd Trimester	76.7% (46)	61.2% (30)	66.2% (51)	78.1% (25)
3rd Trimester	20% (12)	32.7% (16)	28.6% (22)	18.8% (6)

Cell lines

THP-1 cells (cell line isolated from a 1-year-old male) were grown in R10 medium (RPMI plus 10% fetal bovine serum, L-glutamine, and penicillin/streptomycin) supplemented with 0.01% ß-mercaptoethanol at 37°C, seeded at 200,000 cells/ml and split prior to reaching 1,000,000 cells/ml.

METHOD DETAILS

Ig Subclassing/Isotyping and FcR binding

Antigen-specific antibody subclass/isotypes and FcR binding were determined using a high-throughput Luminex-based assay (*197*). Antigens included were: **H1**

A/California/07/2009, H3 A/Perth/16/2009, HA B/Brisbane/60/2008, H3 A/Victoria/361/2011, HA B/Wisconsin/01/2010, H3 A/Singapore/INFIMH-16-0019/2016, HA B/Colorado/06/2017, H1 A/New Caledonia/1999, H3 A/Wisconsin/67/X-161/2005, HA B/Malaysia/2506/2004, all provided from Immune Technology Corp., and EBOV GPdTM from Mayflower Bioscience, St. Louis, MO. Bolded strains indicate vaccine strains during the trial. Antigens were coupled to carboxylate-modified microspheres (Luminex Corp., Austin, TX) by covalent NHS-ester linkages via EDC (ThermoFisher) and Sulfo-NHS (ThermoFisher) per manufacturer's instructions. These antigen-coated microspheres were added to non-binding 384-well plates (Grenier Bio-One, Kremsmunster, Austria) at 1000 beads per well (45µl). Serum samples were heat inactivated at 56°C for 30 minutes and centrifuged to remove aggregates. They were then diluted 1:100 for IgG1, total IgG, and FcRs, and 1:10 for IgG2-4, IgA1-2, and IgM prior to incubation with beads. 5µl of diluted serum samples were added and incubated with microspheres on a shaker overnight at 4°C. Microspheres were washed, and PE-conjugated anti-IgG1, -IgG2, -IgG3, -IgG4, -IgG, -IgM, -IgA1, or -IgA2 detection antibodies (Southern Biotech, Birmingham, AL) or biotinylated FcRs (Duke Human Vaccine Institute(*246*)) conjugated to streptavidin-PE (Prozyme, Hayward, CA) were added for 1 hour at room temperature. The microspheres were washed and read on an iQue Screener Plus (Sartorius). All samples were run in duplicate and correlation between duplicates is ensured. Data are reported as the median fluorescence intensity (MFI) of detection antibody for the average of two replicates.

Antibody-dependent cellular phagocytosis (ADCP)

THP-1 phagocytosis of HA-coated beads was performed as previously described (*194*). HA antigens (H1 A/California/07/2009, H3 A/Perth/16/2009, H3 A/Victoria/361/2011, HA B/Wisconsin/01/2010, and HA B/Brisbane/60/2008) were purchased from Immune

Technologies Corp, New York, NY. Each recombinant antigen was biotinylated with EZ-link NHS-LC-LC Biotin per manufacturer's instructions (Thermo Fisher Scientific). Biotinylated protein was adsorbed onto 1 μm fluorescent neutravidin beads at a ratio of 10μg of protein to 10μl of beads (Invitrogen, Carlsbad, CA). 10 μl of antigen-coated beads were then incubated with equal volume of serum samples diluted 1:200 in PBS for 2 hours at 37°C in 96-well plates. Unbound antibody was washed away, and THP-1 cells added and incubated at 37°C for 16 hours, then fixed. Phagocytosis was measured by flow cytometry on an iQue Screener Plus (Intellicyt, Albuquerque, NM). Data are reported as phagocytic scores, calculated as the % of bead positive cells × geometric mean fluorescence intensity (GMFI)/1,000. Each experiment was performed in two independent replicates and correlation between replicates was ensured.

Antibody-dependent neutrophil phagocytosis (ADNP)

Primary human neutrophil phagocytosis was performed as previously described (*247*). HA-coated 1 μm fluorescent neutravidin beads were prepared and incubated with equal volume 1:50 diluted serum samples as in the ADCP assay. Primary human leukocytes were isolated from healthy donors using Ammonium-Chloride Potassium (ACK) lysis, then added to the opsonized beads and incubated at 37°C for 1 hour. The cells were then stained with fluorescent anti-human CD66b (Biolegend, San Diego, CA) and fixed prior to analysis on an iQue Screener Plus. Data are reported as phagocytic scores, calculated as the % of bead positive CD66+ cells × GMFI/1,000. Each sample was assayed on two healthy PBMC donors and correlation between donors was ensured ($p<0.0001$).

Antibody-dependent complement deposition (ADCD)

Serum samples were heat inactivated at 56°C for 30 minutes and centrifuged to remove aggregates. Bead-based antibody-dependent complement deposition was analyzed

as previously described (*248*). The 5 HA molecules used for the ADCP and ADNP assays were pooled in equal amounts and adsorbed to 1 µm fluorescent neutravidin beads as in the ADCP assay. HA-coated beads were incubated with 1:25 diluted, heat inactivated serum samples for 2 hours at 37°C. Lyophilized guinea pig complement (Cedarlane, Burlington, Canada) was resuspended in ice cold water, then diluted 1:60 in veronal buffer with calcium, magnesium, and gelatin (Boston Bioproducts, Ashland, MA). 150µl diluted complement was added to the opsonized beads and incubated for 20 minutes at 37°C. Beads were then washed with 15 mM EDTA and stained with anti-guinea pig C3 (MP Biomedicals, Santa Ana, CA). Samples were washed and analyzed on an iQue Screener Plus. Each experiment was performed in two independent replicates and correlation between replicates was ensured. Data are reported as the GMFI of C3 antibody for the average of two replicates.

Antibody-dependent NK Cell Activation (ADNKA)

Antibody-dependent NK cell activation and degranulation were measured as previously described (*195*, *196*). ELISA plates (ThermoFisher NUNC MaxiSorp) were coated with pooled HAs (as in ADCD), then blocked. 50µl of 1:25 diluted serum sample was added to each well and incubated for 2 hours at 37°C. NK cells were isolated from buffy coats from healthy donors using the RosetteSep NK cell enrichment kit (STEMCELL Technologies, Vancouver, Canada) and rested in 1 ng/ml IL-15 at 37°C until needed. NK cells, with anti-CD107a PE-Cy5 (BD), brefeldin A (Sigma-Aldrich, St. Louis, MO), and GolgiStop (BD), were added and incubated for 5 hours at 37°C. Cells were stained for surface markers using anti-CD56 PE-Cy7 (BD), anti-CD16 APC-Cy7 (BD), and anti-CD3 PacBlue (BD), then fixed and permeabilized using FIX & PERM® Cell Permeabilization Kit (ThermoFisher). Cells were stained for intracellular markers using anti-MIP-1β PE (BD)

and anti-IFNγ FITC (BD). Fixed cells were analyzed by flow cytometry on an iQue Screener Plus. NK cells were defined as CD3- and CD16/56+. Each sample was assayed on two healthy NK cell donors and correlation between donors was ensured ($p<0.0001$). Further, each donor was independently quality controlled to ensure that positive control values were at least two standard deviations above negative control values. Data are reported as the percentage of cells positive for each marker (CD107a, IFN-γ, and MIP-1β).

Quantification and statistical analysis

Transfer ratios were calculated by dividing the levels of cord blood antibodies by the levels of maternal antibodies. One major outlier was removed from the FCGR3A vaccinee group for visualization purposes. Numbers of samples in each group analyzed can be found in **Figure 3.1**. All univariate statistical analyses were performed using GraphPad Prism. Statistical analyses for specific assays are detailed in the figure legends. Flower plots in Figure 4 were generated in RStudio version 3.5.1 on z-scored and percentile-ranked data using the package ggplot2. Correlation matrices in Figure 4 were generated in RStudio version 3.5.1 using the package corrplot.

Classification models were developed in MATLAB. Missing values due to experimental error were imputed using k-nearest neighbor. Data was normalized using z scoring. Models were built using a previously published approach (*249*). Briefly, Elastic Net least absolute shrinkage and selection operator (LASSO) was used to select the fewest number of features to create separation between the groups. This modeling approach was evaluated through repeated fivefold cross validation, and fold-specific support vector machine (SVM) classifier model was trained using the LASSO-selected features and training data. LASSO was performed in a fivefold cross validation framework, meaning that for each fold 4/5 of the data was used for training and 1/5 of the data was used to test,

with each fifth serving as the test set once. Data was visualized using a partial least squares discriminant analysis (PLSDA). The predictive model significance was measured using a null control model with permuted labels where features were not altered, which preserves the correlation structure within the data. Each control model was repeated a hundred times to generate the distribution of model accuracies and tested against the predictive power of the actual model. The p value represents the tail probability of the true classification accuracy in the distribution of control model accuracies. For the vaccination models, all measured features were input to the model. For the H3N2 infection models, features of H3-specific antibodies were input to the model. Correlation networks were visualized in Cytoscape with correlations calculated in MATLAB. Pairwise Spearman R values describe the correlation strength and false discovery rate (FDR)-corrected q values <0.05 were used as a significance cutoff for inclusion in the correlation network.

RESULTS

VACCINATION BOOSTS ANTIBODY LEVELS, FCGR BINDING, AND FUNCTIONALITY

Previous studies have demonstrated that influenza vaccination during pregnancy results in a significant augmentation of influenza-specific antibody titers (*250*), as well as serum levels of hemagglutination inhibition (HAI) (*228*) and neutralization (*251*). However, it remains unclear whether vaccination also is able to improve or alter antibody functionality. Thus, we applied systems serology (*193*) to comprehensively profile influenza-specific antibodies in vaccinated and unvaccinated mothers and their infants. Given that there was a change in vaccine strains over the study period, the humoral immune response was dissected across all hemagglutinin (HA) strains included in the trivalent vaccine

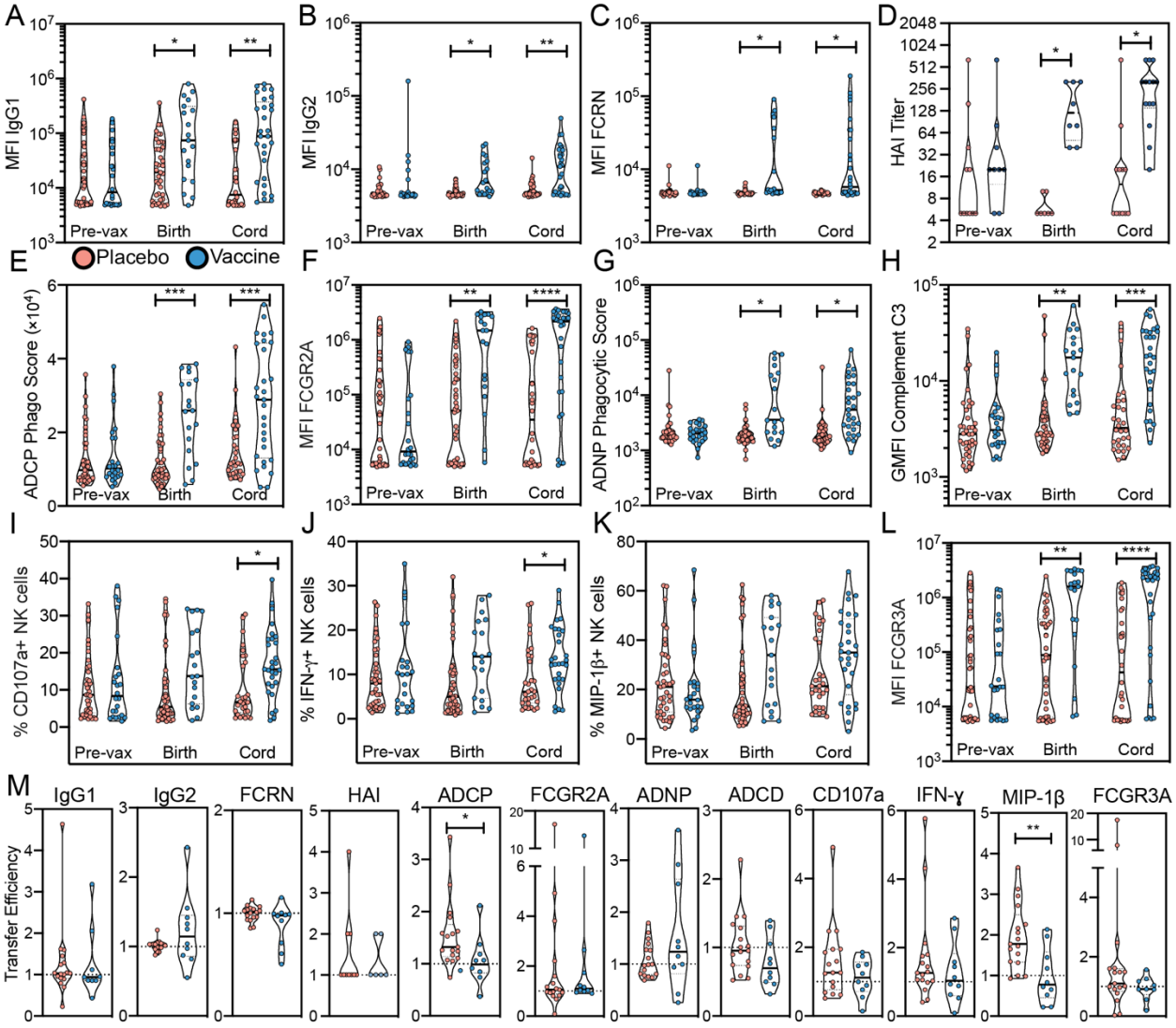

Figure 3.2 Vaccination boosts maternal and fetal antibodies, but not transfer efficiency. Violin plots (**A-L**) show isotype amounts, FCGR binding levels, HAI titers, or functional levels of H1 A/California/07/2009-specific antibodies pre-vaccination in maternal circulation, at the time of birth in maternal circulation, and in the cord blood at the time of birth. (**A**): H1-specific IgG1 MFI by Luminex bead-based assay; (**B**): H1-specific IgG2 MFI by Luminex bead-based assay; (**C**): H1-specific FCRN-binding antibody MFI by Luminex bead-based assay; (**D**): H1N1 HAI titer; (**E**): score of antibody-dependent cellular phagocytosis of immune complexed H1-coated beads; (**F**): H1-specific FCGR2A-binding antibody MFI by Luminex bead-based assay; (**G**): score of antibody-dependent neutrophil phagocytosis of immune complexed H1-coated beads; (**H**): MFI of antibody-dependent C3 deposition on immune complexed H1-coated beads; (**I**): H1-specific antibody-dependent CD107a expression by NK cells; (**J**): H1-specific antibody-dependent IFN-y expression by NK cells; (**K**): H1-specific antibody-dependent MIP-1b expression by NK cells; (**L**): H1-specific FCGR3A-binding antibody MFI by Luminex bead-based assay. Each dot represents an individual and violins show the distribution of the group. Red dots represent pairs where the mother received a placebo injection and blue dots represent pairs where the mother received seasonal influenza vaccination. (Pre-vax placebo n = 39; pre-vax vaccinee n = 24; time of birth placebo n = 41; time of birth vaccinee n = 29; cord placebo n = 30; cord vaccine n = 29.) Significance was determined by mixed-effects analysis followed by Sidak's multiple comparisons test between placebo and vaccine groups within each timepoint. Violin plots (**M**) show transfer efficiencies calculated as the ratio between cord blood experimental value and maternal experimental value at time of birth for a given antibody isotype, FCGR-binding, or function. (Placebo pairs n = 17; vaccinee pairs n = 10.) Significance was determined by Mann-Whitney U test. * $p < 0.05$, ** $p < 0.01$, *** $p < 0.001$, **** $p < 0.0001$.

during the study period. For analyses comparing vaccination to placebo (**Figure 3.2A-B**), we focused on H1-specific antibodies, as the influenza A H1N1 strain did not change during the study period, giving our analysis increased power and removing strain variability as a confounding factor.

No differences were observed in H1-specific IgG1 levels across vaccinated and unvaccinated mothers prior to vaccination, while increased H1-specific IgG1 levels were observed in vaccinated compared to unvaccinated mothers at the time of birth (**Figure 3.2A**). This maternal antibody elevation resulted in increased H1-specific IgG1 levels in the cord blood as well. A similar trend was observed for H1-specific IgG2 levels (**Figure 3.2B**), whereas no significant change following vaccination was observed for any other antibody subclass (**Figure 3.3A-B**) or isotype (**Figure 3.3D-F**). Little to no transfer of IgA or IgM was observed, as expected (**Figure 3.3D-F**).

IgG transfer across the placenta depends on the neonatal Fc-receptor (FcRn) (*252*, *253*). To determine whether vaccination altered FcRn binding, thereby improving antibody transfer, we next examined H1-specific FcRn binding. H1-specific antibodies in sera from vaccinees bound at higher levels to FcRn compared to the placebo serum (**Figure 3.2C**); however, only a subset of vaccinees (n=7) displayed this increase while others remained at baseline levels. This study was not powered to determine why that subset responded at higher levels; although all responders were term births, not all the non-responders were preterm births. Similarly, enhanced binding of H1-specific antibodies to FcRn was also observed in a subset of cord blood samples (n=10) from the vaccine arm (**Figure 3.2C**). This elevation in FcRn binding is likely at least partially attributable to the presence of higher influenza-specific IgG levels after vaccination (**Figure 3.2A, C**). These findings indicate that

vaccination both qualitatively and quantitatively changes the antibody response, enhancing the placental transfer of antibodies.

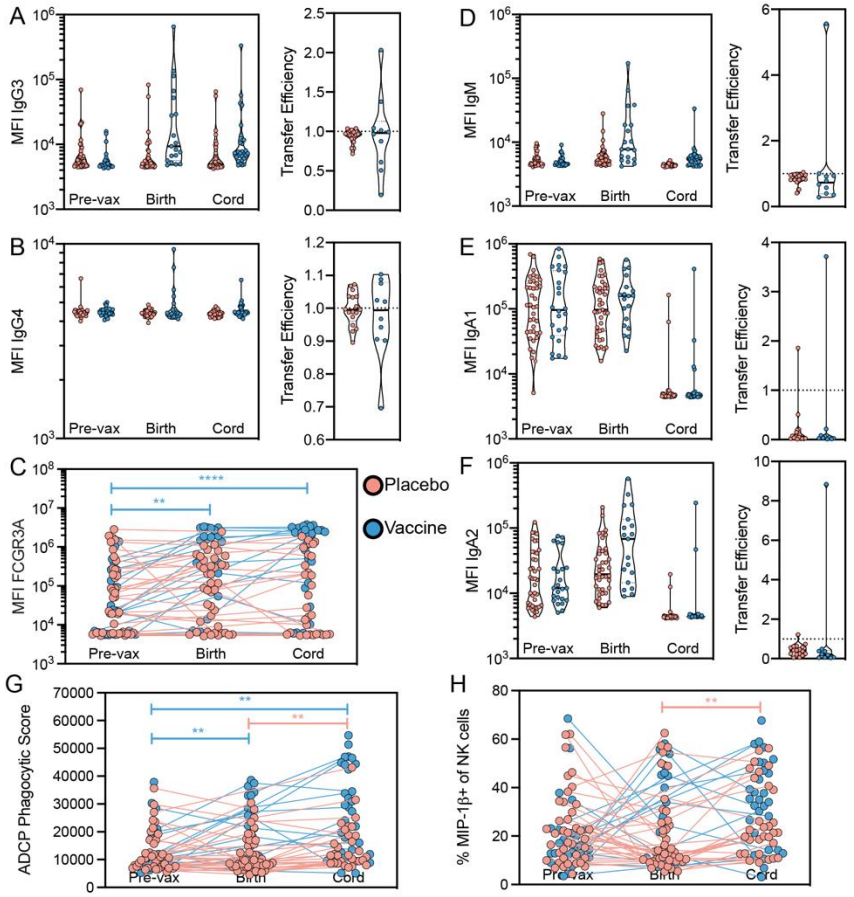

Figure 3.3 Vaccination has isotype- and subclass-specific effects. Paired violin plots show levels of H1 A/California/07/2009-specific antibodies pre-vaccination in maternal circulation, at the time of birth in maternal circulation, and in fetal circulation in the cord blood at the time of birth and the transfer efficiency of each type of antibody across the placenta at the time of birth. Each dot represents an individual and violins show the distribution of the group. Red dots represent pairs where the mother received placebo and blue dots represent pairs where the mother received influenza vaccination. Violin plots show transfer efficiencies calculated as the ratio between cord blood antibodies and maternal antibodies at time of birth. (**A**) H1-specific IgG3 by Luminex MFI; (**B**) H1-specific IgG4 by Luminex MFI; (**D**) H1-specific IgM by Luminex MFI; (**E**) H1-specific IgA1 by Luminex MFI; (**F**) H1-specific IgA2 by Luminex MFI. Dot plots show change over time for connected maternal:fetal dyads. (**C**) H1-specific FCGR3A by Luminex MFI; (**G**) Phagocytosis by monocytes of H1-coated immune complexed beads; (**H**) MIP-1b expression by H1-specific antibody-stimulated NK cells. Significance was calculated by mixed effects analysis with Sidak's multiple comparisons test or Mann-Whitney U test as appropriate, * $p < 0.05$, ** $p < 0.01$, *** $p < 0.001$, **** $p < 0.0001$.

In addition to enhanced binding to FcRn, vaccination also improved neutralizing antibody titers, antibody-dependent innate immune functions, and binding to activating Fc γ receptors (FCγRs). Specifically, HAI titers, the major correlate of vaccine-induced

protection against influenza infection, were significantly increased in both maternal and cord circulation following vaccination (**Figure 3.2D**). Additionally, antibody-dependent cellular phagocytosis (ADCP) by monocytes was increased following vaccination; this increase was transferred to neonates (**Figure 3.2E**), as was binding to the FCγR most commonly associated with phagocytosis, FCGR2A (**Figure 3.2F**). Similarly, both increases in antibody-dependent neutrophil phagocytosis (ADNP) and antibody-dependent complement deposition (ADCD) were elevated in maternal and cord blood following vaccination (**Figure 3.2G-H**). Interestingly, levels of H1-specific antibodies capable of inducing NK cell cytotoxicity (measured by CD107a expression) and cytokine release (measured by IFN-γ) were augmented in cord blood by vaccination, but vaccination had a limited effect on altering the levels of NK cell chemokine release-inducing antibodies (**Figure 3.2I-K**), corroborating previous data pointing to preferential transfer of NK cell activating antibodies (*244*). Interestingly, FCGR3A-binding antibodies increased spontaneously during pregnancy for some individuals (**Figure 3.2L**, **Figure 3.3C**), pointing to a shift in the quality of H1-specific antibodies during pregnancy, augmented by vaccination, poised for placental transfer.

To directly compare placental transfer efficiencies across all antibody features, the ratio between cord and maternal antibodies were calculated for each measurement at the time of birth. A transfer efficiency of 1 indicates equal levels of antibodies in maternal and fetal circulation, while a transfer efficiency of greater than 1 indicates that the antibodies are being selectively transferred to the cord. For most measurements, no difference was observed in transfer efficiencies between vaccinated and placebo groups (**Figure 3.2M**), indicating that the overall antibody increases in the cord blood are the direct result of increased antibody in the maternal circulation. Surprisingly, significant decreases in

transfer efficiency were observed in the vaccinated group for ADCP and antibody-mediated MIP-1β production by NK cells (**Figure 3.2M**). Whereas in placebo recipients, placental transfer enriched the levels of ADCP and MIP-1β inducing antibodies in the cord compared to maternal circulation, transfer in vaccine recipients was not consistently enriched (**Figure 3.3G-H**). This suggests that the placenta may have a maximal transfer capacity for these antibodies, and when maternal levels exceed those at which the placenta can transfer, no more antibody is provided to the fetus. Collectively, these data point to an overall shift in vaccine-induced antibody levels during pregnancy that lead to a concordant augmentation of functionally enhanced antibodies in neonates, governed partially in a quantitative manner by augmented antibody levels, but also driven by qualitative changes in FcRn binding and NK cell activating antibodies.

FCγR-BINDING ANTIBODIES ARE SELECTIVELY ENHANCED FOLLOWING VACCINATION IN MOTHERS AND CORD

Given the broad improvement of antibody amounts, FcR binding capacity, and functional activation in response to vaccination, we next aimed to determine which humoral features were most significantly altered by vaccination. To avoid overfitting, an Elastic Net-Least Absolute Shrinkage and Selection Operator (LASSO) feature selection was first utilized to minimize the features to only include the fewest features that explained the overall variance in the dataset. Feature reduction was then followed by Partial Least Squares Discriminant Analysis (PLSDA) to visualize the separation between groups (*249*). These analyses were initially run including all samples for which antibody subclass, FcR binding, and functional data were available (**Figure 3.4**). Secondly, the analysis was run with only samples for which HAI titer values were calculated (**Figure 3.5**), a subset of the initial sample set. Importantly, while there were no differences between the mothers prior

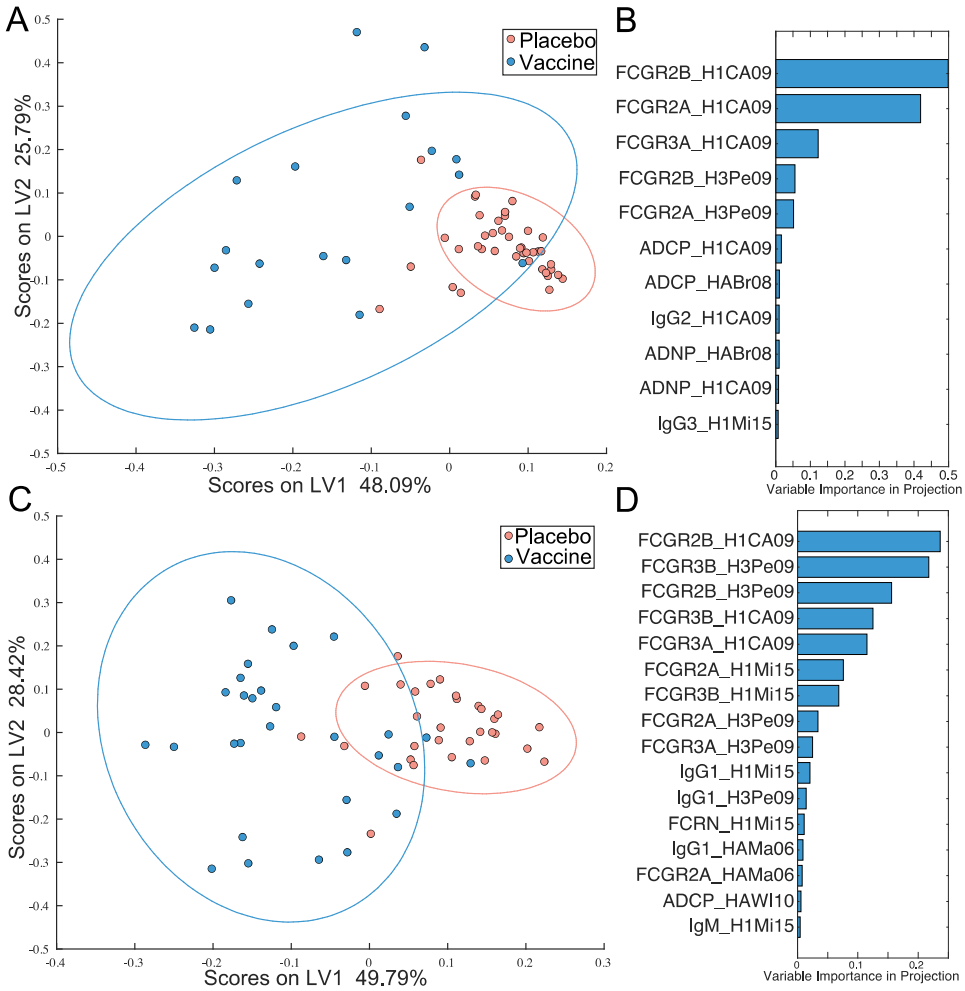

Figure 3.4 FCGR binding levels separate vaccinee mother-child pairs from placebo recipients. Dot plots show Partial Least Squares Discriminant Analysis (PLSDA) scores along latent variable 1 (LV1) and latent variable 2 (LV2) for maternal samples at the time of birth (**A**) and cord blood samples (**C**). PLSDA was modeled using Least Absolute Shrinkage and Selection Operator (LASSO)-selected features out of the total pool of measured humoral biophysical and innate immune functional features. LV percentages represent the amount of total variance between samples captured by that LV. Bar plots show Variable Importance in Protection (VIP) scores for the LASSO-selected features separating vaccinees from placebo recipients for maternal samples at the time of birth (**B**) and cord blood samples (**D**). VIP scores reflect the contribution of a feature across all latent variables.

to vaccination, separation was observed across the placebo and vaccinated mothers after vaccination, at the time of birth (**Figure 3.4A**). Interestingly, this separation was not dependent on HAI, as when it was included in the model it was not selected by the LASSO algorithm as a contributing feature to separation across LV1 and LV2 (**Figure 3.5A-B**). Specifically, using Fc-features alone, vaccinated and unvaccinated mothers could be

resolved with nearly 80% cross-validation accuracy, with model significance of p <0.001 compared to permuted label model (**Figure 3.4A**). This separation was primarily driven by binding of both H1- and H3-specific antibodies to FCGRs, as summarized by the variable importance in projection (VIP) scores, which rank the minimal set of features required to discriminate the groups based on their relative importance in driving separation across the groups (**Figure 3.4B**). Additionally, phagocytic functions and levels of some H1-specific antibody IgG subclasses were enriched in the vaccinee serum compared to the placebo

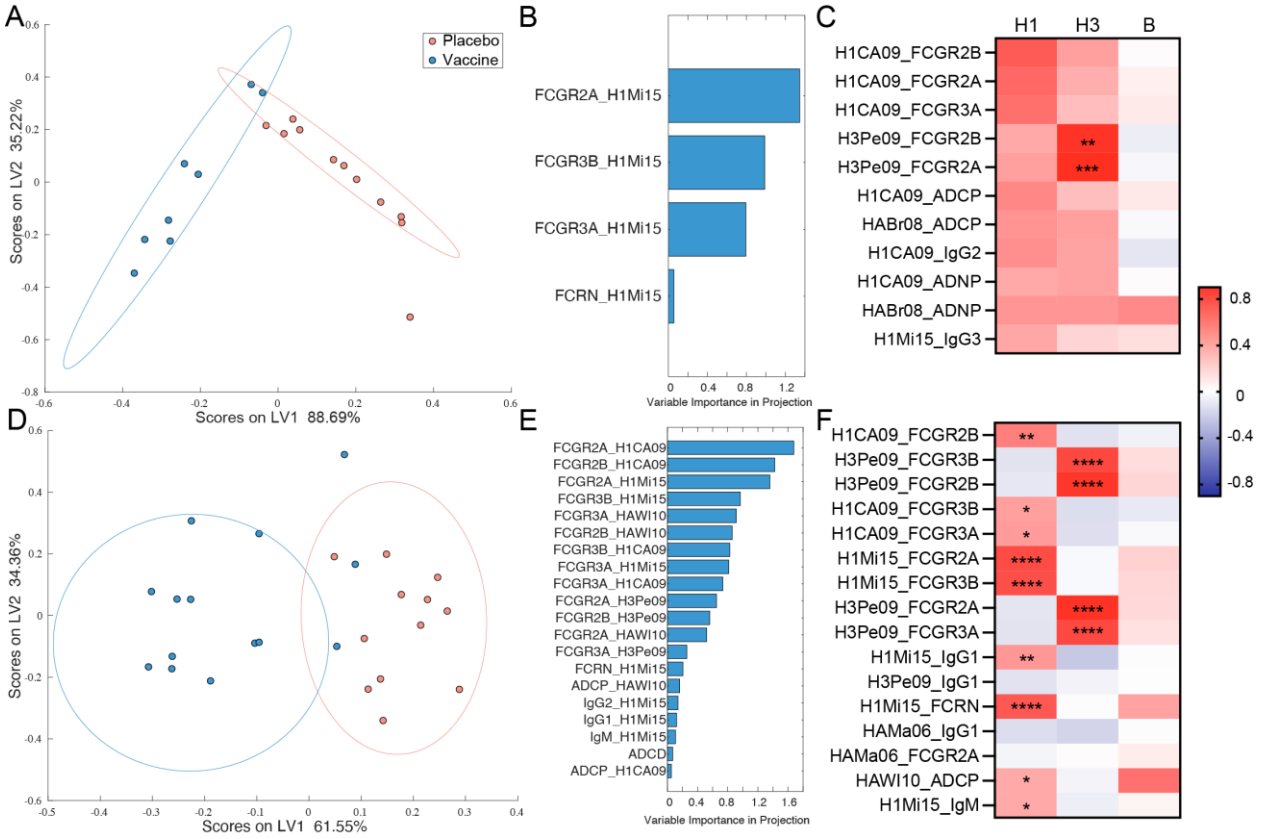

Figure 3.5 HAI is not a key feature separating vaccinees from placebo recipients. Dot plots show PLSDA scores along latent variable 1 (LV1) and latent variable 2 (LV2) for maternal samples at the time of birth (**A**, p < 0.001 compared to permuted label model) and cord blood samples (**D**, p < 0.01 compared to permuted label model). PLSDA was modeled using LASSO-selected features out of the total pool of measured humoral features, including HAI. LV percentages represent the amount of total variance between samples captured by that LV. Bar plots show VIP scores for the LASSO-selected features separating vaccinees from placebo recipients for maternal samples at the time of birth (**B**) and cord blood samples (**E**). VIP scores reflect the contribution of a feature across all latent variables. Correlation matrices show Spearman correlation R values calculated pairwise between HAI titers and LASSO-selected features for samples taken from maternal circulation (**C**) and cord blood (**F**) at the time of birth. Stars indicate Bonferroni-corrected p values: * < 0.05, ** < 0.01, *** < 0.001, **** <0.0001.

serum. While HAI was not selected by the model (**Figure 3.5B**), HAI was correlated with some model selected features (**Figure 3.5C**). At the maternal time of birth, many of the FCGR-binding levels and antibody-dependent functions induced by vaccination were positively, although not significantly, correlated with HAI titers. This is consistent with the univariate analyses (**Figure 3.2**), highlighting vaccine-induced changes in antibody levels and HAI titers, but most significantly in FCGR-binding antibodies following vaccination.

Similar to maternal blood, robust separation was observed in HA-specific antibodies in cord blood using Fc-profiling. Specifically, vaccinated and unvaccinated cord bloods could be discriminated with over 75% cross-validated accuracy using as few as 16 LASSO-selected features out of the overall 146 features measured for each sample ($p<0.01$ compared to permuted label model, **Figure 3.4C**), and again, HAI titers were not selected as a discriminatory feature between vaccinated and placebo pairs (**Figure 3.5D-E**). Improved binding to multiple FCγRs were among the top features that distinguished cord antibodies from the infants of vaccinated and unvaccinated mothers (**Figure 3.4D**). Moreover, IgG1 levels were also included in the model, along with FcRn binding, suggesting both quantitative and qualitative features independently improved in the cord following vaccination (**Figure 3.4D**). Again, while HAI was not highlighted by the machine learning model (**Figure 3.5E**), HAI titers do correlate significantly with FCγR binding levels and HAI for both H1N1 and H3N2 influenza (**Figure 3.5F**). This increase in intercorrelation when compared to the maternal blood samples perhaps suggests a preferential transfer of antibodies capable of driving both neutralizing and extra-neutralizing antibody functions. These data illustrate the parallel shift in maternal (**Figure 3.4A-B**) and cord (**Figure 3.4C-**

D) sera, highlighting the continuum across the mother and fetus resulting in the transfer of highly functional antibodies to the infant following vaccination.

FCγR-BINDING ANTIBODIES, RATHER THAN OVERALL ANTIBODY CONCENTRATIONS, DISCRIMINATE INFANTS THAT LATER DEVELOP INFLUENZA INFECTION

Follow-up of both vaccinated and unvaccinated mother-infant pairs allowed the identification of a number of infant influenza cases in this study (*228*). Here we aimed to determine whether antibody Fc profiles also tracked with differential infant outcomes after birth. Thus mother-infant pairs were divided into those who remained uninfected for the duration of this study and those who went on to have infant infection with H3N2 (**Figure 3.1C-D**). We focused on H3N2 infection as it was the most common strain of influenza responsible for infant infections in this study. No differences were observed in IgG1 and IgG2 levels across those with and without infant influenza infection (**Figure 3.6A-B**). Additionally, no differences were observed in the level of H3-specific FCRN-binding antibodies across the groups (**Figure 3.6C**). However, significant differences in H3-specific FCγR binding capacity were observed in the cord blood of infants who later became infected with influenza compared to those who did not (**Figure 3.6D-F**). Infants who would ultimately become infected had lower levels of FCγR-binding antibodies specific to the infecting strain of influenza when compared to infants who were not infected. These data point to the importance of qualitative changes in FCγR-binding antibodies transferred across the placenta, rather than the overall levels of HA-binding antibodies, in protection from influenza infection in early life.

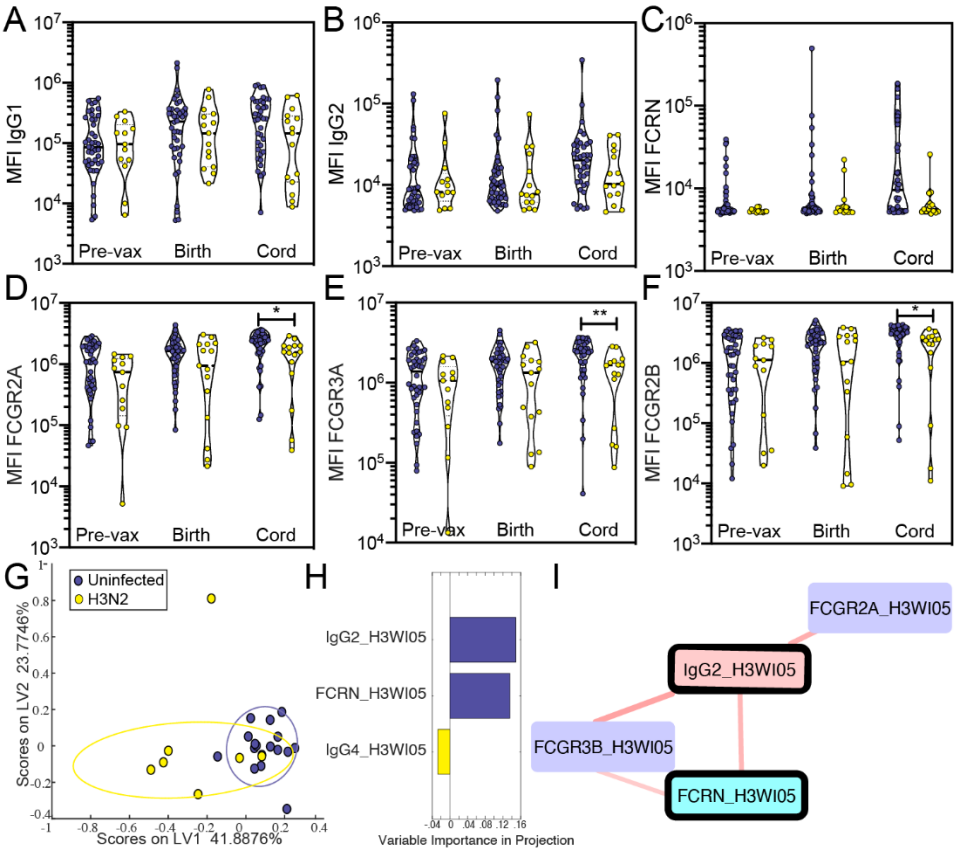

Figure 3.6 FCGR binding levels separate infected infants from uninfected infants. Violin plots (**A-F**) show isotype or FCGR binding levels of H3 A/Perth/16/2009-specific antibodies pre-vaccination, at the time of birth in maternal circulation, and in the cord blood at the time of birth. **A**): H3 A/Perth/16/2009-specific IgG1 MFI by Luminex bead-based assay; (**B**): H3 A/Perth/16/2009-specific IgG2 MFI by Luminex bead-based assay; (**C**): H3 A/Perth/16/2009-specific FCRN-binding antibody MFI by Luminex bead-based assay; (**D**): H3 A/Perth/16/2009-specific FCGR2A-binding antibody MFI by Luminex bead-based assay; (**E**): H3 A/Perth/16/2009-specific FCGR3A-binding antibody MFI by Luminex bead-based assay; (**F**): H3 A/Perth/16/2009-specific FCGR3A-binding antibody MFI by Luminex bead-based assay. Each dot represents an individual and violins show the distribution of the group. Purple dots represent pairs where the infant would not be infected with influenza in the first six months of life and yellow dots represent pairs where the infant would be infected with influenza A/H3N2 in the first six months of life. (Pre-vax control n = 42; pre-vax case n = 21; time of birth control n = 40; time of birth case n = 20; cord control n = 39; cord case n = 20.) Significance was determined by mixed-effects analysis followed by Sidak's multiple comparisons test between placebo and vaccine groups within each timepoint. * $p < 0.05$, * $p < 0.01$. Dot plot (**G**) shows PLSDA scores along latent variable 1 (LV1) and latent variable 2 (LV2) for transfer efficiencies. (Control pairs n = 17; case pairs n = 7.) PLSDA was modeled using LASSO-selected features out of the total pool of H3-specific transfer efficiencies. Bar plot (**H**) shows VIP scores for the LASSO-selected features separating H3N2-infected infant transfer efficiencies from uninfected infant transfer efficiencies. Correlation network (**I**) shows positive correlation between LASSO-selected features (thick borders) and their co-correlates with a significance cutoff for inclusion at false discovery rate (FDR)-corrected q values <0.05. Purple boxes indicate FCGRs, blue boxes indicate FCRN, and pink boxes indicate IgG amounts.

To further dissect the minimal Fc-features that were uniquely enriched in infants who did not develop influenza infection, we next used a similar LASSO-PLSDA model to our previous analysis (**Figure 3.6G**). Here, because of the differences in cord but not

maternal antibodies, we focused on transfer ratios for all measured antibody Fc features across mother-infant pairs, comparing infants with and without H3N2 influenza infection at follow-up. Using these data, separation was achieved between the two groups, with nearly 80% cross-validation accuracy ($p = 0.02$). Interestingly, just 3 features were necessary to split the groups including enhanced transfer of IgG2 and FCRN binding in the uninfected mother:cord pairs and elevated IgG4 transfer ratios in infected mother:cord pairs (**Figure 3.6H**). Enhanced transfer of H3-specific IgG2 and FCRN transfer efficiencies may mark overall enhanced transfer of H3-specific antibodies. Conversely, increased levels of H3-specific IgG4s, known to drive reduced FCGR activity (*65*), may mark dysregulated transfer of poorly functional antibodies in infants who went on to develop H3N2 infection.

Because LASSO does not select features based on their biological significance, but rather simply based on their overall influence on the variance across the sample groups, we next examined whether additional co-correlates existed that could provide information on the LASSO-selected features. In addition to IgG2 and FcRn transfer, transfer of H3-specific-FCGR2A- and FCGR3B-binding antibodies were positively correlated to the LASSO-selected features (**Figure 3.6I**). As a particular point of interest, the features selected in this analysis were not significantly correlated with HAI titer in these infants (**Figure 3.7**), indicating that extra-neutralizing antibody effector mechanisms may play a central part in preventing disease in infants. Overall, the results of this analysis point to IgG2 as a biomarker of more robust transfer of a protective immune response, resulting in the transfer of antibodies able to bind more effectively to FCGRs. These FCGR-binding antibodies may mechanistically underlie protection from influenza outcomes in neonates.

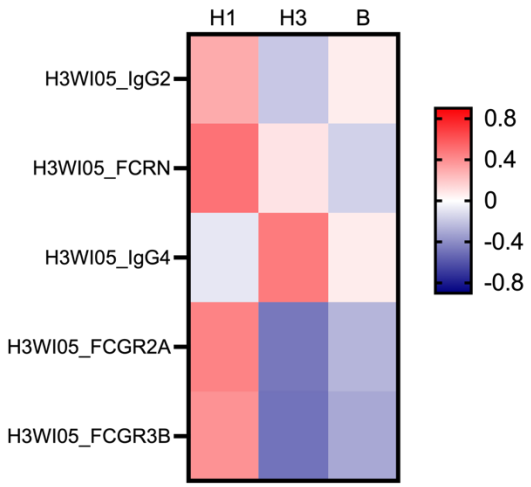

Figure 3.7 Correlations between LASSO-selected features and HAI. Correlation matrix shows Spearman correlation R values calculated pairwise between HAI titers and LASSO-selected features for samples cord blood at the time of birth for infants who went on to become infected with H3N2 influenza or remained uninfected throughout the trial. No correlations were significant when corrected for multiple comparisons.

CORD BLOOD FROM UNINFECTED INFANTS SHOWS TARGETED HUMORAL IMMUNE PROFILE

Given the presence of both univariate and multivariate humoral discriminators across the infected and uninfected infants and their mothers, we next aimed to get a sense of the overall architecture of the polyclonal humoral immune response. Flower plots showing the relative magnitude of response within each group at each timepoint (**Figure 3.8A**) reveal overall higher humoral responses across influenza-specific antibody-dependent functions, antibody FCγR binding, and antibody isotype levels within the uninfected group as compared to the infected group at each timepoint. Levels of IgA were similar across the maternal groups and time points, emphasizing that current vaccination strategies do not induce robust IgA responses. Furthermore, expanded FCγR-binding profiles were observed among the uninfected maternal timepoints, but there was selective and more striking expansion of FCγR-binding antibodies in the cord blood of uninfected infants, linked to

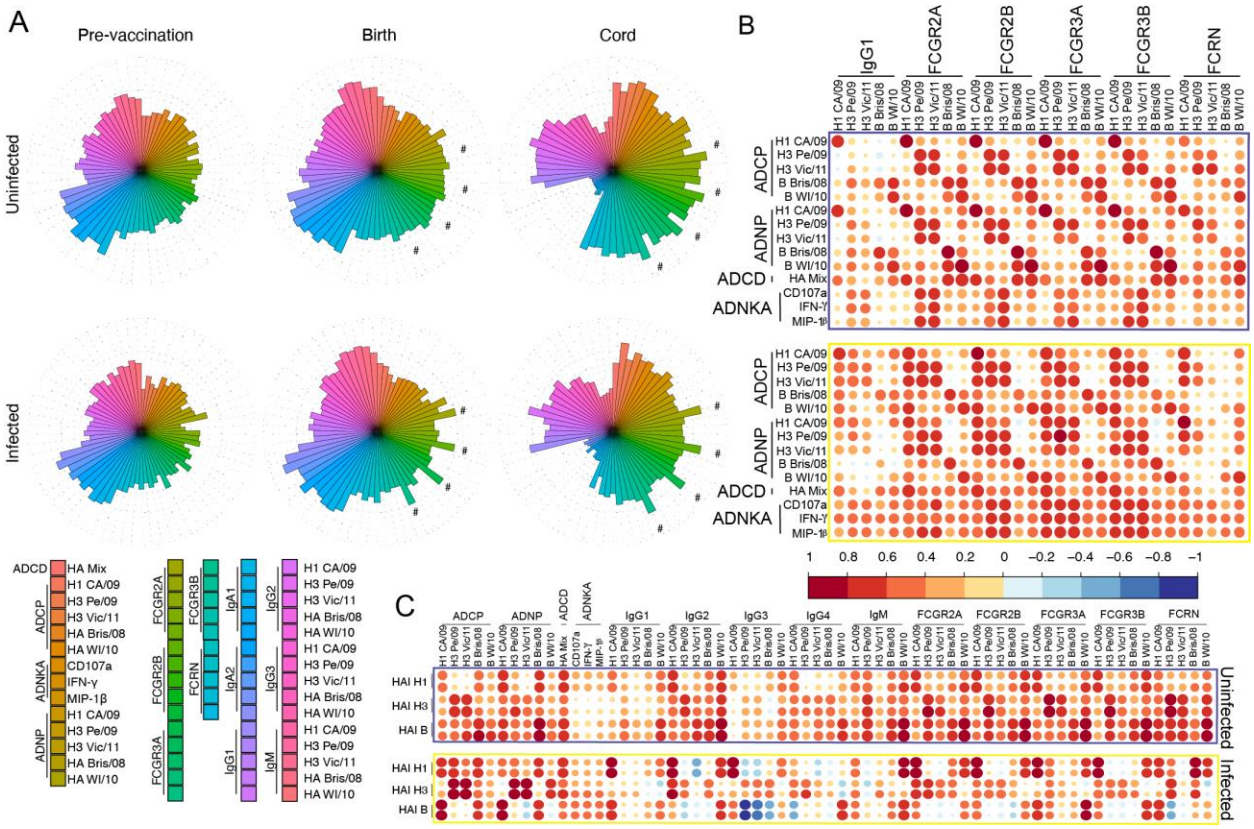

Figure 3.8 Humoral intercorrelation in cord blood differentiates infected infants from uninfected infants. Flower plots (**A**) show average relative magnitude of measured humoral features within a timepoint (maternal pre-vaccination, maternal time of birth, and cord blood) and group (uninfected vs infected). # marks the wedges representing H1 CA/09 FCGR binding levels, as referenced in the text. Heat maps (**B, C**) show Spearman correlation coefficients for intercorrelations between measured antibody features. Within all features (except ADCD and ADNKA) the five rows correspond to antigens specific for the five vaccine antigens: H1 A/California/07/2009, H3 A/Perth/16/2009, H3 A/Victoria/361/2011, B/Brisbane/06/2008, and B/Wisconsin/01/2010. ADCD and ADNKA were performed on pooled HA antigens, and ADNKA rows correspond to NK activation readouts: CD107a, IFN-γ, and MIP-1β. Matrices represent data for all cord blood samples pooled by infection outcome. For the subset of samples with HAI titers measured, matrix (**C**) represents Spearman correlation coefficients between HAI against vaccine strains (vertical) and antibody functional and biophysical features along the horizontal.

enhanced FCRN-binding antibodies in the cord, which indicate increased placental transfer. Specifically, we observed a selective enrichment of FCγR-binding antibodies specific to H1 CA/09 in the infected group both in maternal circulation at the time of birth and in cord blood (shown by the wedges marked with # in those plots). Since most of these infants were infected with H3N2, these data may point to a mis-directed immune response primarily targeting H1N1 influenza, resulting in increased susceptibility to H3N2

influenza. In the uninfected group, the relative magnitude of the immune response was similar across all influenza strains (H1N1, H3N2, B).

To further dissect the humoral profile in the cord blood of infants, correlation matrices were calculated and visualized across functions, IgG1 levels, and FCγR-binding levels (**Figure 3.8B**). Focused and robust relationships between the same subtype of influenza and function were observed in uninfected infants, in contrast to the heterogeneous response patterns in the infected infant cord blood samples. In the uninfected infants (**Figure 3.8B top**), robust and highly focused correlations were observed between phagocytic functions and FCγR-binding antibodies to the same antigen specificity, with strong coordination within H1, H3, or B immune profiles. Infected infants exhibited a diffuse positive, but weaker, correlational profile marking a lower level of functional coordination that may be insufficient to drive protective immunity (**Figure 3.8B bottom**). Within the sample group for which HAI titers were available, correlations were plotted between HAI and influenza-specific antibody-dependent innate immune functions, isotypes, and FCγR binding (**Figure 3.8C**). Here, increased correlation between neutralizing and extra-neutralizing functions/FCγR binding across isotypes was observed in the uninfected cord blood, whereas infected cord blood shows higher levels of strain-specific correlations. This further reinforces the conclusions drawn by the multivariate analyses in **Figure 3.6** that protection tracks with FCγR-binding levels as well as the previously reported HAI titers (*228*). Thus, in addition to the individual biomarkers of protective humoral immunity, these data point to distinct humoral architecture in infants that ultimately are protected from influenza infection.

VACCINATION SHAPES THE TRANSFER OF PROTECTIVE IMMUNITY TO THE CORD

Finally, we examined whether LASSO-selected features that distinguish vaccinee and placebo cord blood profiles are sufficient to predict protection from subsequent influenza infection. A model built on vaccine-augmented features classified infants into those that remained uninfected or became infected significantly better than a model using all features (**Figure 3.9A-B**). The vaccine-modified features were not uniformly associated with protection, but some features were enriched in the uninfected infants and others were enriched in the infected infants (**Figure 3.9C**). H3-specific FCγR responses were enriched in uninfected infants (**Figure 3.9C**), which was likely influential in protection given that dominant seasonal infections were H3N2 during the study period (*228*). Conversely, H1-specific FCγR responses were enriched in infected infants, supporting the critical importance of strain-specific immunity in protection from disease. However, beyond IgG levels, when considered holistically as part of latent variables in the PLSDA model, HA strain-specific FCγR-binding features were highly discriminatory across the two groups (**Figure 3.9C**, **Figure 3.10**). These data suggest that vaccine strategies able to tune FCγR binding in a strain specific manner could potentially drive enhanced protection in the first months of life. The observation that the FCγR-binding levels of antibodies, but not overall amounts, were both enriched in cord blood by the vaccine (**Figure 3.4**) and involved in protection (**Figure 3.6**, **Figure 3.9**) suggests that the mechanism of protection by this vaccine may be driven by increased levels of the antibodies capable of recruiting FCγRs. Thus, beyond neutralizing antibody transfer from mother to child in the cord blood of vaccinated mothers (*228*), the data presented here point to a cooperative role of FCGR2A and FCGR3A in vaccine-induced protection from influenza infection.

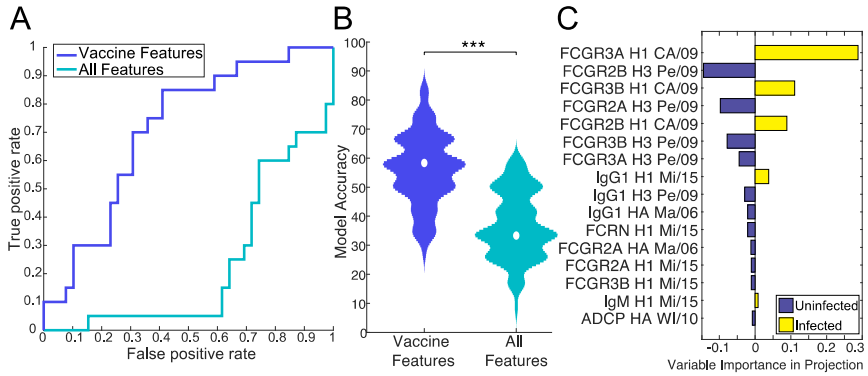

Figure 3.9 Vaccination strongly affects the protective humoral features in cord blood. PLSDA models were trained to distinguish between cord blood of infants who go on to be infected versus those who do not, using either all measured features (light blue) or just those features determined to distinguish between cords of infants whose mothers were vaccinated and those who were not as shown in Figure 2B (dark blue). Receiver Operating Characteristic (ROC) curves for final models are represented in (**A**). Positive rates refer to the model's ability to correctly classify cords into infected or uninfected – a false positive indicates an incorrect designation as a case where a true positive indicates a correct designation as a case. Model accuracy in identifying cords of infected versus uninfected infants was tested for each fold- and replicate-specific test data set. These values are represented in the violin plot (**B**). Significance was determined by Mann-Whitney U test (*** $p<0.001$). Bar plot (**C**) shows VIP scores for the vaccine LASSO-selected features separating infected infant transfer efficiencies from uninfected infant transfer efficiencies. Bars in yellow show features enriched in infected infants while bars in purple show features enriched in uninfected infants.

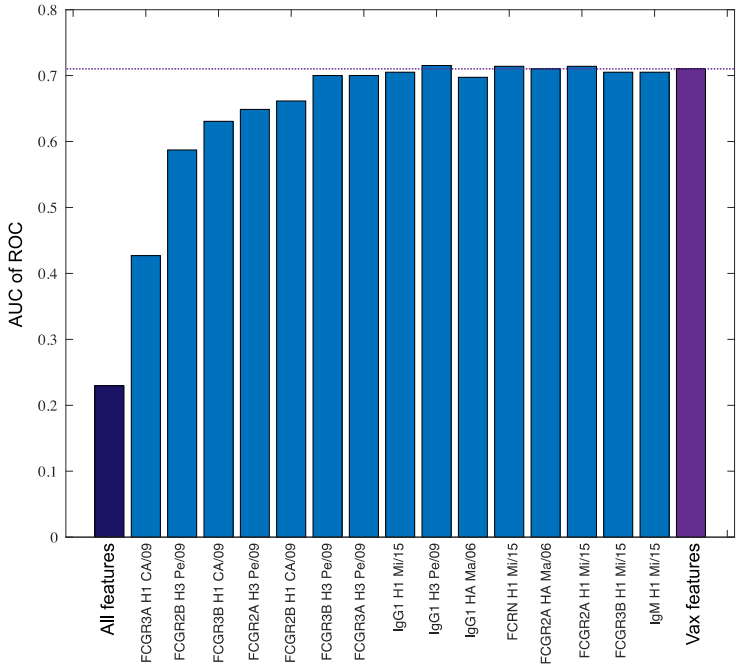

Figure 3.10 Vaccine-induced features separate infected from uninfected infants. Bar plot shows the area under the curve for ROC of the PLSDA separating H3-infected infants from uninfected infants. Dark blue bar (left) shows AUC of ROC for all measured humoral features. Purple bar (right) shows AUC of ROC for vaccine LASSO-selected humoral features (**Figure 3.9**). Blue bars in between show sequential addition of individual features; leftmost blue bar shows only FCGR3A H1 CA/09, then each sequential feature is added moving from left to right.

DISCUSSION

Beyond neutralization, mounting evidence points to a critical role of Fc effector functions in protection against influenza infection in adults (*62*, *254*). However, whether these responses are also critical for protection in infants, and whether they are tunable via influenza vaccination remain unclear. Using a unique cohort of longitudinally followed pregnant women who were enrolled in a randomized clinical trial of influenza vaccine or placebo, here we had a unique opportunity not only to probe the influence of vaccination on shaping Fc-effector function across the maternal:fetal dyad, but also to probe the antibody features that tracked with protection against infection. While naturally, irrespective of vaccination, the production of increased levels of FCγR and FcRn binding antibodies occurred over the course of pregnancy, vaccination during pregnancy led to a robust augmentation of neutralizing and extra-neutralizing functional antibodies. Moreover, seasonal inactivated influenza vaccination preferentially increased the transfer of FCγR-binding antibodies across the placenta in coordination with the enrichment of both FCγR-binding and HAI titers in the cord blood. Yet most critically, lower levels of FCγR-binding antibody transfer and diffuse HA-specific functional antibody-coordination was correlated with increased risk of infection independently of HAI titer. These data point to both a critical role for Fc-effector function in protection from infection in early life, as well as opportunities for vaccination to selective augment functions that may be most desirable for protection.

Previous studies of pertussis and influenza have indicated that maternal vaccination is protective for both pregnant individuals and neonates (*225*, *245*, *255–257*). Here we show that influenza vaccination in pregnancy increases Fc-effector functions, highlighting that the quality of the humoral immune response increases with quantitative changes in

vaccine-induced antibody amounts. Moreover, influenza-specific FCγR-binding levels were significant co-correlates of influenza vaccination and were chosen by an unbiased modeling approach over HAI titers when both were included in the model dataset. However, the ability to compare HAI to other humoral features in this dataset is limited, owing to the lack of available HAI data across many of the vaccinees. Further studies specifically designed to answer this question will be required to fully define the key correlates of protection. Given that the placenta selectively transfers highly effective antibodies to the infant, developing vaccine strategies that can maximize the induction of functional antibodies in pregnancy may be key to improving neonatal immunity. Among proposed strategies, the use of adjuvants may bolster vaccine-induced immune responses (*258*, *259*) and could be used to selectively promote the most efficacious humoral immune responses. Future studies of adjuvanted influenza vaccination during pregnancy that characterize the functional humoral immune response would further elucidate these mechanisms and ensure that vaccines given during pregnancy are as efficacious as possible.

In this study, participants were under weekly respiratory virus symptom surveillance from enrollment to six months after birth, which captured symptomatic infections but did not track disease severity and may have missed asymptomatic infections or sub-clinical disease. While we cannot fully determine whether the uninfected dyads were exposed, clear deficits and differences were observed in antibody transfer across the dyads. However, to reduce variability in this study, we elected to focus solely on the dyads that became infected with H3N2, given the predominance of infections with this strain throughout the study. Moreover, due to the limited number of dyads infected with non-H3N2 strains, the power was insufficient to perform a secondary analysis. With future studies, focused on validation across years, it may be possible to determine whether the

humoral features linked to protection here apply to additional influenza strains or other geographically distinct cohorts, and to further analyze the interplay of HAI with extra-neutralizing antibody functions, which was outside the scope of the current study. Finally, comorbidities, malnutrition, and coinfections may alter both vaccine-induced immunity in mothers, as well as Fc-placental transfer and correlates of immunity, confounding issues that will be of critical interest in countries such as Nepal, which has high rates of diarrheal diseases (*260*), tuberculosis (*261*), and child malnutrition (*262*). We note that Nepal also has a low prevalence of HIV (*263*) and malaria (*264*), which have been shown to diminish transplacental antibody transfer.

Previous studies in the elderly have shown mixed results as to the efficacy of seasonal influenza vaccines at eliciting FCγR-binding antibodies (*79*, *237*). However, elderly individuals are known to have decreased responses to traditional influenza vaccination strategies (*265*, *266*). Vaccination during pregnancy does increase both HAI titers and influenza-specific IgG concentrations (*236*, *267*), but the impact of pregnancy on the functional humoral immune response to influenza vaccination is only beginning to be understood. As shown in the primary results from the clinical trial (*228*), maternal influenza vaccination was linked to protection in infants that could not be fully explained by overall antibody transfer. While other factors, such as antibodies in breastmilk (*268*, *269*) and decreased exposure risk from a vaccinated mother likely also contribute to this protection, in this study, vaccine impacts on the influenza-specific immune response, beyond antibody neutralization or hemagglutination inhibition titers, were identified. Influenza vaccination enriched the serum of both mothers and infants to induce more antibody-dependent innate immune functions and increased influenza-specific IgGs overall. Vaccinees and their infants were distinguished from placebo recipients by an enrichment of

FCγR-binding antibodies. Moreover, the transplacental transfer from maternal to cord blood of these vaccine-induced FCγR-binding antibodies was linked to protection against influenza infection in infants. In sum, these functionally efficient antibodies are enriched by maternal vaccination and, when transferred to the infant, appear to be providing protection after birth. The data presented here provide a critical new dimension to our understanding of maternal influenza vaccination, highlighting the presence of functionally potent antibodies that can be boosted by vaccination during pregnancy and transported to the infants, resulting in protection of the infants from influenza infection. Which specific mechanisms are most critical for neonatal influenza infection or disease remain to be determined, as well as efforts to define the specific vaccine strategies that may selectively elicit these functions to protect this vulnerable population.

Chapter 4: VACCINE-INDUCED ANTIBODY MEDIATED NK CELL ACTIVATION AS A KEY CORRELATE OF IMMUNITY AGAINST INFLUENZA IN OLDER ADULTS

Based on a manuscript in preparation:

Boudreau, C.M., Burke, J.S. IV, Yousif, A.S., Jastrzebski, S., Verschoor, C.P., McElhaney, J.E., Kuchel, G.A., Lingwood, D., Sridhar, S., Kleanthous, H., Landolfi, V. & Alter G. Vaccine-induced antibody mediated NK cell activation as a key correlate of immunity against influenza.

Author contributions: CMB, DL, HK, VL, SS, and GA designed the research study. IDB and VL participated in the original clinical study from which samples were drawn. SJ, CV, JM, and GK provided older adult NK cells and designed that experiment together with CMB and GA. CMB, JSB, and ASY conducted experiments and acquired data. MS provided and tittered influenza virus for animal studies. CMB analyzed data. CMB and GA wrote the manuscript.

Antibodies play a critical role in protection against influenza; however, antibody levels and direct viral neutralization alone represent incomplete correlates of immunity. Instead, the ability of antibodies to leverage the antiviral power of NK cells, monocytes, neutrophils, and complement have all been implicated in protection from or clearance of influenza infection. Yet, the precise antibody effector functions most critical for protection against influenza infection remain unclear. Using systems serology, the humoral immune response to influenza was comprehensively profiled in a cohort of older adult (>65 years of age) vaccinees monitored for infection over the influenza season. Robust vaccine-induced humoral immune responses were observed against both the vaccine H3N2 and circulating (H1N1, H3N2 and influenza B) strains. Influenza HA- and NA-specific Fc γ receptor 3A (FCGR3A) binding antibodies and NK cell activating antibodies were identified as key

correlates of protection from infection, strongly arguing for a role for NK cells in protection against influenza. Similarly, mature mice showed no protection mediated by enhanced NK cell activating antibodies, and NK cells from older adults were less reactive to FCGR3A-mediated stimulation. Together, these data pointed to the critical need for a selective induction of influenza-specific NK activating antibodies to achieve protection in older adults. Furthermore, these data provide clues related to mechanistic correlates of immunity in the population aged 65 years and older that may provide a targeted path to improved vaccine design, and further implicates NK cells as key players in host defense against influenza.

INTRODUCTION

Over the past decades, seasonal influenza has caused increasing numbers of deaths in the United States, explained in part by the growth of our aging population (*270*). Older individuals suffer from a disproportionate burden of severe disease and hospitalization following influenza infection, even in the setting of broad vaccine campaigns (*271*). While seasonal vaccination has resulted in a 40% reduction in hospitalizations in older adults (*272*), the current vaccine is estimated to provide a range of protection from 10-60% in the general population, depending on the match between vaccine and circulating strains each year (*273*). In frail older adults, vaccine effectiveness drops substantially lower (*274*). Thus, beyond the goal of developing a universal vaccine able to induce broad immunity across varying strains, our lack of understanding of the key correlates of immunity against influenza across the age spectrum has severely limited next generation influenza vaccine design and development.

Influenza strains for each year's vaccine are selected by the World Health Organization during the previous year to allow for production of vaccine doses in chicken eggs (*275*). During the 2012-2013 influenza season, an H3 antigen was selected that underwent an adaptation in the egg culture, resulting in the acquisition of three amino acid mutations across two important antigenic sites (*276*). Despite high titer humoral immune responses to the vaccine, neutralizing titers to the circulating wild type strain were decreased by approximately eight-fold compared with responses to the egg adapted strain (*276*), which was associated with reduced protection against the virus (*277*). However, correlates analyses observed that remaining hemagglutination inhibition (HAI) accounted for only about 60% of protection observed over the season (*16*, *19*, *278*), suggesting that other antibody effector functions were likely to contribute to protection, even in the setting of the viral adaptation. The additional functional correlates of immunity remain incompletely defined but could provide key insights for the design of both broadly specific and functionally optimized immune responses required for universal protection against influenza.

The identification of broadly reactive monoclonal antibodies, such as CR6261(*162*) and CR9114 (*279*), that provide robust *in vivo* protection (*214*, *280*) even in the absence of HAI titers have raised the possibility that additional humoral mechanisms beyond HAI titers may be critical for immunity against influenza (*39*, *40*, *62*). Several antibody effector functions have been implicated in protection from influenza infection (*62*), including antibody mediated macrophage phagocytosis (*56, 60*), neutrophil activation (*56*), antibody-dependent cellular cytotoxicity (ADCC) (*57*) by NK cells, monocytes, and neutrophils, and complement-specific lysis (*54*, *55*, *60*, *61*). HA-specific functional antibodies capable of inducing ADCC arise earlier following infection and are more broadly reactive than

neutralizing antibodies (*199*), and have been shown to decrease symptom severity and increase viral clearance (*78*). Furthermore, in older adults, increased ADCC activity correlated with strong HAI responses following vaccination (*79*), although HAI antibodies may compete with ADCC antibodies for access to antigenic epitopes (*86*). However, whether ADCC alone is critical for protection, or whether ADCC antibodies work in tandem with other antibody effector functions to provide maximal protection from infection, remains incompletely understood.

In order to further define the functional humoral correlates of immunity against influenza, we deeply profiled the functional humoral immune response to influenza at the time of peak immunogenicity in a unique cohort of vaccinated older adults. These older adults (≥65 years old) without moderate or severe acute illnesses were enrolled in the FIM12 study (*278*, *281*) and immunized with either standard or high dose trivalent influenza vaccines in October of 2012. Within the randomly selected immunogenicity subset, serum samples were collected at peak immunogenicity, 28 days post vaccination. Individuals were tracked throughout the influenza season, with twice weekly surveillance calls during the peak of the influenza season (January-February), followed by once weekly calls until the end of the season (April 30). Any individuals with respiratory illness were tested for influenza by PCR, culture, or both. During the influenza season when this study took place (2012-2013), the CDC classified the epidemic as moderate severity for children and adults, but high severity in older adults (*282*), related to increases in hospitalization and deaths in the population ≥65 years old (*283*). Decreased vaccine effectiveness was observed for the H3N2 strain, the major circulating variant that year (*283*), later linked to an adaptation to the egg culture (*276*), including a three amino acid mutation altering two critical antigenic sites (*276*) compromising neutralizing antibody activity (*276*, *277*). While

dosing improved HAI activity, HAI levels alone, even to the egg-adapted strain, were an incomplete predictor of protection (*278*). Specifically, whether neutralization alone among antibody-mediated defenses or in combination with other humoral functions previously linked to protection against influenza (*62*) contributed to protection remained unclear.

METHODS

Samples

100 samples drawn 28 days post-vaccination from older individuals were selected from a previous published clinical trial (*278*). This trial compared the standard 15µg per HA dose or high-dose 60µg per HA Fluzone (Sanofi Pasteur) seasonal influenza vaccines (*278*), so individuals were included who received one of these doses (n=50 per vaccine type). These individuals were followed for the duration of the flu season and influenza infection status confirmed by both PCR and culture. This was not a controlled exposure study, so the influenza exposure status of uninfected individuals is unknown. 14 individuals selected for this study were infected with influenza (any subtype), of which 3 received the high dose vaccine. This study was approved by the Massachusetts General Hospital Institutional Review Board.

Antibody isotyping, subclassing, and FCGR binding

Antigen-specific antibody isotype, subclass, and FCGR binding titers in participant serum were measured using a custom Luminex-based array as previously published (*197*, *246*, *284*). Antigens of interest from past, concurrent, and later influenza seasons were coupled to Luminex beads (Luminex Corp.) through carboxyl chemistry. Antigens assayed were: wild type H3 A/Victoria/361/2011, egg adapted H3 A/Victoria/361/2011, H1 stem, H1 A/California/07/2009, N1 A/California/07/2009, H1 A/Brisbane/59/2007, H1 A/Chile/1983,

H1 A/New Caledonia/20/1999, H3 A/Texas/50/2102, N2 A/Texas/50/2012, H3 A/Brisbane/10/2007, H3 A/Hong Kong/4108/2014, N2 A/Hong Kong/4108/2014, H3 A/Panama/2007/1999, H3 A/Singapore/19/2016, H3 A/Switzerland/9715293/13, HA B/Brisbane/60/2008, HA B/Phuket/3073/2013, HA B/Colorado/06/2017, and ZEBOV GPdTM. All antigens were provided by Sanofi Pasteur except the A/Victoria/361/2011 HAs, which were provided by the Ragon Protein Production Core Facility, and the ZEBOV GPdTM, purchased from Mayflower Biosciences. Antigen-coated beads were incubated with diluted serum overnight at 4C, shaking. For IgG1 and FCGR detection, samples were diluted to a final concentration of 1:500. For IgG3, IgA1, and IgM detection, samples were diluted to a final concentration of 1:100. Following immune complex formation, beads were washed and incubated with a PE-labeled detection reagent. For antibody isotypes IgG1, IgG3, IgA1, and IgM, PE-labeled detection antibodies were purchased from Southern Biotech. For FCGRs FCGR2A (R), FCGR2B, and FCGR3A (V), proteins were acquired from the Duke University Protein Production Facility and incubated at a 4:1 molar ratio with streptavidin-PE (Prozyme). After 1 hour incubation at room temperature, excess detector was washed away and labeled immune complexes resuspended in QSol buffer (Intellicyt). Plates were read using an iQue Screener PLUS with Forecyt software (Intellicyt), and antibody levels quantified by PE median fluorescence intensity. All samples were assayed in duplicate.

Antibody-dependent cellular phagocytosis (ADCP)

Antigens (wild type H3 A/Victoria/361/2011, egg adapted H3 A/Victoria/361/2011, and N2 A/Texas/50/2012) were biotinylated using ezLink NHS-LC-LC-biotin (ThermoFisher) for 30 minutes at room temperature, cleaned up with Zeba spin columns (ThermoFisher), and coupled to Neutravidin fluorescent beads (ThermoFisher) for two hours at 37C. Antigen-coated beads were incubated with diluted serum samples (1:200 dilution for HA antigens and 1:100 dilution for NA antigen) for 2 hours at 37C, washed, and

incubated overnight with 25,000/well THP-1 monocytes (ATCC) to allow for phagocytosis. Cells were washed to remove unphagocytosed immune complexes, then fixed. Plates were read using an iQue Screener PLUS with Forecyt software (Intellicyt). Results are reported as phagocytic scores, which were calculated by multiplying the percentage of monocytes that had undergone phagocytosis by the geometric mean fluorescence intensity of bead-positive monocytes (a proxy for the number of beads phagocytosed by each cell), then dividing by 10,000. All samples were assayed in two independent replicates.

Antibody-dependent neutrophil phagocytosis (ADNP)

ADNP was assayed as described in (*247*). Fluorescent beads were coupled to antigens as for ADCP and incubated with diluted serum samples (1:50 dilution for HA antigens and 1:25 dilution for NA antigen) for 2 hours at 37C, washed, and incubated with healthy donor white blood cells isolated by ACK lysis for one hour at 37C. Cells were washed to remove unphagocytosed immune complexes, then stained with CD66b to positively identify neutrophils. Cells were fixed and plates were read using an iQue Screener PLUS with Forecyt software (Intellicyt). Results are reported as phagocytic scores, which were calculated by multiplying the percentage of neutrophils that had undergone phagocytosis by the geometric mean fluorescence intensity of bead-positive neutrophils, then dividing by 10,000. All samples were assayed using two independent white blood cell donors.

Antibody-dependent dendritic cell phagocytosis (ADDCP)

Dendritic cells were derived from blood monocytes isolated from buffy coats (Massachusetts General Hospital Blood Donor Center) by CD14 positive selection (Miltenyi). Following isolation, cells were differentiated in MoDC media (Miltenyi) for 6-7 days. Antigens (wild type H3 A/Victoria/361/2011, egg adapted H3 A/Victoria/361/2011, and N2 A/Texas/50/2012) were coated onto fluorescent beads (ThermoFisher) via carboxy

chemistry. Antigen coated beads were incubated with diluted serum (1:50 dilution for HA antigens and 1:25 dilution for NA antigen) for 2 hours at 37C to form immune complexes. Beads were washed and incubated with differentiated DCs for 4 hours at 37C. DCs were then fixed and stained for cell surface activation makers (HLA-DR, CD86, and CD83; all from BD Biosciences). Plates were read using an iQue Screener PLUS with Forecyt software (Intellicyt). Results are reported as phagocytic scores, which were calculated by multiplying the percentage of neutrophils that had undergone phagocytosis by the geometric mean fluorescence intensity of bead-positive neutrophils, then dividing by 10,000, and as percentage of cells that are positive for activation markers. All samples were assayed using two independent DC donors.

Antibody-dependent complement deposition (ADCD)

ADCD was assayed as described in (*248*). Fluorescent beads were coupled to antigens as for ADCP and incubated with diluted serum samples (1:25 dilution for HA antigens and 1:12.5 dilution for NA antigen) for 2 hours at 37C, washed, and incubated with purified guinea pig complement (Cedarlane) for 20 minutes at 37C. Beads were washed with EDTA-containing buffer, then incubated with anti-C3 fluorescent detection antibody (MP Biomedical) for 15 minutes at room temperature. Beads were washed and read using an iQue Screener PLUS with Forecyt software (Intellicyt). Results are reported as geometric mean fluorescence intensity of anti-C3 on beads. All samples were assayed in two independent replicates.

Antibody-dependent NK cell activation (ADNKA)

NK cells were isolated from healthy donor buffy coats (Massachusetts General Hospital Blood Donor Center) using the RosetteSep NK cell enrichment kit (StemCell). Antigens (wild type H3 A/Victoria/361/2011, egg adapted H3 A/Victoria/361/2011, and N2 A/Texas/50/2012) were adsorbed onto 96-well ELISA plates (ThermoFisher), and plates

were blocked in 5% bovine serum albumin (Sigma) in PBS (Corning). Coated plates were then incubated with diluted serum samples (1:25 dilution for HA antigens and 1:12.5 dilution for NA antigen) for 2 hours at 37C, washed, and incubated with purified donor NK cells for 5 hours at 37C. The NK cells were then removed from antigen-coated plates, fixed, permeabilized, and stained for both cell surface and intracellular markers (CD3, CD16, CD56, CD107a, MIP-1β, IFN-γ; all from BD Biosciences). Cells were analyzed with an iQue Screener PLUS with Forecyt software (Intellicyt). Results are reported as percent of NK cells (CD3-, CD56/CD16+) positive for each activation marker (CD107a, IFN-γ, and MIP-1β). All samples were assayed using two independent NK cell donors.

For comparisons of NK cells from younger and older adults, cryopreserved PMBCs were provided from the UCONN Center on Aging from a previous study(*285*). The younger adult samples came from participants aged 22-40 years old and 70% were female. The older adult samples came from participants aged 65-90 years old and 70% were female. Within the older adults, 50% scored robust on the clinical frailty score, 40% were pre-frail, and 10% were frail. CD16 antibody (Biolegend) was adsorbed onto 96-well ELISA plates (ThermoFisher), and plates were blocked in 5% bovine serum albumin (Sigma) in PBS (Corning). PBMCs were added and incubated for 5 hours. The cells were then removed from coated plates, fixed, permeabilized, and stained for live/dead, cell surface, and intracellular markers (CD107a, CD3, CD56, CD57, CD14, CD69, and MIP-1b all from BD Biosciences; CD16, KIR, NKG2D, NKp46, and Perforin all from Biolegend; NKG2A and NKG2C both from R & D Systems). Cells were analyzed on a BD Fortessa 5-laser cytometer with Diva software. Flow cytometry files were analyzed with Flowjo. This study was approved by the Massachusetts General Hospital Institutional Review Board.

Antibody glycan analysis

Serum samples were heat inactivated at 56C for one hour, then spun down at >20,000g to remove debris. Samples were pre-cleared by incubation with streptavidin-coated magnetic beads (NEB) for 1 hour, rotating. Antigens (wild type H3 A/Victoria/361/2011 and N2 A/Texas/50/2012) were biotinylated as for ADCP and coupled to streptavidin-coated magnetic beads. Antigen-coated beads and pre-cleared samples were incubated for one hour at 37C, rotating. Samples were then washed three times and resuspended in IDEZ (NEB) to cleave at the Fc-Fab hinge. Fc glycans were isolated and labeled using the GlycanAssure kit (ThermoFisher) and APTS-labeled glycans were analyzed by capillary electrophoresis on a 3500xL genetic analyzer with GlycanAssure software (Applied Biosystems). Pre-labeled libraries are used as references. Results are reported for each identified peak as percentage of total isolated glycans, and samples without identifiable traces are excluded from the analysis. Peaks are combined into glycoform groups for visualization and statistical testing (e.g. combining all sialylated glycoforms).

Fc-engineered monoclonal antibodies

The antibody CR9114 (*279*) was cloned onto three different Fc backgrounds (WT IgG1, N297Q-aglycosylated, and SDIEALGA (*286*)) to investigate the impact of enhanced versus ablated NK cell activation in immune complexes using a Golden Gate cloning platform (*287*). Antibodies were produced in HCK-293F cells and purified by protein A/G resin (*287*). These antibodies were characterized by analysis in the systems serology pipeline as described above, using inactivated H3N2 X-31 influenza as antigenic bait and with each antibody at a concentration of 5ug/ml for ADCP, ADNP, and ADNKA and a concentration of 50ug/ml for ADCD. The antibodies were further characterized by Luminex using H3 stem antigen (laboratory of Dr. Daniel Lingwood) as bait with human (as above) and murine (Sino Biological) FCGRs as detection reagents.

Murine experiments

CR9114-IgG1, CR9114-N297Q, and CR9114-SDIEALGA were administered at indicated doses to C57BL6/J mice at ages 6-8 weeks or 35 weeks by intraperitoneal injection. Two hours following antibody administration, mice were intranasally challenged with H3N2 X-31 at 5 LD_{50}. Mice were monitored for disease progression for 1 week following infection. This study was approved by the Massachusetts General Hospital Institutional Animal Care and Use Committee.

Statistical and machine learning analysis

Univariate analyses and visualizations were completed in Prism (Graphpad). Statistical tests are detailed in figure legends.

HA comparison heatmap and correlation heatmaps were created in RStudio using the corrplot package (https://cran.r-project.org/web/packages/corrplot/). Chord diagram was also created in RStudio using the circlize package (https://cran.r-project.org/web/packages/circlize/index.html). Function heatmaps were created in JMP Pro 14 (SAS) using the hierarchical clustering function.

Multivariate and machine learning analyses and visualizations were completed in Matlab R2020a (Mathworks). For Elastic Net-Partial Least Squares analysis of influenza infected compared to uninfected individuals, a dataset containing antigen-specific antibody isotypes, FCGR binding, neutralization, and antibody-dependent functional data for all 100 study subjects was used. Missing datapoints were imputed using K-nearest neighbor and data were normalized using z-scoring. Elastic Net machine learning was performed in a 5-fold cross-validation framework. The Elastic Net lambda coefficient was chosen within this cross-validation framework. A minimum of 5 antibody features were selected in each

replicate. Random size-matched and label permuted datasets were compared for each model within the cross-validation framework.

Networks were plotted in Cytoscape v3.8.1 using pairwise correlation data calculated in Matlab.

RESULTS

ENHANCED RESPONSES TO EGG-ADAPTED HA CORRELATE WITH RESPONSES TO CIRCULATING HA

Using this highly characterized cohort, linked to well defined viral breakthrough, we aimed to objectively define humoral correlates of protection in the elderly population. Specifically, we applied our systems serology platform (*193*) to agnostically measure antigen-specific antibody-dependent innate immune functions, antigen-specific antibody isotype titers, and antigen-specific Fc-γ receptor (FCγR) binding titers at peak immunogenicity blindly across the samples, and then examined differences across antigens, doses, and ultimately protection status.

Consistent with previous neutralizing data (*278*), antibody titers to the vaccine egg-adapted H3 were significantly higher than to the circulating wild type H3 for all measured isotypes and FCGRs (**Figure 4.1A**), including both IgG1, the most abundant circulating antibody isotype, and IgM, the precursor to IgG in the development of the humoral immune response (*288*) (**Figure 4.1B**) Antibody-dependent innate immune functions mediated by monocytes (antibody-dependent cellular phagocytosis, ADCP), neutrophils (antibody-dependent neutrophil phagocytosis, ADNP), complement (antibody-dependent complement

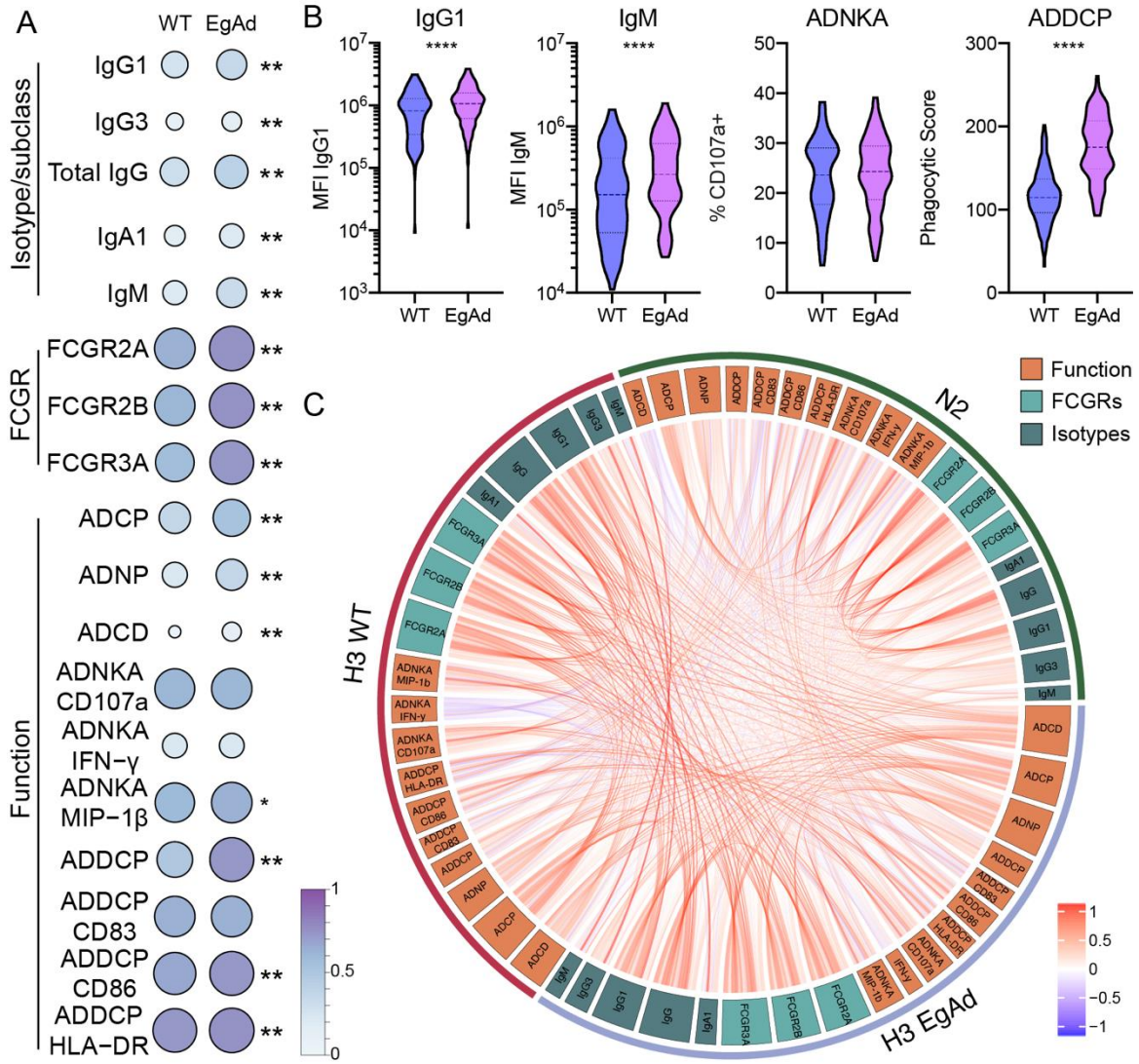

Figure 4.1 Responses to circulating H3 and vaccine H3 are highly correlated but vaccine H3 responses have higher magnitude. (**A**) Circles represent average antigen-specific antibody-dependent functional response, FCGR binding titer, or isotype titer across all participants to both circulating H3 (H3 WT) and vaccine H3 (H3 EgAd). Sample values were z-score normalized across both antigens, then mean values represented in circle plots. (**B**) Violin plots depict responses across all samples for selected univariate antibody features. (**A & B**) Significance of difference between magnitude of response to each antigen is represented by stars and was determined by Wilcoxon matched pairs signed rank test with Bonferroni's correction. * $p < 0.05$, ** $p < 0.01$, **** $p < 0.001$ (**C**) Chord diagram shows correlations between antigen-specific antibody-dependent functional response, FCGR binding titer, or isotype titer across circulating H3, vaccine H3, and N2 antigens. Red chords represent positive Spearman R values and blue chords represent negative Spearman R values, with more intense color representing stronger correlation.

deposition, ADCD), and dendritic cells (antibody-dependent DC phagocytosis, CD83, and HLA-DR expression) were also significantly increased to the egg-adapted strain (**Figure 4.1A**). The increase in ADDCP (**Figure 4.1B**) further underscored augmented antibody-mediated antigen delivery, activity that could also promote enhanced T cell immunity (*289*), selectively to the egg-adapted strain. Surprisingly, despite the higher overall titers of H3 egg-adapted antibodies, antibody dependent NK cell activation (ADNKA), and specifically degranulation (CD107a) and cytokine release (IFN-γ), were not differentially induced to the egg-adapted strain (**Figure 4.1A-1B**). Conversely, chemokine secretion by NK cells, measured by MIP-1β, was enhanced to the egg adapted H3 when compared to the wild type H3 (**Figure 4.1A**).

However, despite the enhanced boosting of humoral immunity to the egg-adapted antigen, antibody isotypes, FCGR binding, and antibody-dependent innate immune functions were highly correlated across the H3 and egg-adapted antigen (**Figure 4.1C**). Thus, despite differences in the magnitude of the response across the wildtype and egg-adapted HAs, the specific humoral features were correlated across H3 antigens, suggesting that rather than altering the functional response to HA, the egg-adapted HA induced a less robust, but proportional response to the wildtype circulating HA strain. Moreover, beyond HA, neuraminidase (NA) is also included at lower and variable concentrations in the vaccine (*290*), and also experienced a proportional boost (**Figure 4.1C**). Thus, these data collectively suggest that while the vaccine induced more robust responses to the egg-adapted HA, vaccination also induced a parallel augmentation of humoral immunity across the wildtype HA and NA, pointing to the presence of functional humoral immune responses that could still contribute to protection against the circulating strain.

HIGH DOSE VACCINATION INDUCES A MULTIPRONGED FUNCTIONAL ANTIBODY RESPONSE

In order to better understand the mechanisms of immunity in older adults, this trial measured the protective capacity of high dose (60µg of HA per strain) compared to standard dose (15µg of HA per strain) vaccination (*278*). To additionally probe the impact of dosing on the evolution of the functional humoral immune response, we profiled the differences in the vaccine-induced Fc-profiles. Significant heterogeneity was observed in HA-specific Fc profiles across all vaccine recipients (**Figure 4.2A**), with no two individuals possessing an identical HA-specific Fc profile. Interestingly, individuals that received the high dose did not exhibit an overall shift in the magnitude of their vaccine-specific responses. Conversely, while previous data pointed to an increase in HAI with the higher dose (*278*), here, limited differences were noted in either IgG1 or IgM titers to HA or NA antigens (**Figure 4.2B**). Yet, selective increases were noted in particular antibody effector functions including elevated H3 egg-adapted-specific NK cell degranulation, and, surprisingly, reduced wildtype H3 and N2-specific antibody mediated DC activation with the high dose (**Figure 4.2B**). These data suggest that while dosing may not have an effect on IgG antibody titers, it may play a role in shaping the qualitative immune response.

To further probe the qualitative impact of dosing, we next examined the architecture of the vaccine-induced humoral immune response by calculating the functional coordination across the standard dose (**Figure 4.2C**, top) and high dose (**Figure 4.2C**, bottom) vaccine recipients. Positive correlations were observed within opsonophagocytic functions (ADCP, ADNP, ADCD) across H3 egg-adapted and wildtype strains (**Figure 4.2C**, top purple box), as evidenced by strong reds and oranges with larger circles. Conversely, these responses were poorly, and even inversely, correlated across opsonophagocytic versus NK cell and DC

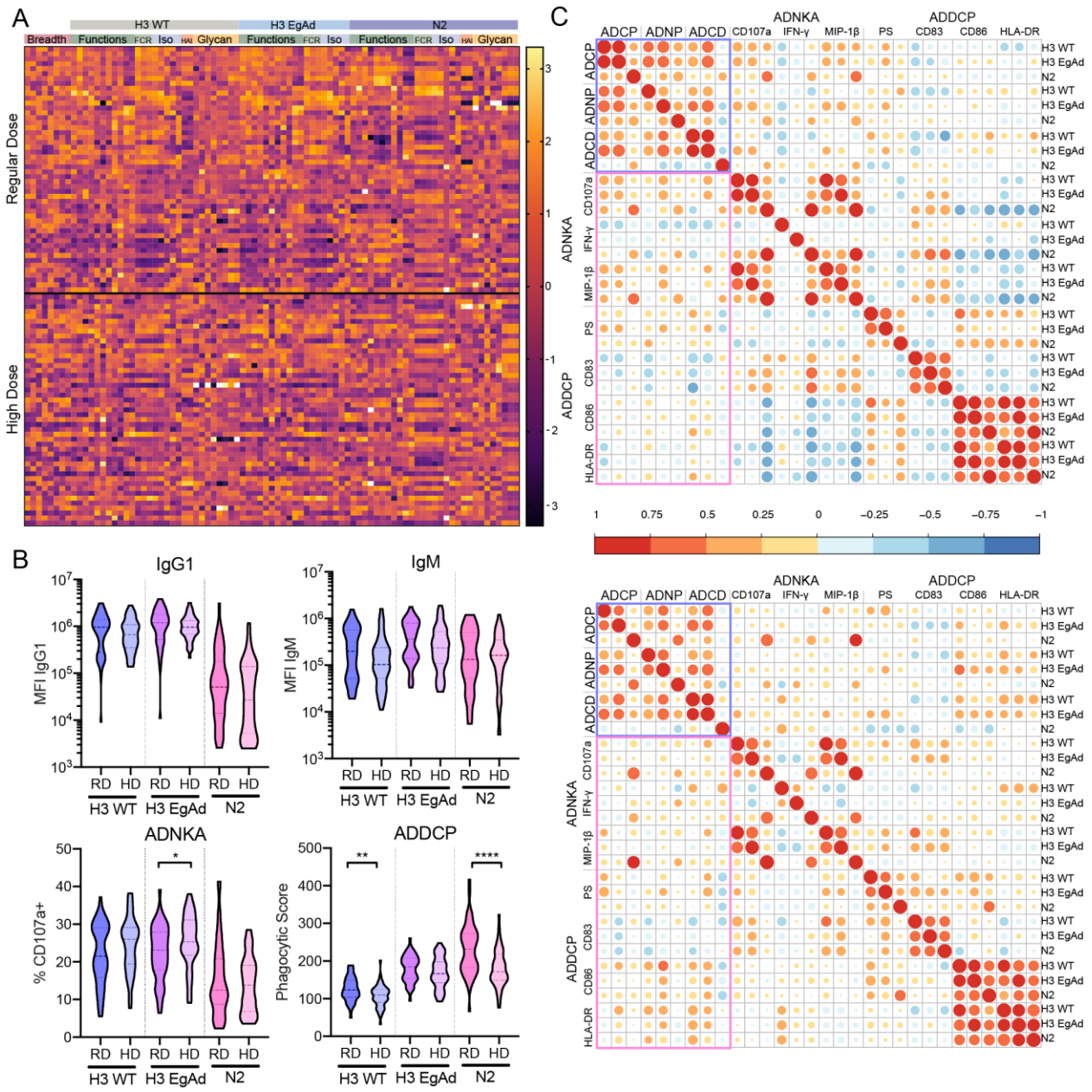

Figure 4.2 Regular and high dose vaccines induce different functional humoral responses. (**A**) Heat map depicts responses across all measured antibody features for regular dose and high dose vaccine recipients. Each row represents an individual sample. Each column represents a measured feature. Values for all measurements were z-score normalized. (**B**) Violin plots depict responses for regular dose (RD) and high dose (HD) vaccine recipients across three antigens: circulating H3 (H3 WT), vaccine H3 (H3 EgAd), and N2 for selected univariate antibody features. Significance of difference between RD and HD recipients for each antigen is represented by stars and was determined by Mann-Whitney U test. * $p < 0.05$, ** $p < 0.01$, **** $p < 0.001$ (**C**) Correlation matrices show Spearman R correlations between antigen-specific antibody-dependent functions for RD (top) and HD (bottom) vaccine recipients. The size of the circles and the color of the circles represent the strength of the correlation, with red for positive and blue for negative correlations. For ADNKA and ADDCP, included measurements are: ADNKA: CD107a, IFN-y, MIP-1b; ADDCP: Phagocytic Score, CD83, CD86, HLA-DR. For each function, responses to H3 WT, H3 EgAd, and N2 are included in that order.

activating functions in the standard dose group (**Figure 4.2C**, top pink box) as shown by small circles and blue colors in the heatmap. Conversely, coordination improved with the high dose vaccination, with weak but positive correlations across all functions (**Figure 4.2C**, bottom). Thus, while increased dosing may not induce individually elevated antibody effector functions to influenza, increased dosing may improve the overall capability of antibodies to recruit many antibody effector functions including HAI, opsonophagocytic, NK cell, and DC activating functions. However, the precise functions required to mediate protection remain unclear.

PROTECTED VACCINEES INDUCE MORE COORDINATED HUMORAL IMMUNE RESPONSES

Given the presence of a spectrum of coordinated humoral profiles across HA and NA antigens in the population (**Figure 4.1**), we next aimed to determine whether differences existed in the antibody profiles across vaccinees that were protected versus those that got infected over the follow up period. Thus, data were grouped by individuals who were infected during the study (cases) and individuals who remained uninfected (controls) (**Figure 4.3A**). While cases exhibited a trend towards lower IgG1 and ADNKA (**Figure 4.3A and B**), these differences were not significant. Furthermore, vaccine specific IgG1 and IgM titers were not predictive of protection from infection (**Figure 4.3B**), highlighting the lack of a univariate predictor of protection at peak immunogenicity. Conversely, the coordination of the immune response varied across the cases and controls (**Figure 4.3C**), marked by enhanced coordination in the controls across all antibody functions. More negatively correlated relationships were observed among cases, marked by a strong correlation between opsonophagocytic functions that excluded NK cell activating functions. These data point to the inclusion of NK cell functions in the polyfunctional antibody response in

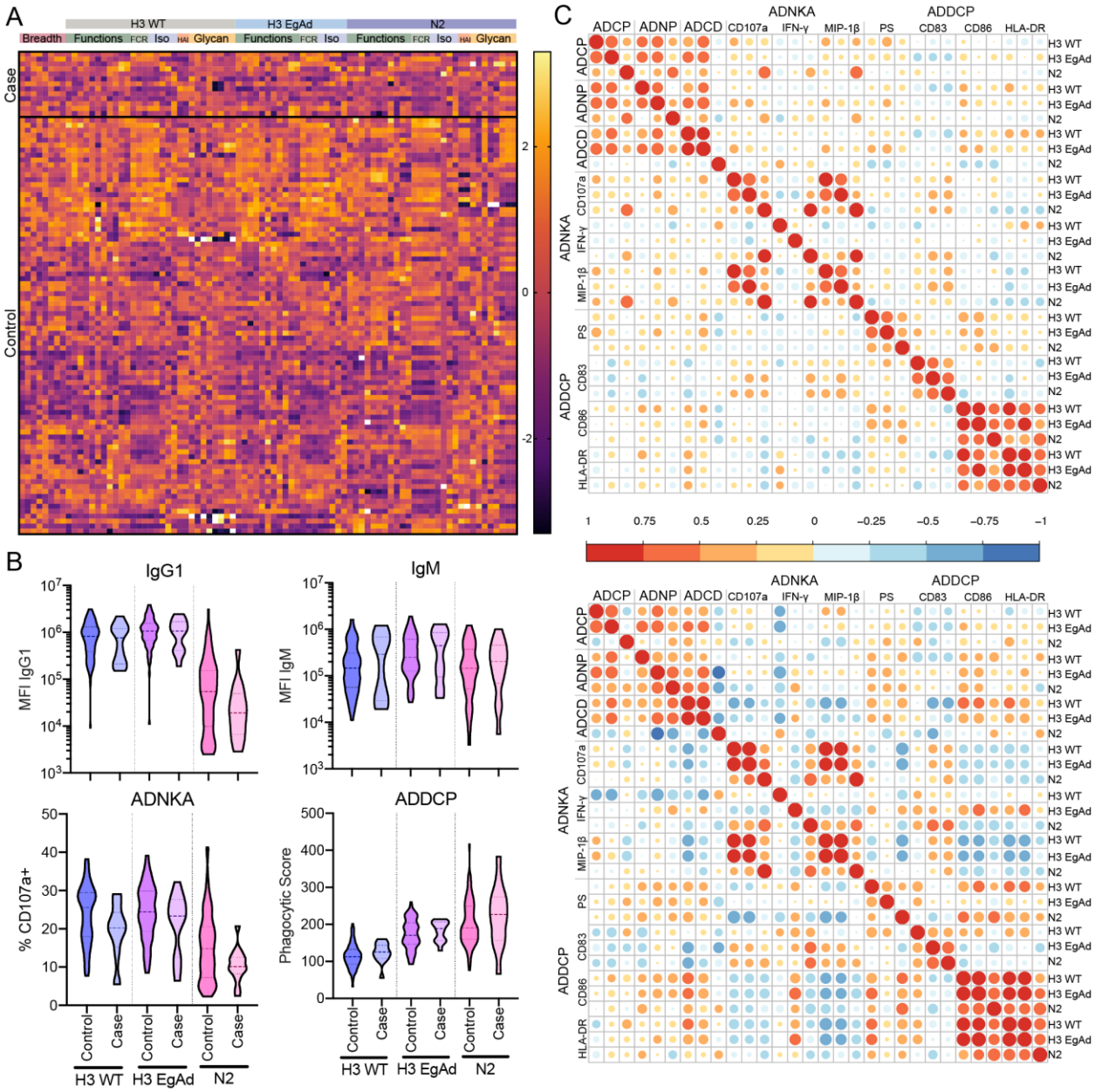

Figure 4.3 Protected vaccinees induce more coordinated humoral immune response. (**A**) Heat map depicts responses across all measured antibody features for vaccine recipients who did (case) or did not (control) develop influenza infection. Each row represents an individual sample. Each column represents a measured feature. Values for all measurements were z-score normalized. (**B**) Violin plots depict responses for vaccine recipients who did (case) and did not (control) develop influenza infection across three antigens: circulating H3 (H3 WT), vaccine H3 (H3 EgAd), and N2 for selected univariate antibody features. Significance of difference between RD and HD recipients for each antigen is represented by stars and was determined by Mann-Whitney U test. * $p < 0.05$, ** $p < 0.01$, **** $p < 0.001$ (**C**) Correlation matrices show Spearman R correlations between antigen-specific antibody-dependent functions for control samples (top) and case samples (bottom). The size of the circles and the color of the circles represent the strength of the correlation, with red for positive and blue for negative correlations. For ADNKA and ADDCP, included measurements are: ADNKA: CD107a, IFN-y, MIP-1b; ADDCP: Phagocytic Score, CD83, CD86, HLA-DR. For each function, responses to H3 WT, H3 EgAd, and N2 are included in that order.

controls, but the selective exclusion of these functions in cases, highlighting a possible role for antibody mediated NK cell recruitment in protective immunity.

NK CELL ACTIVATION SEPARATES INFECTED FROM UNINFECTED VACCINEES

Differences in the correlation matrix across cases and controls pointed to a more complex (**Figure 4.3C**), rather than single biomarker, correlate of immunity against influenza. Given the highly correlated nature of humoral immune features, we used a Least Absolute Shrinkage and Selection Operator (LASSO)-Elastic Net algorithm (*212*, *249*) to identify key features. LASSO collapsed the measured antibody features to a minimal set that accounted for the greatest variation in antibody profiles across the cases and controls, potentially able to predict protective antibody profiles at peak vaccine-induced immunogenicity and prior to exposure. Separation was observed in Fc profiles across cases and controls (**Figure 4.4A,** $p < 0.01$ when compared to both permuted label and random size-matched feature sets, **Figure 4.5**), with the majority of the cases exhibiting higher values across latent variable 1 (LV1) (**Figure 4.4B**). As few as nine of the 198 features captured in our Systems Serological profiling were sufficient to separate out the cases and controls, with five features enriched in the controls and four features that were enriched in the cases, with relative contributions ordered according to Variable Importance in Projection (VIP) (**Figure 4.4C**). The four features enriched in the controls all pointed towards increased functional quality, rather than simple quantitative increases in antibodies, marked by enhanced antibody mediated NK cell activation to both HA and NA, including higher levels of FCGR3A binding and NK cell activating antibodies. Conversely, elevated levels of IgG3 and IgA to HA, IgM to NA and HA-specific DC-activating antibodies were linked to non-protective immunity. These data suggest that increases in antibody

titers across various isotypes/subclasses, in the absence of NK cell recruiting functions, across HA and NA is a marker of a non-protective humoral immune response.

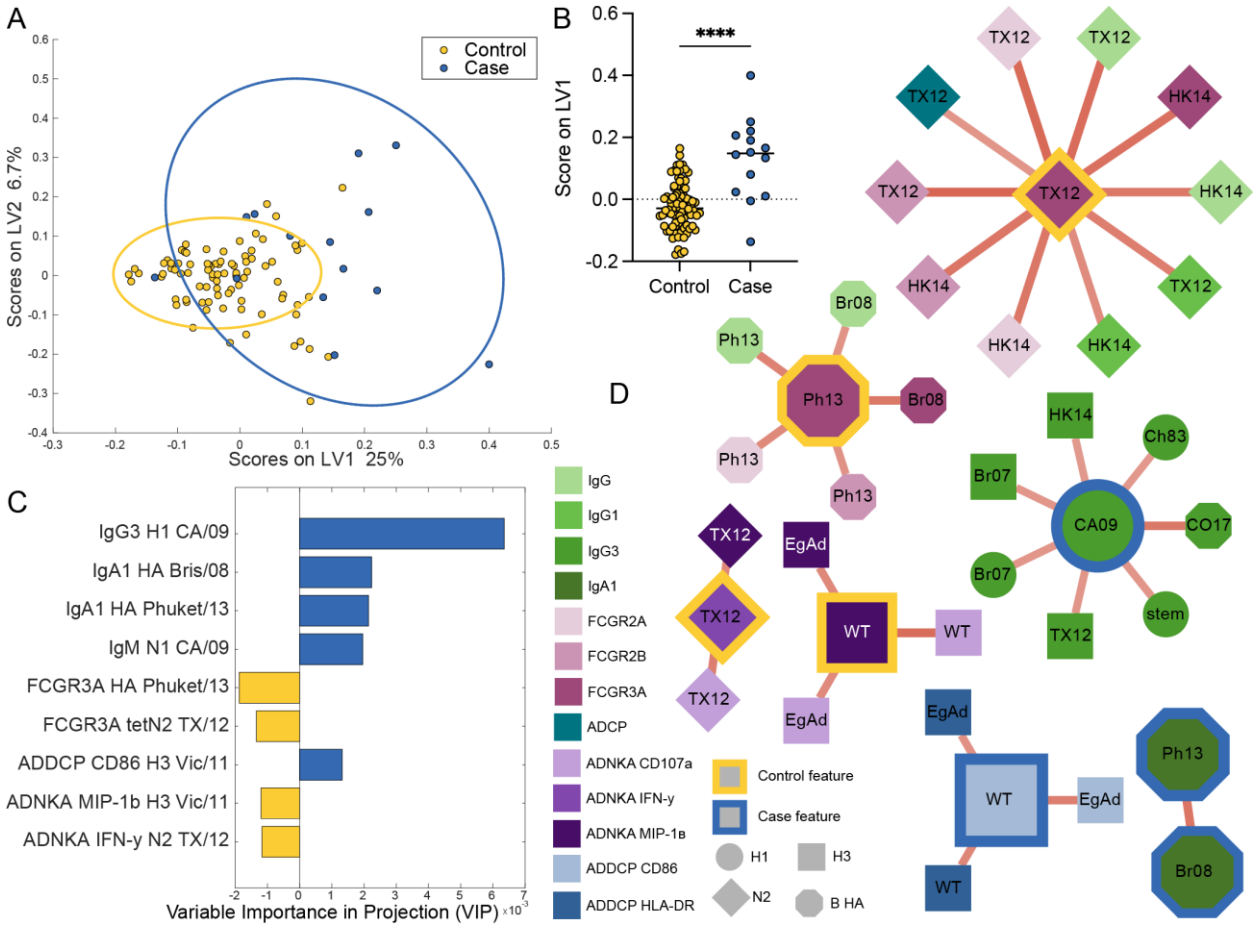

Figure 4.4 Antibody-dependent NK cell activation is a predictor of protection from influenza infection. (**A**) Partial least squares discriminant analysis separating cases (individuals who became infected) from controls (individuals who remained uninfected) using LASSO-Elastic Net machine learning algorithm selected humoral features. Scores across latent variables (LVs) indicate percentage of separation described by that axis. Model is significant ($p < 0.01$) compared to permuted label and random size matched models. (**B**) shows scores for individuals across LV1. Significance tested by Mann-Whitney U test, **** $p < 0.001$. (**C**) Variable importance in projection plot indicates the relative contribution of humoral features to the model depicted in (**A**). (**D**) shows significant co-correlates, defined as spearman $R > 0.6$ and FDR-corrected $Q < 0.01$, of LASSO-Elastic Net selected features enriched in controls (highlighted in yellow) and cases (highlighted in blue).

Because LASSO simply selects features to maximize differences between groups in the absence of any biological knowledge, we took a closer look at the co-correlates of the

LASSO-selected features to gain enhanced insights into additional potential mechanisms of protection. FCGR3A-binding antibody titers were linked to a broad array of additional NK activation readouts across multiple antigens, indicating that a broad FCGR3A binding

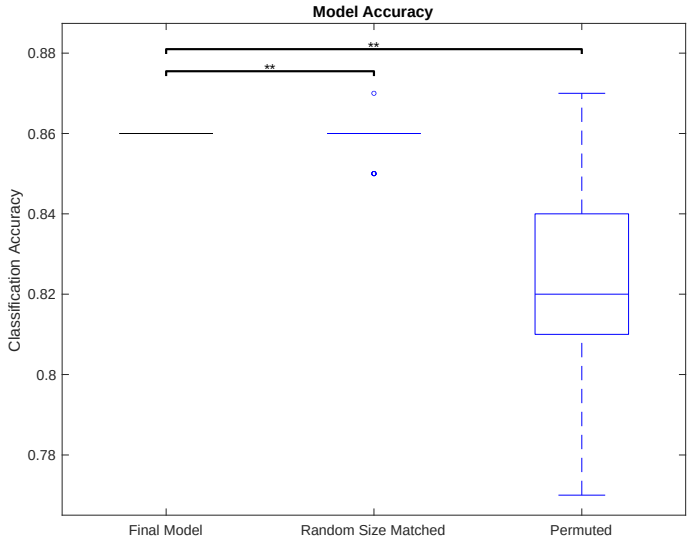

Figure 4.5 Model significance for LASSO-Elastic Net in **Figure 4.4**. The LASSO-Elastic Net model trained to distinguish between cases and controls was validated against random size matched and permuted label models. Significance tested by Mann-Whitney U test, ** $p < 0.01$.

response was present in controls (**Figure 4.4D**). The evolution of broad IgG3 responses, a marker of naïve B cell evolution, as well as ADDCP activity to both the wildtype and egg adapted HA were all enriched among cases (**Figure 4.4D**). These data may indicate that the progression and maturation of the immune response, as evidenced by class switching from IgM, IgA, and IgG3 to IgG1 is required for a fully protective response.

Given the known requirement of afucosylation at the IgG1 Fc glycosylation site for enhanced ADCC (*131*, *291*), we probed the correlation between H3-specific IgG glycosylation and NK cell activation (**Figure 4.6A**). While no particularly strong correlations were observed, negative correlations between fucosylated antibodies and CD107a expression, a proxy for ADCC, and between fucosylated antibodies and MIP-1β expression

were observed. Interestingly, cytokine release by NK cells, measured by IFN-γ expression, was linked to a different glycan profile. Focusing on fucosylation and its possible link to protection via ADCC induction (*291*), we observed that controls had significantly lower levels of fucosylated H3-specific IgG (**Figure 4.6B**). The increased level of afucosylated antibodies suggested a mechanistic driver of the observed NK cell markers of a protective immune response in this cohort, further supporting NK cell activating antibodies as a correlate of protection from infection.

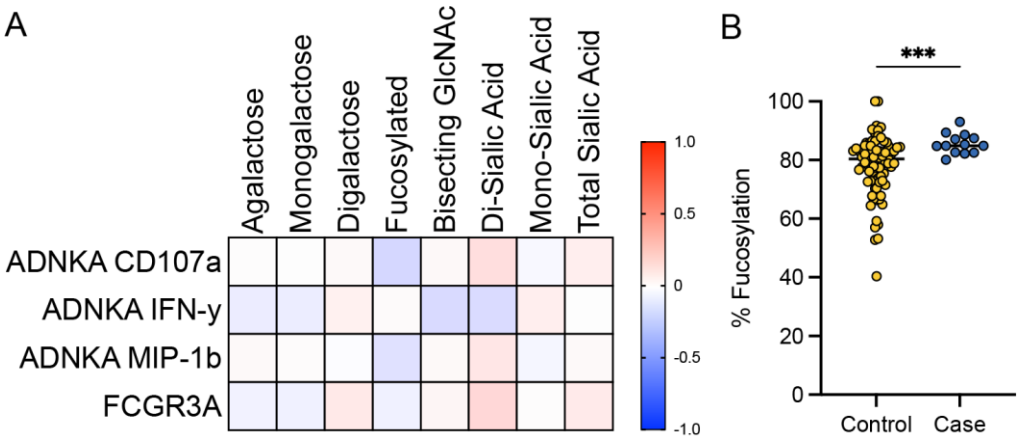

Figure 4.6 Glycosylation and NK cell activation. Heat map (**A**) shows Spearman R correlations between measures of H3 WT-specific NK cell activation and FCGR3A binding and H3 WT-specific antibody Fc glycoforms. Dot plot (**B**) shows levels of Fc fucosylation of H3 WT-specific antibodies in controls and cases. Significance tested by Mann-Whitney U test, *** $p < 0.001$.

AGE DECREASES RESPONSIVENESS TO ANTIBODY-MEDIATED PROTECTION AGAINST INFLUENZA IN MICE

To gain mechanistic insight into the importance of ADCC in protection from influenza, particularly in older adults, we next tested the protective efficacy of influenza-specific ADCC-enhanced antibodies in young (6-8 weeks) and mature (35 weeks) mice. The broadly reactive HA-stem-specific mAb CR9114 was Fc-engineered to express multiple functional profiles (*287*). From these, a primary NK activating profile, SDIEALGA (*279*), was chosen to be compared to both the wild type IgG1 (WT) and the N297Q functionally

ablated mutant to determine whether protection provided by these antibodies differed with age. First, each antibody mutant was tested across antibody-dependent functions and for binding to both human and mouse FCγRs. As expected, the wildtype CR9114 IgG1 mediated variegated antibody effector function linked to variable FcR binding. The N297Q variant demonstrated low level FcR binding and function. Conversely, the SDIEALGA mutant showing enriched functionality and FCγR binding for all functions except complement (**Figure 4.7A**). CR9114 mutants were passively transferred to young and mature mice at 4 mg/kg (*292*), followed by intranasal infection with H3N2 X-31, a strain that CR9114 binds but does not neutralize. While all PBS treated mice succumbed to infection (**Figure 4.7B**), mice that received the wildtype IgG1 or N297Q variant showed variable levels of protection. Conversely, the NK activating SDIEALGA mutant provided significantly increased protection to young mice (**Figure 4.7B**), as previously described (*38*). However, most surprisingly, when administered to older mice, all antibody variants conferred poor protection (**Figure 4.7C**). Moreover, the administration of higher concentrations of the variant mAbs (8 mg/kg) did not enhance protection (**Figure 4.7D**), suggesting that broader immune defects may exist in older mice that prevent the ADCC-enhanced antibodies from mediating their enhanced protective effects.

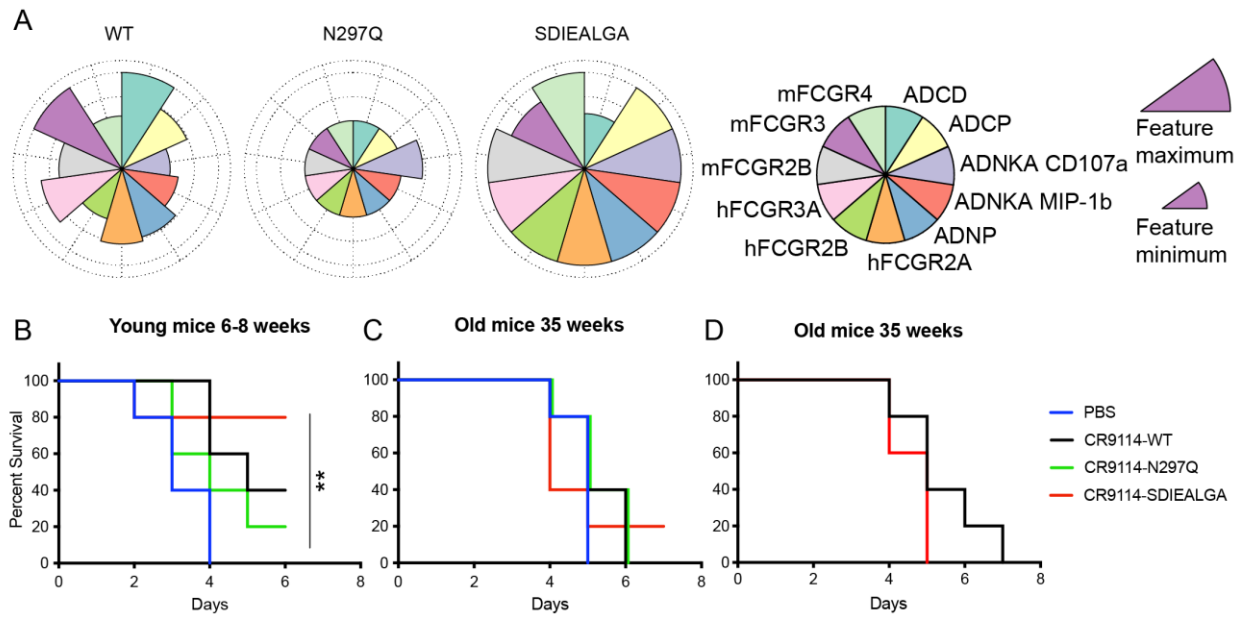

Figure 4.7 NK-activating Fc mutant increases protection in young mice while old mice remain susceptible. (**A**) Flower plots depict H3 X-31-specific functional and Fc-binding profiles of mAb CR9114 Fc mutants where larger petals indicate relative strength of that readout compared to other mutants. (**B**) Survival curves from a preliminary experiment where mice were given mAbs (CR9114 WT, N297Q or SDIEALGA) or PBS control by passive transfer at a dose of 4mg/kg, then infected with H3N2 X-31 influenza. ** $p < 0.01$. (**C**) Survival curves from a follow-up experiment where old mice were given CR9114 WT and SDIEALGA variants at 8mg/kg to attempt to rescue protection.

NK CELLS IN OLDER ADULTS ARE FUNCTIONALLY DIFFERENT THAN NK CELLS IN YOUNGER ADULTS

To ultimately define whether NK cells in humans also experience loss of ADCC activity, PBMCs from either younger (<40) or older (>65) adults were stimulated with an anti-FCGR3A (anti-CD16) activating antibody, a surrogate of activating ADCC. As expected (*293*, *294*), elderly NK cells expressed higher levels of CD57 (**Figure 4.8A**), a marker of maturation, anergy, and decreased functionality (*294*). Stimulated NK cells in younger adults displayed dose-dependent degranulation, measured by increasing levels of CD107a expression following stimulation with increasing amounts of the agonist antibody (**Figure 4.8B**). NK cells from older adults exhibited a significantly diminished response to FCGR3A-crosslinking (**Figure 4.8B**). However, older adult NK cells still remained somewhat

responsive at high levels anti-FCGR3A, highlighting the response is not irreversibly lost in humans, but may be rescued by higher doses of activating antibodies. Interestingly, the ability of NK cells to respond to FCGR3A (CD16)-crosslinking was inversely correlated to CD57 expression on NK cells across the ages, pointing to a potential NK cell biomarker that may provide insights into the levels of ADCC-inducing antibodies required to achieve protection against influenza (**Figure 4.8C**). No correlation existed between CD107a responsiveness and age or clinical frailty index (**Figure 4.10**), highlighting that mechanisms of immune aging may not track linearly with age and other clinical markers. Thus, providing more a more nuanced picture than the mice which experienced a total loss of protection mediated by FCGR3A-activating antibodies associated with aging, this data in humans indicates that next generation vaccines may require higher levels of ADCC-inducing antibodies, able to broadly target influenza, to achieve protection against influenza across the ages.

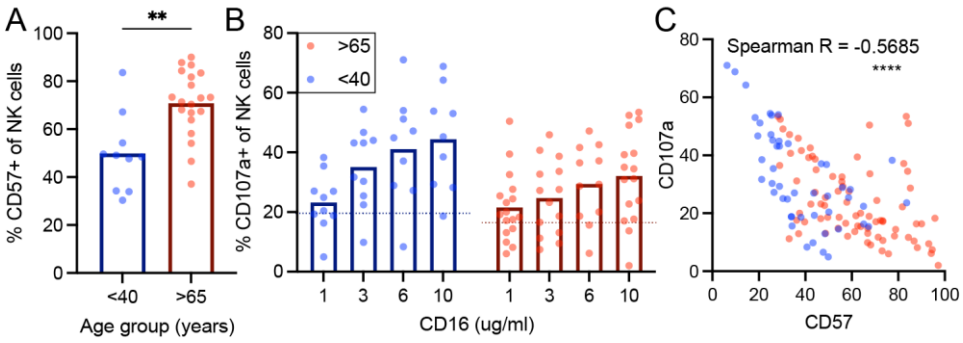

Figure 4.8 NK cells from older adults are less responsive to FCGR3A-mediated stimulation than NK cells from younger adults. Dot plot (**A**) shows percentage of NK cells expressing CD57 in older and younger adults. Representative gating is shown in **Figure 4.9**. Significance tested by Mann-Whitney U test. Dot plot (**B**) shows the percentage of NK cells expressing CD107a following stimulation with increasing concentrations of anti-CD16. Dotted lines show mean PBS control. Correlation plot (**C**) shows correlation between CD57 and CD107a expression across CD16 stimulation conditions. Correlation measured by Spearman's R. * $p < 0.5$, ** $p < 0.01$, **** $p < 0.0001$.

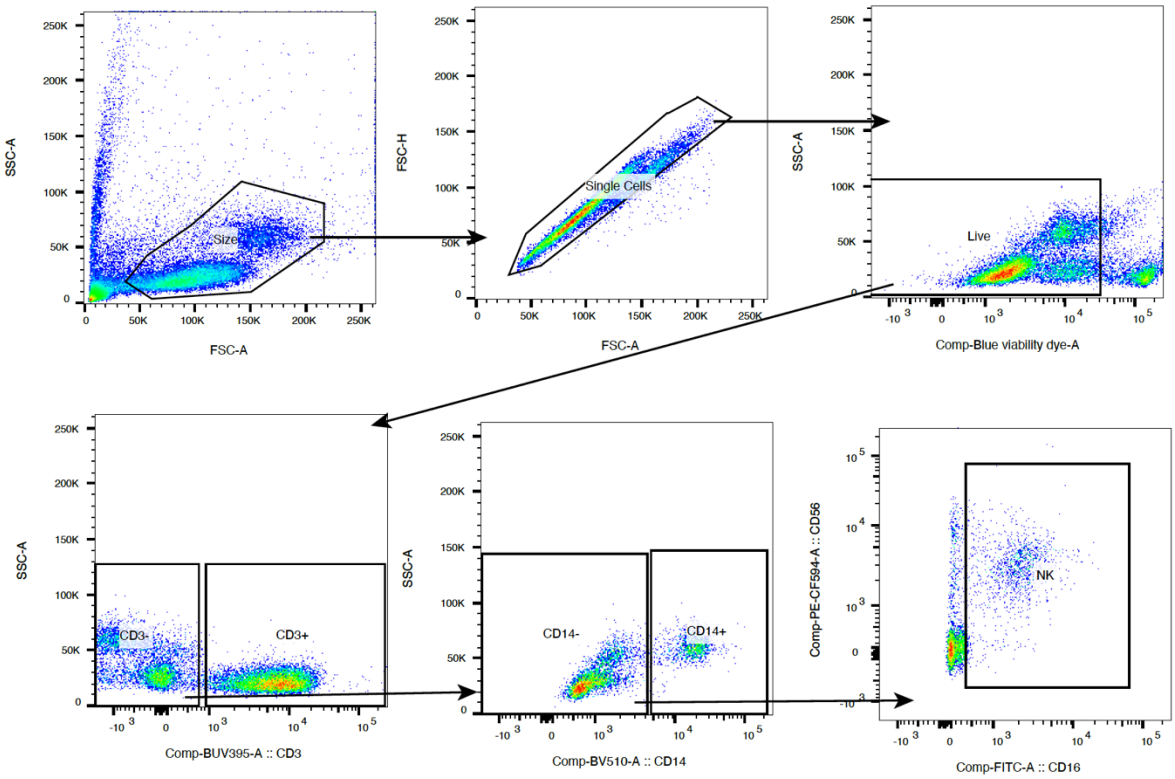

Figure 4.9 Representative gating for NK cells in **Figure 4.8**. PBMCs were gated on Size > Singlets > Live cells > CD3-, CD14-, and CD16+.

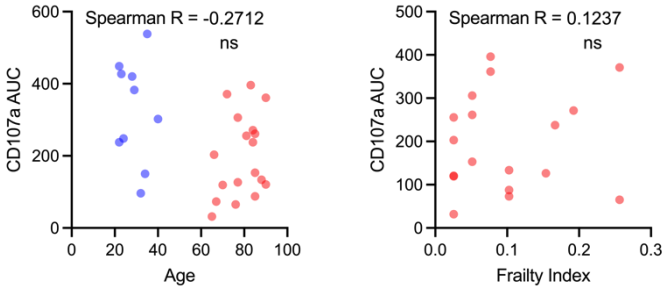

Figure 4.10 Correlations across age and frailty to ADCC activation. Correlation plots shows correlations between age and CD107a AUC and between frailty index and CD107a AUC for CD16 stimulation conditions. Correlation measured by Spearman's R. Not significant.

DISCUSSION

High dose vaccines have successfully increased the relative efficacy of influenza vaccination in older adults (*278*, *295*). This enhanced dosing has been proposed to partially counteract the effects of antigenic seniority, wherein the initial imprinting of the immune system limits the ability of the adaptive immune system to respond to newly evolving influenza strains (*296*). While antigenic seniority, or original antigenic sin, may explain reduced diversification and potency of the humoral immune response (*297*), it does not fully explain the immunologic deficit in protection, wherein some instances vaccination can augment immunity, but older adults remain vulnerable to infection and disease (*16*). Thus, to gain a deeper appreciation for additional mechanisms that may explain vulnerabilities in the elderly population, here we deeply profiled the humoral immune response in a well characterized influenza vaccine efficacy study using both standard and high dose vaccination. Importantly, despite the antigen mismatch observed during the study period, immunity to the circulating strain was induced proportionally to the egg-adapted antigen. Additionally, the inclusion of both the standard and high dose vaccination provided a range of antibody profiles across the population, providing the requisite heterogeneity required to define minimal features of the humoral immune response that were selectively associated with infection. While measurements of phagocytosis, neutrophil activation, complement activation, and DC activation were all captured, a striking and highly selective signal of enhanced FCGR3A binding and NK cell activation, to both HA and NA, were observed in individuals that resisted infection over the study period. These data argue for a highly selective defect in ADCC-inducing antibodies in individuals who ultimately became infected, and objectively point to a critical role for antibody-mediated NK cell activation as a key correlate of immunity against influenza in the population aged 65 years and older.

Moreover, while young mice also clearly benefited from ADCC-inducing antibodies, older mice experienced a loss of responsiveness to ADCC-inducing antibodies even at high levels. Aged humans also experienced a deficient response to ADCC, proportional to their NK cell CD57-marked anergy, but that was partially rescued by increasing doses of FCGR3A cross-ligation. The effect of antibodies on activation of NK cells acts in an age-dependent manner across *in vitro* and *in vivo* models. Thus, these data point to a potential opportunity to improve immunity to influenza in older adults, via the selective induction of elevated titers of ADCC inducing antibodies.

While elevated dosing improved overall antibody titers, HAI (*278*), select antibody functions, and FCGR3A-binding antibodies, dosing did not alter the level of antibodies able to drive NK cell degranulation. Similarly, previous efforts to boost immunity with the use of an adjuvant also resulted in enhanced antibody titers and opsonophagocytic functions, but led to poor induction of NK cell activating antibodies (*258*). Thus, novel strategies may be required to improve the production of ADCC-inducing antibodies. Both changes in antibody isotype usage and Fc-IgG glycosylation have been linked to improved ADCC activity. IgG3 and IgG1 both exhibit enhanced affinity for FCGR3A, involved in driving ADCC activity, however the broad induction of increased IgG3 levels was a correlate of risk in this study. These data suggest that altered IgG1-Fc-glycosylation is likely to be a key immune target for enhanced vaccine-mediated protection in older adults. However, the precise signals required to reduce fucosylation, the key glycan modification required to improve affinity for FCGR3A(*298*), remains incompletely understood. Emerging data suggest that specific adjuvants may differentially shape influenza-specific antibody effector function (*299*, *300*), however whether the same changes will be observed across the ages and through durable

changes in Fc-glycosylation is unknown but could represent a unique opportunity to shape immunity to influenza and beyond.

A unique observation in this study relates to the emergence of protective ADCC signals against both the influenza HA and NA proteins. While both proteins are included in the seasonal inactivated influenza vaccine, only the concentration of HA is controlled. NA, along with other viral proteins, is included in the vaccine but are not quantified precisely. Studies on the level and stability of NA have shown variability from one vaccine to the next (*290*, *301*). It is likely that high dose vaccines include more NA compared to standard dose vaccines, but that the levels of individual NAs vary by strain, vaccine season, and manufacturer (*47*, *290*, *302*). Due to this variation, typical seasonal influenza vaccination has been linked to lower NA responses, or no NA responses, in healthy adults (*47*). Conversely, high dose vaccination in older adults has been shown to induce an anti-NA response in a higher proportion of vaccinees (*302*), as has been observed in mice (*290*). While we did not observe a significant N2-specific titer enhancement in this study, significant differences were observed in the N2-specific humoral immune response across cases and controls, arguing for a critical role for NA, not just HA, -specific functional immunity in older adults. Given our emerging appreciation for the importance of NA as a functional target for ADCC-inducing antibodies, these data suggest that future vaccines able to drive synergistic functional immunity to HA and NA may synergistically improve immunity in the population aged 65 years and older.

The mechanistic finding presented here that "aging" NK cells are less able to respond to FCGR3A-mediated stimulation builds on previous literature in older adults, especially in the presence of cytomegalovirus (CMV) (*293*, *294*). While some studies have indicated that the cytotoxicity of NK cells is comparable between young and old adults

(*303*), here we clearly demonstrate that the level of activation required differs across the ages in humans, pointing to an activation threshold effect, that was linked to the level of CD57 surface expression. Thus, while mice that mediate ADCC via monocytes rather than NK cells (*179*) may experience a more significant defect in ADCC activity, higher levels of ADCC-inducing antibodies may overcome the NK cell anergy that evolves in aging humans. Thus, whether CD57 levels can ultimately be used to determine and guide the level of ADCC required to achieve protective immunity across populations is unclear but provides the first insights on novel biomarkers that may help guide the development of vaccine strategies able to reduce the morbidity and mortality associated with influenza across the ages.

While neutralization is likely to play a critical role in yearly protection from infection, neutralization and HAI alone represent incomplete metrics of immunity, particularly in older adults (*16*, *304*). Unlike human challenge studies, individuals in this study were likely exposed to influenza at variable times following peak immunogenicity (*305*), resulting in highly variable signals particularly among the controls. Yet, despite this heterogeneity, the enrichment of FCGR3A and NK cell activating signals in controls, that were significantly lacking in the cases, coalesced on an NK cell signature of potential protective immunity. Given that vaccination remains the most effective strategy to prevent influenza infections in those over age 65 (*265*, *266*, *306*), strategies are urgently needed to improve both HAI and additional functional correlates of immunity in this population (*265*, *266*). Given our emerging appreciation for the importance of ADCC as a correlate of immunity against influenza across multiple animal models (*38*, *39*, *196*, *216*, *307*) as well as a marker of reduced disease burden in humans (*78*), novel strategies including adjuvants and new immunogens able to induce ADCC may complement emerging efforts that show

elevated HAI activity and breadth (*308*). Future studies will determine whether these novel vaccine technologies, including the newest innovations currently used for SARS-CoV-2 vaccination, will yield superior responses against influenza in high-risk populations by eliciting broadly functional and NK cell activating polyclonal humoral immune responses.

Chapter 5: PRE-EXISTING FC PROFILES SHAPE THE EVOLUTION OF NEUTRALIZING ANTIBODY BREADTH TO INFLUENZA

Based on a manuscript in preparation:

Boudreau, C.M., Burke, J.S. IV, Roederer, A., Mundle, S., Delagrave, S., Sridhar, S., Ross, T., Kleanthous, H. & Alter G. Pre-existing Fc profiles shape the evolution of neutralizing antibody breadth following influenza vaccination.

Author contributions: CMB, HK, TR, and GA designed the study. SM, SD, SS, TR, and HK were involved in the original clinical study and provided samples. CMB and JSB conducted experiments. CMB and AR analyzed data. CMB, HK, SS, and GA wrote the manuscript.

Despite ongoing seasonal vaccination campaigns, influenza remains a global health concern, causing significant morbidity and mortality globally. With the ever-present threat of the emergence of a pandemic strain, the need for a universal influenza vaccine has never been more urgent. Emerging data suggest that the evolution of a broad universal neutralizing and functional humoral immune response may hold the key to protection against both circulating and potential emerging influenza strains. Here, we applied a systems approach to profile the unique humoral signatures that tracked with the evolution of broad influenza-specific immunity in a cohort of 108 individuals and validated these findings in an additional cohort of 137 individuals followed over 4 years of seasonal influenza vaccination. Both the biophysical and functional characteristics of the hemagglutinin- (HA) and neuraminidase- (NA) specific responses were profiled across 15 influenza strains, representing both historical and future strains. Multivariate analysis highlighted the presence of a unique Fc γ receptor-binding antibody profile in individuals

that evolved hemagglutination inhibition activity (HAI), marked by the presence of elevated levels of pre-existing FCGR2B-binding antibodies that predicted the evolution of breadth in a second orthogonal cohort. Moreover, vaccination with FCGR2B-binding antibody-opsonized influenza resulted in enhanced antibody titers and HAI activity in a murine model. Together, these data point to a critical role for pre-existing Fc receptor binding antibodies as key correlates of immunity in the evolution of universal influenza specific antibodies, collectively providing key insights for the design of next generation vaccines against influenza.

INTRODUCTION

Despite the availability of seasonal vaccines, influenza remains a major global health concern. Each year, influenza infects 10-20% of the world's population and causes 290,000-650,000 deaths (*180*). The significant burden of influenza is somewhat mitigated by seasonal vaccination. However, between the limited effectiveness of vaccination (10-60% depending on the season (*273*)), caused by antigenic drift, unexpected strain mismatches, production errors, and limited vaccination rates even in areas where the vaccines are widely available, it is estimated that only 5-18% of annual cases are avoided by vaccination in the United States (*181*). Moreover, unpredictable influenza strains that cause increased illness and death, may emerge at any moment, with four major influenza pandemics having occurred just in the 20th and 21st centuries (*13*).

Current influenza vaccines are designed biannually, once annually per hemisphere, based on predictions of the strains that are projected to circulate in the upcoming season (across subtypes H1N1, H3N2, and Influenza B). When these projections are correct,

vaccine efficacy is higher; in seasons where there is a strain mismatch, vaccine efficacy is low (*309*). While this strategy provides some level of annual protection against circulating viruses, it does not appear to boost broad immunity across influenza strains, resulting in a perpetual need for vaccine re-administration to contemporize immunity to both previously encountered and novel strains. More critically, this vaccine strategy does not afford immunity to emerging pandemic influenza strains (*310*). Thus, vaccine strategies that enhance both the breadth of immunity to commonly circulating viral strains and drive immunity to pandemic strains that may represent a global threat are urgently needed.

The development of a broad, "universal" influenza vaccine, has been named a top priority by the National Institutes of Health (*15*), with vaccine-induced protection defined based on the ability of antibodies to block influenza infection in a hemagglutination inhibition assay (HAI). Broad HAI has been documented in naturally immune individuals (*311*), indicating that a stronger heterosubtypic humoral immune response is achievable. However, vaccine design efforts to date continually fail to induce robust breadth of immunity to influenza (*311*). While consensus in the field points to the importance of eliciting vaccine induced immune responses to conserved epitopes (*312*), it remains unclear how natural HAI breadth evolves and whether other key immunological mechanisms may be leveraged to drive protective universal immunity to influenza.

To begin to define whether unique immune mechanisms may underlie the evolution of HAI activity, here we applied an unbiased, comprehensive antibody-profiling strategy to a cohort of 108 individuals sampled prior to and 21 days after influenza vaccination and validated these findings in an additional cohort of 137 individuals followed over four years of seasonal influenza vaccination. HAI was performed on all subjects across 50 strains, providing a comprehensive opportunity to define the predictors of HAI conversion to the

vaccine strain, as well as HAI conversion to non-vaccine strains. Multivariate humoral profiling across the groups pointed to the presence of a unique Fc-effector signature among individuals that evolved HAI, with a selective FCGR2B binding signature among individuals that evolved broad HAI activity, validated across a second cohort of vaccinees. Moreover, immunization of mice with FCGR2B-binding antibody opsonized influenza virus resulted in potent humoral titers and HAI activity, providing unexpected insights into the potentially critical adjuvating activity of pre-existing influenza-specific antibodies that may be required for the evolution of universal influenza specific immune responses.

METHODS

Samples

Samples for the initial dataset were selected from a pool of available samples from a previous study (*313*) conducted in Pittsburgh, Pennsylvania and Stuart, Florida and approved by the Western Institutional Review Board and the Institutional Review Boards of the University of Pittsburgh and the University of Georgia. Samples were chosen for inclusion in this study's initial cohort to answer key questions regarding breadth and durability of the humoral immune response following seasonal vaccination. To address breadth, subjects were selected to include extremes in terms of breadth of both seroprotection and seroconversion. To address durability, subjects were selected who seroconvert to vaccination and either maintain a protective titer to the next season or drop below protective HAI titers (1:40) by the next season.

Samples were collected at the time of vaccination (day 0) and 21-28 days post-vaccination (day 21). Overall, 24 subjects were included with a minimum of two samples each for a total of 198 samples over the three-year study period. For all day 0 samples (n=105), demographics of the samples are: 75% female and 25% male; 19% ages 18-34, 15%

ages 35-49, 38% ages 50-64, and 28% 65+; 74% received regular dose (RD) inactivated vaccine, 17% received high dose (HD) inactivated vaccine, and 9% received intradermal (ID) inactivated vaccine.

Samples were chosen from vaccinees in the 2013-2015 influenza seasons. The vaccine formulations consisted of three or four strains of influenza virus as specified by the U.S. Food and Drug Administration for inclusion each year. For the 2013-2014 and 2014-2015 seasons, the strains included a trivalent formulation of A/California/7/2009 (H1N1), A/Texas/ 50/2012 (H3N2), B/Massachusetts/2/2012 (Yamagata lineage). In the 2015-2016 season, a quadrivalent influenza vaccine formulation composed of A/California/7/2009 (H1N1), A/Switzerland/ 9715293/2013 (H3N2), B/Phuket/3073/2013 (Yamagata lineage), and B/Brisbane/60/2008 (Victoria lineage) was used for vaccination.

For the validation dataset, samples were chosen from the same initial trial. Samples were chosen for inclusion based on the availability of samples for at least three out of four influenza seasons from 2013-2016. Overall, 136 subjects were included with a minimum of six samples each for a total of 835 samples. For all included individuals, demographics of the samples are: 74% female and 26% male; 9% ages 18-34, 9% ages 35-49, 37% ages 50-64 and 46% ages 65+ at study end. Breakdown of vaccine types varied by year: year 1 had 466% RD, 9% HD, 26% ID; year 2 had 89% RD, 11% HD; year 3 had 76% RD, 24% HD; and year 4 had 63% RD, 37% HD. In years 1-3, vaccine composition was as described above. In year 4, vaccine composition included A/California/7/2009 (H1N1), A/Hong Kong/4801/2014 (H3N2), B/Phuket/3073/2013 (Yamagata lineage), and B/Brisbane/60/2008 (Victoria lineage).

The current studies were approved by the Massachusetts General Hospital Institutional Review Board.

Antibody isotyping/subclassing

HA and NA antigens (H1 stem, H1 A/California/07/2009, N1 A/California/07/2009, H1 A/Brisbane/59/2007, H1 A/Chile/1983, H1 A/New Caledonia/20/1999, H3 A/Texas/50/2012, N2 A/Texas/50/2012, H3 A/Brisbane/10/2007, H3 A/Hong Kong/4108/2014, N2 A/Hong Kong/4108/2014, H3 A/Panama/2007/1999, H3 A/Singapore/19/2016, H3 A/Switzerland/9715293/2013, HA B/Brisbane/60/2008, HA B/Phuket/3073/2013, HA B/Colorado/06/2017; all from Sanofi Pasteur), H1 and H3 stem antigens (from Daniel Lingwood), additional NA antigens (N1 A/California/07/2009 from Florian Krammer), and EBOV GPdTM (Mayflower Biosciences) were coupled via carboxyl chemistry to Magplex® fluorescently bar-coded beads (Luminex Corp.) with sulfo-NHS and EDC (Thermo Fisher) per manufacturer's instructions. These beads were then incubated with diluted, heat inactivated serum samples overnight at 4C, shaking. To detect total IgG, IgG1, and FCGR binding, samples were incubated with beads at a final dilution of 1:500. To detect IgG3, IgA1, and IgM, samples were incubated with beads at a final dilution of 1:100. Each sample was assayed in duplicate. Beads were then washed to remove unbound sample and incubated with PE-labeled secondary detection reagents (anti-Ig isotypes from Southern Biotechnology and FCRs from the Duke University Protein Production Facility). Excess detection antibody was washed away, and samples were quantified on the iQue Screener Plus using Forecyt software (Intellicyt).

For the validation cohort, urea wash affinity measurements were taken for antigen-specific antibodies. Protocol was as above, with each sample run four times. One set of duplicates was washed with 7M urea for 15 minutes while the other was washed with

buffer. Affinity was quantified as the fraction of antibodies remaining after urea wash by dividing the urea wash median fluorescence intensity (MFI) by the buffer wash MFI.

Antibody-dependent cellular phagocytosis

HA antigens (H1 A/California/07/2009 and H3 A/Texas/50/2012) were biotinylated with Sulfo-NHS-LC-LC Biotin (Thermo Fisher) and excess biotin was removed using a Zeba size exclusion column (Thermo Fisher). Biotinylated antigens were coupled to Neutravidin fluorescent beads (Thermo Fisher). Antigen-coupled beads were incubated with 1:200 diluted serum samples for two hours at 37C, then washed to remove unbound sample. THP-1 cells (ATCC) were added to immune complexes and incubated for 16 hours at 37C. Cells were then washed to remove unbound immune complexes, fixed, and quantified on the iQue Screener Plus using Forecyt software (Sartorius). Phagocytic scores were calculated by multiplying the percentage of bead positive cells by the bead fluorescence GMFI of bead positive cells and dividing by 10,000. Each sample was assayed in two independent replicates.

Antibody-dependent neutrophil phagocytosis

Antibody-dependent neutrophil phagocytosis was adapted from the previously published protocol (*247*). HA-coated beads were created as for ADCP. Antigen-coupled beads were incubated with 1:50 diluted serum samples for two hours at 37C, then washed to remove unbound sample. Fresh primary human white blood cells, isolated by ACK lysis, were incubated with immune complexes for one hour at 37C. Cells were then washed to remove unbound immune complexes, labeled for CD66b (anti-human CD66b fluorescent antibody from Biolegend), fixed, and quantified on the iQue Screener Plus using Forecyt software (Intellicyt). Neutrophils were identified as CD66b positive. Phagocytic scores were calculated by multiplying the percentage of bead positive cells by the bead fluorescence

GMFI of bead positive cells and dividing by 10,000. Each sample was assayed for two healthy blood donors.

Antibody-dependent complement deposition

Antibody-dependent complement deposition was adapted from the previously published protocol (*248*). HA-coated beads were created as for ADCP. Antigen-coupled beads were incubated with 1:25 diluted heat inactivated serum samples for two hours at 37C, then washed to remove unbound sample. Immune complexes were then incubated with reconstituted lyophilized guinea pig complement (Cedarlane) for 20 minutes at 37C, and excess complement washed off. Immune complexes were stained with anti-guinea pig C3 fluorescent antibody (MP Biomedicals). Excess staining antibody was removed by washing and immune complexes were quantified on the iQue Screener Plus using Forecyt software (Intellicyt). Complement deposition was indicated by the C3 GMFI of immune complexes. Each sample was assayed in two independent replicates

Antibody-dependent NK cell activation

ELISA plates (NUNC, Thermo Fisher) were coated with HA antigens (H1 A/California/07/2009 and H3 A/Texas/50/2012), washed to remove unbound antigen, and blocked with 5% bovine serum albumin (Sigma) in PBS. Primary human NK cells were isolated from fresh buffy coats using the RosetteSep NK cell enrichment kit (StemCell) and rested overnight at 37C with 1 ng/ml IL-15 (StemCell). 1:25 diluted serum samples were added to the washed, HA-coated plates and incubated for 2 hours at 37C. Immediately prior to use, brefeldin A (Sigma), GolgiStop (BD), and fluorescent anti-CD107a (BD) were added to primary NK cells. Immune complexed plates were washed, and NK cells were added for 5 hours at 37C. After incubation, NK cells were removed and stained with fluorescent antibodies for cell surface markers CD3, CD56, and CD16 (BD). NK cells were fixed and permeabilized using Fixation & Permeabilization Media A & B (BD). Permeabilized NK

cells were stained for intracellular makers MIP-1β and IFN-γ (BD). NK cells were quantified on the iQue Screener Plus using Forecyt software (Intellicyt). NK cells were defined as CD3 negative, CD16 positive. Each sample was assayed on two buffy coat donors.

Antibody-dependent Dendritic Cell phagocytosis

Primary human Dendritic Cells (DCs) were derived from buffy coats through isolation with CD14 microbeads (Miltenyi) and culture in MoDC media (Miltenyi) for 6-7 days. HA antigens (H1 A/California/07/2009 and H3 A/Texas/50/2012) were coupled to fluorescently-labeled beads (Thermo Fisher) through carboxyl chemistry as for antibody isotyping/subclassing. Antigen-coupled beads were incubated with 1:50 diluted serum samples for two hours at 37C, then washed to remove unbound sample. Immune complexes were then incubated with differentiated DCs for 4 hours at 37C. DCs were then fixed and stained for cell surface activation markers HLA-DR, CD86, and CD83. DCs were quantified on the iQue Screener Plus using Forecyt software (Intellicyt). Phagocytic scores were calculated by multiplying the percentage of bead positive cells by the bead fluorescence GMFI of bead positive cells and dividing by 10,000. Other activation markers were quantified as GMFI of each marker as a percentage of total cells. Each sample was assayed on two buffy coat donors.

Antigen-specific antibody Fc glycan analysis

HA and NA antigens (H1 A/California/07/2009, H3 A/Texas/50/2012, N2 A/Texas/50/2012) were coated onto magnetic beads through biotin-streptavidin as for ADCP. Serum samples were pre-cleared with non-coupled magnetic beads to remove nonspecific serum binding components. Pre-cleared samples were incubated with antigen-coated beads for 2 hours at 37C to form immune complexes. Beads were washed and Fc regions were cleaved off from beads by IDEZ digestion (New England Biolabs). Resulting

solubilized Fc regions were then deglycosylated and labeled with APTS per GlycanAssure kit instructions (Thermo Fisher). Labeled glycans were analyzed by capillary electrophoresis (GeneScan 3500XL, Applied Biosciences) and GlycanAssure software (ThermoFisher). Peaks were called based on known labeled glycan standards and reported as a percentage of total glycan peak area.

Breadth Score

Sequences were aligned and pairwise distances between the amino acids of the sequences were generated (**Figure 5.1**) (*314*). All hemagglutinin sequences were obtained through the NIH data base in MEGAX (*315–317*) or provided by Sanofi Pasteur. Sequences were aligned with the MUSCLE algorithm (*318*). MEGAX software was then used to generate the pairwise distance between amino acids of the sequences using the Jones-Taylor-Thornton Model with a gamma distributed rate among sites and pairwise deletion for gaps/missing treatment (*319*). The pairwise distances were used to calculate the overall breadth score of all neutralized viruses with the formula $breadth = \Omega \frac{\sum_{i,j \in N} d(s_i,s_j)}{|N|}$, where the sum of $d(s_i,s_j)$ represents the sum of pairwise distances by amino acid change between strains, and N is the number of strains used. Ω is an arbitrary breadth factor calculated such that the breadth score for a hypothetical individual who neutralizes all strains included in the dataset will equal 1 for the ease of analysis.

Multivariate and statistical analyses

Univariate visualizations and statistics were generated using Prism 8 (Graphpad Software, LLC). Statistical tests are described in figure legends.

Multivariate analyses were completed using MATLAB (The Mathworks, Inc.) For Elastic Net-Partial Least Squares analyses, a dataset containing antigen-specific antibody isotypes, FCGR binding, neutralization, and antibody-dependent functional data for study

subjects was used. Missing datapoints were imputed using K-nearest neighbor and data were normalized using z-scoring. Elastic Net machine learning was performed in a 5-fold cross-validation framework. The Elastic Net lambda coefficient was chosen within this

cross-validation framework. A minimum of 3 antibody features were selected in each replicate. Random size-matched and label permuted datasets were compared for each model within the cross-validation framework. Networks were created from highly significant (false discovery rate adjusted q value < 0.01 and absolute value of r greater than 0.6) co-correlates of LASSO-selected features and visualized using Cytoscape.

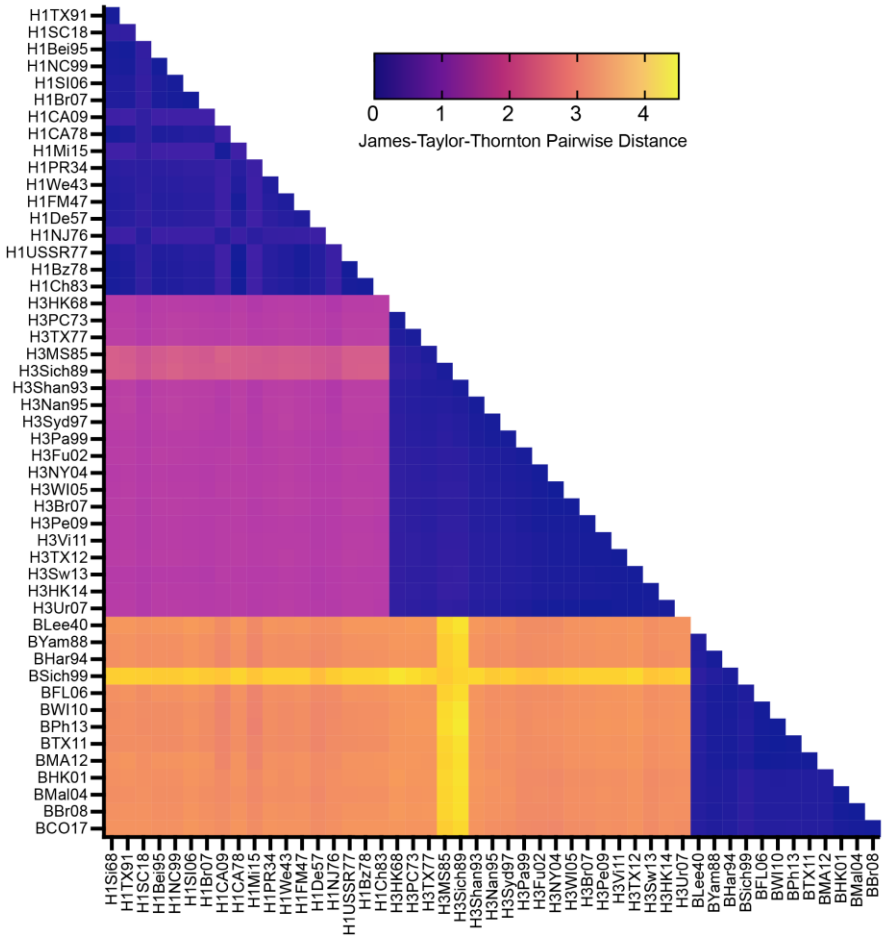

Figure 5.1 Pairwise distances show subtype variation. Heatmap depicts James-Taylor-Thornton pairwise distance values between influenza strains.

RESULTS

RESPONSE TO SEASONAL INFLUENZA VACCINATION IS HIGHLY HETEROGENEOUS

A cohort of 108 healthy adults was sampled prior to and 21 days following inactivated influenza vaccination. Serum samples were profiled for hemagglutinin inhibition (HAI) across 50 influenza strains (**Table 5.1**). Individuals were selected for inclusion in this cohort based on their HAI conversion profiles against vaccine strains H1N1 A/California/07/2009 and H3N2 A/Texas/50/2012. Annual HAI conversion profiles for each influenza strain could be divided into four patterns (**Figure 5.2A**): 1) individuals that did not experience seroconversion (*non-converters*), 2) individuals who were HAI positive (≥1:40 (*320*)) prior to vaccination and did not experience significant (4-fold) increase in HAI titer (*positives*), 3) individuals who had sub-protective (<1:40) HAI titers prior to vaccination but seroconverted following vaccination (*converters*), and 4) individuals who were HAI positive prior to vaccination but also experienced a greater than or equal to four-fold increase in HAI titer following vaccination (*positive/converters*).

To begin to define the humoral immune profile changes that could potentially provide mechanistic insights into these different vaccine response profiles, systems serology (*209*) was used to deeply profile the biophysical and functional characteristics of the influenza-specific antibodies elicited by vaccination. Over 200 measurements were taken per serum sample, mapped across 23 influenza antigens (**Table 5.2**), resulting in a comprehensive analysis of the polyclonal humoral response to influenza vaccination. For each individual, a delta from pre- to post-vaccination was calculated to account for pre-existing immunity, enabling the comparison of vaccine induced immunity. Striking

Table 5.1 Influenza strains tested in HAI assays and abbreviations used.

Influenza strain	Abbreviation
H1N1 A/South Carolina/1/1918	H1SC18
H1N1 A/Puerto Rico/8/1934	H1PR34
B/Lee/1940	BLee40
H1N1 A/Weiss/1943	H1We43
H1N1 A/Fort Monmouth/1/1947	H1FM47
H1N1 A/Denver/1957	H1De57
H3N2 A/Hong Kong/1/1968	H3HK68
H3N2 A/Port Chalmers/12/1973	H3PC73
H1N1 A/New Jersey/1976	H1NJ76
H1N1 A/USSR/90/1977	H1USSR77
H3N2 A/Texas/1/1977	H3TX77
H1N1 A/Brazil/11/1978	H1Bz78
H1N1 A/California/10/1978	H1CA78
H1N1 A/Chile/1/1983	H1Ch83
H3N2 A/Mississippi/1/1985	H3MS85
H1N1 A/Singapore/6/1986	H1Si68
B/Yamagata/16/1988	BYam88
H3N2 A/Sichuan/60/1989	H3Sich89
H1N1 A/Texas/36/1991	H1TX91
H3N2 A/Shandong/9/1993	H3Shan93
B/Harbin/7/1994	BHar94
H1N1 A/Beijing/262/1995	H1Bei95
H3N2 A/Nanchang/933/1995	H3Nan95
H3N2 A/Sydney/5/1997	H3Syd97
B/Sichuan/379/1999	BSich99
H1N1 A/New Caledonia/29/1999	H1NC99
H3N2 A/Panama/2007/1999	H3Pa99
B/Hong Kong/330/2001	BHK01
H3N2 A/Fujian/411/2002	H3Fu02
B/Malaysia/2506/2004	BMal04
H3N2 A/New York/55/2004	H3NY04
H3N2 A/Wisconsin67/2005	H3WI05
B/Florida/4/2006	BFL06
H1N1 A/Solomon Islands/03/2006	H1SI06
H1N1 A/Brisbane/59/2007	H1Br07
H3N2 A/Brisbane/10/2007	H3Br07
B/Brisbane/60/2008	BBr08
H3N2 A/Kentucky/UR07-0028/2008	H3Ur07
H1N1 A/California/07/2009	H1CA09
H3N2 A/Perth/16/2009	H3Pe09
B/Wisconsin/1/2010	BWI10
B/Texas/06/2011	BTX11
H3N2 A/Victoria/361/2011	H3Vi11
B/Massachusetts/2/2012	BMA12
H3N2 A/Texas/50/2012	H3TX12
B/Phuket/3073/2013	BPh13
H3N2 A/Switzerland/9715293/2013	H3Sw13
H3N2 A/Hong Kong/4801/2014	H3HK14
H1N1 A/Michigan/45/2015	H1Mi15
B/Colorado/06/2017	BCO17

heterogeneity in influenza specific humoral immune responses were observed across the vaccinees, where no two individuals possessed an identical response (**Figure 5.2B**). The data were therefore collapsed into the 4 groups to begin to visualize potential differences in profiles across HAI conversion to the vaccine strain H1N1 A/California/07/2009 (**Figure 5.2C**). As expected, non-converters exhibited the lowest overall reactivity compared to the other 3 groups. Conversely, robust induction of humoral immune responses was noted in HAI converters and positive/converters, surprisingly with a marked increase also in influenza- specific FCGR binding antibody levels among HAI positive individuals.

Table 5.2 Systems serologic measurements by sample cohort and influenza strain.

Influenza strain	Abbreviation	Ag-specific Ab isotype titers & FCR binding		Ag-specific Ab isotype & FcR binding affinity		Ag-specific Ab functions		Ag-specific Ab glycosylation	
		Cohort 1	*Cohort 2*	*Cohort 1*	*Cohort 2*	*Cohort 1*	*Cohort 2*	*Cohort 1*	*Cohort 2*
		FCGR2A *FCGR2B* *FCGR3A* *IgA1* *IgG1* *IgG3* *IgM* *Total IgG*	*FCGR2A* *FCGR2B* *FCGR3A* *FCGR3B* *IgA1* *IgA2* *IgG1* *IgG2* *IgG3* *IgG4* *IgM*		*FCGR2A* *FCGR2B* *FCGR3A* *FCGR3B* *IgA1* *IgA2* *IgG1* *IgG2* *IgG3* *IgG4* *IgM*	*ADCP* *ADNP* *ADCD* *ADNKA* *ADDCP*	*ADCP* *ADNP* *ADCD*		
H1N1 A/Chile/1/1983	H1Ch83	HA	HA		HA				
H1N1 A/New Caledonia/29/1999	H1NC99	HA	HA		HA				
H3N2 A/Panama/2007/1999	H3Pa99	HA	HA		HA				
H1N1 A/Brisbane/59/2007	H1Br07	HA	HA		HA				
H3N2 A/Brisbane/10/2007	H3Br07	HA	HA		HA				
B/Brisbane/60/2008	BBr08	HA	HA		HA				
H1N1 A/California/07/2009	H1CA09	HA, NA	HA, NA		HA, NA	HA	HA	HA	
H1N1 A/Belgium/145-MA/2009	H1Be09		NA		NA				
H3N2 A/Texas/50/2012	H3TX12	HA, NA	HA, NA		HA, NA	HA	HA	HA, NA	
B/Phuket/3073/2013	BPh13	HA	HA, NA		HA, NA				
H3N2 A/Switzerland/9715293/2013	H3Sw13	HA	HA, NA		HA, NA				
H3N2 A/Hong Kong/4801/2014	H3HK14	HA, NA	HA, NA		HA, NA				
H1N1 A/Michigan/45/2015	H1Mi15		NA		NA				
H3N2 A/Singapore/19/2016	H3Si16	HA	HA		HA				
B/Colorado/06/2017	BCO17	HA	HA, NA		HA, NA				
H1 stabilized stem	H1 stem	HA	HA		HA				
H3 stabilized stem	H3 stem		HA		HA				

To gain a precise understanding of the specific vaccine-induced features that distinguished converters from non-converters to the vaccine strain H1N1 A/California/07/2009, all systems serology data were combined and a Least Absolute Shrinkage and Selection Operator (LASSO)-Elastic Net (*212*, *249*) was used to define the minimal set of antibody features required to discriminate converters and non-converters. Partial Least Squares Discriminant Analysis (PLSDA) was then used to visualize the differences across the groups. Highly significant separation was observed across the two groups (**Figure 5.2D**) compared to random size-matched and permuted label models ($p<0.001$, **Figure 5.3**). As few as five of the total 239 humoral features captured for each

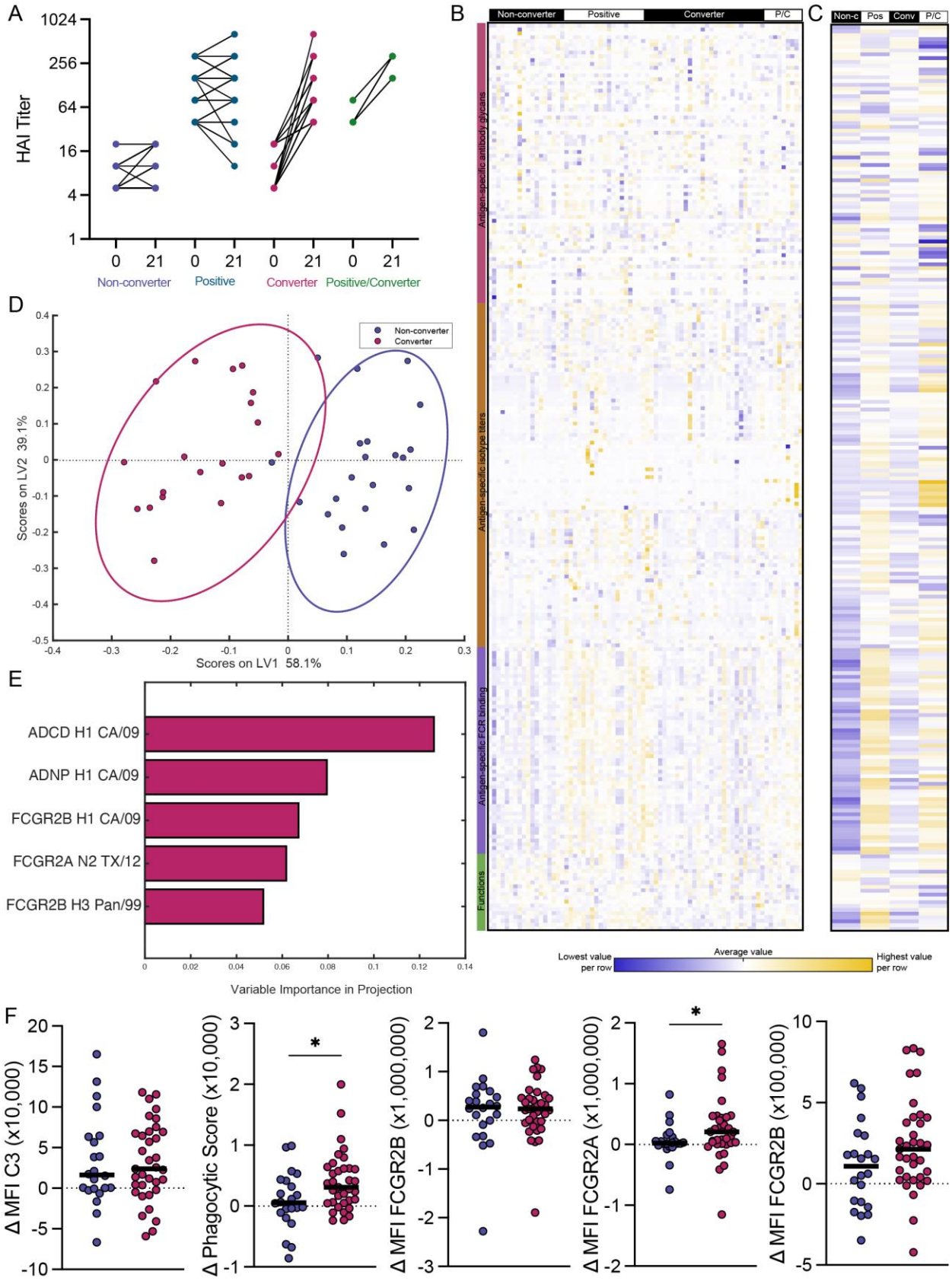

Figure 5.2 Seasonal influenza vaccine produces highly heterogeneous responses in healthy adults.

Figure 5.2 cont. Line plot (**A**) shows before-and-after HAI titers against H1N1 A/California/07/2009, with individuals broken out into groups based on HAI conversion as described. Heat map (**B**) shows normalized Δ day 21 – day 0 values for all antibody biophysical and functional features measured with rows grouped by type of antibody feature measured. All features are listed in Table S3. Each column represents an individual subject, grouped by H1N1 A/California/07/2009 HAI response to vaccination. Yellow represents high values and blue represents low values. Smaller heat map (**C**) shows median value for each H1N1 seroconversion group by column and the same antibody features in (**B**) by row. Dot plot (**D**) shows PLSDA of H1N1 A/California/07/2009 converters and non-converters graphed across latent variables 1 and 2. Percentages indicate amount of variation explained by each latent variable. Multivariate modeling in this analysis used Δ values calculated as the change from pre- to post-vaccination. Bar graph (**E**) shows LASSO-Elastic Net selected features contributing to the separation in (**D**) graphed by variable importance in projection (VIP) score. VIP scores indicate contribution to the model. Dot plots (**F**) show LASSO-Elastic Net selected features (Δ day 21 – day 0) as univariate plots. Significance was tested by Kruskal-Wallis test followed by Dunn's multiple comparisons correction. * $p < 0.05$

plasma sample were sufficient to build this model (**Figure 5.2E-F**), pointing to a highly focused humoral signature of conversion. Interestingly, no identified features were enriched in the non-converters, pointing to limited negative predictors of HAI conversion. Conversely, while antibody titers were not a correlate of conversion, the "converter signature" included vaccine strain-specific antibody-dependent complement deposition (ADCD), antibody-dependent neutrophil phagocytosis (ADNP), and binding to both the activating and inhibitory FCGR2 receptors. Given that univariate differences across the

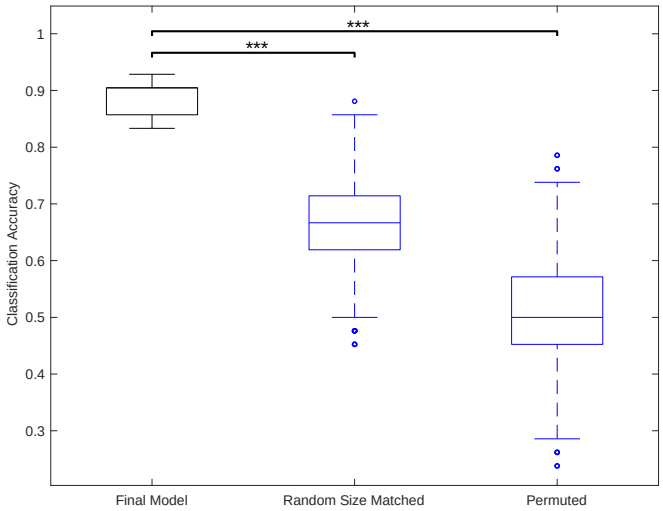

Figure 5.3 Accuracy and significance of non-converter vs converter model in **Figure 5.2**. Box plot shows model accuracy for LASSO classification model, random size matched models, and permuted label models. LASSO was run for 20 replicates of 5-fold data separation. Random size matched and permuted label models were run 100 permutations per replicate. Stars indicate significance by Mann-Whitney U test. *** $p < 0.001$.

five "correlates of conversion" were modest (**Figure 5.2E**), these data point to the importance of a functional multivariate signature of conversion, indicating that the evolution of HAI occurs in concert with a significant shift in Fc biology.

DEFINING CORRELATES FOR THE EVOLUTION OF BREADTH OF HAI

Across this cohort, differences were seen in seroconversion to different viral strains (**Figure 5.2A, Figure 5.4**), with more individuals seroconverting to the H3N2 strain A/Texas/50/2012 than to the H1N1 A/California/07/2009 (**Figure 5.5A, inner rings**).

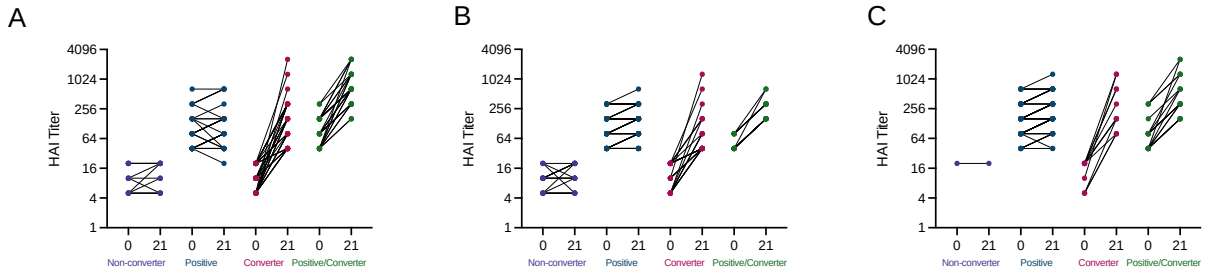

Figure 5.4 HAI titers by group for vaccine antigens. Line plots show before-and-after HAI titers against (**A**) H3N2 A/Texas/50/2012, (**B**) B/Brisbane/60/2008, and (**C**) B/Massachusetts/2/2012 with individuals broken out into groups based on HAI conversion for each strain: 1) individuals that did not experience seroconversion (non-converters), 2) individuals who were HAI positive prior to vaccination and did not experience significant increase in HAI titer (positives), 3) individuals who had subprotective HAI titers prior to vaccination but seroconverted following vaccination (converters), and 4) individuals who were HAI positive prior to vaccination but saw a significant (greater than or equal to four-fold) increase in HAI titer following vaccination (positive/converters).

However, interestingly, when we examined how many individuals converted their HAI responses to both strains, only a small fraction of individuals converted simultaneously to both strains (**Figure 5.5A, 2 strain ring**). Furthermore, an even smaller fraction showed seroconversion to all four strains included in the quadrivalent vaccine (**Figure 5.5A, 4 strain outer ring**). Given our ultimate goal of defining the predictors of broad seroconversion, we calculated a breadth score, encompassing the normalized average pairwise HA genetic sequence distance between strains to which an individual seroconverted. A breadth score of 0 indicated seroconversion to no or only one strain, whereas higher scores indicated

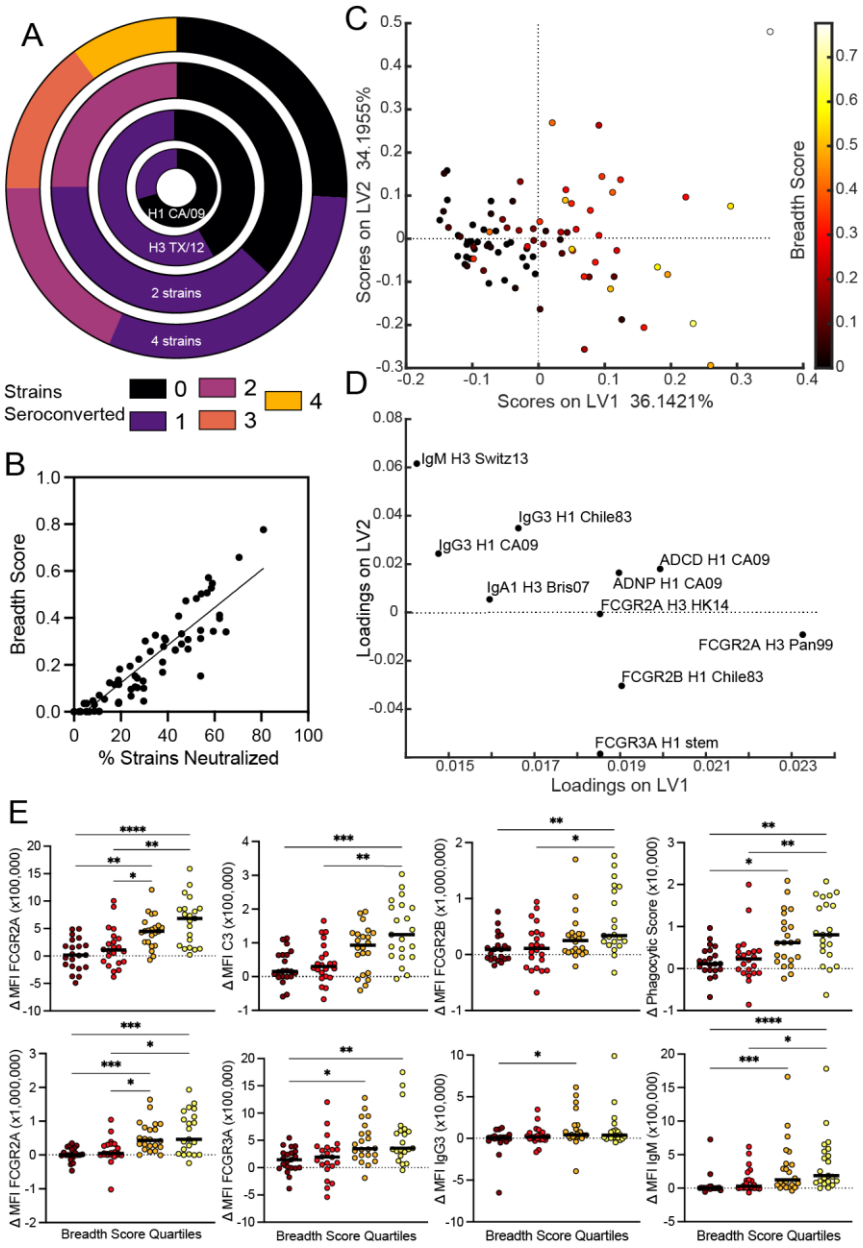

Figure 5.5 FCGR-binding titers are correlates of the development of neutralizing breadth. Pie charts (**A**) show fraction of individuals who seroconvert to a given strain or strains. In order from smallest to largest: H1N1 A/California/07/2009; H3N2 A/Texas/50/2012; both; both plus B/Brisbane/60/2008 and B/Massachusetts/01/2012. Dot plot (**B**) shows correlation between percentage of strains seroconverted and breadth score. Dot plot (**C**) represents PLSR for delta values regressed against breadth in the test cohort. Loadings plot (**D**) represents relative contributions of LASSO-Elastic Net selected features for the model, with features plotted to represent where they have highest values if overlaid on the PLSR plot. Dot plots (**E**) show significantly different LASSO-Elastic Net selected features as univariate plots binned by quartile of breadth score. Significance (**E**) was tested by Kruskal-Wallis test followed by Dunn's multiple comparisons correction. * $p < 0.05$, ** $p < 0.01$, *** $p < 0.001$, **** $p < 0.0001$.

increased breadth of seroconversion. Furthermore, conversion of HAI to two strains that have low sequence similarity resulted in a higher breadth score than conversion of HAI to two genetically similar strains. A seroconversion breadth score was generated for each individual and compared to percentage of strains neutralized. Individuals with percentage values from 0-20% represented those with low total number of strains neutralized; however, within this group breadth and percentage neutralized was poorly correlated (**Figure 5.5B**). On the high end, percentages above 60% indicated individuals who seroconverted to a large number of strains, and again within this group the breadth score allowed discrimination between those who converted to a large number of genetically similar strains (e.g. breadth scores < 0.5) and those who converted to a large number of genetically different strains.

Using seroconversion breadth, we next explored which humoral features developed in concert with the evolution of breadth using LASSO-Elastic Net and Partial Least Squares Regression (PLSR). Using the change in antibody humoral features from pre- to post-vaccination (delta), individuals with broader responses were separated across LV1 (**Figure 5.5C**, model $p < 0.001$, **Figure 5.6**). Specifically, 10 of a total of 239 analyzed features per plasma sample were sufficient to separate individuals that evolved broad neutralizing responses. The features overlapped with features captured in the single HAI conversion model (**Figure 5.2**), and included FCGR2A, FCGR2B, FCGR3A, and functional titers to both vaccine strains and additional breadth strains (**Figure 5.5D-E, Figure 5.7**). Interestingly, the breadth strains included in this analysis reflected a wide diversity of H3N2 influenza HA antigens, spanning nearly twenty years of antigenic drift. For H1N1, a more focused response on the 2009 pandemic strain was observed. This accumulation of Fc-features, rather than titers, again emphasized the involvement of the Fc region in Fab evolution.

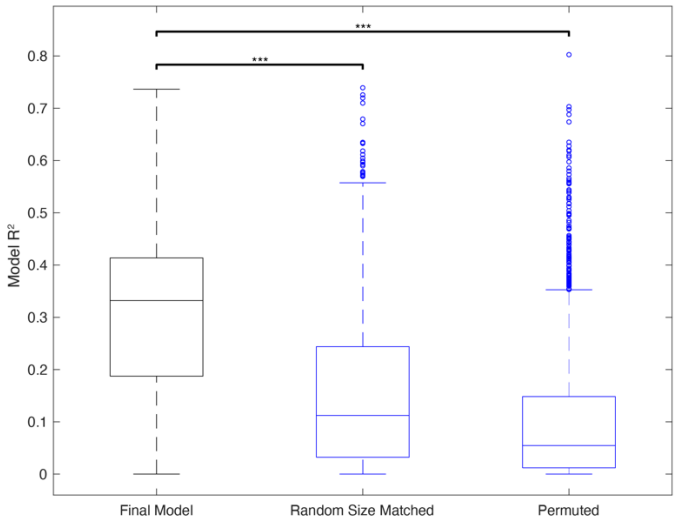

Figure 5.6 Accuracy and significance of breadth model in **Figure 5.5**. Box plot shows model accuracy (R^2) for LASSO-Elastic Net classification model, random size matched models, and permuted label models. LASSO-Elastic Net was run for 20 replicates of 5-fold data separation. Random size matched and permuted label models were run 100 permutations per replicate. Stars indicate significance by Mann-Whitney U test. *** $p < 0.001$.

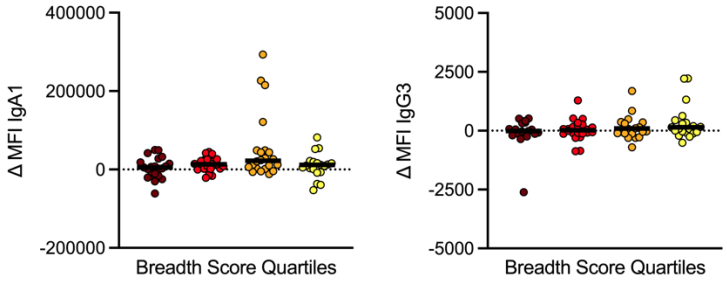

Figure 5.7 Additional univariate plots for LASSO-Elastic Net selected features (**Figure 5.5**). Dot plots show significantly different LASSO-Elastic Net selected features as univariate plots binned by quartile of breadth score. Significance was tested by Kruskal-Wallis test followed by Dunn's multiple comparisons correction. Not significant.

VALIDATION OF NEUTRALIZING BREADTH CORRELATES IN AN ORTHOGONAL COHORT OF VACCINEES

Given the potential role of Fc profiles in tuning both conversion to a single HA as well as in the development of breadth, we next aimed to validate these signatures in an orthogonal cohort of vaccinated individuals. Specifically, influenza-specific systems serology was performed on a second cohort of 137 vaccinated individuals followed over multiple years, for a total of 430 pairs of before- and after-vaccination samples. Over 450 distinct humoral features, including antigen-specific antibody-dependent functions, subclass/isotype titers, FCγR binding titers, and isotype-and FCγR-specific affinities, were mapped in the validation cohort across 23 influenza antigens (HA and NA) representing 15 distinct strains (**Table 5.2**). Like the first cohort, the validation cohort showed a broad heterogeneity in response to vaccination across the antibody functional and biophysical features measured (**Figure 5.8A**). Patterns emerged across individuals, with visibly enhanced functionality and Fc-receptor binding among individuals with higher breadth scores. This was more apparent when individuals were grouped into breadth quartiles (**Figure 5.8B**). To test the generalizability of the correlates of breadth defined in the first discovery cohort, we built a model using the features selected using the first cohort but used the data from the second cohort. The five features selected in the discovery model were able to significantly separate the converters from non-converters in the second, independent cohort (**Figure 5.9**). Additionally, breadth scores were calculated for the second cohort using the same approach used on the first discovery cohort, with breadth scores ranging from 0 to 0.73, which reflected a wide range of neutralizing breadth (**Figure 5.10**). To validate our previous findings, a model was built for the evolution of breadth of neutralization based on the 10

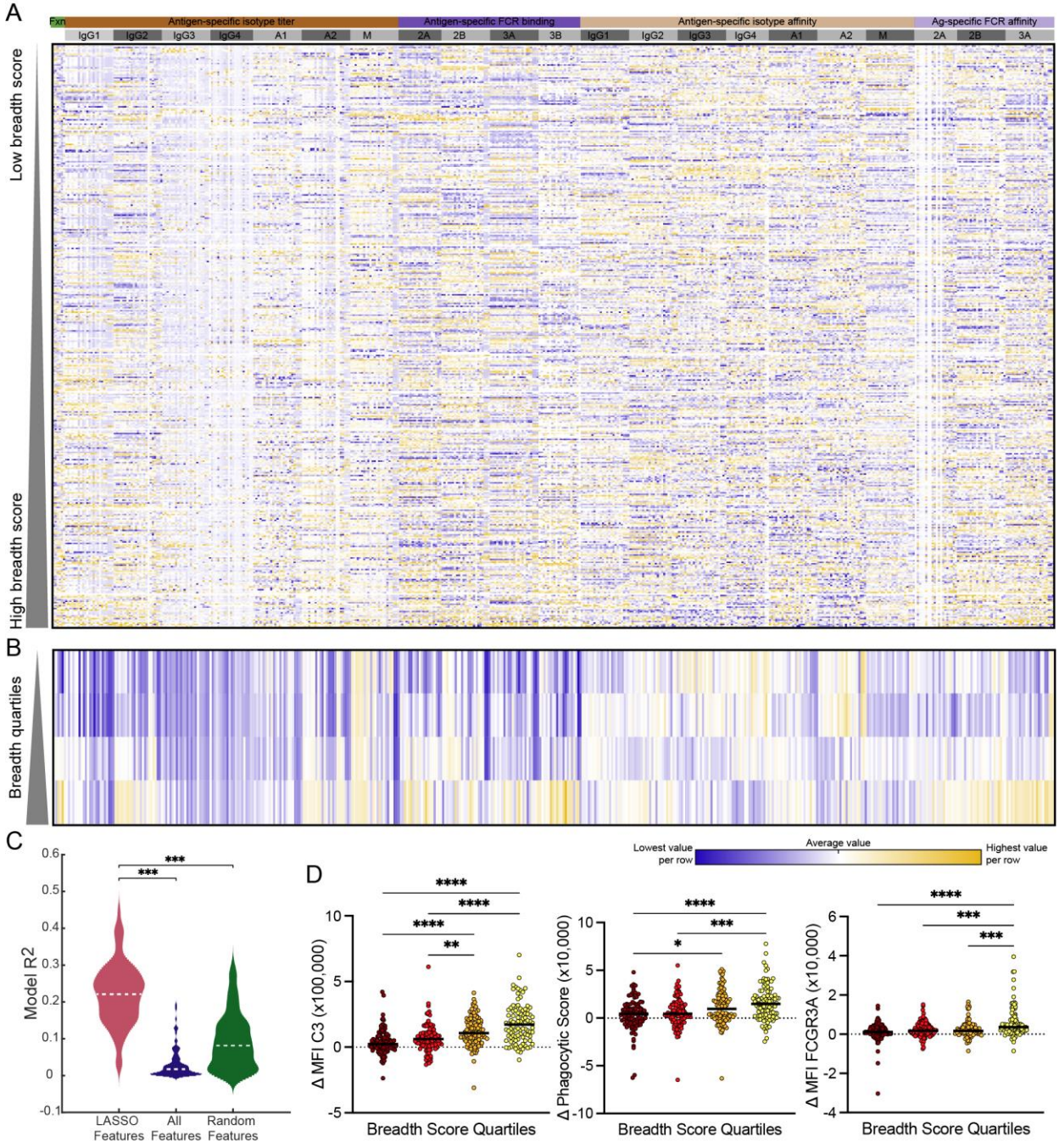

Figure 5.8 Validation of breadth findings in an independent cohort. Heat map (**A**) shows normalized Δ day 21 – day 0 values for all antibody biophysical and functional features measured with columns grouped by type of antibody feature measured. Each row represents an individual subject, ordered by HAI conversion breadth score. Yellow represents high values and blue represents low values. Smaller heat map (**B**) shows median value for each breadth score quartile by row and the same antibody features in (**A**) by column. Violin plot (**C**) shows validation model system in validation cohort, comparing the LASSO-Elastic Net selected features, to all features, to a random equal sized subset of features. Dot plots (**D**) show a subset of LASSO-Elastic Net selected features as univariate plots binned by quartile of breadth score. Significance in (**C**) and (**D**) was tested by Kruskal-Wallis test followed by Dunn's multiple comparisons correction. * $p < 0.05$, ** $p < 0.01$, *** $p < 0.001$, **** $p < 0.0001$.

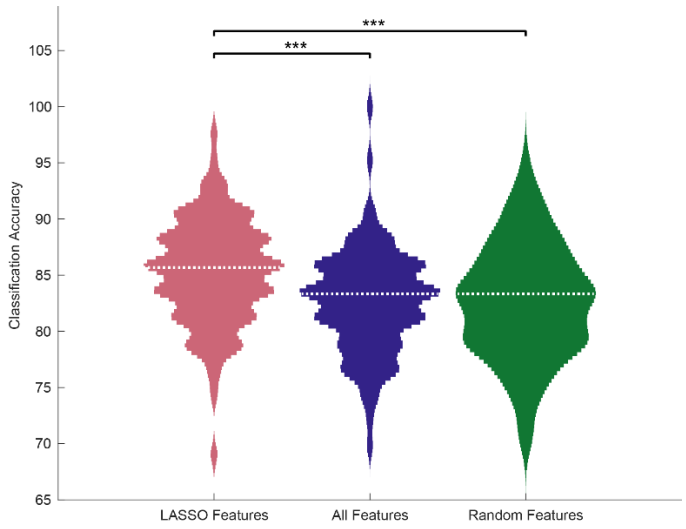

Figure 5.9 Validation of the seroconversion model in **Figure 5.2** with an orthogonal cohort. Features selected by LASSO on the training cohort (pink) were compared to all measured features (blue) and a size-matched set of random features (green). Significance determined by Mann-Whitney U test. *** $p < 0.01$.

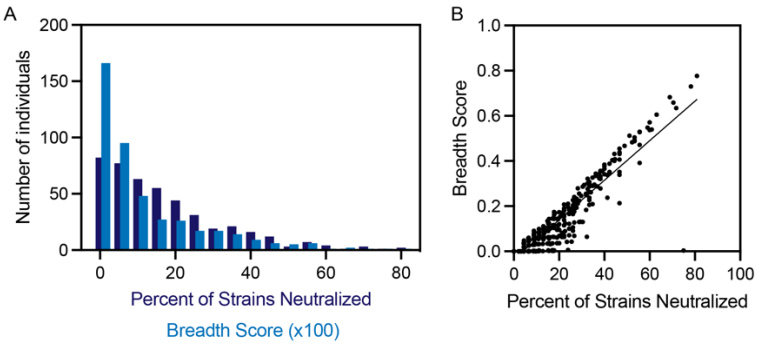

Figure 5.10 Breadth score distribution and comparison to percentage of strains neutralized for the larger cohort used for validation. Histogram (**A**) shows both percentage seroconversion and breadth score. Dot plot (**B**) shows correlation between percentage of strains seroconverted and breadth score.

features selected using the original cohort (**Figure 5.5D**). When applied to the second cohort, these 10 features were able to robustly differentiate individuals across neutralizing breadth (**Figure 5.8C**). These data suggest that conserved Fc-profiles are linked to the development of a broad neutralizing responses across individuals, with orthogonal validation highlighting that these features are not unique to one cohort but represent conserved features of a broadly neutralizing polyclonal humoral immune response. Furthermore, analysis of these humoral features on a univariate basis shows significant

differences developing in coordination with neutralizing breadth (**Figure 5.8D, Figure 5.11**). This emphasized and reinforced the findings from the first cohort, showing that a broad neutralizing response to vaccination develops in concert with extra-neutralizing functions driven by the binding of influenza-specific antibodies to FCγRs.

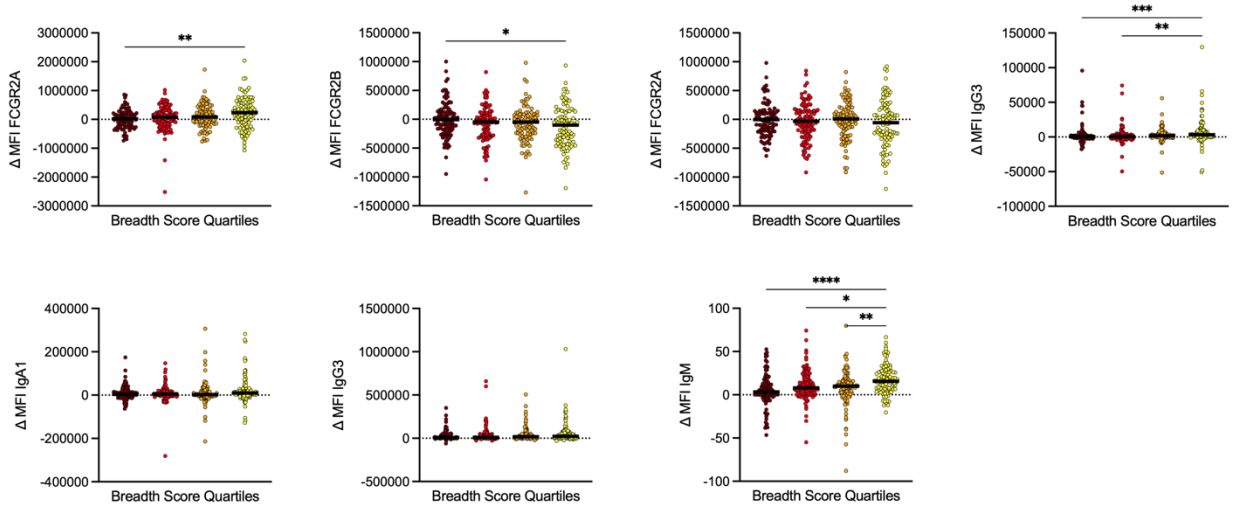

Figure 5.11 Additional univariate plots for LASSO-Elastic Net selected features (**Figure 5.8**). Dot plots show significantly different LASSO-Elastic Net selected features as univariate plots binned by quartile of breadth score. Significance was tested by Kruskal-Wallis test followed by Dunn's multiple comparisons correction. * $p < 0.05$, ** $p < 0.01$, *** $p < 0.001$, **** $p < 0.0001$.

PRE-EXISTING FCγR-BINDING ANTIBODY TITERS PREDICT A BROAD NEUTRALIZING VACCINE RESPONSE

Collectively, these data pointed to the existence of conserved Fc-signatures that co-evolve with breadth of neutralization across cohorts. However, whether any Fc-features exist prior to immunization that could help predict or explain the response to vaccination remains incompletely understood. Thus, we next aimed to determine whether the evolution of breadth could be predicted from pre-vaccine humoral profiles. LASSO-PLSR was performed on pre-vaccination systems serology data from the second validation cohort, where more samples were tested to increase power to see predictive differences. The model

successfully discriminated individuals that evolved broad neutralizing antibody responses (**Figure 5.12A**, p<0.001, **Figure 5.13**) using only pre-existing humoral profiles.

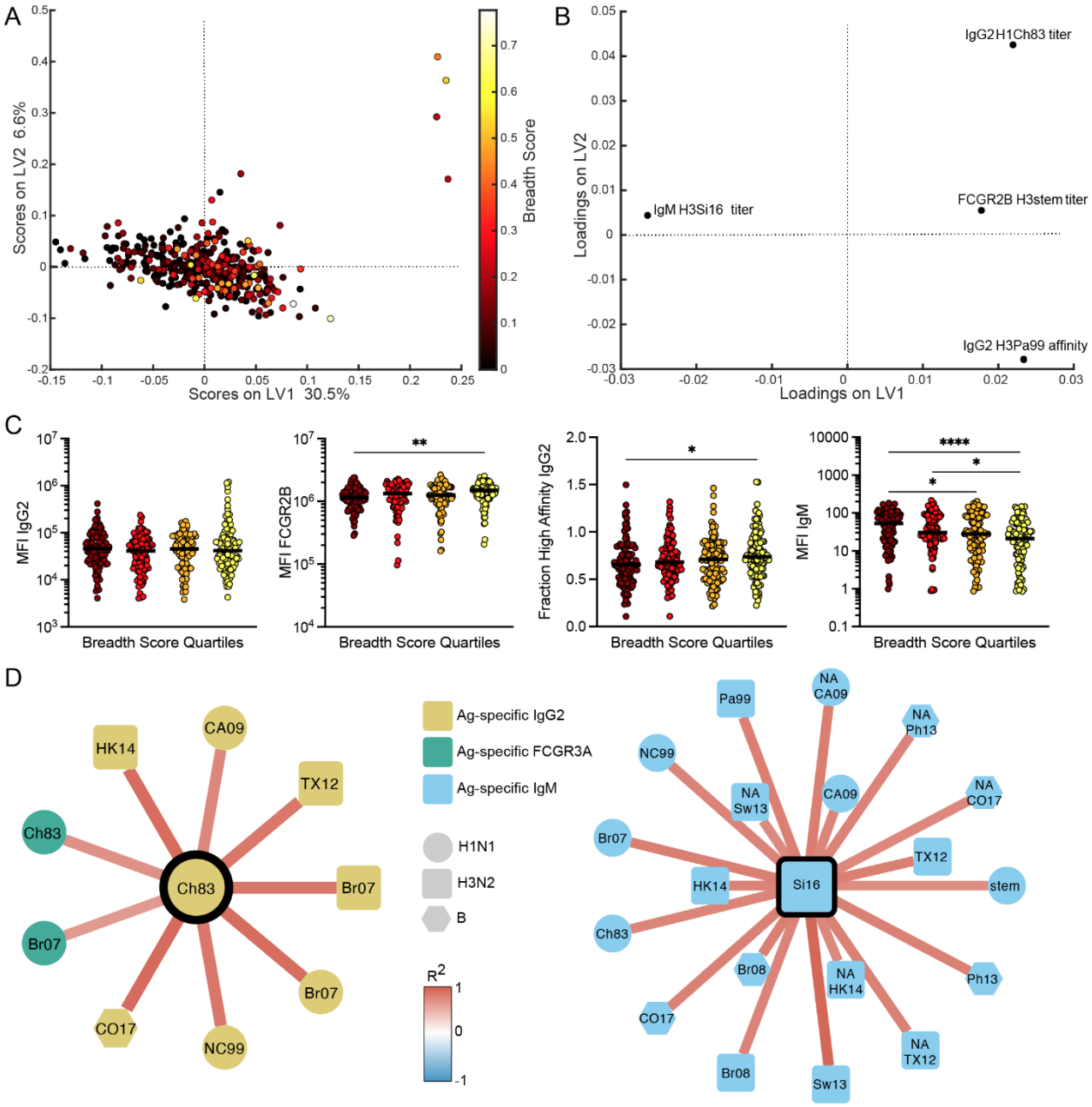

Figure 5.12 FCGR2B-binding antibodies are a predictor of neutralizing breadth. Dot plot (**A**) represents PLSR for day 0 values regressed against breadth score in the validation cohort. Loadings plot (**B**) represents relative contributions of LASSO-Elastic Net selected features for each model. Dot plots (**C**) represent univariate values for the LASSO-Elastic Net selected features, with individual samples binned by quartile of breadth score. Significance was tested by Kruskal-Wallis test followed by Dunn's multiple comparisons correction. * $p < 0.05$, ** $p < 0.01$, **** $p < 0.0001$. Networks (**D**) show significant (R >0.6 and FDR-corrected Q <0.01) co-correlates of LASSO-Elastic Net selected features as shown in (**B**), where stronger red edges indicate stronger correlations and node shape and color reflects strain and measurement type. All antigens are HA unless otherwise noted.

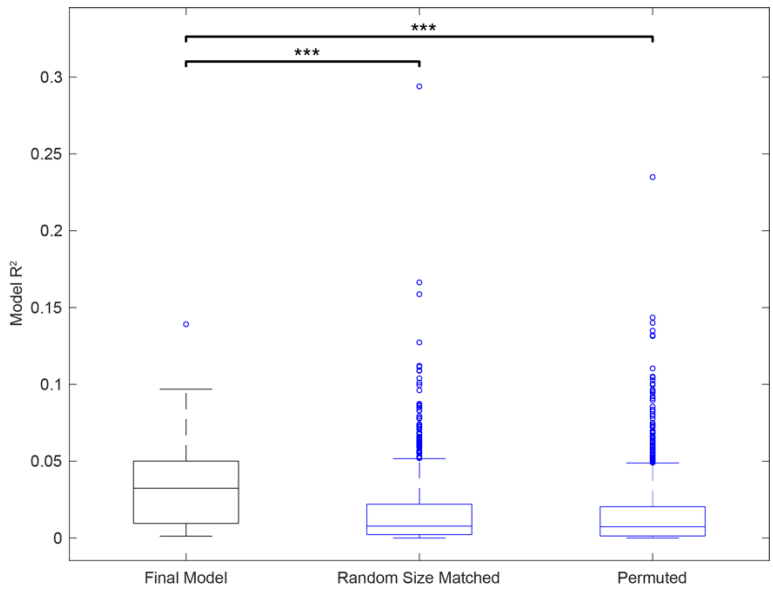

Figure 5.13 Accuracy and significance of breadth model in **Figure 5.12**. Box plot shows model accuracy (R^2) for LASSO-Elastic Net classification model, random size matched models, and permuted label models. LASSO-Elastic Net was run for 20 replicates of 5-fold data separation. Random size matched and permuted label models were run 100 permutations per replicate. Stars indicate significance by Mann-Whitney U test. *** $p < 0.001$.

Among the 524 features analyzed per sample in the second validation cohort, as few as four features were required to predict the evolution of breadth. Specifically, these features included titers of IgG2 antibodies specific to H1 A/Chile/1/1983, FCGR2B binding antibody titers to conserved stem of H3, affinity of IgG2 antibodies for H3 A/Panama/2007/1999, IgM titers specific to H3 A/Panama/2007/1999. Among the predictive features, HA-specific FCGR2B binding antibodies were selectively enriched among individuals that elicited the broadest responses (**Figure 5.12B-C**). FCGR2B-binding antibody levels, rather than IgG levels, were positively associated with breadth of seroconversion highlighting the importance of quality, not just quantity, of pre-existing antibodies in the evolution of breadth. Additionally, pre-existing avidity/affinity and titer of IgG2 antibody titers were also among the predictors, potentially pointing to the importance of efficient antigen capture by subclasses that drive less aggressive antigen destruction and

enhanced presentation. Conversely, IgM antibody titers were a negative predictor of neutralizing breadth (**Figure 5.12B-C**), possibly related to the overly efficient role of IgM in opsonization and rapid antigen clearance prior to deposition in germinal centers.

Given that the LASSO model selects a minimal set of features that differ most across populations without consideration for biological relevance, we next aimed to further define the additional co-correlates of the model-selected features to gain a deeper appreciation of the biological differences across the groups. Thirty highly significant ($R > 0.6$ and FDR-corrected $q < 0.01$) co-correlates were identified (**Figure 5.12D**). Co-correlates of the positive predictor IgG2 titer included a variety of H1N1, H3N2, and influenza B antigen-specific IgG2 titers, as well as FCGR3A binding antibodies to the two H1 antigens (**Figure 5.12D, left**), indicating coordination across both the Fab and Fc domains. The negative IgM co-correlate was linked to a broad array of H1N1, H3N2, and flu B antigen IgM titers. This breadth of epitope specificity highlights the coordination of this response across strain diversity, suggesting that a broad pre-existing IgM repertoire inhibits the development of a broad neutralizing response, while the existence of pre-existing IgG antibodies capable of binding to FCγRs may enhance the developing immune response.

PRE-EXISTING FCGR-BINDING ANTIBODIES INCREASE HUMORAL RESPONSE TO INFLUENZA VACCINATION IN MICE

Given the enrichment of particular IgG subclasses with FCGR2B-binding properties both in the post- and pre-vaccine predictors of evolution of HAI and breadth of HAI, we next aimed to test whether binding to FCGR2B was key to the evolution of HAI. To address the role of FCGR2B, a panel of antibody Fc variants were engineered on a broadly cross-reactive HA stem-specific CR9114 monoclonal antibody (*216*, *287*). The panel included a

wildtype human (WT) IgG1 backbone; an IgG1-Fc with an N297Q mutation (*287*), known to ablate FCGR binding and complement activity; a KWES mutant IgG1 Fc (*321*), known to exhibit increased complement and monocyte phagocytic activity; and an EFTEA mutant IgG1 Fc (*322*), known to increase FCGR2B and general FCγR binding. Each variant was tested in our systems serological assays for antibody-mediated innate immune functions and binding across both mouse and human FCGRs (**Figure 5.14A**). WT IgG1 CR9114 showed moderate phagocytic and complement activity and strong NK cell activation, while N297Q decreased binding to all FCγRs and functions to background levels, as expected. The KWES mutant showed the highest level of complement and monocyte phagocytosis, but

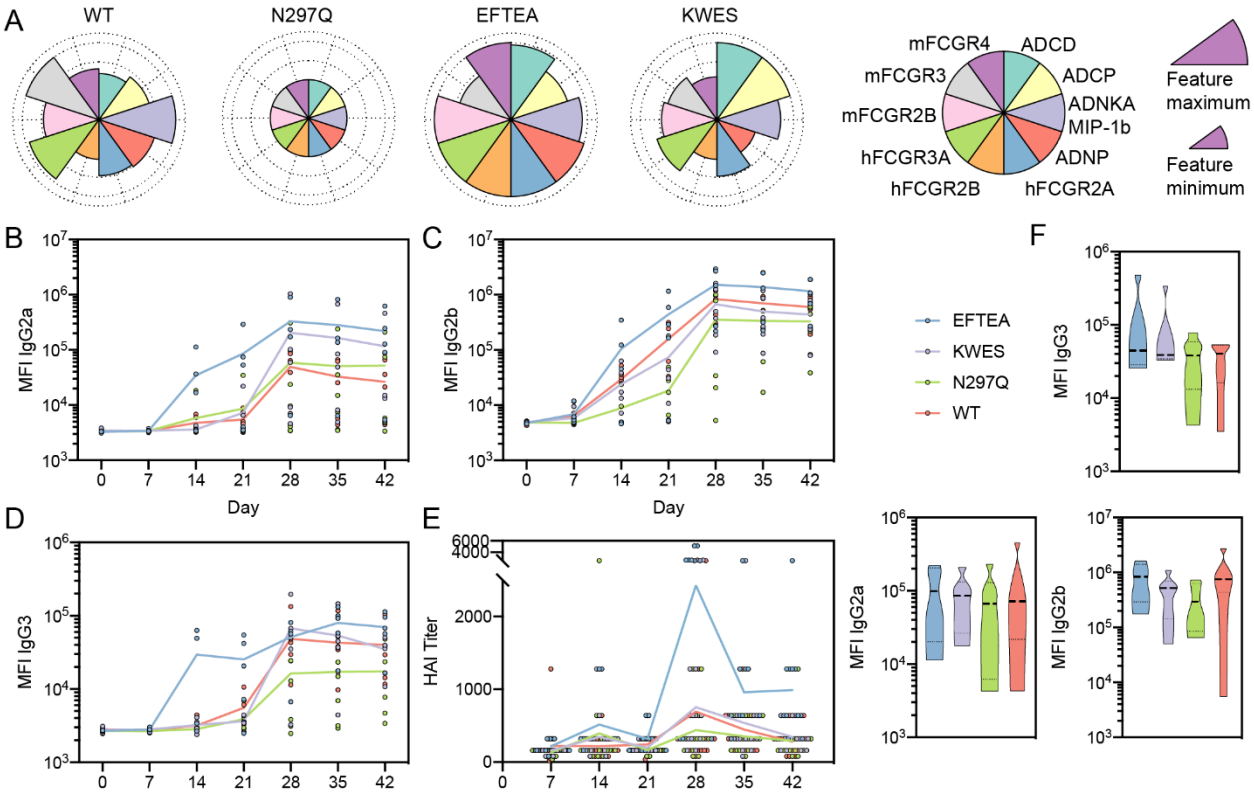

Figure 5.14 Presence of FCGR-binding antibodies in immunization drives improved humoral immune response in mice. Flower plots (**A**) show relative capacity of each Fc-mutant of CR9114 to bind to FCGRs (both mouse and human) and elicit antibody-dependent functionalities, normalized to the minimum and maximum observed values for each feature. Line graphs show antibody isotypes (**B**: IgG2a; **C**: IgG2b; **D**: IgG3) and HAI titers (**E**) of mouse serum against vaccine strain H3N2 X-31 and antibody isotype Luminex MFIs against vaccine strain recombinant H3 A/Aichi/2/1968. Violin plots (**F**) show antibody isotype Luminex MFIs at day 28 against vaccine strain recombinant N2 A/Aichi/2/1968.

with decreased overall FCγR binding. Finally, the EFTEA mutant showed high levels of binding to human and mouse FCGR2s and generally mid- to high binding of FCγRs across both mouse and human. Importantly, we observed a strong correlation between human and mouse FCγR binding, with EFTEA demonstrating high human and mouse FCGR2, and especially FCGR2B, binding.

Using this panel of Fc-variant monoclonal antibodies (mAbs) that bound to HA equally (**Figure 5.15**) but differentially to Fc receptors/complement (**Figure 5.14A**), immune complexes were generated by incubating inactivated influenza virus to mimic the current vaccine with mAbs to mimic pre-existing antibodies. Mice were then immunized, and serum samples were collected weekly to measure the development of both antigen-specific antibody titers (**Figure 5.14B-D**) and HAI (**Figure 5.14E**). Mice immunized with WT immune complexes exhibited a robust response to vaccination following boosting across antibody subclasses (**Figure 5.14B-D**), with similar performance by all Fc variants, except for the EFTEA variant which induced higher titers across subclasses. The WT and KWES variants induced comparable HAI (**Figure 5.14E**), with a trend towards reduced HAI with the N297Q variant, confirming the importance of Fc-binding to improved Fab qualitative evolution. Conversely, the EFTEA variant, which exhibited enhanced binding to both human and mouse FCGR2B, exhibited the most rapid antibody titer evolution across subclasses (**Figure 5.14B-D**) as well as the most robust HAI induction (**Figure 5.14E**). Importantly, no differences were noted in the evolution of NA-specific antibody titers, further suggesting that the target of the pre-existing monoclonal antibody specifically focuses the response to precise immunological targets (**Figure 5.14F**). These data clearly confirm the importance of pre-existing antibodies in shaping the evolution of the humoral immune response, and suggest that broad FcR binding, and specifically FCGR2B binding,

by pre-existing antibodies may accelerate the speed of class switching and the evolution of HAI.

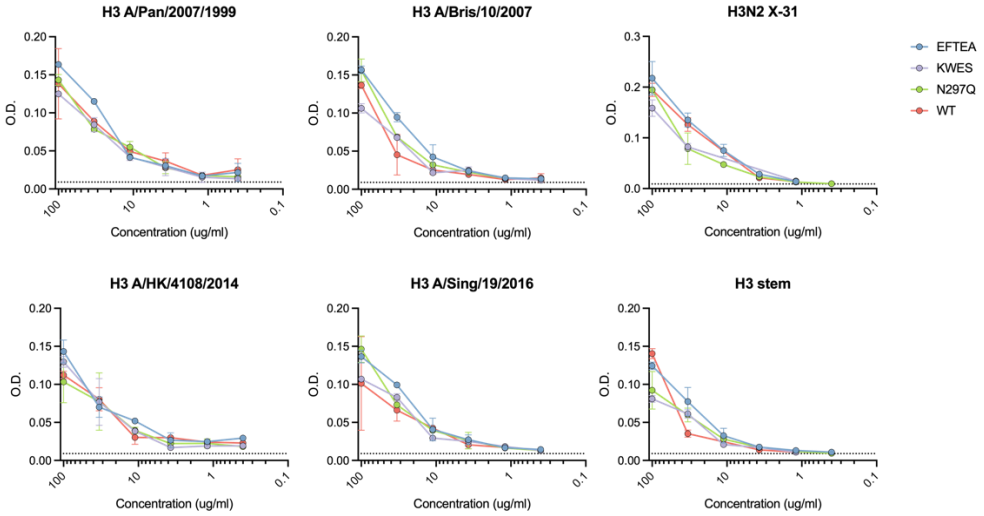

Figure 5.15 Binding of CR9114 Fc variants to multiple H3N2 antigens. Line plots show serial dilution curves for CR9114 variants binding to H3N2 antigens. Each point represents two independent measurements.

DISCUSSION

The rapid spread and unpredictable disease caused by SARS-CoV-2 and its variants has clearly illustrated the urgent need for vaccines against pathogens that have the potential to cause pandemics. While multiple vaccines exist for influenza, these vaccines largely confer strain-specific immunity, requiring annual redesign and delivery. However, emerging data suggest that broadly reactive influenza-specific immune responses can evolve in rare individuals (*279*). Thus, understanding the mechanisms by which these individuals are able to induce protective immune responses may provide critical insights for the design of next generation vaccines that capitalize on this biology to drive enhanced immunity to influenza. Both *in vitro* and *in vivo* data presented here point to the critical role for pre-existing FCGR-binding IgG antibodies as potential adjuvants for the evolution

of qualitatively superior humoral immune responses against influenza. Thus, next generation vaccines able to harness the immunomodulatory role of pre-existing antibodies or deliver similar signals may improve the breadth and quality of the vaccine-induced immune response to influenza and beyond.

The development of a broad and effective humoral immune response to vaccination is dependent on both antigen specificity and Fc functionality. Here, we observed that HAI seroconversion to a single vaccine antigen occurred in concert with the evolution of several opsonophagocytic functions. Specifically, A/California/07/2009 HAI evolved in tandem with increased levels of H1 A/California/07/2009-specific antibody-mediated complement deposition, neutrophil activation, and FCGR2B binding. Additionally, HAI conversion also evolved in concert with FCGR2A-binding NA responses highlighting the presence of broader, more holistic responses to the vaccine among individuals who seroconverted in response to the vaccine. Given the emerging appreciation for the importance of NA-specific immunity to protection against influenza (*323*), these data suggest that functional humoral immunity to both targets may contribute to enhanced HAI conversion. Moreover, both complement and neutrophil functions have been implicated in protective immunity against influenza (*54*, *56*), thus co-evolution of HAI and opsonophagocytosis to multiple antigenic targets may collectively drive the broadest universal immunity. These data highlight the coevolution of multiple lines of protective humoral immunity pointing to an overall enhanced immune response to influenza.

Among the theories that have been proposed to explain the poor evolution of breadth in response to current seasonal vaccines and infections, "original antigenic sin" (*25*) suggests that pre-existing responses to influenza dominate all subsequent responses and prevent the evolution of breadth (*324–326*). The unbiased nature of systems serology

allowed us to broadly profile the humoral immune response across many historical strains, contemporaneous strains, and "future" strains relative to when the samples were drawn. Interestingly, IgM titer to H3 A/Singapore/INFIMH/16-0019/2016 was the sole feature negatively associated with the development of vaccine-induced breadth. Importantly, IgM titers to H3 A/Singapore/INFIMH/16-0019/2016 were correlated to IgM responses across tested virus antigens, arguing that IgM responses prior to vaccination are highly negatively associated with the evolution of breadth. IgM deposition on antigens/pathogens results in rapid complement activation (*327*) and opsonophagocytic uptake via complement receptors (*328*) that leads to rapid antigen degradation (*329*). Conversely, FCGR2B binding and IgG2 antibodies were enriched in individuals who developed breadth. IgG2 antibodies have poor affinity for complement and Fc-receptors (*113*), and thus likely create complexes that are poorly phagocytosed and not readily cleared by immune cells. Moreover, in the setting of FCR2B-binding antibodies, these immune complexes may bind to FCGR2B on the surface of circulating B cells and traffic into germinal centers. In the germinal center, FCGR2B binding on follicular dendritic cells (FDCs) likely competes for deposition, and ultimately presentation, to evolving B cells (*51*, *109*). Thus, the ability of pre-existing antibodies to redirect the response to either myeloid or follicular DCs may contribute mechanistically to shifting the response to vaccination, increasing affinity maturation in germinal centers and the evolution of broader neutralization (*104–106*).

To define whether these observed changes in Fc-profiles were simple biomarkers or mechanistic players in the evolution of HAI breadth, immune complex-based immunization was performed in mice. Given the redundancy of the human and murine Fc-receptor system, where human IgG1 binds murine FCγRs and FcRn (*63*, *330*), we were able to select a set of Fc-modifications that tuned human and murine Fc-receptor binding in an analogous

manner. However, some differences exist between murine human FCγR function and affinity for antibodies. ADCC in mice is primarily mediated by monocytes/macrophages via mFCGR4 (*179*), rather than exclusively by FCGR3A on NK cells in humans (*63*). Additionally, mice do not express FCGR2A, instead relying on mFCGR3 as a more generalized activating receptor (*178*). In contrast, FCGR2B expression and function are relatively conserved across mice and humans, with this lone inhibitory FCGR serving to limit the development of auto-antibodies, heighten the affinity threshold in germinal centers, maintain tolerance, and decrease other pro-inflammatory functions of cells (*331–333*). As shown in the human studies, the EFTEA variant, with the most robust FCGR2B binding, exhibited rapid induction of antibody titers as well as HAI. Despite the fact that the EFTEA variant exhibited the single highest binding to both the murine and human FCR2B receptors, the EFTEA antibody also showed enhanced binding to a wide array of FcγRs. Combined with previous studies indicating that IgG1 and FCGR2A-binding variants resulted in comparable antibody responses and HAI activity following challenge (*334*), these data suggest a role for FCGR2B specifically in the development of the humoral immunity, both broadly and in a strain-specific manner. This observed mechanism supports previous studies indicating that FCGR2B-binding antibodies are important to the development of neutralization capacity against influenza (*109*), likely acting through its dual role in the germinal center, both raising the B cell activation threshold and trapping antigen-containing immune complexes on FDCs (*51*). Thus, future studies using larger panels of variants may further dissect the precise Fc-receptor binding patterns required for optimal evolution of the Fab and the immunological mechanisms occurring in the germinal center following seasonal influenza vaccination.

Altogether, the *in vitro* and *in vivo* findings from this study emphasize the importance of systems level immunological dissection of the humoral immune response to identify unexpected insights into the key mechanics that may be required to achieve universal immunity to influenza. Emerging data argue that distinct inflammatory responses, induced, for example, by adjuvants (*335*), could shape antibody Fc-profiles and thereby drive enhanced Fab activity. Thus, whether next generation vaccines seek to include existing or emerging adjuvants (*336*), prime-boost strategies with chimeric antigens (*337*), or targeted exploitation of pre-existing antibodies (*338*), several avenues now exist to rationally exploit the correlates of breadth identified here. These data suggest that future influenza vaccine studies, in particular those exploiting repeated boosting, should include some considerations for the recruitment and elicitation of FCGR-binding antibodies.

Chapter 6: DISCUSSION

The protective efficacy of the antibody response to influenza is shaped by the antibodies' ability to both recognize the infecting influenza strain and activate the innate and adaptive immune systems. This dissertation explored the functional humoral immune response in natural immunity to influenza and in response to influenza vaccination, highlighting the effects of adjuvants, pre-existing antibodies, placental transfer, and aging to create snapshots of the influenza-specific immune response under different states. Across clinical cohorts, systems serology was used to generate a comprehensive description of the humoral immune response to vaccination and further mechanistic insights were gained through *in vitro* and *in vivo* experimentation. Across these disparate study populations, an image of the influenza-specific immune response across stages of life emerged. Repeated exposures led to the development of heterosubtypic breadth in a subset of individuals, but for most this broadly protective immune response remained out of reach. The overall coordination of the immune response across antigens and Fc-functions altered the susceptibility to influenza across populations. While FcγR binding antibodies emerged as a key vaccine-induced mechanism of protection in neonates, antibodies capable of activating NK cells arose as a key correlate of protection in older adults. The titers of these NK-activating antibodies were not boosted to the same level as overall IgG titers by the inclusion of adjuvants. Together, this work emphasizes the importance of moving beyond simply measuring neutralization and considering the antibody Fc when developing novel universal influenza vaccine candidates.

USE OF SYSTEMS SEROLOGY IN EVALUATING INFLUENZA VACCINES

Systems serology (*193*) is a comprehensive, unbiased platform of experiments for evaluating the biophysical and functional features of a polyclonal humoral immune response to infection or vaccination (**Figure 6.1**).

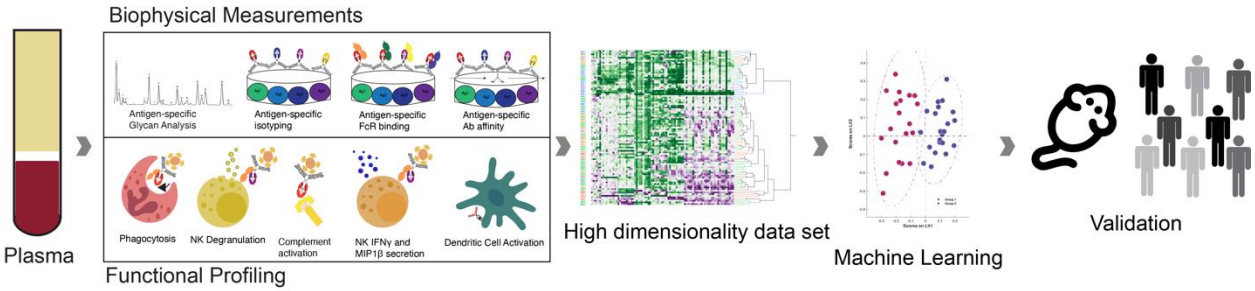

Figure 6.1 Schematic depicting the systems serology analysis pipeline. Plasma from influenza vaccinees is analyzed through a variety of antibody functional and biophysical measurements, yielding a high dimensionality dataset comprehensively capturing the antigen-specific humoral immune response. These large datasets were then analyzed through machine learning to provide key correlates or predictors of relevant outcomes, which were then validated through additional cohorts, in vitro, and in vivo studies.

INNOVATIONS TO THE PLATFORM

Within this dissertation, systems serology was applied to study influenza-specific immune responses across a variety of vaccination strategies and populations. With the current understanding in the literature of the importance of extra-neutralizing functions to protection from influenza (*40*, *62*) in animal models, this was a ripe area for investigation with human clinical samples. The high-throughput nature of the systems serology platform, which allowed for interrogation of a high number of patient samples, combined with the low sample volume required to gather hundreds of vaccine-specific datapoints, yielded rich datasets with significant power to ask a wide variety of interesting, important scientific questions. Furthermore, this work expanded the systems serology platform beyond the previous standard. First, increases to the high-throughput capacity of the platform allowed

the analysis of additional, inter-related antigens (e.g. influenza HAs from over 25 strains and subtypes at a time) and large, diverse cohorts (over 800 individual samples). Beyond these expansions, this work pushed the platform forwards by exploring the interaction between changes in the Fab (avidity) and Fc-function (FcR binding). This created the ability, in influenza and beyond, to assay the evolution of a humoral immune response from both an antigen-specific avidity perspective and a functional perspective within the same individual. In future studies of influenza, interrogating the ability of antibodies to recruit innate immune cells and function in the mucosal environment of the upper respiratory tract will be essential. Murine studies have indicated the importance of alveolar macrophages to the clearance of influenza infection (*58*), which has not yet been modeled for human cells *in vitro* as part of this platform. Furthermore, the mucosa is the site of infection within the upper respiratory tract, and influenza-specific mucosal IgG and IgA antibodies are known to provide protection (*339*). This represents an area of open exploration, and novel assays will be required to add these key measurements to the systems serology platform.

COMPUTATIONAL BIOLOGY ANALYSES

In conjunction with the systems serology experimental platform, sophisticated machine learning algorithms were used to identify the key features that track with desired vaccination outcomes, including humoral breadth, protection from disease, and placental transfer. The specific approaches chosen here to identify key humoral features that drive outcomes of interest were selected based on their ability to prevent overfitting while distinguishing between groups in a high dimensionality dataset (*212*, *249*). Elastic Net combines the features of linear regression with the prevention of overfitting provided by the Least Absolute Shrinkage and Selection Operator (LASSO) (*340*). Similar approaches have also been used in studies of malaria vaccines (*341*), HIV patients (*249*), Ebola antibodies

(*212*, *287*), an anthrax vaccine (*342*), a typhoid fever vaccine (*343*), and SARS-CoV-2 patients (*344*, *345*) to identify correlates of protection. Furthermore, the analysis presented here represented a step forward for these algorithms, wherein validation was achieved in an independent cohort, not just through subsetting an individual cohort. Combining the rich datasets and the power of cutting-edge computational techniques allowed for a deep analysis of the polyclonal, polyfunctional humoral immune response to influenza vaccination across the studies presented here.

HUMORAL BREADTH: EPITOPES & FUNCTIONALITY

DEFINING HUMORAL BREADTH

Previous studies in the field have characterized breadth using landscapes (*346*), which provide detailed information on strain interrelatedness and are useful in comparing different populations, or by isolating specific memory B cells (*347*), which can provide a deep understanding of single monoclonal antibodies but limited information about the total polyclonal response. The breadth score, described in Chapter 5, is a single measurement to describe the cross-reactivity of an individual's antibody repertoire at a moment in time or in response to vaccination. It is informed by the genetic sequence distance between strains and can be applied to any set of strains tested for any single antibody metric for which positive and negative can be identified (e.g. neutralization, titer). Compared to previous methods (*346*, *347*), the breadth score is widely and easily applicable to many datasets and captures more information than a simple percentage of neutralized strains over tested strains, which may over-emphasize closely related strains. Here, we used machine learning algorithms and the breadth score to show that the development of breadth was predicted by FCGR2B-binding antibodies. Future studies may be able to use this metric, as well as

further analysis of breadth, to elucidate the precise mechanisms by which these antibodies contribute to that development.

HUMORAL BREADTH IN RESPONSE TO VACCINATION

Humoral breadth develops in response to exposure to multiple strains and subtypes of influenza, either by vaccination or infection, over the course of an individual's life. For this reason, adults have been shown to have more serum cross-reactivity against a variety of influenza strains than is present in young children (*346*). Antibody responses to natural infection are known to be broader and longer-lived than those arising following seasonal influenza vaccination (*311*). Seasonal vaccination induces limited breadth, instead engaging only high affinity B cells to strain specific epitopes and shifting the response towards the immunodominant globular head (*50*, *348*), giving rise to the same plasmablast clones over years of repeated vaccination (*349*). Novel influenza exposures, in contrast, can shift the response to conserved epitopes creating a wider breadth of binding, a phenomenon known as GC steering (*50*). The data presented here begin to elucidate some of the mechanisms at work in those few individuals who develop a broadly neutralizing polyclonal response following seasonal vaccination. These individuals making the ideal breadth response comprised a small segment of the study population, and this population had already been highly selected to include those who seroconverted following vaccination. Therefore, one limitation of this study is that the overall distribution of this population not reflective of natural population diversity and is likely biased to over-represent these rare individuals. However, this finding is still important and interesting as it points the way towards the possibility of engaging these mechanisms in a wider swath of the population in the future.

Specifically, in these rare individuals, pre-existing antibodies at the time of vaccination that are able to bind to FCGR2B lead to a wider breadth of reactivity, likely by

enhancing binding of the immune complexes in germinal centers and steering the response away from antigen destruction (**Figure 6.2**). Mechanistically, when the antigens from vaccination enter the body, they are bound by pre-existing antibodies forming immune complexes (*101*). If these antibodies have high binding affinity for FCGR2B, this can target them to be deposited in germinal centers via interactions with follicular dendritic cells (FDCs), which act to trap antigen-containing immune complexes that are crucial to driving the germinal center response productively forward (*51*). Furthermore, FCGR2B decreases antibody-dependent cellular phagocytosis (*332*), limiting antigen destruction by phagocytic cells prior to deposition in the germinal center. In germinal centers, FCGR2B increases the B cell activation threshold, decreasing the output of antibodies overall but increasing levels of affinity maturation (*331*, *332*). Indeed, sialylated IgG engagement of CD23 on B cells induces the upregulation of FCGR2B, thereby increasing affinity maturation and

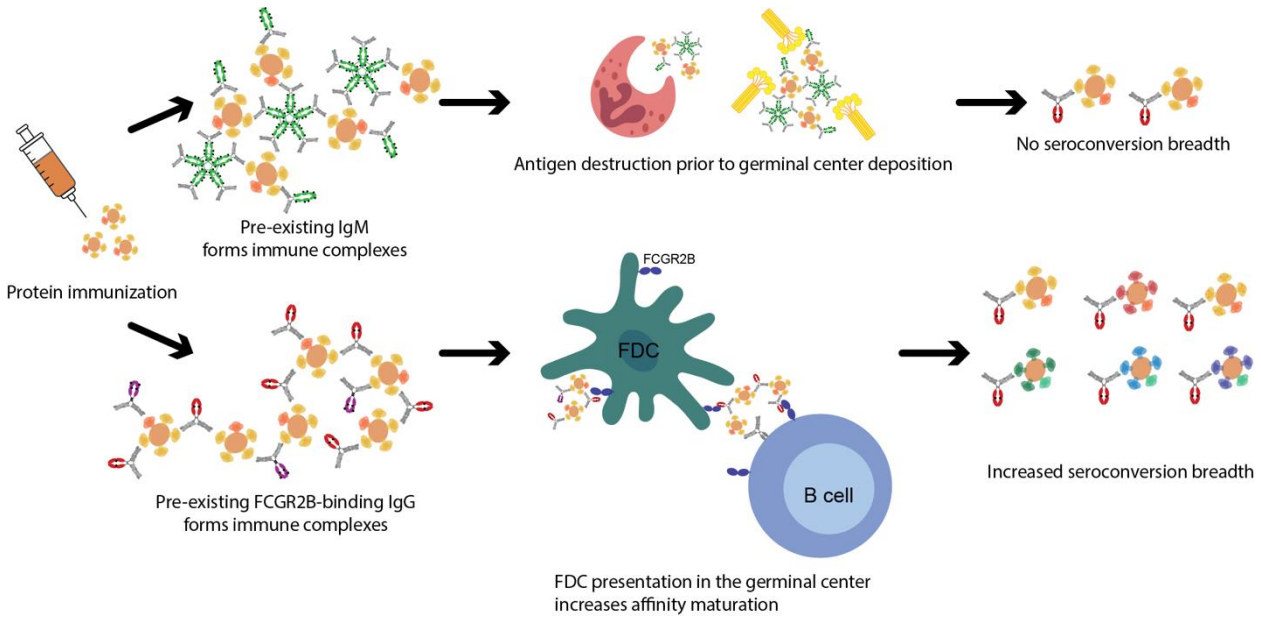

Figure 6.2 Effects of pre-existing antibodies at the time of vaccination. Pre-existing IgM antibodies target antigen for destruction, whereas FCGR2B-binding antibodies allow for trafficking to the germinal center, presentation by FDCs, and enhanced affinity maturation of B cells leading to increased seroconversion breadth.

generating higher affinity IgG response with broad protective affinity (*109*), emphasizing that this pathway may be the key to driving these responses. Together, the downstream functions of FCGR2B may serve to prolong the half-life of antigen in a vaccinated individual, increasing affinity maturation and thereby creating additional broadly reactive and/or neutralizing antibodies. This FCGR2B-dependent mechanism could provide a target for future universal influenza vaccine designs (*15*). Protein engineering can be used to target vaccine antigens into this pathway is the use of Fc-fusion antigens, which have been studied across a wide range of diseases including Ebola (*350*), Epstein-Barr Virus (*351*), SARS-CoV-2 (*352*), and cancer (*353*). The Fc domain of these recombinant fusion antigens could be specifically altered to preferentially enhance binding to FCGR2B (*354*), mimicking the effects seen here in rare individuals with high levels of pre-existing FCGR2B-binding antibodies and carrying the antigens more effectively into the germinal centers. Alternately, adjuvants can be used to increase the vaccine-specific IgG sialylation (*355*), as sialylated IgG upregulates FCGR2B expression (*108*, *109*), leading to potentially similar downstream effects. Both of these strategies provide mechanisms that potentially allow for exploitation of the FGGR2B pathway, thereby increasing antibody breadth and affinity.

EPITOPES AND IMMUNODOMINANCE

Antigenic match to circulating strains is known to be a significant predictor of seasonal influenza vaccine effectiveness. In seasons where there is a mismatch, the effectiveness of the vaccine is lower across all age groups (*277*). In the 2013-2014 influenza season, there was a 3 amino acid change caused by viral adaptation to egg cultures used to grow the vaccines (*276*). This mismatch, which was not discovered until after the influenza season, caused significantly lower effectiveness but also provided an opportunity to study the humoral immune response and how a polyclonal response differs across these two

antigens. The study of influenza vaccination in older adults presented here (Chapter 4) occurred during this particular vaccine season and indicated that while responses were qualitatively similar across egg-adapted and circulating antigens, the magnitude of responses to the circulating antigen was lower, suggesting that the misdirection of the antibodies changed the specificity but not functional development of the humoral response.

The HA head is immunodominant, leading most responses to be directed to these variable epitopes. Indeed, the evidence observed here of decreased responses to the circulating strain in comparison to the mutated vaccine strain (Chapter 4) emphasizes the importance of the immunodominant HA head epitope labeled antigenic site B, also one of the sites of antigenic cluster transitions (*276*, *277*). This immunodominance can be circumvented by high titers of pre-existing antibodies, which suppress responses to similar antigenic sites and enable B cells specific for non-dominant sites to mature (*153*). However, in contrast, memory B cells may dominate the response in the absence of high antibody titers, leading to original antigenic sin (*153*, *356*), despite naïve B cells having similar frequencies of specificities to both the immunodominant HA head and subdominant HA stem (*348*). This is consistent with the findings presented here indicating that seroconversion occurs in the presence of pre-existing antibodies (Chapter 5).

Beyond epitope specificity, antigen specificity can also play a role in the immune response. While HA overall is immunodominant compared to other influenza proteins (*34*), particularly in the context of vaccination, seasonal inactivated influenza vaccination is also known to induce antibodies to the other surface protein of influenza, NA (*290*) (**Figure 1.1**). These NA-specific antibodies have been shown to induce ADCC and reduce disease severity in mice, with correlative epidemiology in humans (*46*, *170*). Coordination between antibodies targeting both HA and NA as antigenic targets may be a key driver of protection,

particularly in older adults whose innate immune cells are less responsive to immune complex-driven stimulation, as was shown in the study of older adults presented here (Chapter 4).

The antigenic target of antibodies present at the time of vaccination is a key contributor to the development of further humoral immune responses, as data presented here indicated an antigen-specific effect of pre-existing antibodies (Chapter 5). Specifically, pre-existing antibodies to HA had no effect on the development of the anti-NA response. Further research is needed to determine if the effects on the developing humoral immune response exerted by pre-existing antibodies are consistent against multiple antigenic targets. However, this evidence of antigen-specific developments indicates that future universal influenza vaccine strategies may be able to capitalize on different functionalities of antigenically distinct antibodies.

THE DEVELOPMENT OF THE INFLUENZA-SPECIFIC IMMUNE RESPONSE ACROSS A LIFETIME

Using the data presented here, a trajectory of the anti-influenza immune response across a lifetime can begin to be assembled (**Figure 6.3**). Correlates of protection from influenza may be fundamentally different across age groups, leading to the requirement for different vaccine designs targeting specific humoral outcomes. The development of the immune system and repeated exposures to influenza and influenza vaccines shape the humoral immune response, while the capability of innate immune cells to respond to Fc-mediated signals also changes with age (*357*).

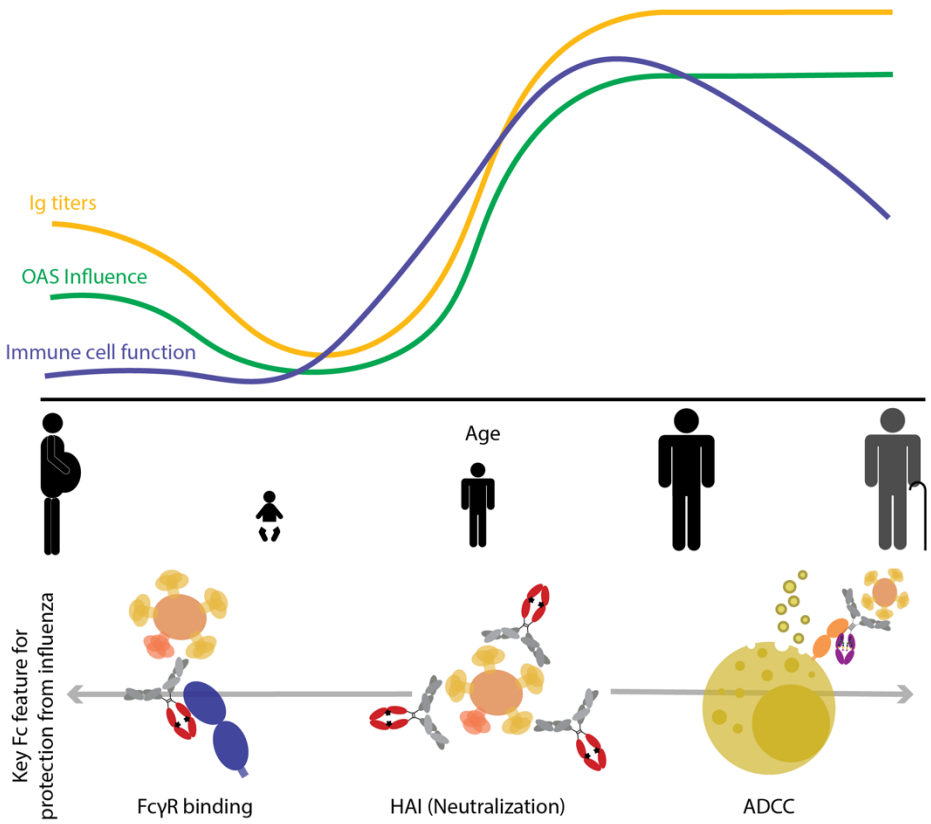

Figure 6.3 The development of the influenza-specific immune response over a lifetime. Lines show relative levels of IgG titers (orange), the influence of original antigenic sin (green), and overall immune cell function (blue). Below the chart, pictograms depict the key protective antibody qualities described here: FcγR binding antibodies as a fetus and neonate, and ADCC-inducing antibodies as an older adult, as well as the current correlate of protection, HAI.

PLACENTAL SIEVING

The immune response to influenza begins during fetal development, as antibodies developed by the pregnant parent during infection or vaccination are transferred across the placenta to provide protection to the neonate (*227*, *230*, *235*). These antibodies provide essential immune protection in the first months of life, since at birth, the immune system is attenuated, with reduced adaptive immune responses and increased regulation preventing immune activation (*358*, *359*). Previous work in the Alter laboratory has shown that placental transfer favors antibodies that can bind to both the neonatal Fc receptor (FcRn) and Fc γ receptor IIIA (FCGR3A) independently of antigen specificity (*244*). The data

presented here (Chapter 3) broadly supported these conclusions and have built upon this foundation to understand more about how placentally sieved antibodies can provide protection to a neonate via binding to FCγRs and activating innate immune functions.

Furthermore, these data demonstrated that the impact of vaccination is not on the rate of placental transfer itself but rather alters the makeup of available antibodies on the maternal side of the placental barrier (Chapter 3). Data from this same study population indicated that maternal vaccination against influenza, in this medically underserved community, increased protection of both pregnant individuals and their neonates from infection with influenza and serious complications if infected (*228*, *245*). However, this protection was incomplete. Here, the data indicated that protection was linked to how well the vaccination could induce FCγR-binding antibodies. This has important implications for maternal vaccine design, indicating that vaccination has not overcome the previously described requirements of a galactosylated Fc capable of binding to FcRn and FCGR3A for placental transfer (*244*). However, vaccination can skew the transfer by changing what is available in maternal circulation to be transferred (Chapter 3). Future vaccination efforts in pregnant individuals should consider the mechanisms of placental transfer to achieve the goal of protecting neonates following birth.

ORIGINAL ANTIGENIC SIN

As these maternal antibodies wane over the first few months of life (*231*, *232*), young children begin to mount an anti-influenza immune response to early exposures, even sub-clinical exposures. As children mount their own responses, strain-specific antibodies dominate and breadth remains low until there is a sufficient reservoir of recall responses (*346*). Initial exposures to influenza drive antigenic seniority, or original antigenic sin (OAS). Antigenic seniority is the concept that hemagglutination inhibition (HAI) titers of

previously encountered strains are boosted upon re-exposure to influenza, resulting in the highest overall titers for the strains which an individual encountered earliest in their life (*296*). OAS encompasses this concept and associates it with negative outcomes to vaccination with current strains (*26*). This process has been described in humans over the decades since its original identification (*25*, *26*) and experimentally modeled in mice (*100*). Here, however, limited evidence of OAS was observed. Across age groups, limited negative predictors of response to vaccination were observed, with only IgM levels presaging a limited breadth of response to vaccination (Chapter 5). Thus, whether this only relates to the broadening of the immune response or is related to different populations, in this agnostic analysis no evidence was found that pre-existing IgG response prevented the evolution of immunity. Instead, most pre-existing antibodies were seen to be neutral, and a small group of highly selective antibody features were associated with better immunity, particularly antibodies binding to FCGR2B.

REPEATED INFLUENZA EXPOSURE

As adults, individuals are repeatedly exposed to H1N1, H3N2, and influenza B strains through yearly influenza exposure and/or vaccination. These repeated exposures tune the immune response, generating a wide polyclonal reactivity in some individuals. Memory B cells in humans can undergo additional somatic hypermutation upon influenza re-exposure, which occurs within seven days following exposure (*360*). In others, the presence of pre-existing antibodies limits the development of new germinal centers (Chapter 5). Exposure to closely related HA antigens leads to a response dominated by highly mutated memory B cells, which is a less protective response than the primary response (*361*). However, despite the wide body of knowledge around the effect of memory B cell presence on Fab evolution, little is known about their role in directing the evolution of

the Fc. Here, we begin to observe the development of breadth across influenza specificities in some, but not all individuals. Seasonal vaccination provides yearly boosts in antibody titer, and exposures to circulating influenza can also boost natural immunity. While the effects on the evolution of antigen specificity have been studied (*361*), far less has been understood about how the Fc domain of antibodies changes over the lifetime.

AGING

In older adults, responsiveness to individual challenges with influenza antigens declines (*297*, *313*). However, the humoral immune response is more critical than ever as the responsiveness and effectiveness of the overall immune system wanes (*357*, *362*). Innate immune cells, including neutrophils (*363*), macrophages (*364*), NK cells (*293*), dendritic cells (*365*), and adaptive immune cells, including B (*366*, *367*) and T cells (*368*), show increasing dysfunction and decreased anti-viral responses as age increases. Specifically in the humoral immune response, vaccination against influenza elicits limited adaptation to novel strains in older adults, instead favoring antibodies to historic epitopes where antigenic drift has evaded immunity (*297*). Here, we observed that, likely due to decreased NK cell activation potential, antibodies able to activate NK cell–mediated ADCC are a correlate of post-vaccine protection from symptomatic influenza infection (Chapter 4). More studies will be needed to elucidate the precise mechanisms by which vaccine-elicited antibodies can best activate NK cells.

High dose vaccination has been shown to be protective in older adults, surpassing the protection achieved by standard inactivated influenza vaccines without increasing negative side effects (*278*, *369*, *370*). While the exact efficacy varies based on the matching of the vaccine to circulating strains (*273*), high dose vaccination is now licensed by the CDC for all US adults over the age of 65 each year. Despite high heterogeneity within regular

dose and high dose vaccinees, the data presented here suggested that there was a difference in coordination in the immune responses, with those receiving the high dose vaccination increasing antibody functionality across measured functions while the regular dose vaccination only induced high levels of opsonophagocytic functions (Chapter 4). This suggests that high dose vaccination may also serve to overwhelm the innate targeting of the response towards certain influenza-specific functions, boosting antibodies across functional modalities.

However, high dose vaccination is not without risk as high dosing has been shown to have deleterious effects on humoral immune development in the context of HIV. Repeated high dose protein vaccination resulted in the generation of IgG4 antibodies which are poorly functional but can compete for antigen binding with more effective subclasses (*209*). Over time, high dosing in older adults, who already have compromised effector function, may lead to a compromised immune response. The effect of repeated high dosing could not be evaluated in this trial, as this was the first high dose vaccination received by trial participants (*278*). Understanding the key protective modalities in older adults, such as the NK cell-mediated correlate of protection identified here, may ultimately provide the key to targeting a more effective immune response that is durable over the lifetime, as well as able to be activated in a possible pandemic setting, rather than already driven to anergy.

DEFINING ADDITIONAL CORRELATES OF PROTECTION

NEUTRALIZATION AND ANTIBODY TITERS

Historically, HAI titers have been identified as the correlates of protection against influenza infection and have been used to evaluate vaccine immunogenicity (*23*). However, HAI is an inadequate correlate of protection that does not fully explain the protection

afforded by a humoral and cellular immune response, instead focusing on only antibodies that bind and block the receptor binding domain of HA (*16*, *17*). Individuals with seemingly protective HAI titers have gone on to be infected with influenza following vaccination (*18*). Notably, age has been identified as an independent risk factor for influenza infection (*16*). Furthermore, HA-binding antibodies targeting the HA1 domain, the full length HA molecule, and the HA stalk domain have each been recently identified as independent correlates of protection from influenza infection across age groups (*304*). These findings create the opportunity to identify and put into practice additional correlates of protection against which future vaccines could be tested.

NK CELLS AS A KEY CORRELATE OF PROTECTION AGAINST INFLUENZA

Antibodies capable of inducing innate immune effector functions via FCγR binding have been identified as protective in the absence of neutralization in animal models (*39*, *58*). Furthermore, ADCC-inducing antibodies have been linked to shorter duration and less severe infection in humans (*78*). Here, antibodies capable of binding to FCGR3A and activating NK cells were identified as a key correlate of protection against influenza in older adults. Given the finding that older adult NK cells were also less responsive to FCγR-mediated stimulation (Chapter 4) and the current literature (reviewed in (*40*, *199*)), we propose that these antibodies capable of activating NK cells can provide protection across age groups. In neonates, another high-risk group, NK cell–activating antibodies have been linked to increased placental transfer of IgG from mother to child (*244*), working in tandem with the increased NK cell functionality (compared to other innate immune cells) in neonates (*244*). While we did not see a measurable effect on ADCC-inducing antibodies enriched by placental transfer, we did observe an increase in FCGR3A-binding antibodies, suggesting that the effect may be below the detection sensitivity of ADCC assays. Together,

these findings suggest that influenza vaccines that induce antibodies with ADCC activity may be protective across age risk groups, but particularly in older adults where NK cells are anergic (*293*).

While HAI is important for blocking infection, ADCC-inducing antibodies may be acting to prevent disease from occurring after infection or to clear an existing infection (*213*, *371*). The mechanisms by which ADCC-inducing antibodies provide protection is an active area of study. The current model of ADCC induction by HA-specific antibodies requires a two-step activation cascade whereby the antibody bound to the HA molecule activates FCGR3A while the sialic acid binding site of HA provides a second intermolecular bridge between the infected cell and NK cell surfaces (*85*). This model posits that epitope specificity plays a key role in ADCC induction, namely limiting ADCC functionality to stem-specific and head-specific but not sialic acid binding site–specific antibodies (*86*, *214*). While the work presented here did not interrogate specific HA epitopes as targets, it clearly showed that the polyclonal response to vaccination, across populations, elicited ADCC functionality by NK cells as a key component of protection.

These ADCC-inducing antibodies may not be working alone to provide protection. Across cohorts, even in those not specifically linked to protection, we observed high levels of polyfunctionality and coordination between ADCC-inducing antibodies and antibodies capable of inducing other innate immune functions. This finding is supported by previously published animal model studies, wherein many antibody-dependent innate immune effector functions have been linked to both protection against and clearance of influenza infection (*38–40*, *53–59*). Whether these antibodies provide mechanistic input to the response to infection or serve as biomarkers remains to be investigated.

FCγR-BINDING ANTIBODIES AS A PREDICTOR OF PROTECTION IN NEONATES

At birth, neonates have a compromised immune system with many innate immune cells not yet fully matured and little to no antibody production capacity (*359*). In order to protect neonates and their parents, Tdap and seasonal influenza vaccines are recommended during pregnancy (*372*). Here, antibodies that bound to FcγRs emerged as a predictor of protection of infants from influenza infection when measured at the time of birth. These FcγR-binding antibodies, separate from any specific innate immune effector function, were both enriched by maternal vaccination and were a biomarker of protection in the neonate (Chapter 3:). One hypothesis is that these antibodies are a biomarker of successful placental transfer. This cord blood biomarker would exist in contrast to innate immune cells in the cord, which have been shown not to correlate with immune cells in the peripheral blood of newborns (*373*). They may also serve as a biomarker for the higher transfer of breastmilk antibodies by these vaccinated mothers (*257*), which is another route through which protection is transferred from parent to child. Alternately, these FcγR-binding antibodies could be playing a role to counteract the predominant transfer of anti-inflammatory glycoforms observed in some studies (*374*, *375*) in an antigen-specific manner, upregulating an inflammatory response to pathogens but not to microbial antigens or allergens. Further work is needed to determine the precise contribution of these antibodies to immunity; however, this finding does emphasize the importance of eliciting this type of response to vaccination to provide maximal protection in neonates.

This correlate is distinct from the correlate of protection of ADCC-inducing antibodies identified in older adults. In older adults, NK cells are anergic and less responsive to FCGR3A-mediated stimulation (Chapter 4). On the contrary, NK cells are the most effective and abundant of neonatal innate immune cells, despite all cells in the

neonate being functionally down-regulated (*244*, *359*). While much of the immune system is distracted by acquiring tolerance to the gut microbiome (*373*), vaccine-induced antibodies may be able to provide some level of protection in the neonate by engaging widely with Fc-mediated functions. These findings indicate that future vaccine strategies may differ across populations to induce the most protective effects, with a vaccine for pregnant individuals targeting cross-FcγR binding antibodies and a vaccine for older adults targeted towards ADCC.

OVERALL COORDINATION OF THE HUMORAL IMMUNE RESPONSE ALTERS SUSCEPTIBILITY TO INFLUENZA

In addition to single measures and identification of key features, these rich datasets allowed for analysis of the overall coordination of the immune response across both antigen targets and Fc features. A striking pattern was observed across the two cohorts presented here that have data for protection: a more coordinated immune response, with high levels of polyfunctionality and concomitant FcR binding, was found in individuals who were protected from influenza infection by vaccination (Chapters 3 & 4). This finding suggests that antibody-induced effector functions work in concert and that enriching for one specific function, while beneficial especially in the case of NK cells, does not capture the important diversity of the humoral response.

Beyond Fc, matching the immune response to the circulating virus was key, as expected. However, it seemed that those whose immune response was well matched to that year's circulating virus responded broadly across vaccine antigens, not just with the unique strain-specific response required for the current circulating strain (Chapter 4). In both adults and older adults (>65 years of age), antibody Fc-features were highly correlated

across antigen specificities; for example, individuals with high pre-vaccination IgM titers against one H3 antigen were likely to have high pre-vaccination IgM titers across a wide range of influenza A and B antigens. These data suggest that those who are protected are more likely to generate responses across vaccine strains, leading not only to a quality Fc effector response but one that targets multiple subtypes of influenza.

Beyond matching to the circulating strain, coordination between the site of infection and the site of enhanced immunity may also play a critical role. Mucosal immune responses, namely IgA and IgG capable of binding to cell-surface mucins, have been identified as key modulators of infection (*376–379*), highlighting that the immune response in the nasal mucosa may be important in providing protection in influenza. Additional studies will be needed to identify key correlates of protection in the nasal mucosa, and define how these nasal correlates interact with the systemic correlates of protection described here (Chapters 3 & 4).

ROLE OF ADJUVANTS IN DEVELOPING PROTECTIVE RESPONSES

Oil-in-water adjuvants, such as MF59 and AS03, have been used successfully to boost immune responses to influenza vaccination in multiple high-risk populations (*380*), including older adults (*381*), children (*140*), and infants (*382*). However, studies have not shown consistent results in boosting protection despite increases in HAI and/or overall anti-influenza titers (*188*, *189*). In further investigations into this mismatch between increased biomarkers of immunity and immunity itself in the context of adjuvanted vaccination, here we observed that the reduced efficacy of MF59, compared to expectations based on HAI immunogenicity (*138*, *140*, *184*, *188*, *189*, *205*), may be the result of biasing the humoral immune response away from NK cell and monocyte activating antibodies (Chapter 2). While MF59 induced more antibodies overall, the quality of those antibodies was altered by the

inclusion of the adjuvant. These data presented here demonstrate that the effects of adjuvants on the resulting vaccine-induced humoral immune response are more nuanced than previously identified, with implications for future vaccine studies.

Another promising class of adjuvants are Toll-like receptor (TLR) ligands. TLR ligands engage these evolutionarily conserved pattern recognition receptors to boost immune responses (*135*). Studies of a TLR agonist used in a murine model of influenza vaccination have shown that activation of TLR7/8 boosted type 1 humoral and cellular immunity in both adult and early-life vaccinations (*145*). Another TLR agonist adjuvant Monophosphoryl lipid A (MPLA) targets TLR4, and is part of two adjuvants, AS01 and AS04, that have been licensed in vaccines against other pathogens (*383*). MPLA has shown promising results in multiple murine studies of influenza vaccination, both with traditional (*384*) and novel vaccine preparations (*385*). Additional adjuvants, including liposomes, virosomes, saponins, and ISCOMs, are being tested widely in animal models but human clinical data is not yet available (*135*). The findings presented here that MF59 alters the qualitative humoral profile of the influenza-specific vaccine response, together with recent data on the impact of adjuvants in SARS-CoV-2 vaccination (*335*), motivate deeper analysis to find those adjuvants that can tune both the antibody epitope specificity (Fab) and functional profile (Fc) most effectively to provide protection customized to each pathogen.

FUTURE DIRECTIONS

IMPACT OF REPEATED SEASONAL VACCINATION

Repeated seasonal influenza vaccination provides increased cumulative protection to individuals, but the magnitude of the immune response following each single vaccination decreases over time (*31*, *386*). With the contributions of original antigenic sin and immune

imprinting, seasonal vaccinations must overcome significant immune pressure to generate *de novo* responses as opposed to activating cross reactive but low neutralization antibodies. The seasonal vaccination cohort studies here provide the unique opportunity to investigate the effect of repeated vaccination on the whole humoral immune response and how antibodies change over multiple years. Preliminary analyses have indicated that, for the majority of individuals, breadth is boosted by yearly vaccination but returns to pre-vaccination levels by the next season (**Figure 6.4**). Studying the rare individuals in this cohort whose breadth durability increased following vaccination, may provide insights into what effects pre-existing immunity has on this process and how vaccines could be designed to best induce a durable, broad polyclonal humoral immune response. Already, the data presented here hint at a tiny fraction of the already pre-enriched population studied here who are elite responders to vaccination with wide response breadth across influenza A and B, driven by antibodies that bind to pre-existing antibodies that bind FCγRs. Further research will seek to identify how these individuals are different from others and what tunes their immune response to recognize influenza across subtype and strain variation.

This work builds on previous investigations in the field detailing the protective efficacy of repeated influenza investigation (*31*), providing key information to maximize the response to future novel influenza vaccines. This work has shown that there are very specific humoral profiles that pre-exist repeated vaccination and predict the evolution of breadth, with evidence that this can boost protection during subsequent influenza seasons, even despite antigenic drift (*386*). At a single season level, FCGR2B antibodies have been shown to be a key predictor of the evolution of breadth (Chapter 5); however, how these antibodies evolve over time in this rare population in yet to be determined. Further

research will be needed to elucidate the mechanisms of cross-seasonal protection in both adults and the elderly, for whom vaccines provide lower levels of durable protection (*272*).

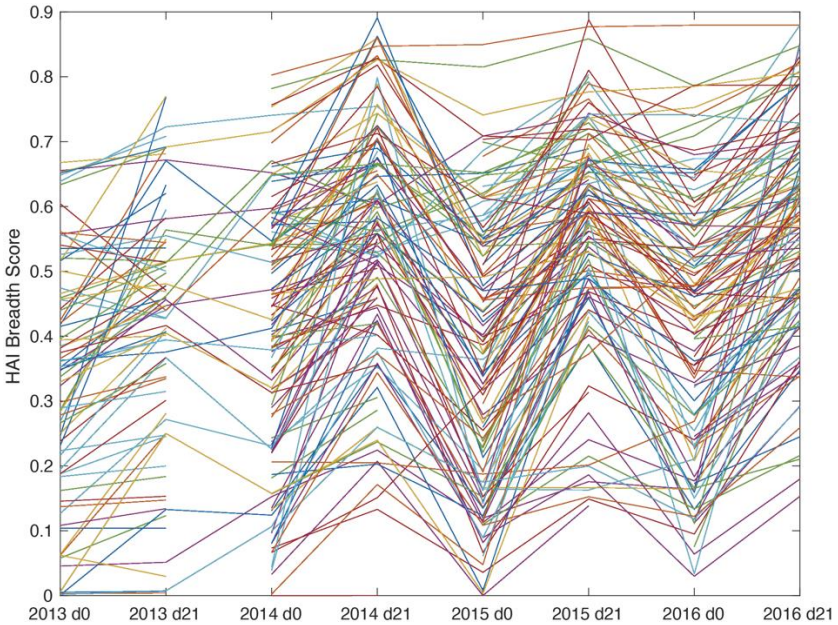

Figure 6.4 HAI breadth over multiple influenza vaccinations. Line graph depicts HAI breadth score, as described in Chapter 5, calculated at each timepoint across four vaccination seasons. Higher numbers indicate increased neutralizing breadth. Day 0 samples were drawn prior to that season's vaccination, and Day 21 was post-seasonal vaccination date during the autumn of that year. Each line represents one individual.

IMPACTS OF NOVEL VACCINE FORMULATIONS

Novel influenza vaccine strategies have been in testing for many years (*15*). One promising candidate, stem chimera vaccines, show promise at eliciting a strong humoral immune response targeting the conserved HA stalk domain (*337*). However, in the correlates analyses presented here, antibodies targeting the HA stem were not correlates of either protection or a broad response to vaccination (Chapters 4 & 5), suggesting that there is more to be understood about the mechanisms involved in protection afforded by these vaccines. Following the recent successes against COVID-19, mRNA vaccine technology is being investigated for use in influenza. Given emerging data indicating that there are differences in SARS-CoV-2-specific antibody Fc profiles even between different mRNA

vaccines in high-risk populations (*387*), it remains to be seen how mRNA will compare to inactivated virus immunization such as is typical in influenza. Because mRNA vaccination presents antigen bound to the membranes of cells instead of in solution, it has been hypothesized that there will be increased BCR crosslinking, leading to enhanced affinity maturation and overall humoral immune response (*388*). Furthermore, the rapid production timelines of mRNA and other emerging technologies may enable better strain matching each season.

Various adjuvanted vaccines, including MF59 vaccines, similar to the one described here, are already in use or in active development. Initial data from this study on the impact of MF59 indicate that the functional humoral response may vary widely depending on adjuvant inclusion (Chapter 2). One interesting area of research is vaccination wherein recombinant HA is bound to C3d have a proposed mechanism of activating B cells via the complement receptors found on their surface (CR2 or CD21) (*389*); this may provide a similar mechanism to the FCGR2B-mediated development of breadth discussed here. This cDNA-based immunization strategy has, in mice, modestly increased heterosubtypic HAI and provided protection against heterosubtypic challenge (*390*, *391*). As seen in the data presented here and in the literature (*371*), increasing breadth and Fc-functionality are frequently tied together, with the understanding that by targeting more conserved epitopes, which may not mediate neutralization, a broad antibody response requires functionality to elicit maximal protection. Current novel vaccine strategies are already seeking to leverage this interaction to provide heterosubtypic protection (*60*).

ANTIGENIC TARGETS BEYOND HA & NA

Another strategy to create a heterosubtypic response to an influenza vaccine is to direct the immune response against a conserved viral antigen (*14*). One attractive

conserved antigen is NP, the influenza nucleoprotein (*171*). NP is about 90% conserved across influenza A viruses, so immunity directed towards NP would be heterosubtypic (*392*, *393*). NP is not expressed on the surface of virions but is expressed on the surface of infected cells (*5*, *7*, *394–396*). NP-specific T cell responses and antibodies have been observed in adults with prior exposure to influenza (*397*, *398*). However, current vaccination strategies do not increase the titer of these antibodies (*397*). Experimental NP vaccination in mice provides heterosubtypic protection from lethal challenge, but does not prevent infection (*397*, *399–404*). NP antibodies are not neutralizing; therefore, infection is established but is cleared quicker and with less severe symptoms than in naïve animals (*399*, *401*). FCγRs are required for protection, as *FcR γ chain*$^{-/-}$ mice receive significantly less benefit from the passive transfer of NP-specific IgG (*43*, *173*).

Vaccination with the M2 ion channel protein of influenza A has also shown protective efficacy in animal models (*45*, *169*). M2 is conserved across all known human influenza A viruses (*405*), and immunity to M2 is heterosubtypic (*406*). M2-specific immune responses have been observed in adults with prior exposure to influenza, but current vaccine strategies do not elicit M2-specific immunity (*311*, *407–409*). Like NP, M2-specific antibodies rely on FCγRs to provide protection and additional immunity is mediated by T cells (*410*). The mechanism by which these antibodies directed towards highly conserved influenza-specific proteins mediate protection is unknown, but the systems serology platform is uniquely poised to measure these immune responses.

CONCLUSION

Historically, influenza vaccines have been evaluated on their ability to induce HAI titers. This work emphasized the importance of taking a holistic approach to the humoral immune response, evaluating antibodies not only on their binding and neutralization capacity but also on their ability to recruit the rest of a protective immune response and, indeed, to shape the development of future humoral development. The data presented here indicate that NK cell-activating antibodies provide protection in older adults and FCγR-binding antibodies provide protection in neonates; however, the heterogeneity of the influenza-specific vaccine response acts as a crucial barrier to improved vaccination. Further, these data present the tantalizing suggestion that pre-existing FCGR2B-binding antibodies act as adjuvants and offer a new opportunity to drive breadth of vaccine-induced immune response. While there is much to be done to fully understand the immune response to influenza, both humoral and cellular, these data provide key insights into what antibody qualities are necessary for the next generation of influenza vaccines to elicit on a population-specific level and a starting point for understanding the influenza-specific immune response over a lifetime.

REFERENCES

1. J. K. Taubenberger, D. M. Morens, The Pathology of Influenza Virus Infections. *Annu. Rev. Pathol. Mech. Dis.* **3**, 499–522 (2008).

2. R. Webster, W. Bean, Evolution and ecology of influenza A viruses. *Microbiol. Rev.* **56**, 152–179 (1992).

3. S. B. Kasloff, H. M. Weingartl, Swine alveolar macrophage cell model allows optimal replication of influenza A viruses regardless of their origin. *Virology*. **490**, 91–98 (2016).

4. S. J. Gamblin, J. J. Skehel, Influenza hemagglutinin and neuraminidase membrane glycoproteins. *J. Biol. Chem.* **285**, 28403–28409 (2010).

5. J. W. Yewdell, E. Frank, W. Gerhard, Expression of influenza A virus internal antigens on the surface of infected P815 cells. *J. Immunol.* **126**, 1814–1819 (1981).

6. K. Das, J. M. Aramini, L.-C. Ma, R. M. Krug, E. Arnold, Structures of influenza A proteins and insights into antiviral drug targets. *Nat. Struct. Mol. Biol.* **17**, 530–538 (2010).

7. K. M. Bialas, K. A. Bussey, R. L. Stone, T. Takimoto, Specific Nucleoprotein Residues Affect Influenza Virus Morphology. *J. Virol.* **88**, 2227–2234 (2014).

8. Y. H. Jang, B. L. Seong, The Quest for a Truly Universal Influenza Vaccine. *Front. Cell. Infect. Microbiol.* **9**, 1–24 (2019).

9. A. J. Hay, V. Gregory, A. R. Douglas, P. L. Yi, The evolution of human influenza viruses. *Philos. Trans. R. Soc. B Biol. Sci.* **356**, 1861–1870 (2001).

10. M. A. Carlock *et al.*, Impact of age and pre-existing immunity on the induction of human antibody responses against influenza B viruses. *Hum. Vaccines Immunother.* **15**, 2030–2043 (2019).

11. WHO, Influenza (2008), (available at http://www.who.int/immunization/topics/influenza/en/).

12. N. I. for O. S. and H. O. of the Director, Influenza in the Workplace (2018), (available at https://www.cdc.gov/niosh/topics/flu/activities.html).

13. WHO, Influenza virus infections in humans (February 2014) (2014), (available at http://www.who.int/influenza/human_animal_interface/virology_laboratories_and_vaccines/influenza_virus_infections_humans_feb14.pdf).

14. C. I. Paules, H. D. Marston, R. W. Eisinger, D. Baltimore, A. S. Fauci, The Pathway to a Universal Influenza Vaccine. *Immunity*. **47**, 599–603 (2017).

15. E. J. Erbelding *et al.*, A Universal Influenza Vaccine: The Strategic Plan for the National Institute of Allergy and Infectious Diseases. *J. Infect. Dis.* **218**, 347–354 (2018).

16. A. Fox *et al.*, Hemagglutination inhibiting antibodies and protection against seasonal and pandemic influenza infection. *J. Infect.* **70**, 187–196 (2015).

17. X. Zhao *et al.*, Quantifying Protection Against Influenza Virus Infection Measured by Hemagglutination-inhibition Assays in Vaccine Trials. *Epidemiology*. **27**, 143–151 (2016).

18. S. E. Ohmit, J. G. Petrie, R. T. Cross, E. Johnson, A. S. Monto, Influenza hemagglutination-inhibition antibody titer as a correlate of vaccine-induced protection. *J. Infect. Dis.* **204**, 1879–1885 (2011).

19. M. J. Memoli *et al.*, Evaluation of antihemagglutinin and antineuraminidase antibodies as correlates of protection in an influenza A/H1N1 virus healthy human challenge model. *MBio*. **7**, 1–12 (2016).

20. CDC, Seasonal Influenza Vaccine Effectiveness, 2005-2017 (2017), (available at https://www.cdc.gov/flu/professionals/vaccination/effectiveness-studies.htm).

21. W. H. Organisation, WHO recommendations on the composition of influenza virus vaccines (2017), (available at http://www.who.int/influenza/vaccines/virus/recommendations/en/).

22. S. J. Zost *et al.*, Contemporary H3N2 influenza viruses have a glycosylation site that alters binding of antibodies elicited by egg-adapted vaccine strains. *Proc. Natl. Acad. Sci.* **114**, 12578–12583 (2017).

23. CDC, Influenza (Flu) (2018), (available at https://www.cdc.gov/flu/index.htm).

24. J. E. J. E. Salk, W. J. W. J. J. Menke, T. J. Francis, A clinical, epidemiological and immunological evaluation op vaccination against epidemic influenza. *Am. J. Epidemiol.* **42**, 57–93 (1945).

25. T. J. Francis, On the Doctrine of Original Antigenic Sin. *Proc. Am. Philos. Soc.* **104**, 572–578 (1960).

26. A. Zhang, H. D. Stacey, C. E. Mullarkey, M. S. Miller, Original Antigenic Sin: How First Exposure Shapes Lifelong Anti–Influenza Virus Immune Responses. *J. Immunol.* **202**, 335–340 (2019).

27. K. M. Gostic, M. Ambrose, M. Worobey, J. O. Lloyd-Smith, Potent protection against H5N1 and H7N9 influenza via childhood hemagglutinin imprinting. *Science (80-.).* **354**, 722–726 (2016).

28. T. W. Hoskins, J. R. Davies, A. J. Smith, C. L. Miller, A. Allchin, Assessment of Inactivated Influenza-a Vaccine After Three Outbreaks of Influenza a At Christ'S Hospital. *Lancet.* **313**, 33–35 (1979).

29. W. A. Keitel, T. R. Cate, R. B. Couch, L. L. Huggins, K. R. Hess, Efficacy of repeated annual immunization with inactivated influenza virus vaccines over a five year period. *Vaccine.* **15**, 1114–1122 (1997).

30. W. E. P. Beyer, I. A. de Bruijn, A. M. Palache, R. G. J. Westendorp, A. D. M. E. Osterhaus, Protection Against Influenza After Annually Repeated Vaccination. *Arch. Intern. Med.* **159**, 182 (1999).

31. L. C. Ramsay *et al.*, The impact of repeated vaccination on influenza vaccine effectiveness: a systematic review and meta-analysis. *BMC Med.* **15**, 159 (2017).

32. J. Wrammert *et al.*, Rapid cloning of high-affinity human monoclonal antibodies against influenza virus. *Nature.* **453**, 667–671 (2008).

33. P. S. Lee, I. A. Wilson, in *Life Science Journal* (2014; http://link.springer.com/10.1007/82_2014_413), vol. 6, pp. 323–341.

34. D. Angeletti, J. W. Yewdell, Is It Possible to Develop a "Universal" Influenza Virus Vaccine? Outflanking Antibody Immunodominance on the Road to Universal Influenza Vaccination. *Cold Spring Harb. Perspect. Biol.*, a028852 (2017).

35. A. H. Ellebedy, R. Ahmed, Re-engaging cross-reactive memory B cells: The influenza puzzle. *Front. Immunol.* **3**, 1–7 (2012).

36. D. C. Ekiert, I. A. Wilson, Broadly neutralizing antibodies against influenza virus and prospects for universal therapies. *Curr. Opin. Virol.* **2**, 134–141 (2012).

37. G. S. Tan *et al.*, A Pan-H1 Anti-Hemagglutinin Monoclonal Antibody with Potent Broad-Spectrum Efficacy In Vivo. *J. Virol.* **86**, 6179–6188 (2012).

38. D. J. Dilillo, G. S. Tan, P. Palese, J. V. Ravetch, Broadly neutralizing hemagglutinin stalk – specific antibodies require Fc γ R interactions for protection against influenza virus in vivo. *Nat. Med.* **20** (2014), doi:10.1038/nm.3443.

39. D. J. DiLillo, P. Palese, P. C. Wilson, J. V. Ravetch, Broadly neutralizing anti-influenza antibodies require Fc receptor engagement for in vivo protection. *J. Clin. Invest.* **126**, 605–610 (2016).

40. S. Jegaskanda, H. A. Vanderven, A. K. Wheatley, S. J. Kent, Fc or not Fc; that is the question: Antibody Fc-receptor interactions are key to universal influenza vaccine design. *Hum. Vaccines Immunother.* **13**, 1288–1296 (2017).

41. H. L. Dugan *et al.*, Preexisting immunity shapes distinct antibody landscapes after influenza virus infection and vaccination in humans. *Sci. Transl. Med.* **12**, 1–15 (2020).

42. L. Bimler *et al.*, Matrix Protein 2 Extracellular Domain-Specific Monoclonal Antibodies Are an Effective and Potentially Universal Treatment for Influenza A. *J. Virol.* (2020), doi:10.1128/JVI.01027-20.

43. M. W. LaMere *et al.*, Contributions of Antinucleoprotein IgG to Heterosubtypic Immunity against Influenza Virus. *J. Immunol.* **186**, 4331–4339 (2011).

44. M. W. LaMere *et al.*, Regulation of Antinucleoprotein IgG by Systemic Vaccination and Its Effect on Influenza Virus Clearance. *J. Virol.* **85**, 5027–5035 (2011).

45. A. Jegerlehner, N. Schmitz, T. Storni, M. F. Bachmann, Influenza A Vaccine Based on the Extracellular Domain of M2: Weak Protection Mediated via Antibody-Dependent NK Cell Activity. *J. Immunol.* **172**, 5598–5605 (2004).

46. E. R. Job *et al.*, Fcγ Receptors Contribute to the Antiviral Properties of Influenza Virus Neuraminidase-Specific Antibodies. *MBio.* **10**, 1–14 (2019).

47. T. J. Wohlbold *et al.*, Vaccination with adjuvanted recombinant neuraminidase induces broad heterologous, but not heterosubtypic, cross-protection against influenza virus infection in mice. *MBio.* **6**, 1–13 (2015).

48. J. A. Roco *et al.*, Class-Switch Recombination Occurs Infrequently in Germinal Centers. *Immunity.* **51**, 337-350.e7 (2019).

49. L. Mesin, J. Ersching, G. D. Victora, Germinal Center B Cell Dynamics. *Immunity.* **45**, 471–482 (2016).

50. G. D. Victora, P. C. Wilson, Germinal Center Selection and the Antibody Response to Influenza. *Cell.* **163**, 545–548 (2015).

51. K. G. C. Smith, M. R. Clatworthy, FcγRIIB in autoimmunity and infection: Evolutionary and therapeutic implications. *Nat. Rev. Immunol.* **10**, 328–343 (2010).

52. M. Espéli *et al.*, FcγRIIb differentially regulates pre-immune and germinal center B cell tolerance in mouse and human. *Nat. Commun.* **10**, 1–14 (2019).

53. S.-S. Wong *et al.*, The immune correlates of protection for an avian influenza H5N1 vaccine in the ferret model using oil-in-water adjuvants. *Sci. Rep.* **7**, 44727 (2017).

54. K. B. O'Brien, T. E. Morrison, D. Y. Dundore, M. T. Heise, S. Schultz-Cherry, A protective role for complement C3 protein during pandemic 2009 H1N1 and H5N1 influenza a virus infection. *PLoS One*. **6** (2011), doi:10.1371/journal.pone.0017377.

55. A. Rattan *et al.*, Synergy between the classical and alternative pathways of complement is essential for conferring effective protection against the pandemic influenza A(H1N1) 2009 virus infection. *PLoS Pathog.* **13** (2017), doi:10.1371/journal.ppat.1006248.

56. C. E. Mullarkey *et al.*, Broadly neutralizing hemagglutinin stalk-specific antibodies induce potent phagocytosis of immune complexes by neutrophils in an Fc-dependent manner. *MBio*. **7**, 1–12 (2016).

57. V. C. Huber, J. M. Lynch, D. J. Bucher, J. Le, D. W. Metzger, Fc Receptor-Mediated Phagocytosis Makes a Significant Contribution to Clearance of Influenza Virus Infections. *J. Immunol.* **166**, 7381–7388 (2001).

58. W. He *et al.*, Alveolar macrophages are critical for broadly-reactive antibody-mediated protection against influenza A virus in mice. *Nat. Commun.* **8**, 1–13 (2017).

59. M. Terajima, M. D. T. Co, J. Cruz, F. A. Ennis, High Antibody-Dependent Cellular Cytotoxicity Antibody Titers to H5N1 and H7N9 Avian Influenza A Viruses in Healthy US Adults and Older Children. *J. Infect. Dis.* **212** (2015), doi:10.1093/infdis/jiv181.

60. S. Jegaskanda, The Potential Role of Fc-Receptor Functions in the Development of a Universal Influenza Vaccine. *Vaccines*. **6**, 27 (2018).

61. M. Kopf, B. Abel, A. Gallimore, M. Carroll, M. F. Bachmann, Complement component C3 promotes T-cell priming and lung migration to control acute influenza virus infection. *Nat. Med.* **8**, 373–378 (2002).

62. C. M. Boudreau, G. Alter, Extra-Neutralizing FcR-Mediated Antibody Functions for a Universal Influenza Vaccine. *Front. Immunol.* **10**, 1–14 (2019).

63. P. Bruhns, Properties of mouse and human IgG receptors and their contribution to disease models. *Blood*. **119**, 5640–5650 (2012).

64. S. Bournazos, J. V. Ravetch, Fcγ Receptor Function and the Design of Vaccination Strategies. *Immunity*. **47**, 224–233 (2017).

65. P. Bruhns *et al.*, Specificity and affinity of human Fc gamma receptors and their polymorphic variants for human IgG subclasses. *Receptor*. **113**, 3716–3725 (2009).

66. F. Ana-Sosa-Batiz *et al.*, Influenza-Specific Antibody-Dependent Phagocytosis. *PLoS One*. **11**, e0154461 (2016).

67. S. Bournazos, J. M. Woof, S. P. Hart, I. Dransfield, Functional and clinical consequences of Fc receptor polymorphic and copy number variants. *Clin. Exp. Immunol.* **157**, 244–254 (2009).

68. B. Perussia *et al.*, Human natural killer cells analyzed by B73.1, a monoclonal antibody blocking Fc receptor functions. II. Studies of B73.1 antibody-antigen interaction on the lymphocyte membrane. *J. Immunol.* **130**, 2142–2148 (1983).

69. J. Ritz, R. E. Schmidt, J. Michon, T. Hercend, S. F. Schlossman, Characterization of Functional Surface Structures on Human Natural Killer Cells. *Adv. Immunol.* **42**, 181–211 (1988).

70. C. R. Wilcox, B. Holder, C. E. Jones, Factors affecting the FcRn-mediated transplacental transfer of antibodies and implications for vaccination in pregnancy. *Front. Immunol.* **8** (2017), doi:10.3389/fimmu.2017.01294.

71. R. P. Junghans, C. L. Anderson, The protection receptor for IgG catabolism is the beta2-microglobulin-containing neonatal intestinal transport receptor. *Proc. Natl. Acad. Sci.* **93**, 5512–5516 (1996).

72. P. Palmeira, C. Quinello, A. L. Silveira-Lessa, C. A. Zago, M. Carneiro-Sampaio, IgG placental transfer in healthy and pathological pregnancies. *Clin. Dev. Immunol.* **2012** (2012), doi:10.1155/2012/985646.

73. U. J. E. Seidel, P. Schlegel, P. Lang, Natural killer cell mediated antibody-dependent cellular cytotoxicity in tumor immunotherapy with therapeutic antibodies. *Front. Immunol.* **4**, 1–8 (2013).

74. T. Werfel *et al.*, Activation of cloned human natural killer cells via Fc gamma RIII. *J Immunol.* **142**, 1102–1106 (1989).

75. A. De Maria, F. Bozzano, C. Cantoni, L. Moretta, Revisiting human natural killer cell subset function revealed cytolytic CD56dimCD16+ NK cells as rapid producers of abundant IFN-γ on activation. *Proc. Natl. Acad. Sci.* **108**, 728–732 (2011).

76. A. Oliva *et al.*, Natural killer cells from human immunodeficiency virus (HIV)-infected individuals are an important source of CC-chemokines and suppress HIV-1 entry and replication in vitro. *J. Clin. Invest.* **102**, 223–231 (1998).

77. H. Jacobsen *et al.*, Influenza virus hemagglutinin stalk-specific antibodies in human serum are a surrogate marker for in vivo protection in a serum transfer mouse challenge model. *MBio.* **8** (2017), doi:10.1128/mBio.01463-17.

78. S. Jegaskanda *et al.*, Generation and Protective Ability of Influenza Virus-Specific Antibody-Dependent Cellular Cytotoxicity in Humans Elicited by Vaccination, Natural Infection, and Experimental Challenge. *J. Infect. Dis.* **214**, 945–952 (2016).

79. H. A. Vanderven *et al.*, Antibody-Dependent Cellular Cytotoxicity Responses to Seasonal Influenza Vaccination in Older Adults. *J. Infect. Dis.* **217**, 12–23 (2017).

80. G. Hashimoto, P. F. Wright, T. David, Antibody-Dependent Cell-Mediated Cytotoxicity against Influenza Virus-Infected Cells. *J. Infect. Dis.* **148**, 785–794 (1983).

81. M. D. T. Co *et al.*, Relationship of Preexisting Influenza Hemagglutination Inhibition, Complement-Dependent Lytic, and Antibody-Dependent Cellular Cytotoxicity Antibodies to the Development of Clinical Illness in a Prospective Study of A(H1N1)pdm09 Influenza in Children. *Viral Immunol.* **27**, 375–382 (2014).

82. S. Jegaskanda *et al.*, Induction of H7N9-cross-reactive antibody-dependent cellular cytotoxicity antibodies by human seasonal influenza a viruses that are directed toward the nucleoprotein. *J. Infect. Dis.* **215**, 818–823 (2017).

83. S. Jegaskanda *et al.*, Age-Associated Cross-reactive Antibody-Dependent Cellular Cytotoxicity Toward 2009 Pandemic Influenza A Virus Subtype H1N1. *J. Infect. Dis.* **208**, 1051–1061 (2013).

84. A. W. Mesman *et al.*, Influenza virus A(H1N1)2009 antibody-dependent cellular cytotoxicity in young children prior to the H1N1 pandemic. *J. Gen. Virol.* **97**, 2157–2165 (2016).

85. P. E. Leon *et al.*, Optimal activation of Fc-mediated effector functions by influenza virus hemagglutinin antibodies requires two points of contact. *Pnas*, E5944–E5951 (2016).

86. W. He *et al.*, Epitope specificity plays a critical role in regulating antibody-dependent cell-mediated cytotoxicity against influenza A virus. *Proc. Natl. Acad. Sci.* **113**, 11931–11936 (2016).

87. G. N. Barber, Host defense, viruses and apoptosis. *Cell Death Differ.* **8**, 113–126 (2001).

88. Y. Ren, J. Savill, Apoptosis: The importance of being eaten. *Cell Death Differ.* **5**, 563–568 (1998).

89. Y. Hashimoto, T. Moki, T. Takizawa, A. Shiratsuchi, Y. Nakanishi, Evidence for Phagocytosis of Influenza Virus-Infected, Apoptotic Cells by Neutrophils and Macrophages in Mice. *J. Immunol.* **178**, 2448–2457 (2007).

90. A. Mócsai, Diverse novel functions of neutrophils in immunity, inflammation, and beyond. *J. Exp. Med.* **210**, 1283–1299 (2013).

91. V. Brinkmann, A. Zychlinsky, Beneficial suicide: Why neutrophils die to make NETs.

Nat. Rev. Microbiol. **5**, 577–582 (2007).

92. K. Lim *et al.*, Neutrophil trails guide influenza-specific CD8+ T cells in the airways. *Science (80-.).* **349**, aaa4352–aaa4352 (2015).

93. M. A. Otten *et al.*, FcR gamma-Chain Dependent Signaling in Immature Neutrophils is Mediated by Fc alpha RI , but Not by Fc gamma RI 1. *J. Immunol.* **179**, 2918–2924 (2007).

94. H. Fujisawa, Neutrophils play an essential role in cooperation with antibody in both protection against and recovery from pulmonary infection with influenza virus in mice. *J. Virol.* **82**, 2772–2783 (2008).

95. H. Fujisawa, S. Tsuru, M. Taniguchi, Y. Zinnaka, K. Nomoto, Protective mechanisms against pulmonary infection with influenza virus. I. Relative contribution of polymorphonuclear leukocytes and of alveolar macrophages to protection during the early phase of intranasal infection. *J. Gen. Virol.* **68**, 425–432 (1987).

96. J. T. Hicks, F. A. Ennis, E. Kim, M. Verbonitz, The importance of an intact complement pathway in recovery from a primary viral infection: influenza in decomplemented and in C5-deficient mice. *J Immunol.* **121**, 1437–1445 (1978).

97. M. Terajima *et al.*, Complement-Dependent Lysis of Influenza A Virus-Infected Cells by Broadly Cross-Reactive Human Monoclonal Antibodies. *J. Virol.* **85**, 13463–13467 (2011).

98. K. Baker *et al.*, Immune and non-immune functions of the (not so) neonatal Fc receptor, FcRn. *Semin. Immunopathol.* **31**, 223–236 (2009).

99. Y. Bai *et al.*, Intracellular neutralization of viral infection in polarized epithelial cells by neonatal Fc receptor (FcRn) -mediated IgG transport. *Pnas*, 2–7 (2011).

100. J. H. Kim, I. Skountzou, R. Compans, J. Jacob, Original Antigenic Sin Responses to Influenza Viruses. *J. Immunol.* **183**, 3294–3301 (2009).

101. T. T. Wang, S. Bournazos, J. V Ravetch, Immunological responses to influenza vaccination: lessons for improving vaccine efficacy. *Curr. Opin. Immunol.* **53**, 124–129 (2018).

102. G. D. Victora, M. C. Nussenzweig, Germinal Centers. *Annu. Rev. Immunol.* **30**, 429–457 (2012).

103. T. G. Phan, J. A. Green, Y. Xu, J. G. Cyster, Immune complex relay by subcapsular sinus macrophages and noncognate B cells drives antibody affinity maturation. *Nat. Immunol.* **10**, 786–796 (2009).

104. B. A. Heesters *et al.*, Endocytosis and Recycling of Immune Complexes by Follicular Dendritic Cells Enhances B Cell Antigen Binding and Activation. *Immunity*. **38**, 1164–1175 (2013).

105. J. G. Tew, T. E. Mandel, Prolonged antigen half-life in the lymphoid follicles of specifically immunized mice. *Immunology*. **37**, 69–76 (1979).

106. Y. Fu *et al.*, A broadly neutralizing anti-influenza antibody reveals ongoing capacity of haemagglutinin-specific memory B cells to evolve. *Nat. Commun.* **7** (2016), doi:10.1038/ncomms12780.

107. F. Klein *et al.*, Somatic mutations of the immunoglobulin framework are generally required for broad and potent HIV-1 neutralization. *Cell*. **153**, 126–138 (2013).

108. G. Lofano *et al.*, Antigen-specific antibody Fc glycosylation enhances humoral immunity via the recruitment of complement. *Sci. Immunol.* **3**, eaat7796 (2018).

109. T. T. Wang *et al.*, Anti-HA Glycoforms Drive B Cell Affinity Selection and Determine Influenza Vaccine Efficacy. *Cell*. **162**, 160–169 (2015).

110. R. Nachbagauer *et al.*, Defining the antibody cross-reactome directed against the influenza virus surface glycoproteins. *Nat. Immunol.* **18** (2017), doi:10.1038/ni.3684.

111. F. Nimmerjahn, J. V. Ravetch, Immunology: Divergent immunoglobulin G subclass activity through selective Fc receptor binding. *Science (80-.).* **310**, 1510–1512 (2005).

112. D. Frasca *et al.*, Effects of age on H1N1-specific serum IgG1 and IgG3 levels evaluated during the 2011-2012 influenza vaccine season. *Immun. Ageing*. **10**, 14 (2013).

113. G. Vidarsson, G. Dekkers, T. Rispens, IgG subclasses and allotypes: From structure to effector functions. *Front. Immunol.* **5**, 1–17 (2014).

114. H. Einarsdottir *et al.*, H435-containing immunoglobulin G3 allotypes are transported efficiently across the human placenta: Implications for alloantibody-mediated diseases of the newborn. *Transfusion*. **54**, 665–671 (2014).

115. A. S. El-Madhun, R. J. Cox, L. R. Haaheim, The effect of age and natural priming on the IgG and IgA subclass responses after parenteral influenza vaccination. *J. Infect. Dis.* **180**, 1356–1360 (1999).

116. M. Muramatsu *et al.*, Comparison of antiviral activity between IgA and IgG specific to influenza virus hemagglutinin: Increased potential of IgA for heterosubtypic immunity. *PLoS One*. **9**, 1–8 (2014).

117. V. Snoeck, I. R. Peters, E. Cox, The IgA system: a comparison of structure and

function in different species. *Vet. Res.* **37**, 455–467 (2006).

118. K. B. Renegar, P. A. Small, L. G. Boykins, P. F. Wright, Role of IgA versus IgG in the Control of Influenza Viral Infection in the Murine Respiratory Tract. *J. Immunol.* **173**, 1978–1986 (2004).

119. E. Van Riet, A. Ainai, T. Suzuki, H. Hasegawa, Mucosal IgA responses in influenza virus infections; thoughts for vaccine design. *Vaccine*. **30**, 5893–5900 (2012).

120. C. W. Seibert *et al.*, Recombinant IgA Is Sufficient To Prevent Influenza Virus Transmission in Guinea Pigs. *J. Virol.* **87**, 7793–7804 (2013).

121. M. F. Jennewein, G. Alter, The Immunoregulatory Roles of Antibody Glycosylation. *Trends Immunol.* **38**, 358–372 (2017).

122. P. Stanley, N. Taniguchi, M. Aebi, in *Essentials of Glycobiology*, A. Varki, R. Cummings, J. Esko, Eds. (Cold Spring Harbor Laboratory Press, NY, ed. 3, 2017).

123. M. Pučić *et al.*, *Mol. Cell. Proteomics*, in press, doi:10.1074/mcp.M111.010090.

124. S. Krapp, Y. Mimura, R. Jefferis, R. Huber, P. Sondermann, Structural analysis of human IgG-Fc glycoforms reveals a correlation between glycosylation and structural integrity. *J. Mol. Biol.* **325**, 979–989 (2003).

125. G. P. Subedi, A. W. Barb, The Structural Role of Antibody N-Glycosylation in Receptor Interactions. *Structure*. **23**, 1573–1583 (2015).

126. M. E. Ackerman *et al.*, Natural variation in Fc glycosylation of HIV-specific antibodies impacts antiviral activity. *J. Clin. Invest.* **123**, 2183–2192 (2013).

127. R. Parekh *et al.*, Association of rheumatoid arthritis and primary osteoarthritis with changes in the glycosylation pattern of total serum IgG. *Nature*. **316**, 452–457 (1985).

128. T. Li *et al.*, Modulating IgG effector function by Fc glycan engineering (2017), doi:10.1073/pnas.1702173114.

129. R. M. Anthony *et al.*, Recapitulation of IVIG Anti-Inflammatory Activity with a Recombinant IgG Fc. *Science (80-.).* **320**, 373–376 (2008).

130. Y. Kaneko, F. Nimmerjahn, J. V Ravetch, Anti-Inflammatory Activity of Immunoglobulin G Resulting from Fc Sialylation. *Science (80-.).* **313**, 670–673 (2006).

131. R. L. Shields *et al.*, Lack of fucose on human IgG1 N-linked oligosaccharide improves binding to human FcγRIII and antibody-dependent cellular toxicity. *J. Biol. Chem.* **277**, 26733–26740 (2002).

132. A. E. Mahan *et al.*, Antigen-Specific Antibody Glycosylation Is Regulated via Vaccination. *PLoS Pathog.* **12**, 1–18 (2016).

133. M. H. J. Selman *et al.*, *Mol. Cell. Proteomics*, in press, doi:10.1074/mcp.M111.014563.

134. J. S. Tregoning, R. F. Russell, E. Kinnear, Adjuvanted influenza vaccines. *Hum. Vaccines Immunother.* **14**, 550–564 (2018).

135. G. Leroux-Roels, Unmet needs in modern vaccinology. Adjuvants to improve the immune response. *Vaccine*. **28** (2010), doi:10.1016/j.vaccine.2010.07.021.

136. D. T. O'Hagan, G. S. Ott, E. De Gregorio, A. Seubert, The mechanism of action of MF59 - An innately attractive adjuvant formulation. *Vaccine*. **30**, 4341–4348 (2012).

137. F. Liang *et al.*, Vaccine priming is restricted to draining lymph nodes & controlled by adjuvant-mediated antigen uptake. *Sci. Transl. Med.* **9** (2017), doi:10.1126/scitranslmed.aal2094.

138. D. T. O'Hagan, R. Rappuoli, E. De Gregorio, T. Tsai, G. Del Giudice, MF59 adjuvant: the best insurance against influenza strain diversity. *Expert Rev. Vaccines*. **10**, 447–462 (2011).

139. D. I. Bernstein *et al.*, Effects of Adjuvants on the Safety and Immunogenicity of an Avian Influenza H5N1 Vaccine in Adults. *J. Infect. Dis.* **197**, 667–675 (2008).

140. S. Khurana *et al.*, MF59 Adjuvant Enhances Diversity and Affinity of Antibody-Mediated Immune Response to Pandemic Influenza Vaccines. *Sci. Transl. Med.* **3**, 85ra48-85ra48 (2011).

141. M. J. Hocart, J. S. Mackenzie, G. A. Stewart, The immunoglobulin G subclass responses of mice to influenza A virus: the effect of mouse strain, and the neutralizing abilities of individual protein A-purified subclass antibodies. *J. Gen. Virol.* **70**, 2439–2448 (1989).

142. J. Coutelier, J. T. M. Van Der Logt, F. W. A. Heessen, G. Warnier, J. V. A. N. Snick, IgG2a restriction of murine antibodies elicited by viral infections. *J. Exp. Med.* **165**, 64–69 (1987).

143. C. Savard *et al.*, Improvement of the trivalent inactivated flu vaccine using papmv nanoparticles. *PLoS One*. **6** (2011), doi:10.1371/journal.pone.0021522.

144. I. D. Davis *et al.*, Recombinant NY-ESO-1 protein with ISCOMATRIX adjuvant induces broad integrated antibody and CD4+ and CD8+ T cell responses in humans. *Proc. Natl. Acad. Sci.* **101**, 10697–10702 (2004).

145. F. Borriello *et al.*, Identification and Characterization of Stimulator of Interferon

Genes As a Robust Adjuvant Target for Early Life Immunization. *Front. Immunol.* **8**, 1–14 (2017).

146. B. M. Giles *et al.*, A computationally optimized hemagglutinin virus-like particle vaccine elicits broadly reactive antibodies that protect nonhuman primates from H5N1 infection. *J. Infect. Dis.* **205**, 1562–1570 (2012).

147. B. M. Giles, S. J. Bissel, D. R. DeAlmeida, C. A. Wiley, T. M. Ross, Antibody breadth and protective efficacy are increased by vaccination with computationally optimized hemagglutinin but not with polyvalent hemagglutinin-based H5N1 virus-like particle vaccines. *Clin. Vaccine Immunol.* **19**, 128–139 (2012).

148. D. M. Carter *et al.*, Design and Characterization of a Computationally Optimized Broadly Reactive Hemagglutinin Vaccine for H1N1 Influenza Viruses. *J. Virol.* **90**, 4720–4734 (2016).

149. T. M. Wong *et al.*, Computationally Optimized Broadly Reactive Hemagglutinin Elicits Hemagglutination Inhibition Antibodies against a Panel of H3N2 Influenza Virus Cocirculating Variants. *J. Virol.* **91**, e01581-17 (2017).

150. J. E. M. Van Der Lubbe *et al.*, Mini-HA is superior to full length hemagglutinin immunization in inducing stem-specific antibodies and protection against group 1 influenza virus challenges in mice. *Front. Immunol.* **9**, 1–13 (2018).

151. W.-C. Liu, J.-T. Jan, Y.-J. Huang, T.-H. Chen, S.-C. Wu, Unmasking Stem-Specific Neutralizing Epitopes by Abolishing N-Linked Glycosylation Sites of Influenza Virus Hemagglutinin Proteins for Vaccine Design. *J. Virol.* **90**, 8496–8508 (2016).

152. D. D. Raymond *et al.*, Conserved epitope on influenza-virus hemagglutinin head defined by a vaccine-induced antibody. *Proc. Natl. Acad. Sci.* **115**, 168–173 (2018).

153. D. Angeletti *et al.*, Defining B cell immunodominance to viruses. *Nat. Immunol.* **18**, 456–463 (2017).

154. J. Steel *et al.*, Influenza Virus Vaccine Based on the Conserved Hemagglutinin Stalk Domain. *MBio.* **1**, 259–265254 (2010).

155. R. Nachbagauer *et al.*, A universal influenza virus vaccine candidate confers protection against pandemic H1N1 infection in preclinical ferret studies. *npj Vaccines.* **2**, 1–12 (2017).

156. S.-Y. Sunwoo *et al.*, A Universal Influenza Virus Vaccine Candidate Tested in a Pig Vaccination-Infection Model in the Presence of Maternal Antibodies. *Vaccines.* **6**, 64 (2018).

157. A. T. Harding, N. S. Heaton, Efforts to Improve the Seasonal Influenza Vaccine.

Vaccines. **6**, 19 (2018).

158. J. V. Roedig, E. Rapp, D. Höper, Y. Genzel, U. Reichl, Impact of host cell line adaptation on quasispecies composition and glycosylation of influenza a virus hemagglutinin. *PLoS One*. **6** (2011), doi:10.1371/journal.pone.0027989.

159. J. Schwarzer *et al.*, Glycan analysis in cell culture-based influenza vaccine production: Influence of host cell line and virus strain on the glycosylation pattern of viral hemagglutinin. *Vaccine*. **27**, 4325–4336 (2009).

160. J. Hutter *et al.*, Toward Animal Cell Culture-Based Influenza Vaccine Design: Viral Hemagglutinin N-Glycosylation Markedly Impacts Immunogenicity. *J. Immunol.* **190**, 220–230 (2013).

161. A. S. Gambaryan *et al.*, Effects of host-dependent glycosylation of hemagglutinin on receptor- binding properties of H1N1 human influenza A virus grown in MDCK cells and in embryonated eggs. *Virology*. **247**, 170–177 (1998).

162. D. C. Ekiert *et al.*, Antibody Recognition of a Highly Conserved Influenza Virus Epitope. *Science (80-.).* **324**, 246–251 (2009).

163. Y. Abe, E. Takashita, K. Sugawara, Y. Matsuzaki, Y. Muraki, Effect of the Addition of Oligosaccharides on the Biological Activities and Antigenicity of Influenza A/H3N2 Virus Hemagglutinin. *J. Virol.* **78**, 9605–11 (2004).

164. W. Wang *et al.*, Glycosylation at 158N of the Hemagglutinin Protein and Receptor Binding Specificity Synergistically Affect the Antigenicity and Immunogenicity of a Live Attenuated H5N1 A/Vietnam/1203/2004 Vaccine Virus in Ferrets. *J. Virol.* **84**, 6570–6577 (2010).

165. M. D. Tate, E. R. Job, A. G. Brooks, P. C. Reading, Glycosylation of the hemagglutinin modulates the sensitivity of H3N2 influenza viruses to innate proteins in airway secretions and virulence in mice. *Virology*. **413**, 84–92 (2011).

166. M. D. Tate, A. G. Brooks, P. C. Reading, Specific Sites of N-Linked Glycosylation on the Hemagglutinin of H1N1 Subtype Influenza A Virus Determine Sensitivity to Inhibitors of the Innate Immune System and Virulence in Mice. *J. Immunol.* **187**, 1884–1894 (2011).

167. C.-Y. Wu *et al.*, Influenza A surface glycosylation and vaccine design. *Proc. Natl. Acad. Sci.* **114**, 280–285 (2017).

168. X. Sun *et al.*, N-Linked Glycosylation of the Hemagglutinin Protein Influences Virulence and Antigenicity of the 1918 Pandemic and Seasonal H1N1 Influenza A Viruses. *J. Virol.* **87**, 8756–8766 (2013).

169. K. El Bakkouri *et al.*, Universal Vaccine Based on Ectodomain of Matrix Protein 2 of Influenza A: Fc Receptors and Alveolar Macrophages Mediate Protection. *J. Immunol.* **186**, 1022–1031 (2011).

170. G. Marcelin, M. R. Sandbulte, R. J. Webby, Contribution of antibody production against neuraminidase to the protection afforded by influenza vaccines. *Rev. Med. Virol.* **22**, 267–279 (2012).

171. M. Zheng, J. Luo, Z. Chen, Development of universal influenza vaccines based on influenza virus M and NP genes. *Infection.* **42**, 251–262 (2014).

172. S. Jegaskanda, P. C. Reading, S. J. Kent, Influenza-Specific Antibody-Dependent Cellular Cytotoxicity: Toward a Universal Influenza Vaccine. *J. Immunol.* **193**, 469–475 (2014).

173. W. Gerhard, K. Mozdzanowska, M. Furchner, G. Washko, K. Maiese, Role of the B-cell response in recovery of mice from primary influenza virus infection. *Immunol. Rev.* **159**, 95–103 (1997).

174. Y. Matsuoka, E. W. Lamirande, K. Subbaran, The mouse model for influenza. *Curr. Protoc. Microbiol.*, 1–30 (2009).

175. R. R. Thangavel, N. M. Bouvier, Animal models for influenza virus pathogenesis, transmission, and immunology. *J. Immunol. Methods.* **410**, 60–79 (2014).

176. C. M. Oshansky, P. G. Thomas, The human side of influenza. *J. Leukoc. Biol.* **92**, 83–96 (2012).

177. C. Langlet *et al.*, CD64 Expression Distinguishes Monocyte-Derived and Conventional Dendritic Cells and Reveals Their Distinct Role during Intramuscular Immunization. *J. Immunol.* **188**, 1751–1760 (2012).

178. P. Bruhns, F. Jönsson, Mouse and human FcR effector functions. *Immunol. Rev.* **268**, 25–51 (2015).

179. M. B. Overdijk *et al.*, Crosstalk between Human IgG Isotypes and Murine Effector Cells. *J. Immunol.* **189**, 3430–3438 (2012).

180. A. D. Iuliano *et al.*, Estimates of global seasonal influenza-associated respiratory mortality : a modelling study. *Lancet.* **391**, 1285–1300 (2018).

181. CDC, Disease Burden of Influenza. *Influ.* (2018).

182. World Health Organization, H5N1 avian influenza : Timeline of major events (2012), (available at http://www.who.int/influenza/human_animal_interface/H5N1_avian_influenza_updat

e200412.pdf).

183. WHO, "Avian influenza: assessing the pandemic threat" (2005), (available at https://www.who.int/influenza/resources/documents/h5n1_assessing_pandemic_threat/en/).

184. A. Banzhoff *et al.*, MF59-adjuvanted H5N1 vaccine induces immunologic memory and heterotypic antibody responses in non-elderly and elderly adults. *PLoS One*. **4** (2009), doi:10.1371/journal.pone.0004384.

185. R. L. Coffman, A. Sher, R. A. Seder, Vaccine adjuvants: Putting innate immunity to work. *Immunity*. **33**, 492–503 (2010).

186. Centers for Disease Control and Prevention, FLUAD Flu Vaccine with Adjuvant (2017), (available at https://www.cdc.gov/flu/protect/vaccine/adjuvant.htm).

187. A. Seubert, E. Monaci, M. Pizza, D. T. O'Hagan, A. Wack, The adjuvants aluminum hydroxide and MF59 induce monocyte and granulocyte chemoattractants and enhance monocyte differentiation toward dendritic cells. *J. Immunol.* **180**, 5402–5412 (2008).

188. T. Vesikari *et al.*, Efficacy, immunogenicity, and safety evaluation of an MF59-adjuvanted quadrivalent influenza virus vaccine compared with non-adjuvanted influenza vaccine in children: a multicentre, randomised controlled, observer-blinded, phase 3 trial. *Lancet Respir. Med.* **6**, 345–356 (2018).

189. A. Domnich *et al.*, Effectiveness of MF59-adjuvanted seasonal influenza vaccine in the elderly: A systematic review and meta-analysis. *Vaccine*. **35**, 513–520 (2017).

190. L. L. Lu, T. J. Suscovich, S. M. Fortune, G. Alter, Beyond binding: antibody effector functions in infectious diseases. *Nat. Rev. Immunol.* **18**, 46–61 (2018).

191. B. M. Gunn, G. Alter, Modulating Antibody Functionality in Infectious Disease and Vaccination. *Trends Mol. Med.* **22**, 969–982 (2016).

192. M. E. Ackerman *et al.*, Polyfunctional HIV-Specific Antibody Responses Are Associated with Spontaneous HIV Control. *PLOS Pathog.* **12**, e1005315 (2016).

193. A. W. Chung *et al.*, Dissecting Polyclonal Vaccine-Induced Humoral Immunity against HIV Using Systems Serology. *Cell.* **163**, 988–998 (2015).

194. M. E. Ackerman *et al.*, A robust, high-throughput assay to determine the phagocytic activity of clinical antibody samples. *J. Immunol. Methods*. **366**, 8–19 (2011).

195. L. L. Lu *et al.*, A Functional Role for Antibodies in Tuberculosis. *Cell.* **167**, 433-443.e14 (2016).

196. S. Jegaskanda, J. T. Weinfurter, T. C. Friedrich, S. J. Kent, Antibody-Dependent Cellular Cytotoxicity Is Associated with Control of Pandemic H1N1 Influenza Virus Infection of Macaques. *J. Virol.* **87**, 5512–5522 (2013).

197. E. P. Brown *et al.*, High-throughput, multiplexed IgG subclassing of antigen-specific antibodies from clinical samples. *J. Immunol. Methods*. **386**, 117–123 (2012).

198. D. Kao *et al.*, IgG subclass and vaccination stimulus determine changes in antigen specific antibody glycosylation in mice. *Eur. J. Immunol.* **47**, 2070–2079 (2017).

199. H. A. Vanderven, S. Jegaskanda, A. K. Wheatley, S. J. Kent, Antibody-dependent cellular cytotoxicity and influenza virus. *Curr. Opin. Virol.* **22**, 89–96 (2017).

200. L. C. Lambert, A. S. Fauci, Influenza Vaccines for the Future. *N. Engl. J. Med.* **363**, 2036–2044 (2010).

201. H. Ren, P. Zhou, Epitope-focused vaccine design against influenza A and B viruses. *Curr. Opin. Immunol.* **42**, 83–90 (2016).

202. K. Houser, K. Subbarao, Influenza Vaccines: Challenges and Solutions. *Cell Host Microbe*. **17**, 295–300 (2015).

203. S. S. Ahmed, S. A. Plotkin, S. Black, R. L. Coffman, Assessing the Safety of Adjuvanted Vaccines. *Sci. Transl. Med.* **3**, 93rv2-93rv2 (2011).

204. C. H. Clegg, J. A. Rininger, S. L. Baldwin, Clinical vaccine development for H5N1 influenza. *Expert Rev. Vaccines*. **12**, 767–777 (2013).

205. G. Galli *et al.*, Fast rise of broadly cross-reactive antibodies after boosting long-lived human memory B cells primed by an MF59 adjuvanted prepandemic vaccine. *Proc. Natl. Acad. Sci. U. S. A.* **106**, 7962–7967 (2009).

206. J. R. Francica *et al.*, Innate transcriptional effects by adjuvants on the magnitude, quality, and durability of HIV envelope responses in NHPs. *Blood Adv.* **1**, 2329–2342 (2017).

207. A. M. Kerrigan, G. D. Brown, C-type lectins and phagocytosis. *Immunobiology*. **214**, 562–575 (2009).

208. D. H. Barouch *et al.*, Protective Efficacy of a Global HIV-1 Mosaic Vaccine against Heterologous SHIV Challenges in Rhesus Monkeys. *Cell*. **155**, 531–539 (2013).

209. A. W. Chung *et al.*, Polyfunctional Fc-effector profiles mediated by IgG subclass selection distinguish RV144 and VAX003 vaccines. *Sci. Transl. Med.* **6**, 228–238 (2014).

210. R. W. Tiendrebeogo *et al.*, Antibody-Dependent Cellular Inhibition Is Associated With Reduced Risk Against Febrile Malaria in a Longitudinal Cohort Study Involving Ghanaian Children. *Open Forum Infect. Dis.* **2**, 1–8 (2015).

211. A. Jafarshad *et al.*, A Novel Antibody-Dependent Cellular Cytotoxicity Mechanism Involved in Defense against Malaria Requires Costimulation of Monocytes Fc RII and Fc RIII. *J. Immunol.* **178**, 3099–3106 (2007).

212. B. M. Gunn *et al.*, A Role for Fc Function in Therapeutic Monoclonal Antibody-Mediated Protection against Ebola Virus. *Cell Host Microbe*. **24**, 221-233.e5 (2018).

213. S. Jegaskanda *et al.*, Cross-Reactive Influenza-Specific Antibody-Dependent Cellular Cytotoxicity Antibodies in the Absence of Neutralizing Antibodies. *J. Immunol.* **190**, 1837–1848 (2013).

214. F. Cox *et al.*, HA Antibody-Mediated FcγRIIIa Activity Is Both Dependent on FcR Engagement and Interactions between HA and Sialic Acids. *Front. Immunol.* **7**, 1–10 (2016).

215. M. Q. Ge *et al.*, NK Cells Regulate CD8+ T Cell Priming and Dendritic Cell Migration during Influenza A Infection by IFN- and Perforin-Dependent Mechanisms. *J. Immunol.* **189**, 2099–2109 (2012).

216. A. Impagliazzo *et al.*, A stable trimeric influenza hemagglutinin stem as a broadly protective immunogen. *Science (80-.).* **349**, 1301–1306 (2015).

217. S. P. Kasturi *et al.*, Programming the magnitude and persistence of antibody responses with innate immunity. *Nature*. **470**, 543–550 (2011).

218. A. Wack *et al.*, Combination adjuvants for the induction of potent, long-lasting antibody and T-cell responses to influenza vaccine in mice. *Vaccine*. **26**, 552–561 (2008).

219. J. R. Ortiz, J. A. Englund, K. M. Neuzil, Influenza vaccine for pregnant women in resource-constrained countries: A review of the evidence to inform policy decisions. *Vaccine*. **29**, 4439–4452 (2011).

220. C. El Guerche-Séblain *et al.*, Epidemiology and burden of influenza in healthy children aged 6 to 35 months: Analysis of data from the placebo arm of a phase III efficacy trial. *BMC Infect. Dis.* **19**, 4–9 (2019).

221. H. Nair *et al.*, Global burden of respiratory infections due to seasonal influenza in young children: A systematic review and meta-analysis. *Lancet*. **378**, 1917–1930 (2011).

222. J. M. Tielsch *et al.*, Designs of two randomized, community-based trials to assess the

impact of influenza immunization during pregnancy on respiratory illness among pregnant women and their infants and reproductive outcomes in rural Nepal. *BMC Pregnancy Childbirth*. **15**, 1–10 (2015).

223. X. Wang *et al.*, Global burden of respiratory infections associated with seasonal influenza in children under 5 years in 2018: a systematic review and modelling study. *Lancet Glob. Heal.*, 497–510 (2020).

224. World Health Organization, Vaccines against influenza WHO position paper - November 2012. *Wkly. Epidemiol. Rec.* **47**, 461–476 (2012).

225. S. B. Omer *et al.*, Three randomized trials of maternal influenza immunization in Mali, Nepal, and South Africa: Methods and expectations. *Vaccine*. **33**, 3801–3812 (2015).

226. K. M. Neuzil, G. W. Reed, E. F. Mitchel, L. Simonsen, M. R. Griffin, Impact of influenza on acute cardiopulmonary hospitalizations in pregnant women. *Am. J. Epidemiol.* **148**, 1094–1102 (1998).

227. T. J. Doyle, K. Goodin, J. J. Hamilton, Maternal and Neonatal Outcomes among Pregnant Women with 2009 Pandemic Influenza A(H1N1) Illness in Florida, 2009-2010: A Population-Based Cohort Study. *PLoS One*. **8**, 2009–2010 (2013).

228. J. Katz *et al.*, Impact of timing of influenza vaccination in pregnancy on transplacental antibody transfer, influenza incidence, and birth outcomes: A randomized trial in Rural Nepal. *Clin. Infect. Dis.* **67**, 334–340 (2018).

229. J. R. Jarvis, R. B. Dorey, F. D. M. Warricker, N. A. Alwan, C. E. Jones, The effectiveness of influenza vaccination in pregnancy in relation to child health outcomes: Systematic review and meta-analysis. *Vaccine*. **38**, 1601–1613 (2020).

230. M. D. Tapia *et al.*, Maternal immunisation with trivalent inactivated influenza vaccine for prevention of influenza in infants in Mali: a prospective, active-controlled, observer-blind, randomised phase 4 trial. *Lancet Infect. Dis.* **16**, 1026–1035 (2016).

231. K. Zaman *et al.*, Effectiveness of Maternal Influenza Immunization in Mothers and Infants. *N. Engl. J. Med.* **359**, 1555–1564 (2008).

232. M. C. Nunes, S. A. Madhi, Influenza vaccination during pregnancy for prevention of influenza confirmed illness in the infants: A systematic review and meta-analysis. *Hum. Vaccines Immunother.* **14**, 758–766 (2018).

233. G. Dabrera *et al.*, Effectiveness of seasonal influenza vaccination during pregnancy in preventing influenza infection in infants, England, 2013/14. *Eurosurveillance*. **19**, 1–4 (2014).

234. S. B. Omer, Maternal immunization. *N. Engl. J. Med.* **376**, 1256–1267 (2017).

235. J. A. Englund *et al.*, Maternal immunization with influenza or tetanus toxoid vaccine for passive antibody protection in young infants. *J. Infect. Dis.* **168**, 647–656 (1993).

236. Z. Zhong *et al.*, The impact of timing of maternal influenza immunization on infant antibody levels at birth. *Clin. Exp. Immunol.* **195**, 139–152 (2019).

237. H. A. Vanderven *et al.*, Fc functional antibody responses to adjuvanted versus unadjuvanted seasonal influenza vaccination in community-dwelling older adults. *Vaccine*. **38**, 2368–2377 (2020).

238. M. D. T. Co, J. Cruz, A. Takeda, F. A. Ennis, M. Terajima, Comparison of complement dependent lytic, hemagglutination inhibition and microneutralization antibody responses in influenza vaccinated individuals. *Hum. Vaccines Immunother.* **8**, 1218–1222 (2012).

239. B. T. Costa-Carvalho *et al.*, Transfer of IgG subclasses across placenta in term and preterm newborns. *Brazilian J. Med. Biol. Res.* **29**, 201–204 (1996).

240. N. M. Stapleton *et al.*, Competition for FcRn-mediated transport gives rise to short half-life of human IgG3 and offers therapeutic potential. *Nat. Commun.* **2** (2011), doi:10.1038/ncomms1608.

241. H. Akbulut, A. Çelik, A. Akbulut, A. Ayar, Placental Transfer of Total IgG and IgG Subclasses in a Turkis Population Living in Eastern Anatolia. *Nobel Med.* **8**, 59–64 (2012).

242. T. Clements *et al.*, Update on Transplacental Transfer of IgG Subclasses: Impact of Maternal and Fetal Factors. *Front. Immunol.* **11**, 1–17 (2020).

243. S. Hashira, S. Okitsu-Negishi, K. Yoshino, Placental transfer of IgG subclasses in a Japanese population. *Pediatr. Int.* **42**, 337–342 (2000).

244. M. F. Jennewein *et al.*, Fc glycan-mediated regulation of placental antibody transfer. *Cell.* **178**, 202-215.e14 (2019).

245. M. C. Steinhoff *et al.*, Year-round influenza immunisation during pregnancy in Nepal: a phase 4, randomised, placebo-controlled trial. *Lancet Infect. Dis.* **17**, 981–989 (2017).

246. A. W. Boesch *et al.*, Highly parallel characterization of IgG Fc binding interactions. *MAbs*. **6**, 915–927 (2014).

247. C. B. Karsten *et al.*, A versatile high-throughput assay to characterize antibody-mediated neutrophil phagocytosis. *J. Immunol. Methods*. **471**, 46–56 (2019).

248. S. Fischinger *et al.*, A high-throughput, bead-based, antigen-specific assay to assess the ability of antibodies to induce complement activation. *J. Immunol. Methods*. **473**, 112630 (2019).

249. M. E. Ackerman *et al.*, Route of immunization defines multiple mechanisms of vaccine-mediated protection against SIV. *Nat. Med.* **24**, 1590–1598 (2018).

250. S. Takeda *et al.*, Influenza vaccination during pregnancy and its usefulness to mothers and their young infants. *J. Infect. Chemother.* **21**, 238–246 (2015).

251. A. W. Kay *et al.*, Pregnancy Does Not Attenuate the Antibody or Plasmablast Response to Inactivated Influenza Vaccine. *J. Infect. Dis.* **212**, 861–870 (2015).

252. N. E. Simister, A. R. Rees, Isolation and characterization of an Fc receptor from neonatal rat small intestine. *Eur. J. Immunol.* **15**, 733–738 (1985).

253. N. E. Simister, K. E. Mostov, An Fc receptor structurally related to MHC class I antigens. *Nature*. **337** (1989).

254. H. A. Vanderven, S. J. Kent, The protective potential of Fc-mediated antibody functions against influenza virus and other viral pathogens. *Immunol. Cell Biol.* **98**, 253–263 (2020).

255. E. Henkle *et al.*, Incidence of influenza virus infection in early infancy: A prospective study in South Asia. *Pediatr. Infect. Dis. J.* **30**, 170–173 (2011).

256. S. A. Madhi *et al.*, Influenza vaccination of pregnant women and protection of their infants. *N. Engl. J. Med.* **371**, 918–931 (2014).

257. C. Switzer, C. D'Heilly, D. Macina, *Immunological and Clinical Benefits of Maternal Immunization Against Pertussis: A Systematic Review* (Springer Healthcare, 2019; https://doi.org/10.1007/s40121-019-00264-7), vol. 8.

258. C. M. Boudreau *et al.*, Selective induction of antibody effector functional responses using MF59-adjuvanted vaccination. *J. Clin. Invest.* **130**, 662–672 (2019).

259. P. Nguyen-Contant, M. Y. Sangster, D. J. Topham, Squalene-Based Influenza Vaccine Adjuvants and Their Impact on the Hemagglutinin-Specific B Cell Response. *Pathogens*. **10**, 355 (2021).

260. A. Shakya, Diarroheal Diseases; Still a Public Health Problem? *Heal. Prospect.* **10**, 79–80 (2018).

261. R. Basnet, S. G. Hinderaker, D. Enarson, P. Malla, O. Mørkve, Delay in the diagnosis of tuberculosis in Nepal. *BMC Public Health*. **9**, 1–5 (2009).

262. J. Katz *et al.*, Nutritional status of infants at six months of age following maternal influenza immunization: A randomized placebo-controlled trial in rural Nepal. *Vaccine*. **35**, 6743–6750 (2017).

263. S. Cousins, Reaching Nepal's mobile population at risk of HIV. *lancet. HIV*. **5**, e613–e614 (2018).

264. N. Gautam, S. Kakchapati, S. Shrestha, W. Wanishsakpong, Patterns and trends of malaria in 25 risk districts of nepal from 2001 to 2017. *Clin. Exp. Vaccine Res.* **8**, 77–85 (2019).

265. T. M. E. Govaert *et al.*, The efficacy of influenza vaccination in elderly individuals. A randomized double-blind placebo-controlled trial. *JAMA J. Am. Med. Assoc.* **272**, 1661–1665 (1994).

266. P. A. Gross, A. W. Hermogenes, H. S. Sacks, J. Lau, R. A. Levandowski, The efficacy of influenza vaccine in elderly persons. A meta-analysis and review of the literature. *Ann. Intern. Med.* **123**, 518–527 (1995).

267. A. B. Amin *et al.*, Immunogenicity of influenza vaccines administered to pregnant women in randomized clinical trials in Mali and South Africa. *Vaccine*. **38**, 6478–6483 (2020).

268. E. P. Schlaudecker *et al.*, IgA and Neutralizing Antibodies to Influenza A Virus in Human Milk: A Randomized Trial of Antenatal Influenza Immunization. *PLoS One*. **8**, 6–13 (2013).

269. V. Demers-mathieu *et al.*, Breast Milk , and Gastric Contents and Stools from Preterm Infants (2019).

270. W. W. Thompson *et al.*, Mortality Associated With Influenza and Respiratory Syncytial Virus in the United States. *JAMA J. Am. Med. Assoc.* **289**, 179–186 (2003).

271. C. A. Czaja *et al.*, Age-Related Differences in Hospitalization Rates, Clinical Presentation, and Outcomes among Older Adults Hospitalized with Influenza - U.S. Influenza Hospitalization Surveillance Network (FluSurv-NET). *Open Forum Infect. Dis.* **6**, 1–8 (2019).

272. M. Rondy *et al.*, Effectiveness of influenza vaccines in preventing severe influenza illness among adults: A systematic review and meta-analysis of test-negative design case-control studies. *J. Infect.* **75**, 381–394 (2017).

273. Centers for Disease Control and Prevention: National Center for Immunization and Respiratory Diseases, Past Seasons Vaccine Effectiveness Estimates. *Seas. Influ.* (2020), (available at https://www.cdc.gov/flu/vaccines-work/past-seasons-estimates.html).

274. M. K. Andrew *et al.*, The importance of frailty in the assessment of influenza vaccine effectiveness against influenza-related hospitalization in elderly people. *J. Infect. Dis.* **216**, 405–414 (2017).

275. Centers for Disease Control and Prevention: National Center for Immunization and Respiratory Diseases, Selecting Viruses for the Seasonal Influenza Vaccine (2020).

276. D. M. Skowronski *et al.*, Low 2012-13 influenza vaccine effectiveness associated with mutation in the egg-adapted H3N2 vaccine strain not antigenic drift in circulating viruses. *PLoS One.* **9** (2014), doi:10.1371/journal.pone.0092153.

277. D. M. Skowronski, G. De Serres, Role of Egg-adaptation Mutations in Low Influenza A(H3N2) Vaccine Effectiveness During the 2012–2013 Season. *Clin. Infect. Dis.* **67**, 1474–1476 (2018).

278. C. A. DiazGranados *et al.*, Efficacy of High-Dose versus Standard-Dose Influenza Vaccine in Older Adults. *N. Engl. J. Med.* **371**, 635–645 (2014).

279. C. Dreyfus *et al.*, Highly Conserved Protective Epitopes on Influenza B Viruses. *Science (80-.).*, 1343–1349 (2012).

280. T. C. Sutton *et al.*, In Vitro Neutralization Is Not Predictive of Prophylactic Efficacy of Broadly Neutralizing Monoclonal Antibodies CR6261 and CR9114 against Lethal H2 Influenza Virus Challenge in Mice. *J. Virol.* **91**, e01603-17 (2017).

281. A. Chit *et al.*, Cost-effectiveness of high-dose versus standard-dose inactivated influenza vaccine in adults aged 65 years and older: An economic evaluation of data from a randomised controlled trial. *Lancet Infect. Dis.* **15**, 1459–1466 (2015).

282. Centers for Disease Control and Prevention: National Center for Immunization and Respiratory Diseases, How CDC Classifies Flu Severity (2018), (available at https://www.cdc.gov/flu/about/classifies-flu-severity.htm).

283. Centers for Disease Control and Prevention: National Center for Immunization and Respiratory Diseases, Summary of the 2012-2013 Influenza Season (2019), (available at https://www.cdc.gov/flu/pastseasons/1213season.htm).

284. E. P. Brown *et al.*, Multiplexed Fc array for evaluation of antigen-specific antibody effector profiles. *J. Immunol. Methods.* **443**, 33–44 (2017).

285. N. Loeb *et al.*, Frailty is associated with increased hemagglutination- inhibition titers in a 4-year randomized trial comparing standard- And high-dose influenza vaccination. *Open Forum Infect. Dis.* **7** (2020), doi:10.1093/OFID/OFAA148.

286. P. Smith, D. J. DiLillo, S. Bournazos, F. Li, J. V. Ravetch, Mouse model recapitulating human Fc receptor structural and functional diversity. *Proc. Natl.*

Acad. Sci. **109**, 6181–6186 (2012).

287. B. M. Gunn *et al.*, A Fc engineering approach to define functional humoral correlates of immunity against Ebola virus. *Immunity*. **54**, 815-828.e5 (2021).

288. F. Horns *et al.*, Lineage tracing of human B cells reveals the in vivo landscape of human antibody class switching. *Elife*. **5**, 1–32 (2016).

289. C. Biondo, G. Lentini, C. Beninati, G. Teti, The dual role of innate immunity during influenza. *Biomed. J.* **42**, 8–18 (2019).

290. I. Sultana *et al.*, Stability of neuraminidase in inactivated influenza vaccines. *Vaccine*. **32**, 2225–2230 (2014).

291. C. Ferrara *et al.*, Unique carbohydrate-carbohydrate interactions are required for high affinity binding between FcγRIII and antibodies lacking core fucose. *Proc. Natl. Acad. Sci. U. S. A.* **108**, 12669–12674 (2011).

292. D. J. Dilillo, G. S. Tan, P. Palese, J. V. Ravetch, Broadly neutralizing hemagglutinin stalk-specific antibodies require FcR interactions for protection against influenza virus in vivo. *Nat. Med.* **20** (2014), doi:10.1038/nm.3443.

293. A. Przemska-Kosicka *et al.*, Age-related changes in the natural killer cell response to seasonal influenza vaccination are not influenced by a synbiotic: A randomised controlled trial. *Front. Immunol.* **8**, 1–9 (2018).

294. R. Solana, C. Campos, A. Pera, R. Tarazona, Shaping of NK cell subsets by aging. *Curr. Opin. Immunol.* **29**, 56–61 (2014).

295. J. K. H. Lee *et al.*, Efficacy and effectiveness of high-dose versus standard-dose influenza vaccination for older adults: a systematic review and meta-analysis. *Expert Rev. Vaccines*. **17**, 435–443 (2018).

296. M. S. Miller *et al.*, Neutralizing Antibodies Against Previously Encountered Influenza Virus Strains Increase over Time: A Longitudinal Analysis. *Sci. Transl. Med.* **5**, 198ra107-198ra107 (2013).

297. C. Henry *et al.*, Influenza Virus Vaccination Elicits Poorly Adapted B Cell Responses in Elderly Individuals. *Cell Host Microbe*. **25**, 357-366.e6 (2019).

298. D. J. Falconer, G. P. Subedi, A. M. Marcella, A. W. Barb, Antibody Fucosylation Lowers the FcγRIIIa/CD16a Affinity by Limiting the Conformations Sampled by the N162-Glycan. *ACS Chem. Biol.* **13**, 2179–2189 (2018).

299. W. Zhong *et al.*, Antibody-dependent cell-mediated cytotoxicity to hemagglutinin of influenza a viruses after influenza vaccination in humans. *Open Forum Infect. Dis.* **3**,

1–7 (2016).

300. A. P. Y. Li *et al.*, Immunogenicity of standard, high-dose, MF59-adjuvanted, and recombinant-HA seasonal influenza vaccination in older adults. *npj Vaccines*. **6**, 1–12 (2021).

301. M. Getie-Kebtie, I. Sultana, M. Eichelberger, M. Alterman, Label-free mass spectrometry-based quantification of hemagglutinin and neuraminidase in influenza virus preparations and vaccines. *Influenza Other Respi. Viruses*. **7**, 521–530 (2013).

302. T. R. Cate *et al.*, A high dosage influenza vaccine induced significantly more neuraminidase antibody than standard vaccine among elderly subjects. *Vaccine*. **28**, 2076–2079 (2010).

303. R. Solana, E. Mariani, NK and NK/T cells in human senescence. *Vaccine*. **18**, 1613–1620 (2000).

304. S. Ng *et al.*, Novel correlates of protection against pandemic H1N1 influenza A virus infection. *Nat. Med.* (2019), doi:10.1038/s41591-019-0463-x.

305. J. M. Ferdinands *et al.*, Intraseason waning of influenza vaccine protection: Evidence from the US influenza vaccine effectiveness network, 2011-2012 through 2014-2015. *Clin. Infect. Dis.* **64**, 544–550 (2017).

306. R. Praditsuwan, P. Assantachai, C. Wasi, P. Puthavatana, U. Kositanont, The Efficacy and Effectiveness of Influenza Vaccination among Thai Elderly Persons Living in the Community. *J. Med. Assoc. Thail.* **88**, 256–264 (2005).

307. C. Shen *et al.*, A multimechanistic antibody targeting the receptor binding site potently cross-protects against influenza B viruses. *Sci. Transl. Med.* **9**, 1–14 (2017).

308. L. D. Estrada, S. Schultz-Cherry, Development of a Universal Influenza Vaccine. *J. Immunol.* **202**, 392–398 (2019).

309. A. C. Tricco *et al.*, Comparing influenza vaccine efficacy against mismatched and matched strains : a systematic review and meta-analysis. *BMC Med.* **11**, 1 (2013).

310. A. J. Broadbent, K. Subbarao, Influenza virus vaccines : lessons from the 2009 H1N1 pandemic. *Curr. Opin. Virol.* **1**, 254–262 (2011).

311. F. Krammer, The human antibody response to influenza A virus infection and vaccination. *Nat. Rev. Immunol.* **19**, 383–397 (2019).

312. N. Thulin, T. Wang, The Role of Fc Gamma Receptors in Broad Protection against Influenza Viruses. *Vaccines*. **6**, 36 (2018).

313. I. A. Nuñez *et al.*, Impact of age and pre-existing influenza immune responses in humans receiving split inactivated influenza vaccine on the induction of the breadth of antibodies to influenza A strains. *PLoS One*. **12**, 1–23 (2017).

314. N. Tewawong *et al.*, Assessing antigenic drift of seasonal influenza A(H3N2) and A(H1N1)pdm09 viruses. *PLoS One*. **10**, 1–15 (2015).

315. K. Tamura, G. Stecher, D. Peterson, A. Filipski, S. Kumar, MEGA6: Molecular evolutionary genetics analysis version 6.0. *Mol. Biol. Evol.* **30**, 2725–2729 (2013).

316. S. Kumar, G. Stecher, M. Li, C. Knyaz, K. Tamura, MEGA X: Molecular evolutionary genetics analysis across computing platforms. *Mol. Biol. Evol.* **35**, 1547–1549 (2018).

317. G. Stecher, K. Tamura, S. Kumar, Molecular evolutionary genetics analysis (MEGA) for macOS. *Mol. Biol. Evol.* **37**, 1237–1239 (2020).

318. R. C. Edgar, MUSCLE: Multiple sequence alignment with high accuracy and high throughput. *Nucleic Acids Res.* **32**, 1792–1797 (2004).

319. D. T. Jones, W. R. Taylor, J. M. Thornton, The rapid generation of mutation data matrices from protein sequences. *Bioinformatics*. **8**, 275–282 (1992).

320. C. Hannoun, F. Megas, J. Piercy, Immunogenicity and protective efficacy of influenza vaccination. *Virus Res.* **103**, 133–138 (2004).

321. W. Steurer, P. W. Nickerson, A. W. Steele, J. Steiger, T. B. Strom, Ex vivo coating of islet cell allografts with murine CTLA4/Fc promotes graft tolerance. *J. Immunol.* **155**, 1165–1174 (1995).

322. G. L. Moore, H. Chen, S. Karki, G. A. Lazar, Engineered Fc variant antibodies with enhanced ability to recruit complement and mediate effector functions. *MAbs*. **2**, 181–189 (2010).

323. F. Krammer *et al.*, NAction! how can neuraminidase-based immunity contribute to better influenza virus vaccines? *MBio*. **9**, 1–12 (2018).

324. S. F. Andrews *et al.*, High Preexisting Serological Antibody Levels Correlate with Diversification of the Influenza Vaccine Response. *J. Virol.* **89**, 3308–3317 (2015).

325. K. Y. A. Huang, S. C. Chang, Y. C. Huang, C. H. Chiu, T. Y. Lin, Antibody responses to trivalent inactivated influenza vaccine in health care personnel previously vaccinated and vaccinated for the first time. *Sci. Rep.* **7**, 1–10 (2017).

326. J. Lee *et al.*, Molecular-level analysis of the serum antibody repertoire in young adults before and after seasonal influenza vaccination. *Nat. Med.* **22**, 1456–1464 (2016).

327. D. L. Brown, G. D. Harkiss, In vivo generation and clearance of soluble immune complexes containing IgM antibodies in normal and decomplemented rabbits. *Clin. Exp. Immunol.* **43**, 231–239 (1981).

328. B. Mantovani, Phagocytosis of immune complexes mediated by IgM and C3 receptors by macrophages from mice treated with glycogen. *J Immunol.* **126**, 127–130 (1981).

329. M. L. Litvack, M. Post, N. Palaniyar, IgM promotes the clearance of small particles and apoptotic microparticles by macrophages. *PLoS One.* **6**, 1–12 (2011).

330. G. Dekkers *et al.*, Affinity of human IgG subclasses to mouse Fc gamma receptors. *MAbs.* **9**, 767–773 (2017).

331. T. Takai, M. Onot, M. Hikida, H. Ohmori, J. V Ravetcht, Augmented humoral and anaphylactic responses in FcyRll-deficient mice. *Nature.* **379**, 346–349 (1996).

332. R. J. Brownlie *et al.*, Distinct cell-specific control of autoimmunity and infection by FcγRIIb. *J. Exp. Med.* **205**, 883–895 (2008).

333. F. Li, P. Smith, J. V. Ravetch, Inhibitory Fcγ Receptor Is Required for the Maintenance of Tolerance through Distinct Mechanisms. *J. Immunol.* **192**, 3021–3028 (2014).

334. S. Bournazos, D. Corti, H. W. Virgin, J. V. Ravetch, Fc-optimized antibodies elicit CD8 immunity to viral respiratory infection. *Nature.* **11**, 55 (2020).

335. P. S. Arunachalam *et al.*, Adjuvanting a subunit COVID-19 vaccine to induce protective immunity. *Nature.* **594**, 253–258 (2021).

336. W. Zhu, C. Dong, L. Wei, B. Z. Wang, Promising adjuvants and platforms for influenza vaccine development. *Pharmaceutics.* **13**, 1–13 (2021).

337. R. Nachbagauer *et al.*, A chimeric hemagglutinin-based universal influenza virus vaccine approach induces broad and long-lasting immunity in a randomized, placebo-controlled phase I trial. *Nat. Med.* (2020), doi:10.1038/s41591-020-1118-7.

338. T. K. Andersen *et al.*, Enhanced germinal center reaction by targeting vaccine antigen to major histocompatibility complex class II molecules. *npj Vaccines.* **4** (2019), doi:10.1038/s41541-019-0101-0.

339. R. B. Abreu, E. F. Clutter, S. Attari, G. A. Sautto, T. M. Ross, IgA Responses Following Recurrent Influenza Virus Vaccination. *Front. Immunol.* **11**, 1–13 (2020).

340. H. Zou, T. Hastie, Regularization and variable selection via the elastic net. *J. R. Stat. Soc. Ser. B Stat. Methodol.* **67**, 301–320 (2005).

341. T. J. Suscovich *et al.*, Mapping functional humoral correlates of protection against malaria challenge following RTS,S/AS01 vaccination. *Sci. Transl. Med.* **12** (2020), doi:10.1126/scitranslmed.abb4757.

342. L. Chen *et al.*, Comprehensive analysis and selection of anthrax vaccine adsorbed immune correlates of protection in Rhesus Macaques. *Clin. Vaccine Immunol.* **21**, 1512–1520 (2014).

343. C. Jin *et al.*, Vi-specific serological correlates of protection for typhoid fever. *J. Exp. Med.* **218** (2020), doi:10.1084/JEM.20201116.

344. C. Atyeo *et al.*, Distinct early serological signatures track with SARS-CoV-2 survival. *Immunity*, 1–9 (2020).

345. T. Zohar *et al.*, Compromised Humoral Functional Evolution Tracks with SARS-CoV-2 Mortality. *Cell.* **183**, 1508-1519.e12 (2020).

346. P. Meade *et al.*, Influenza Virus Infection Induces a Narrow Antibody Response in Children but a Broad Recall Response in Adults. *MBio.* **11**, 1–15 (2020).

347. K. R. McCarthy *et al.*, Memory B Cells that Cross-React with Group 1 and Group 2 Influenza A Viruses Are Abundant in Adult Human Repertoires. *Immunity.* **48**, 174-184.e9 (2018).

348. D. Angeletti *et al.*, Outflanking Immunodominance to Target Subdominant Broadly Neutralizing Epitopes. *Pnas* (2019), doi:10.1073/pnas.1816300116.

349. S. F. Andrews *et al.*, Immune history profoundly affects broadly protective B cell responses to influenza. *Sci. Transl. Med.* **7** (2015), doi:10.1126/scitranslmed.aad0522.

350. K. Konduru *et al.*, Ebola virus glycoprotein Fc fusion protein confers protection against lethal challenge in vaccinated mice. *Vaccine.* **29**, 2968–2977 (2011).

351. B. Zhao *et al.*, Immunization with Fc-based recombinant Epstein-Barr virus gp350 elicits potent neutralizing humoral immune response in a BALB/c mice model. *Front. Immunol.* **9** (2018), doi:10.3389/fimmu.2018.00932.

352. S. Sun *et al.*, Recombinant vaccine containing an RBD-Fc fusion induced protection against SARS-CoV-2 in nonhuman primates and mice. *Cell. Mol. Immunol.* **18**, 1070–1073 (2021).

353. E. G. Alcaide, S. Krishnarajah, F. Junker, Dendritic cell tumor vaccination via Fc gamma receptor targeting: Lessons learned from pre-clinical and translational studies. *Vaccines.* **9**, 1–20 (2021).

354. S. Y. Chu *et al.*, Inhibition of B cell receptor-mediated activation of primary human B

cells by coengagement of CD19 and FcγRIIb with Fc-engineered antibodies. *Mol. Immunol.* **45**, 3926–3933 (2008).

355. Y. C. Bartsch *et al.*, IgG Fc sialylation is regulated during the germinal center reaction following immunization with different adjuvants. *J. Allergy Clin. Immunol.* **146**, 652-666.e11 (2020).

356. J. S. Turner *et al.*, Human germinal centres engage memory and naive B cells after influenza vaccination. *Nature*. **586** (2020), doi:10.1038/s41586-020-2711-0.

357. R. Solana *et al.*, Innate immunosenescence: Effect of aging on cells and receptors of the innate immune system in humans. *Semin. Immunol.* **24**, 331–341 (2012).

358. A. Saso, B. Kampmann, Vaccine responses in newborns. *Semin. Immunopathol.* **39**, 627–642 (2017).

359. J. C. Yu *et al.*, Innate Immunity of Neonates and Infants. *Front. Immunol.* **9**, 1759 (2018).

360. M. J. Shlomchik, Do Memory B Cells Form Secondary Germinal Centers? *Cold Spring Harb. Perspect. Biol.* **10**, a029405 (2018).

361. M. Auladell *et al.*, Recalling the Future: Immunological Memory Toward Unpredictable Influenza Viruses. *Front. Immunol.* **10**, 1–18 (2019).

362. J. E. McElhaney, G. A. Kuchel, X. Zhou, S. L. Swain, L. Haynes, T-cell immunity to influenza in older adults: A pathophysiological framework for development of more effective vaccines. *Front. Immunol.* **7**, 1–11 (2016).

363. S. Butcher, H. Chahel, J. M. Lord, Ageing and the neutrophil: No appetite for killing? *Immunology*. **100**, 411–416 (2000).

364. R. P. H. De Maeyer, E. S. Chambers, The impact of ageing on monocytes and macrophages. *Immunol. Lett.* **230**, 1–10 (2021).

365. A. Agrawal, S. Gupta, Impact of aging on dendritic cell functions in humans. *Ageing Res. Rev.* **10**, 336–345 (2011).

366. S. Ma, C. Wang, X. Mao, Y. Hao, B Cell Dysfunction Associated With Aging and Autoimmune Diseases. *Front. Immunol.* **10** (2019), doi:10.3389/fimmu.2019.00318.

367. D. Frasca, B. B. Blomberg, Effects of aging on B cell function. *Curr. Opin. Immunol.* **21**, 425–430 (2009).

368. M. Mittelbrunn, G. Kroemer, Hallmarks of T cell aging. *Nat. Immunol.* **22**, 687–698 (2021).

369. H. S. Izurieta *et al.*, Relative Effectiveness of Influenza Vaccines among the United States Elderly, 2018-2019. *J. Infect. Dis.* **222**, 278–287 (2020).

370. H. S. Izurieta *et al.*, Relative Effectiveness of Cell-Cultured and Egg-Based Influenza Vaccines among Elderly Persons in the United States, 2017-2018. *J. Infect. Dis.* **220**, 1255–1264 (2019).

371. H. A. Vanderven *et al.*, Fc functional antibodies in humans with severe H7N9 and seasonal influenza. *J. Clin. Invest.* **2** (2017), doi:10.1172/jci.insight.92750.

372. Centers for Disease Control and Prevention: Department of Health and Human Services, Guidelines for Vaccinating Pregnant Women. *Toolkit Prenat. Care Provid.* (2016), (available at https://www.cdc.gov/vaccines/pregnancy/hcp-toolkit/guidelines.html).

373. A. Olin *et al.*, Stereotypic Immune System Development in Newborn Children. *Cell.* **174**, 1277-1292.e14 (2018).

374. T. Dashivets *et al.*, Multi-angle effector function analysis of human monoclonal IgG Glycovariants. *PLoS One.* **10**, 1–24 (2015).

375. R. L. Shields *et al.*, High Resolution Mapping of the Binding Site on Human IgG1 for FcγRI, FcγRII, FcγRIII, and FcRn and Design of IgG1 Variants with Improved Binding to the FcγR. *J. Biol. Chem.* **276**, 6591–6604 (2001).

376. R. Weltzin, T. P. Monath, Intranasal Antibody Prophylaxis for Protection against Viral Disease. *Clin. Microbiol. Rev.* **12**, 383 (1999).

377. B. M. Gunn *et al.*, Enhanced binding of antibodies generated during chronic HIV infection to mucus component MUC16. *Mucosal Immunol.* **9**, 1–10 (2016).

378. V. M. W. Gould *et al.*, Nasal IgA Provides Protection against Human Influenza Challenge in Volunteers with Low Serum Influenza Antibody Titre. *Front. Microbiol.* **0**, 900 (2017).

379. Y.-Y. Wang *et al.*, Influenza-binding antibodies immobilise influenza viruses in fresh human airway mucus. *Eur. Respir. J.* **49**, 1601709 (2017).

380. J. K. Yin *et al.*, Immunogenicity and safety of pandemic influenza A (H1N1) 2009 vaccine: Systematic review and meta-analysis. *Influenza Other Respi. Viruses.* **5**, 299–305 (2011).

381. P. G. Van Buynder *et al.*, The comparative effectiveness of adjuvanted and unadjuvanted trivalent inactivated influenza vaccine (TIV) in the elderly. *Vaccine.* **31**, 6122–6128 (2013).

382. A. Seubert *et al.*, Adjuvanticity of the oil-in-water emulsion MF59 is independent of Nlrp3 inflammasome but requires the adaptor protein MyD88. *Proc. Natl. Acad. Sci.* **108**, 11169–11174 (2011).

383. N. Garçon, A. Di Pasquale, From discovery to licensure, the Adjuvant System story. *Hum. Vaccines Immunother.* **13**, 19–33 (2017).

384. W. Quintilio *et al.*, Bordetella pertussis monophosphoryl lipid A as adjuvant for inactivated split virion influenza vaccine in mice. *Vaccine*. **27**, 4219–4224 (2009).

385. H. P. Patil *et al.*, Evaluation of monophosphoryl lipid A as adjuvant for pulmonary delivered influenza vaccine. *J. Control. Release*. **174**, 51–62 (2014).

386. H. Q. McLean *et al.*, Impact of Repeated Vaccination on Vaccine Effectiveness Against Influenza A(H3N2) and B During 8 Seasons. *Clin. Infect. Dis.* **59**, 1375–1385 (2014).

387. C. Atyeo *et al.*, COVID-19 mRNA vaccines drive differential Fc-functional profiles in pregnant, lactating, and non-pregnant women. *bioRxiv Prepr. Serv. Biol.* (2021), doi:10.1101/2021.04.04.438404.

388. J. J. Guthmiller, H. A. Utset, P. C. Wilson, B Cell Responses against Influenza Viruses: Short-Lived Humoral Immunity against a Life-Long Threat. *Viruses*. **13**, 965 (2021).

389. A. S. De Groot *et al.*, C3d adjuvant effects are mediated through the activation of C3d-specific autoreactive T cells. *Immunol. Cell Biol.* **93**, 189–197 (2015).

390. J. A. Mitchell, T. D. Green, R. A. Bright, T. M. Ross, Induction of heterosubtypic immunity to influenza A virus using a DNA vaccine expressing hemagglutinin-C3d fusion proteins. *Vaccine*. **21**, 902–914 (2003).

391. G. X. Li *et al.*, Fusion of C3d with hemagglutinin enhances protective immunity against swine influenza virus. *Res. Vet. Sci.* **86**, 406–413 (2009).

392. A. Portela, P. Digard, The influenza virus nucleoprotein: A multifunctional RNA-binding protein pivotal to virus replication. *J. Gen. Virol.* **83**, 723–734 (2002).

393. L. L. Shu, W. J. Bean, R. G. Webster, Analysis of the evolution and variation of the human influenza A virus nucleoprotein gene from 1933 to 1990 . Analysis of the Evolution and Variation of the Human Influenza A Virus Nucleoprotein Gene from 1933 to 1990. *J. Virol.* **67**, 2723–2729 (1993).

394. E. N. Prokudina, N. P. Semenova, Localization of the influenza virus nucleoprotein: Cell-associated and extracellular non-virion forms. *J. Gen. Virol.* **72**, 1699–1702 (1991).

395. S. Patterson, J. Gross, J. S. Oxford, The intracellular distribution of influenza virus matrix protein and nucleoprotein in infected cells and their relationship to haemagglutinin in the plasma membrane. *J. Gen. Virol.* **69 (Pt 8)**, 1859–72 (1988).

396. R. Bodewes *et al.*, In vitro assessment of the immunological significance of a human monoclonal antibody directed to the influenza a virus nucleoprotein. *Clin. Vaccine Immunol.* **20**, 1333–7 (2013).

397. H. A. Vanderven *et al.*, What Lies Beneath: Antibody Dependent Natural Killer Cell Activation by Antibodies to Internal Influenza Virus Proteins. *EBioMedicine*. **8**, 277–290 (2016).

398. L. Chen *et al.*, Immunodominant CD4+ T-Cell Responses to Influenza A Virus in Healthy Individuals Focus on Matrix 1 and Nucleoprotein. *J. Virol.* **88**, 11760–11773 (2014).

399. D. C. Wraith, A. E. Vessey, B. A. Askonas, Purified influenza virus nucleoprotein protects mice from lethal infection. *J. Gen. Virol.* **68 (Pt 2)**, 433–440 (1987).

400. J. B. Ulmer *et al.*, Heterologous Protection Against Influenza by Injection of DNA Encoding a Viral Protein. *Science (80-.).* **259**, 1745–1749 (1993).

401. A. Hessel *et al.*, MVA vectors expressing conserved influenza proteins protect mice against lethal challenge with H5N1, H9N2 and H7N1 viruses. *PLoS One*. **9** (2014), doi:10.1371/journal.pone.0088340.

402. R. J. Cox, E. Mykkeltvedt, J. Robertson, L. R. Haaheim, Non-lethal viral challenge of influenza haemagglutinin and nucleoprotein DNA vaccinated mice results in reduced viral replication. *Scand. J. Immunol.* **55**, 14–23 (2002).

403. S. L. Epstein *et al.*, Protection against multiple influenza A subtypes by vaccination with highly conserved nucleoprotein. *Vaccine*. **23**, 5404–5410 (2005).

404. Q. Chen *et al.*, Comparing the ability of a series of viral protein-expressing plasmid DNAs to protect against H5N1 influenza virus. *Virus Genes*. **38**, 30–38 (2009).

405. R. A. Lamb, S. L. Zebedee, C. D. Richardson, Influenza virus M 2 protein is an integral membrane protein expressed on the infected-cell surface. *Cell*. **40**, 627–633 (1985).

406. J. M. Song *et al.*, Influenza virus-like particles containing M2 induce broadly cross protective immunity. *PLoS One*. **6** (2011), doi:10.1371/journal.pone.0014538.

407. J. Q. Feng *et al.*, Influenza A virus infection engenders a poor antibody response against the ectodomain of matrix protein 2. *Virol. J.* **3**, 1–13 (2006).

408. A. G. Grandea *et al.*, Human antibodies reveal a protective epitope that is highly conserved among human and nonhuman influenza A viruses. *Proc. Natl. Acad. Sci. U. S. A.* **107**, 12658–12663 (2010).

409. W. Zhong *et al.*, Serum antibody response to matrix protein 2 following natural infection with 2009 pandemic influenza A(H1N1) virus in humans. *J. Infect. Dis.* **209**, 986–994 (2014).

410. Y.-N. Lee, M.-C. Kim, Y.-T. Lee, Y.-J. Kim, S.-M. Kang, Mechanisms of Cross-protection by Influenza Virus M2-based Vaccines. *Immune Netw.* **15**, 213 (2015).